

STATUS OF THESIS

Title of thesis

A CHANCE-CONSTRAINED APPROACH FOR
OPTIMIZATION OF GAS PROCESSING PLANT OPERATION
UNDER UNCERTAIN CONDITIONS

I MESFIN GETU

hereby allow my thesis to be placed at the information Resource Center (IRC) of Universiti Teknologi PETRONAS (UTP) with the following conditions:

1. The thesis becomes the property of UTP
2. The IRC of UTP may make copies of the thesis for academic purposes only.
3. This thesis is classified as

Confidential

Non-confidential

If the thesis is confidential, please state the reason:

The contents of the thesis will remain confidential for _____ years.

Remarks on disclosure:

Endorsed by

Signature of Author

Signature of Supervisor

Permanent address:

Assoc. Prof. Dr. Shuhaimi Bin Mahadzir

Faculty of Technology

Addis Ababa University

P.O.Box 385

Addis Ababa, Ethiopia

Date: _____

Date: _____

UNIVERSITI TEKNOLOGI PETRONAS

A CHANCE-CONSTRAINED APPROACH FOR OPTIMIZATION OF
GAS PROCESSING PLANT OPERATION UNDER UNCERTAIN CONDITIONS

By

MESFIN GETU

The undersigned certify that they have read, and recommend to the Postgraduate Studies Programme for acceptance this thesis for the fulfillment of the requirements for the degree stated.

Signature: _____

Main Supervisor: Assoc. Prof. Dr. Shuhaimi Bin Mahadzir

Signature: _____

Head of Department: Assoc. Prof. Dr. Shuhaimi Bin Mahadzir

Date: _____

A CHANCE-CONSTRAINED APPROACH FOR OPTIMIZATION OF
GAS PROCESSING PLANT OPERATION UNDER UNCERTAIN CONDITIONS

By

MESFIN GETU

A Thesis

Submitted to the Postgraduate Studies Programme
as a Requirement for the Degree of

DOCTOR OF PHILOSOPHY
CHEMICAL ENGINEERING DEPARTMENT
UNIVERSITI TEKNOLOGI PETRONAS
BANDAR SRI ISKANDAR
PERAK

JUNE 2011

DECLARATION OF THESIS

Title of thesis

A CHANCE-CONSTRAINED APPROACH FOR
OPTIMIZATION OF GAS PROCESSING PLANT OPERATION
UNDER UNCERTAIN CONDITIONS

I MESFIN GETU

hereby declare that the thesis is based on my original work except for quotations and citations which have been duly acknowledged. I also declare that it has not been previously or concurrently submitted for any other degree at UTP or other institutions.

Witnessed by

Signature of Author

Signature of supervisor

Permanent address:

Name of supervisor:

Faculty of Technology
Addis Ababa University
P.O.BOX 385
Addis Ababa, Ethiopia

Assoc. Prof. Dr. Shuhaimi Bin Mahadzir

Date: _____

Date: _____

ABSTRACT

Natural gas plant operations contribute hugely to the economies of many developed nations that depend on hydrocarbon resources. The plant operation is usually subjected to continuous variations in upstream conditions, such as flow rate, composition, temperature and pressure, which propagate through the plant and affect its stable operations. As a result, decision making for optimal operating conditions of an in-operation plant is a complex problem and it is exacerbated with the changing product specifications and variations in energy supplies. This work presents a new solution method to the problem, which is based on chance constrained optimization method. A deterministic model is initially developed from process simulation using Aspen HYSYS and later converted to a chance constrained model. The probabilistic model is then relaxed to its equivalent deterministic form and solved for optimum solution using GAMS. The optimum solution is determined probabilistically using chance constraints that are held at a user-defined confidence level. Optimal solution is represented graphically as a trade-off between reliability of holding the process constraints and profitability of the plant. Three case studies are presented to demonstrate the new method. Optimization results show that uncertainty of plant parameters significantly affect the economic performance of the plant operation. The solution approach developed in this work is able to increase the reliability of maintaining the profit by more than 95% confidence level. As a result, the risk of constraints violation is reduced from more than 50% using the typical deterministic optimization to less than 5% with the chance constrained optimization approach. In addition, the results from this study indicate that the variation of material flow from the plant inlet has greater impact by more than 85.5% on profit compared to variation from the plant outlet, which is less than 2%. The variations of energy flow affect on profit is mainly changes with confidence level measurement higher than 95%, although material flow uncertainty is more sensitive to profit changes than uncertainty in energy flow. Final computational results also highlight the advantage of the developed chance constrained approach, which combines both the profit and the

reliability of the process constraints, over “worst case” and two-stage programming approaches. Decisions from the “worst case” approach may reach to more than 99% confidence level which can drastically decrease the profit while the optimal decision from the two-stage programming does not clearly show to how much extent that the profit has been held. The developed solution approach in this work can aid as guidelines to flexible plant operation decision making for the in-operating plant by satisfying all the process constraints at certain confidence level.

ABSTRAK

Operasi loji penapisan gas adalah penyumbang besar kepada ekonomi ke banyak negara membangun yang bergantung kepada hasil dari sumber hidrokarbon. Cabaran mengendalikan operasi loji gas selalunya berpunca dari perubahan keadaan huluan yang bertenusan, seperti kadar alir, komposisi, suhu dan tekanan. Kesan dari keadaan yang berubah-ubah ini meningkat ketika melalui unit-unit di dalam loji dan akhirnya membawa kesan buruk kepada kestabilan operasi loji. Justeru itu, proses membuat keputusan untuk keadaan operasi loji yang optimum merupakan masalah yang kompleks dan ini dipertingkatkan lagi dengan spesifikasi produk yang berubah-ubah serta variasi dalam perbekalan tenaga. Tesis ini mencadangkan suatu kaedah penyelesaian baru untuk masalah operasi loji kompleks berdasarkan kepada kaedah pengoptimuman kesempatan terhad. Sebuah model deterministik pada awalnya dikembangkan dari simulasi proses menggunakan perisian Aspen HYSYS dan kemudian diubah menjadi model pengoptimuman kesempatan terhad. Model ini kemudian dikendurkan untuk membentuk model setara deterministik dan diselesaikan menggunakan perisian GAMS. Penyelesaian optimum ditentukan secara kebarangkalian pada had kebolehpercayaan yang ditetapkan pengguna. Penyelesaian optimum dipamerkan secara grafik sebagai “trade-off” antara kebolehpercayaan memegang tingkat had dan keuntungan operasi loji. Tiga kajian kes dianalisa untuk menunjukkan kaedah penyelesaian baru dalam tesis ini. Keputusan penyelesaian optimum menunjukkan bahawa ketidakpastian parameter loji memberi kesan terhadap prestasi ekonomi operasi loji. Pendekatan penyelesaian yang dibangunkan dalam tesis ini mampu meningkatkan kebolehpercayaan keuntungan operasi loji pada tingkat kebolehpercayaan melebihi 95%. Akibatnya, risiko menyalahi had berkurangan daripada lebih 50% menggunakan kaedah biasa pengoptimuman deterministik kepada kurang dari 5% dengan kaedah pengoptimuman kesempatan terhad. Selain itu, hasil dari kajian ini menunjukkan bahawa variasi aliran material huluan loji mempunyai kesan yang lebih besar melebihi 85.5% ke atas keuntungan dibandingkan dengan

variasi dari hiliran kesempatan terhad, yang menggabungkan keuntungan dan kebolehpercayaan had proses, dari kaedah "kes terburuk" dan kaedah pengaturcaraan dua-tahap. Keputusan dari kaedah "kes terburuk" boleh mencapai tingkat kepercayaan lebih dari 99% yang secara drastik boleh mengurangkan keuntungan sedangkan keputusan yang optimum dari pengaturcaraan dua-tahap tidak jelas menunjukkan kepada kuantiti tahap keuntungan dipegang. Pendekatan penyelesaian yang dibangunkan dalam tesis ini dapat membantu sebagai panduan untuk proses membuat keputusan operasi loji yang lebih fleksibel di samping memenuhi semua had proses pada tahap kepercayaan yang tertentu.

In compliance with the terms of the Copyright Act 1987 and the IP Policy of the university, the copyright of this thesis has been reassigned by the author to the legal entity of the university,
Institute of Technology PETRONAS Sdn Bhd.

Due acknowledgement shall always be made of the use of any material contained in, or derived from, this thesis.

© MESFIN GETU, 2011
Institute of Technology PETRONAS Sdn Bhd
All rights reserved.

ACKNOWLEDGEMENTS

First of all, I would like to express my earnest gratitude to my supervisor Assoc. Prof. Dr. Shuhaimi Mahadzir for his encouraging comments and invaluable guidance. Without his guidance, inspiration and support, this work would not be complete. He was always ready to discuss ideas, read and response to the drafts which I submitted to him. His oral and written responses were very helpful for me to improve the work. I am also indebted to Assoc. Prof. Ir. Dr. Kamarul Ariffin.

I am grateful to Universiti Teknologi PETRONAS (UTP) for providing me this opportunity to come and study here under the graduate assistanceship scheme. During my four and half year stay in UTP, I believe that I have earned a good knowledge which will significantly enhance my career in the future. My appreciation also goes to Chemical Engineering Department for creating such a conducive environment by providing all the necessary tools which I used them in this work. I would like also to thank UTP for releasing the required fund to support this work.

I am thankful for the wonderful Ethiopian and other international fellows in UTP whom they showed me their friendship during my stay. I thank Dr. Lemma Dendena, Dr. Dereje Engida, Dr. Akililu Tesfamichael, Dr. Abdelbagi Osman, Dr. Firas Basim Ismail, Mr. Abdulwehab Adem, Mr. Ahmed Nurys, Mr. Anteneh Mesfin, Mr. Biruh Shemkit, Mr. Chanyalew Belachew, Mr. Mesfin Gizaw, Mr. Sintayhu Mekuria, Mr. Tamiru Alemu, Mr. Tilahune Derebe, Mr. Yohannes Tamrat and others. I am also grateful to PhD students at Chemical Engineering Department and wish to them all the best during their research period: Mr. Mamoud Massaad, Mr. Omer Esia, Ms Triana Prihatin and others.

Last but not least, many thanks to my fiancé, Mekdes Gebrestadik, who has always been there and encouraged me to continue.

DEDICATION

This thesis is dedicated to my beloved family whom they encouraged and gave me a constant support throughout my study.

TABLE OF CONTENTS

Abstract	v
Abstrak	vii
Acknowledgements	x
Dedication	xi
Table of Contents	xii
List of figures	xvii
List of tables	xxi
Abbervations	xxi
Nomenclatures	xxvi
CHAPTER 1	1
INTRODUCTION	1
1.1 The basics of natural gas	1
1.2 Gas processing plant (GPP)	3
1.3 Operational issues in GPP	5
1.4 Process optimization	8
1.4.1 Deterministic programming	8
1.4.2 Optimization under uncertainty	10
1.4.2.1 Fuzzy programming	11

1.4.2.2 Two-stage programming	11
1.4.2.3 Chance-constrained programming	12
1.5 Problem statement.....	13
1.6 Research objectives.....	13
1.7 Scope of the research	16
1.8 Overview of the thesis	16
CHAPTER 2	17
LITERATURE REVIEW	17
2.1 Uncertainty in chemical process plant	17
2.1.1 Uncertainty sources and classifications	18
2.1.2 Uncertainty analysis and sampling	19
2.1.3 Uncertainty and optimization.....	22
2.2 Process scheme options and optimization algorithms in GPP.....	25
2.2.1 Gas plant process scheme options.....	26
2.2.2 Gas plant optimizations algorithms	31
2.2.2.1 Statistical method.....	32
2.2.2.2 Equation based method	32
2.2.2.3 Model predictive control.....	35
2.2.2.4 Sequential modular simulation technique	36
2.2.2.5 Simulator response surface modeling technique.....	39

2.2.2.6 Methaheuristic algorithms.....	44
2.2.2.7 Taguchi method	44
2.3 Summary	45
CHAPTER 3	47
DEVELOPMENT OF CHANCE CONSTRAINED OPTIMIZATION METHOD FOR GPP	47
3.1 Preliminary terms.....	47
3.2 Inflows and outflows.....	50
3.3 Modeling material inflow and outflow	51
3.4 Modeling energy inflow and outflow	54
3.5 Deterministic model formulation	59
3.5.1 Uncertain feed inflow	59
3.5.2 Uncertain product outflow	61
3.5.3 Uncertain utility inflow	62
3.5.4 Uncertain energy product outflow	63
3.6 Chance constrained model formulation	64
3.6.1 Single chance constrained.....	65
3.6.2 Joint chance constrained	66
3.7 Relaxed deterministic model formulation.....	67
3.8 Evaluation of probability distribution function.....	71
3.9 Feasibility analysis.....	73

3.10 Reliability vs profitability analysis	74
3.11 ASPEN HYSYS process simulator.....	76
3.12 General algebraic modeling system (GAMS).....	77
3.12.1 GAMS LP solvers	79
3.12.2 GAMS NLP solvers	79
3.13 Summary	81
CHAPTER 4	83
RESULTS AND DISCUSSIONS	83
4.1 Case study 1: Optimal operation of GPP with uncertain feed flows.....	83
4.1.1 Data analysis	85
4.1.2 Optimization	87
4.1.3 Sensitivity analysis.....	94
4.1.4 Computational results	96
4.2 Case study 2: Optimal operation of GPP with uncertain product flows.....	98
4.2.1 Data analysis	100
4.2.2 Optimization	101
4.2.3 Sensitivity analysis.....	107
4.2.4 Computational results	108
4.3 Case study 3: Optimal operation of GPP with uncertain utility and energy product flows	110
4.3.1 Optimization	111

4.3.2 Computational results	116
4.4 Summary	17
CHAPTER 5	119
CONCLUSIONS AND FUTURE WORKS	119
5.1 Conclusions.....	119
5.2 Future works	122
REFERENCES	125
PUBLICATION LISTS	125
APPENDIX A.....	142
SHORTCUT DISTILLATION CORRELATIONS	143
APPENDIX B	147
STANDARD NORMAL DISTRIBUTION FUNCTION	147
APPENDIX C.....	149
HYSYS PROCESS MODEL AND STREAM DATA TABLES.....	149
APPENDIX D.....	178
NORMAL DISTRIBUTION FOR UNCERTAIN MATERIAL FLOWS	178
APPENDIX E	184
GAMS OPTIMIZATION CODE	184

LIST OF FIGURES

Fig.1.1: Primary sources of energy in the world	2
Fig.1.2: Product utilization of natural gas.....	3
Fig.1.3: Simplified flowsheet for a gas processing plant.....	4
Fig.1.4: Deterministic optimization framework.....	9
Fig.2.1: The 1970-vintage turbo-expander process scheme.....	26
Fig.2.2: The gas sub-cooled process scheme.....	27
Fig.2.3: Deethanizer overhead recycle process scheme.....	28
Fig.2.4: Cold residue recycles process scheme.....	29
Fig.2.5: Enhanced NGL recovery process scheme.....	29
Fig.2.6: Three factor inscribed central composite design.....	40
Fig.2.7: Three factor box-Behnken design.....	40
Fig.2.8: Implemented architecture GA algorithm.....	42
Fig.3.1: Classification of linear chance constrained problems.....	50
Fig.3.2: A schematic representation of inflows and outflows of GPP.....	52
Fig.3.3: A schematic representation for material inflow and outflow of GPP.....	55
Fig.3.4: A schematic representation for energy inflow and outflow of GPP.....	54
Fig.3.5: A typical conventional distillation column used in GPP.....	55
Fig.3.6: The standard normal cumulative distribution function.....	72

Fig.3.7: Probable and feasible operating region with specified confidence level.....	74
Fig.3.8: Possible profit profiles with respect to confidence level.....	75
Fig.3.9: Hierarchical tree for simulation environment in HYSYS.....	76
Fig.3.10: General structure of GAMS representation.....	78
Fig.3.11: The overall methodology developed.....	81
Fig.4.1: Simplified block diagram of GPP with uncertain feed flow.....	84
Fig.4.2: The three column arrangement in the PRU section.....	84
Fig.4.3: Optimal profit profile for uncertain feed flows case.....	90
Fig.4.4: Optimal sales gas product profile for uncertain feed flow case.....	91
Fig.4.5: Optimal ethane product profiles for uncertain feed flow case.....	92
Fig.4.6: Optimal propane product profiles for uncertain feed flow case.....	92
Fig.4.7: Optimal butane product profiles for uncertain feed flow case.....	93
Fig.4.8: Joint vs Single confidence level for uncertain feed flow case.....	94
Fig.4.9: Single confidence level vs profit for uncertain feed flow case.....	95
Fig.4.10: Simplified block diagram of GPP with uncertain product flow.....	99
Fig.4.11: The two column arrangements in the PRU section.....	99
Fig.4.12: Optimal profit profiles for uncertain product flows case.....	104
Fig.4.13: Optimal profit profiles for uncertain product flows case.....	105
Fig.4.14: Optimal ethane product profiles for uncertain product flows case.....	106
Fig.4.15: Optimal LPG product profile for uncertain product flow case.....	106

Fig.4.16: Joint vs single confidence level for uncertain product flow case.....	107
Fig. 4.17: Single confidence level vs profit for uncertain product flow case.....	108
Fig.4.18: Optimal profit profile with specified confidence level.....	111
Fig.4.19: Optimal steam flow rate with specified confidence level.....	113
Fig.4.21: Optimal cooling water flow rate with specified confidence level.....	114
Fig.4.22: Optimal reboiler duty with specified confidence level.....	115
Fig.4.23: Optimal condenser duty with specified confidence level.....	116
Fig.A.1: A logarithmic plot for component distribution.....	144
Fig.C.1: HYSYS process model for pretreatment unit (PTU), acid gas removal unit (AGRU) and dehydration unit (DHU).....	149
Fig.C.2: HYSYS process model for condensate treatment unit (CTU).....	150
Fig.C.3:HYSYS process model for low temperature separation unit (LTSU)	151
Fig.C.4:HYSY process model for sales gas compression unit (SGCU)	152
Fig.C.5: HYSYS process model for product recovery unit (PRU).....	153
Fig.C.6: HYSYS process model for C ₃ refrigeration unit (PRU).....	154
Fig D.1: Total C ₁ or methane inflow from the plant inlet.....	178
Fig D.2: Total C ₂ or ethane inflow from the plant inlet.....	179
Fig D.3: Total C ₃ or propane inflow from the plant inlet.....	179
Fig.D.4: Total C _{4s} or butanes inflow from the plant inlet.....	180
Fig.D.5: Total C ₅₊ or condensates inflow from the plant inlet.....	180
Fig.D.6: Total N ₂ or Nitrogen inflow from the plant inlet	181

Fig. D.7: Total CO₂ or carbon dioxide inflow from the plant inlet181

Fig.D.8: C₂ outflow for propane product from the plant outlet182

Fig. D.9: C₃ outflow for propane product from the plant outlet.....182

Fig.D. 10: C₄s outflow for propane product from the plant outlet183

LIST OF TABLES

Table 1.1: Typical natural gas feeds used in gas processing plant.....	6
Table 2.1: Classification of all gas plant optimization algorithms.....	46
Table 4.1: Mean and standard deviations of the uncertain feed component flows.....	85
Table 4.2: Maximum and minimum values of decision variables for uncertain feed flow case.....	86
Table 4.3: Expected price value for products and raw material.....	86
Table 4.4: Final computational result for uncertain feed flow case.....	97
Table 4.5: Mean and standard deviations of the uncertain product component outflow.....	100
Table 4.6: Maximum and minimum values of decision variables for uncertain product component outflow case.....	101
Table 4.7: Final optimization result for uncertain product flow case.....	109
Table 4.8: Final optimization result for uncertain utility and energy product flows.....	117
Table B.1: Standard loss function and standard normal cumulative distribution function $Z(-3, 3)$	147
Table C.1: PTU process stream data table 1.....	155
Table C.2: PTU process stream data table 2.....	156
Table C.3: PTU process stream data table 3.....	157
Table C.4: PTU process stream data table 4.....	158

Table C.5: PTU process stream data table 5.....	159
Table C.6: CTU process stream data table 1.....	160
Table C.7: CTU process stream data table 2.....	161
Table C.8: CTU process stream data table 1.....	162
Table C.9: LTSU process stream data table 2.....	163
Table C.10: LTSU process stream data table 3.....	164
Table C.11: LTSU process stream data table 4.....	165
Table C.12: LTSU process stream data table 5.....	166
Table C.13: SGCU process stream data table 1.....	167
Table C.14: SGCU process stream data table 2.....	168
Table C.15: PRU process stream data table 1.....	169
Table C.16: PRU process stream data table 2.....	170
Table C.17: PRU process stream data table 3.....	171
Table C.18: PRU process stream data table 4.....	172
Table C.19: C ₃ RU process stream data table 1.....	173
Table C.20: C ₃ RU process stream data table 2.....	174
Table C.21: C ₃ RU process stream data table 3.....	175
Table C.22: C ₃ RU process stream data table 4.....	176
Table C.23: C ₃ RU process stream data table 5.....	177

ABBERVATIONS

AGRU	Acid gas removal unit
ANOM	Analysis of means
ANOVA	Analysis of variance
CMO	Constant mass or molar overflow
COM	Component object model
CTU	Condensate treatment unit
EIA	Energy information administration
EPS	Equality probability sampling
FA	Firefly algorithm
GA	Genetic algorithm
GPP	Gas processing plant
GSP	Gas sub-cooled process
HS	Harmony search
HSS	Hammersley sequence sampling
ISS	Inconsistent set of constraints
LHS	Latin hypercube sampling
LP	Linear programming
LPG	Liquefied petroleum gas

LNG	Liquefied natural gas
LSTJ	Linear steady state with time-dependent uncertainties under joint chance constraint
LSTS	Linear steady state with time-dependent uncertainties under single chance constraint
LTSU	Low temperature separation unit
MCS	Monte carlo simulation
MTBE	Methyl tertiary-butyl ether
NDTJ	Non linear dynamic state with time-dependent uncertainties under joint chance constraints
NGLs	Natural gas liquids
NLP	Nonlinear programming
MTBE	Methyl tertiary-butyl ether
NDTJ	Non linear dynamic state with time-dependent uncertainties under joint chance constraints
NGLs	Natural gas liquids
NLP	Nonlinear programming
NMDS	Neider-mead downhill simplex
OHD	Overhead recycle
PRU	Product recovery unit
PSO	Particle swam optimization

PTU	Pre-treatment unit
SA	Simulated annealing
SNR	Signal-to-noise-ratio
SHS	Shifted Hammersley sampling
SGCU	Sales gas compression unit
SQP	Sequential quadratic programming
SF	Sub-flowsheet
TAME	Tertiary amyl methyl ether
TS	Tabu search
VBA	Visual basic

NOMENCLATURES

Letters

$a_{k,j}$	composition for certain product flow
$\hat{a}_{k,j}$	composition for uncertain product flow
$a_{k,j}P_j$	certain product component mass flow
$\hat{a}_{k,j}\hat{P}_j$	uncertain product component mass flow
$b_{k,j}$	composition for certain raw material flow
$\hat{b}_{k,j}$	composition for uncertain raw material flow
$b_{k,i}R_i$	certain raw material component mass flow
$\hat{b}_{k,i}\hat{R}_i$	uncertain raw material component mass flow
B_t	column bottom flow rate
\bar{C}^P	expected price factor for certain product flow
$\bar{C}^{\hat{P}}$	expected price factor for uncertain product flow
\bar{C}^R	expected price factor for certain raw material flow
$\bar{C}^{\hat{R}}$	expected price factor for uncertain raw material flow
\bar{C}^R	expected price factor for uncertain utility flow
\bar{C}^q	expected price factor for uncertain energy product flow
D_s	column distillate flow rate
\bar{C}^q	expected price factor for uncertain product flow
D_s	column distillate flow rate
E	expected value
f	objective function
F	column feed flow

g	inequality constraint
h	equality constraint
h_{B_s}	specific mass enthalpy of column bottom flow
h_{D_s}	specific mass enthalpy of column distillate flow
h^L	specific mass enthalpy of column liquid flow
h^v	specific mass enthalpy of column vapor flow
H	vectors of equation
ΔH_{stm}	latent heat of the steam
J_n	Jacobian matrix
k	component representation
L_N	column bottom liquid flow rate
L_0	column top liquid flow rate (reflux rate)
\dot{M}	mass flow rate for utility
n_d	number of data points
N_{\min}	minimum number of stages
N	actual number of stages
p^ζ	uncertain product component flows
P	certain product flow
p_m	number of parameter
\hat{P}	uncertain product flow
Pr	probability operator
q_c	condenser duty
q_F	feed quality
q^ζ	actual energy product flow
q_R	reboiler duty
Q	certain energy product flow
\hat{Q}	uncertain energy product flow
r^ξ	uncertain feed component flows
R	certain raw material flow

\hat{R}	uncertain raw material flow
R^2	lowest mean square error
R_{flx}	column reflux ratio
R_{flx}^{\min}	minimum reflux ratio
\Re	set of real number
s	state variable
u^ε	actual utility flow
U	certain utility flow
\hat{U}	uncertain total utility flow
Var	variance measurement
V_N	column bottom vapor flow rate
V_o	column top vapor flow rate
w	constrained output variable
x	continuous optimization variable
Y	vector of variable
z_F	composition of column feed flow
Z	standardized parameter

Greek symbols & others

α	probability or confidence level
θ	mean or average
σ	standard deviation
∂	relative volatility
ρ	probability density function (pdf)
Φ	probability distribution function
φ	correlating parameter
ℓ	coefficient in response surface modeling
Δ	delta/ change/
λ_N	specific enthalpy of column bottom vapor flow
λ_o	specific enthalpy of column top vapor flow

λ_s	line search parameter
ε	vectors of uncertain energy inflows
ξ	vectors of the uncertain feed component inflows
ζ	vectors of the uncertain product component outflows
ς	vectors of uncertain energy product outflows
η_c	constant value
τ	boil up ratio
Π	multiplication operator
Σ	summation operator
\int	integration operator

Subscripts

e	index for energy flow
i	index for certain raw material flow
j	index for certain product flow
i'	index for certain utility flow
j'	index for certain energy product flow
k	index for components
l	index for uncertain product flow
l'	index for uncertain energy product flow
m	index for uncertain raw material flow
m'	index for uncertain utility flow
max	maximal
min	minimal

Superscript

$_$	index for expected price value of material and energy flows
\wedge	index for the uncertain material and energy flows

CHAPTER 1

INTRODUCTION

Natural gas, also called “the prince of hydrocarbons”, is the fastest growing energy source in the world [1]. Recent reports showed that the industrial consumption of natural gas in U.S has increased by 7.4 percent [2]. Out of the 7.4 percent growth, the projected 6.7 percent is contributed from increased industrial production index. The production of natural gas by itself involves a number of unit operations before the feed is converted into saleable products. The safe operations of the plant as well as its optimality are very important in order for the plant to generate a higher profit. Moreover, the operation of the plant should also be flexible enough to allow for any variations that arise from both internal and external factors. This chapter presents the basics of natural gas, the main processes involved in gas processing plant, operational issues related to gas processing plant and the different optimization approaches.

1.1 The basics of natural gas

Natural gas is a mixture of gaseous hydrocarbons that developed organically from fossil fuels, remains of plants and animals as well as microorganisms that lived million of years ago. It is formed under pressure, buried several kilometers beneath the earth’s surface and obtained either associated or non-associated gas. Associated gas is produced together with a crude oil, while non-associated gas contains little or no crude oil. Raw natural gas comprises varying amounts of light hydrocarbons. Methane makes up 80-90% of most natural gas mixtures. The balance is made up of those hydrocarbons in decreasing amount towards higher carbon molecules. These gases are sold as natural gas liquids (NGLs) in the form of ethane, propane, butane, LPG and condensate (C₅₊). In addition, raw natural gas may contain non hydrocarbons such as hydrogen sulfide, helium, water, nitrogen and carbon dioxide.

Nowadays, natural gas has become an important fuel in the world due to its steady growth rate, wide availability, clean burning characteristics and easy transportation [3]. Based on the recent assessment made by the U.S. energy information administration, the world demand for natural gas is expected to almost double by 2030 and by then, natural gas is forecasted to overtake oil as the dominant fuel in industrial sector [4]. The share of natural gas and NGLs out of the total world energy resources is shown in Fig. 1.1 [5]. These two form the second most energy sources of the world.

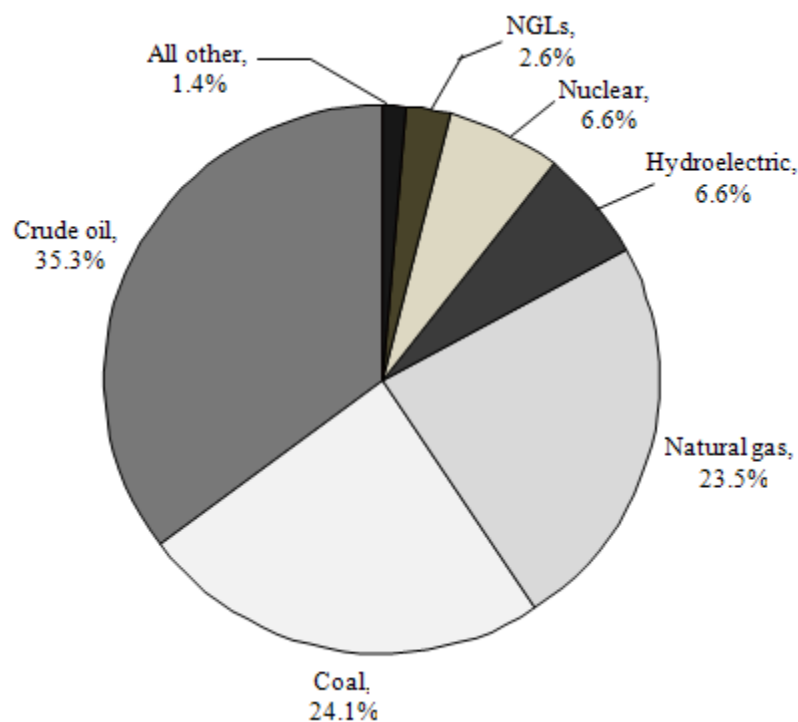


Fig 1.1: Primary sources of energy in the world

The products from natural gas have a number of applications in different sectors as shown in Fig. 1.2. Sales gas is used in residential consumers, transportation and power plants. The NGLs from natural gas are important feedstocks for petrochemical and refinery industries. For example, ethane is used as a petrochemical feedstock to produce ethylene in petrochemical complex plant. Propane is also widely used as a heating and transportation fuel. Beside this, propane can be used as a feedstock for the production of ethylene and propylene. Butanes are also important feedstock in

refinery processes such as alkylation, MTBE (methyl tertiary-butyl ether) and TAME (tertiary amyl methyl ether) production as well as blending stock for gasoline.

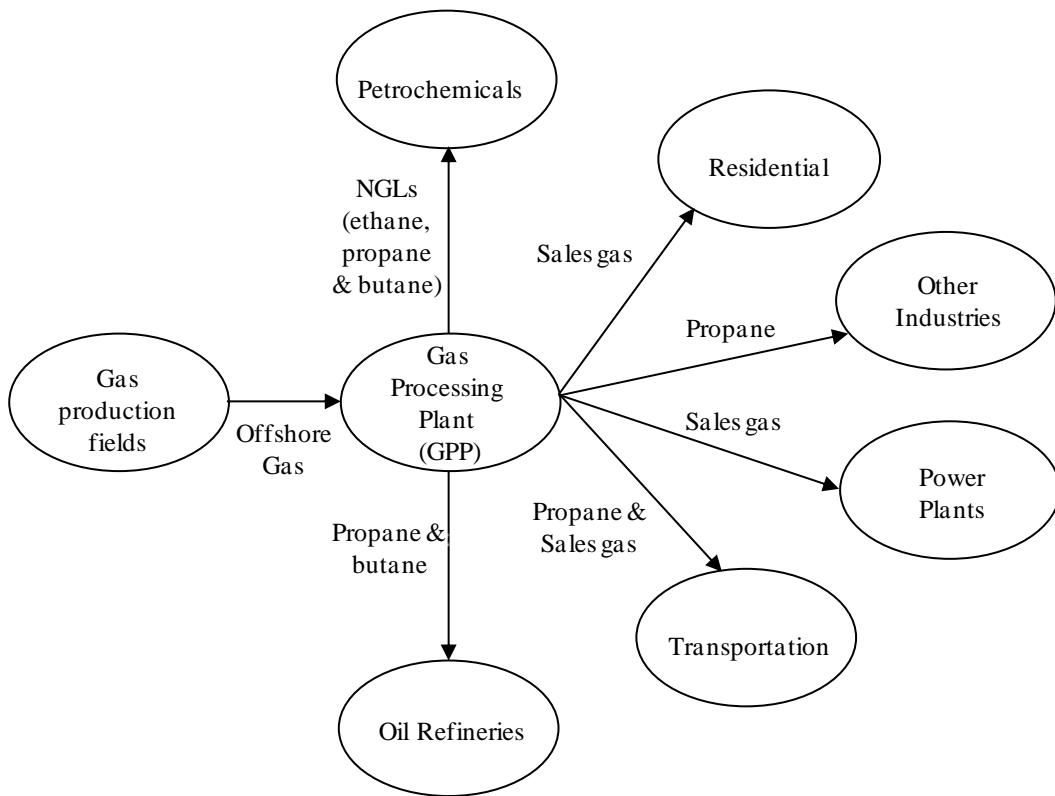


Fig 1.2: Product utilization of natural gas

1.2 Gas processing plant (GPP)

A typical gas processing plant comprises of the following main processes: a) pretreatment unit (PTU); b) acid gas removal unit (AGRU); c) condensate treatment unit (CTU); d) low temperature separation unit (LTSU); e) sales gas compression unit (SGCU) and f) product recovery unit (PRU). The simplified schematic representation of a gas processing plant for the main processes involved is shown in Fig. 1.3. The pretreatment operation is the first step to be performed in the gas processing plant after receiving the raw natural gas from the gas production fields. The presence of impurities such as chlorine, hydrogen sulfide, nitrogen, carbon dioxide, water and heavier hydrocarbons have a profound effect on the performance of the plant. Chlorine and hydrogen sulfide are removed from natural gas because they are toxic

and corrosive. Water is removed from the feed gas to prevent hydrate formation in processing facilities and pipelines. Nitrogen, carbon dioxide and heavier hydrocarbons are removed because they can significantly affect the heating value of sales gas by lowering its level.

After the pretreatment operation, the outlet stream is divided into two. The top stream enters the acid gas removal unit after it has been expanded. The acid gas removal operation uses the Benfield process to capture carbon dioxide and hydrogen sulfide in the feed gas. The presence of carbon dioxide has also an effect on downstream equipment units by exposing them to plugging and corrosion. In addition, the removal of carbon dioxide is also important for ethane product to acquire the required specification.

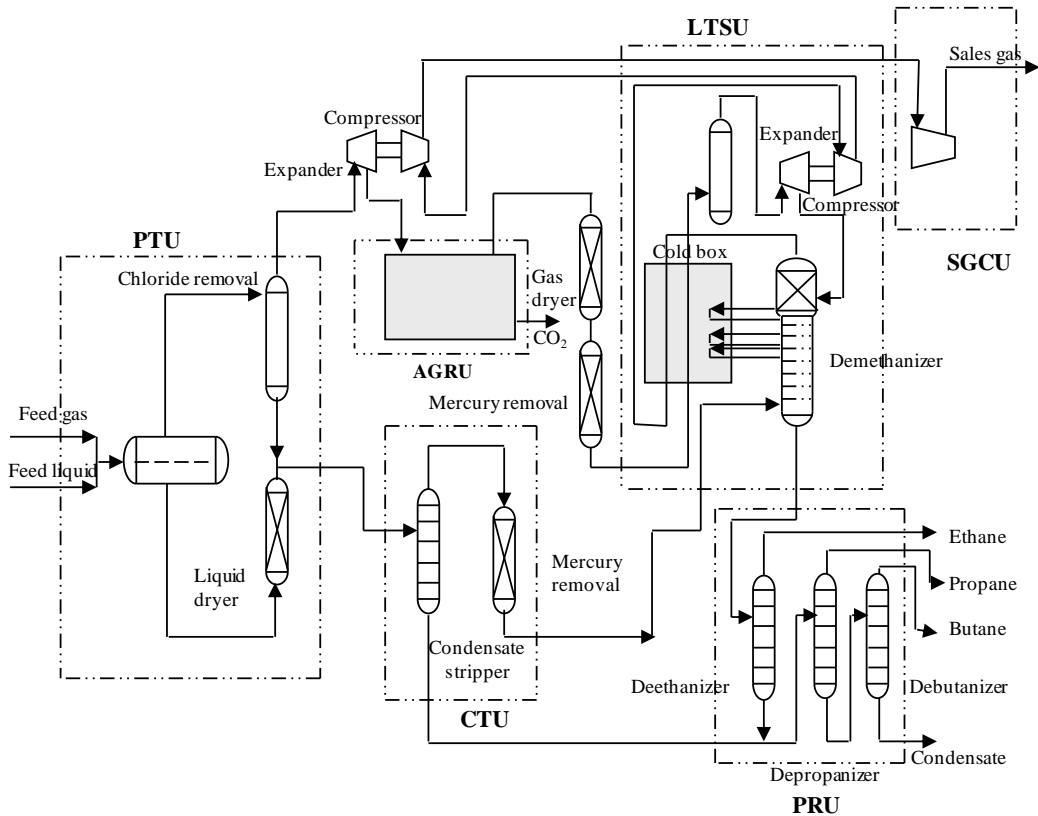


Fig 1.3: Simplified flowsheet for a gas processing plant

The bottom stream from the pretreatment unit then enters to the condensate treatment section. Two main operations, namely water washing and condensate stabilization are performed. Depending upon the associated water quality, the

condensate may require water wash to remove salts and additives. The water often contains high concentrations of methanol or ethylene glycol, which is added to prevent formation of hydrate. After removal of free water, the condensate is sent to a stabilizer, where the lighter hydrocarbons are stripped to the demethanizer column. The heavier hydrocarbons from the bottom of the stabilizer are directly sent to the depropanizer column for further separation.

The outlet stream from the acid gas removal unit is treated using separators to remove mercury before it enters in the low temperature separation unit. Later, the stream is then passed through the cold boxes for cooling. The outlet stream from the cold box is flashed and further chilled in the expander before it finally enters as a top feed in the demethanizer column. The demethanizer is designed to produce an overhead methane vapor stream and a bottom liquid product NGLs. The overhead methane vapor from the demethanizer is compressed and used to cool the overhead vapor stream from the pretreatment section. The methane vapor stream is then sent to the sales gas compression section for a recompression process. The resulting methane vapor produced from this section is sold as sales gas in the market.

The bottom liquid from the demethanizer column is sent to the product recovery unit. This section is well known for its energy intensive process due to its high utility requirement for the separation [6]. It consists of a number of fractionation columns to produce the desired products. The fractionation step takes the advantage of difference in volatility of various hydrocarbons for separation. The fractionators usually contain trays with overflow weirs and downcomers. Reflux from the top of the tower flows across the top tray, into the downer, then across the next tray. The vapor passes up through the tower holes in the trays. In this manner, the vapor and liquid phases are thoroughly contacted, allowing the components to vaporize and condense easily and accomplished the desired separation. The products produced from this section include, ethane from deethanizer column, propane from depropanizer column, butane and condensate from debutanizer column.

1.3 Operational issues in GPP

Changes in feed flow rate and composition are normally expected in a real plant [7]. The feed streams in a gas processing plant originate from upstream production facilities. These facilities may be remote and in turn take their feed directly from gas reservoirs or crude stabilization units [8]. As a result, the plant is usually subjected to variations in upstream conditions such as, feed flow rate and composition, pipeline pressure and ambient temperature [9]. An important requirement in a gas processing plant is that for the process to be flexible to accommodate for a range feed flow rates and compositions which vary from time to time [10]. A sample of different types of feed taken from a real plant operation is shown in Table 1.1.

Table 1.1 Typical natural gas feeds used in gas processing plant

Feed types	1	2	3	4	5	6
Temperature, °C	243.878	129.846	199.155	175.129	183.593	156.672
Pressure, kPa	6707.710	6956.647	6647.088	6878.301	6791.521	7012.446
Flowrate (ton/h)	356.670	345.499	332.810	290.954	297.682	347.691
Composition (Mole %)						
C ₁	81.271	77.768	75.676	71.942	66.569	48.251
C ₂	7.394	7.821	7.197	11.015	13.523	22.142
C ₃	3.460	3.810	2.989	5.362	6.754	12.180
iC ₄	0.794	0.875	0.630	0.966	1.154	1.551
nC ₄	0.728	0.877	0.638	0.944	1.080	1.538
iC ₅	0.247	0.341	0.229	0.411	0.488	0.751
nC ₅	0.185	0.173	0.136	0.225	0.287	0.384
C ₆₊	0.264	0.323	0.153	0.438	0.511	0.767
N ₂	0.364	0.509	0.546	0.396	0.429	0.221
CO ₂	5.289	7.499	11.802	8.295	9.200	12.210

From Table 1.1 in the above, the temperature, pressure, flow rate and compositions for the different types of feeds vary hourly. The feeds generally can be classified as lean and rich based on the compositional value of C₂ and C₃. If the C₂ content of the feed is greater than 10 percent or the C₃ content greater than 4 percent, the feed is considered as rich. Otherwise the feeds are taken as lean. Based on this, the

first three feeds (Feed 1-3) in Table 1.1 are classified under lean feeds, while the latter three feeds (Feed 4-6) are considered as rich feeds.

In order to reduce the effect of the variation in feed composition, different operating mode has been practiced in gas processing plant. Most of the previous works to handle such uncertainty focus on lay out of the sequences from the process design aspect [10, 11]. For instance, for the plant to operate in ethane rejection mode, it follows a different process scheme from the normal mode of operation. Similarly, for ethane recovery, another process scheme is preferred to improve the production level. However, the majority of the time that process engineers spend is not on the design part, but trying to make the existing process work. Hence, the major problem for a process engineer is to address on how to make the process become feasible under such uncertain conditions.

At the plant outlet, some of the compositions of the products have also uncertain product requirements. The plant may seek to maximize the revenue by boosting the production level based on the market conditions. However, due to the competitive nature of the market environment for some of the products, there exist certain restrictions on reliability of meeting the product requirements and quality specification. Due to this, gas processing plant operators want to know long term specifications for the quality of the product to be delivered to their customers. For example, the C_3 and C_{4s} content in propane and butane products may vary depending on the customer's specification. Sometimes, it may be also advantageous to produce liquefied petroleum gas (LPG) based on the market outlook. During such situations, the plant may be operated using the depropanizer column only and the debutanizer column may be shut down for energy saving. As a result, the amount of C_3 and C_{4s} in the LPG may also have different specification. Hence, the need to make an optimal decision under such uncertainty is a major issue which needs to be addressed well.

On the other hand, the continuous variation in operating conditions may aggravate the instability of the plant operation [12, 13]. In industrial practice, such variations are usually handled using trial and error methods. However, this would increase the workload of plant engineers by spending more time in fine tuning the plant. Furthermore, the utility flow to the plant is also another factor which can significantly

affect the plant performance. Hence, it is clearly vital for process engineers to be able to quantify the ability of the plant to be operated feasibly in the presence of uncertainties and to have systematic methods for the plant operation that are both economically optimal and flexible [14].

1.4 Process optimization

Process optimization is a systematic method to determine the most effective and efficient solution to a process problem while meeting all possible operational and design constraints. It is a well known quantitative tool to aid decision making in industries. A wide variety of problems in design, operations, and analysis of industrial processes can be resolved by optimization. A process can be represented by mathematical equations developed from physical principles or experimental data. If a single performance criterion is set, such as maximizing profit, then the goal of process optimization is to find the values of the variables in the process that yield the best value of the performance criterion.

In process operations, benefits arise from improved plant performance such as higher yields of valuable products, lower energy consumption, higher production rates, and longer operation times between shutdowns. However, this requires a critical analysis of the process operation in order to obtain useful information. The process operation can be represented by developing an appropriate mathematical model. The developed model represents “the essence” of reality that captures the behavior of the plant operation [15]. If the mathematical model is well developed, then the solution obtained from the model should also be the solution to the system problem. Thus, the effectiveness of the results of the application of any optimization technique is largely a function of the degree to which the model represents the system studied. The major optimization techniques can be classified as deterministic and optimization under uncertainty. These two optimization approaches will be discussed below.

1.4.1 Deterministic programming

Most conventional process models nowadays in use are largely based on a deterministic framework. The goal of a classical deterministic optimization problem is to determine the values of decision variables that maximize some aspect of the model [16]. The body of the optimization model consists of objective function and constraints. The generalized iterative solution procedure for this classical deterministic optimization problem is illustrated schematically in Fig. 1.4. The model simulates the flow sheet and calculates values for the decision variable as well as values of the objective function and constraints. The information is then utilized by the optimizer to calculate a new set of decision variables. This iterative sequence is continued until the optimization criteria are satisfied.

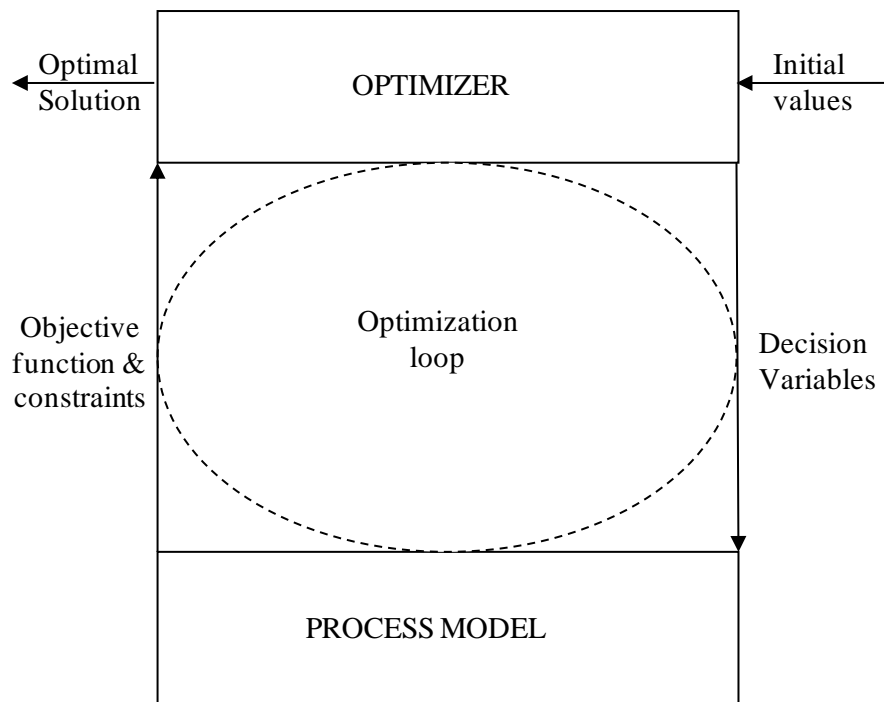


Fig 1.4: Deterministic optimization framework

A number of studies on gas processing plant optimization have also used this deterministic approach. Most of these works have been applied for the turbo-expander section of the plant such as the works in Bandoni et al. [17], Fernández et al. [18], Diaz et al. [19-21], Gomes and Wolf-Maciel [22], and Bullin and Hall [23]. In deterministic approach, the expected values of the uncertain parameters are usually

employed to hold the constraints. However, in reality, the uncertain parameters will deviate from their expected values. As a result, constraint violation may occur and finally the solution becomes not only non-optimal but also infeasible [24, 25]. Such kinds of decisions are usually referred as aggressive decisions. On the other hand, few works have also been done using the “worst case” strategy such as Eliceche et al. [26] and Diaz et al. [9]. In “worst case” approach, the uncertain parameters are expressed in terms of the minimum and maximum displacement from their nominal values. This solution strategy may be very helpful in holding the process constraints; however, the achievable profit will be drastically decreased [27]. Such kind of decisions is referred as conservative decisions.

In some works, the uncertain parameters are provided by specific bounds such as the works by Grossmann and Sargent [28], Grossmann and Halemane [29], and Varvarezos et al. [30]. Most of these works have been used for process design problems under uncertainty. Sometimes, it is also common to couple the uncertain parameters with feasibility test such as the works in Halemane and Grossmann [31] and flexibility index by Swaney and Grossmann [32, 33], Grossmann and Floudas [34], Pistikopoulos and Grossmann [35-37], and Varvarezos et al. [38]. However, there still exist possibilities for violation of constraint to occur since the uncertain parameters are not considered as a continuous variable. In addition, most of these works may not guarantee the optimal profit value by comprising the reliability of holding the process constraints. Furthermore, the optimal solution from such kind of approaches may probably lead to either a conservative or aggressive decision.

1.4.2 Optimization under uncertainty

The optimization techniques used in dealing with uncertainty can be categorized as stochastic programming and fuzzy programming [39]. Stochastic programming also consists of two-stage programming with recourse formulation and probabilistic or chance constrained programming as discussed in the following sections.

1.4.2.1 Fuzzy programming

In fuzzy programming approach, fuzzy numbers are defined on a fuzzy set to represent uncertain parameters in a model. In this approach, some constraint violation is allowed and the degree of satisfaction of a constraint is defined as the membership function of the constraint [40]. Even though fuzzy programming approach gives a better solution compared to the deterministic approach, it has still some limitations compared to stochastic programming.

The main difference between fuzzy programming and stochastic programming is in the way that the uncertainty is modeled. Fuzzy programming considers random parameters as fuzzy numbers and constraints are treated as fuzzy sets [41]. In addition, Liu & Sahinidis [42] have conducted the comparison of fuzzy programming and stochastic programming. Accordingly, fuzzy programming is easier to solve but stochastic programming provides a more rigorous means of solving the optimization problem.

1.4.2.2 Two-stage programming

In two-stage programming approach, the first stage variables are to be decided before the realization of the uncertain variables. Subsequently, the second-stage variables are used as corrective measures or as recourse against any infeasibilities arising during the realization of the uncertainty. In this approach, the random data are represented through a set of discrete outcomes called scenarios with a probability that represent their importance in the overall problem.

One of the limitations of this approach is that the iteration between the first and the second stage variables requires expensive computational effort especially when the size of the problem becomes large [24]. In addition, violation of constraint is allowed but compensated using a penalty term in the objective function. However, the solution with the compensation provides no obvious information on the relation between profitability and reliability of the process which are very crucial in decision making purpose. Some of the works using this method includes the one by Liu and Sahinidis [42], Paules and Floudas [43], Pistikopoulos and Ierapetritou [44], Ahmed

and Sahinidis [45], Gupta and Maranas [46], Rooney and Biegler [47], and Khor et al. [48].

1.4.2.3 Chance-constrained programming

Chance-constrained programming is another stochastic approach which becomes a very competitive tool for optimization under uncertainty [24]. It ensures not only the optimality and flexibility of the plant operation but also the reliability of the process by satisfying the constraints at certain probability or confidence level. The method was initially introduced by Charnes and Copper [49] and later modified by Miller and Wagner [50], Prékopa [51, 52], and Kall and Wallace [53]. The application has been widely used in different disciplines for optimization under uncertainty [54]. In process system engineering, however, very few works can be found using chance constrained programming where most of the applications are limited to theoretical basis such as Schwarm and Nikolau [55], Li et al. [24, 27, 56-58], Wendt et al. [59], Henrion and Möller [60], Arellano-Garcia and Wendt [61].

Li et al. [24] have reported their recent development in the works of chance constrained programming. The authors have extended and employed the method to deal with optimization problems under uncertain operating conditions as well as model parameters. The solution strategy is to relax the probabilistic problem into an equivalent deterministic problem so that it can be solved using the available commercial software routines. The main challenge in solving chance constrained programming is however the computation of the probability and its derivatives of satisfying the inequality constraint. As the number of uncertain variables increases, multivariate integration is required to compute the probability value. Moreover, the probability computation also needs to be developed on a computer program unless there is an available function already built in the software routines. However, some approximation approaches can be used alternatively to represent the probability computation numerically. For gas processing plant, in which, the operation of the plant is challenged with a number of uncertain conditions, the application of this method has a significant importance in dealing with those uncertain variables.

1.5 Problem statement

The increasing uncertainty, complexity and size of process models pose a constant challenge in today's research environment. Up to now, works regarding to gas processing plant operations under uncertain conditions are seldom reported. In reality, however, the variation in feed conditions, product requirement, operating conditions and utility flows are highly uncertain. Developing an efficient optimization method to solve such operational problems related to uncertainty is one of the major issues usually raised by process engineers. In industrial practice, heuristic optimization approach based on trial and error are employed to solve those problems. The main reason for such kind of decision is due to lack of system analysis of the objective functions as well as the reliability of holding the process constraints. As a result, sometimes, aggressive decision may be preferred due to high profit expectation. However, this strategy will deteriorate the objective function and later leads to constraints violation. Therefore, a systematic method is required to evaluate the trade-off between profitability and reliability of holding the process constraints. This requires an efficient optimization approach which incorporates the stochastic description of the uncertain parameters and guarantees the flexibility of the plant operation.

1.6 Research objectives

This thesis combines probabilistic analysis with optimization to solve major problems related with the operation of a gas processing plant. The proposed method represents an original effort to apply chance constrained programming to a real gas processing plant. In this thesis, a probabilistic optimization solution approach is developed, which is also applicable to any other plant. The importance of the problem can be measured by a number of literatures that exists on this topic. The main motivation in this work is that the possibilities of obtaining optimal profit by taking into account the reliability of the process under such uncertain condition. This thesis not only builds upon the existing literatures, but also introduces original method and models not used before to solve those problems. Thus, the objectives of the research are:

- To introduce a solution method for gas processing plant operation that is capable of quantifying the ability of the plant to be operated feasibly in the presence of uncertainties by incorporating all the stochastic description.
- To find the optimum trade-off between the reliability and profitability of the plant which are very crucial in decision making purpose.
- To implement a solution strategy that can provide as guidelines for flexible decision making purpose in plant operations.

To achieve the aforementioned objectives, a rigorous HYSYS [62] model for the whole plant operation has been developed to study parameter and plant performance. All the optimization models have been built on a computer program using GAMS (general algebraic modeling system) [63]. Thus, the main contributions of the work reported in this thesis are:

- Most of the previous works for gas processing plant optimization have used deterministic approach. However, this does not match with reality since it involves an arbitrary approximation for the uncertain parameters. Thus, instead of using such deterministic approach, the proposed model determines the optimal solution probabilistically by using chance constraints. The constraints are held at specified probability level using a user-defined parameter called confidence level. For each of the user-defined confidence level, the corresponding values of the uncertain parameter are obtained from probabilistic analysis using statistical data measurements. The decision maker can take the risk level based on the priority between the profitability and reliability holding the process constraints.
- For other optimization approaches used in gas processing plant, such as “worst case” in which the value of the uncertain parameter is statistically displaced by a certain level, the solution approach developed in this thesis proves by how far that such kind of decisions can significantly affect the economic performance of the plant. In addition, unlike the two-stage programming where the uncertain parameters are considered as a discrete variable, the solution approach developed in this thesis treats the uncertain variable to be

continuous. This can better reflect reality since the uncertain variables are continuously varying from time to time.

- Most of the chance constrained programming approaches that exist in process system engineering are based on theoretical applications. Moreover, the objective function is considered as deterministic optimization without considering the cost evaluation for the uncertain variables. However, this also significantly affects the economic performance of the plant. Hence, the evaluation should incorporate both objective function and constraints, which are the main body of the optimization problem. In this thesis, the cost emulation for the uncertain variables in the objective function has been considered.
- Most of the previous researches on gas processing plant focus on layout the process in sequence in order to solve problems related with uncertain parameters. Even though it is possible to find many structural organizations from the design aspect, a robust decision is required for the plant engineers to overcome those problems using a systematic approach in order to ensure the feasible operation of the plant as well as its flexibility under such circumstances. Thus, in this work, a solution method is introduced which can guarantee not only the optimal operation of the plant but also its flexibility by accommodating any variation that arises from external factors.
- An investigation has been made to observe the effect of each uncertain feed and product components by employing the method developed in this thesis. This is also very important especially to identify those components which can significantly affect the overall plant performance. In addition, the use of LPG column also has been introduced for the plant to shift load when there is a high market demand for LPG product. This has not been investigated before and the results of this research prove in finding the optimal decisions to generate a high profit for the plant.

1.7 Scope of the research

This research mainly focuses on introducing a solution method to a gas processing plant under uncertain: a) feed conditions; b) product requirements; and c) operating conditions and utility flows. The developed approach uses statistical data measurements from a real plant for a steady state operation instead of using or approximated values of the uncertain parameters. The data have been analyzed and used in the case study part to test the performance of the developed method. Generally, the findings from this research ought to be able to demonstrate the usefulness of the method in determining the optimal operation of the plant by considering not only the profitability but also the reliability of the process constraints.

1.8 Overview of the thesis

Chapter 2 provides extensive review on uncertainty and their consideration during optimization in chemical process plant. It also presents previous works in gas processing plant both from design aspect and optimization approaches.

Chapter3 presents the solution approach developed in this thesis. The chapter discusses on the formulation of deterministic and their corresponding chance constrained models used for gas processing plant.

Chapter 4 considers three case studies from a real plant operation. The first case study focuses on the uncertainty of the feeds from the plant inlet. The second case study discusses for the uncertainty of the products from the plant outlet. The third case study presents on uncertain utility and energy product flows.

Chapter 5 summarizes by discussing on the main finding and conclusions made from the research. The chapter also discusses about the future research direction suggested in this thesis.

CHAPTER 2

LITERATURE REVIEW

This chapter can be treated in to three main sections. The first section focuses on a review for uncertainty and optimization in chemical process plants. This includes the sources of uncertainties in chemical process plant and their analysis, sampling and sensitivity approach. In addition, it also presents a review on how these uncertainties are considered during optimization. The second section discusses on related works on gas processing plant which has been addressed before. Here, the review focuses on the different process scheme options and various optimization algorithms applied for gas processing plant to solve the existing problem. Finally, the third section summarizes the chapter by discussing the main issues from the previous sections.

2.1 Uncertainty in chemical process plant

In industrial practice, there are always uncertainties due to variations in design conditions, loading and material properties, physical dimensions and operating conditions. Due to the multivariate and correlated stochastic sequences, these uncertainties or disturbances have a significant influence like a chain effect to each unit operation of the production line. The common practice to avoid these uncertainties is by first considering the nominal values of the uncertain parameters and then applying empirical overdesign factors to the solution obtained. However, such kinds of corrections are somehow arbitrary and hence may lead to an infeasible and non-optimal solution.

Several approaches have also been proposed based on optimization formulations to address uncertainties in process design. In these approaches, the uncertain parameters are described using a probability distribution functions and the problem design is formulated based on the probabilistic decision criterions. The solution obtained from the optimization represents the best decision in the face of actual knowledge available

about the process. Other approaches have also been developed to incorporate operational issues such as process flexibility and robustness as well as controllability. The process flexibility is based on the ability of the plant to operate feasibly under variable inputs. The robustness of the process is measured on how the plant responds to the variable inputs with relatively invariable outputs. The controllability of the plant refers to the ability of the plant to respond efficiently to the disturbances of the input variables.

In addition, issues related to decision theory to reduce the effect of uncertainty has also been addressed. In terms of applications, the optimization under uncertainty tools initially developed for process synthesis and design problems have also been extended to other process system engineering problems, such as process planning, design and operation of batch processes and product design. The following section discusses the sources of and classification of uncertainties and their analysis and how they are incorporated in the optimization problem by reviewing previous works.

2.1.1 Uncertainty sources and classifications

From process operation point of view, the sources of uncertainty may be internal such as inaccurate model parameter or external such as unknown future feed stock. From the context of process system engineering, Ierapetritou et al. [64] categorized the different uncertainty that involved in process models as follows:

- i)* Model-inherent uncertainty: this includes kinetic constants, physical properties and transfer coefficients. Information regarding to such uncertainty is obtained from experimental or pilot scale data. The uncertainty is described either in a range of possible realizations or some approximation of probability distribution function. As a result, the model may not be able to predict the actual process [65]. Furthermore, process models developed by considering such uncertainties are usually an approximation and thus can not describe the real behaviours of the process exactly [66].

- ii)* Process-inherent uncertainty: this consists of flowrate, composition, temperature, pressure variations as well as product specifications, stream quality fluctuations and so on. Such uncertainties are usually described by probability distributions obtained from on-line measurements of the uncertain parameters. The realization of these uncertain parameters for any desired range could in principle be achieved through the implementation of a suitable control scheme [67].

- iii)* External uncertainty: this includes uncertainties beyond the production process such as feed stream availability, product demands, prices and environmental conditions. In addition, the outlet stream from an upstream unit and the recycle stream from a downstream unit are also considered as external uncertain parameters [12]. Usually, forecasting techniques based on historical data, customers orders and market indicators are used to obtain approximate ranges of uncertainty levels or the corresponding probability distribution.

- iv)* Discrete uncertainty: this is mostly used to describe equipment availability and other random discrete events. The probability distribution function of such uncertain parameters commonly obtained from available data and manufacturers' specifications [67].

Another classification can also be made by considering the uncertain time dependence in the future horizon. Thus, the representation of the uncertainty is an important modelling question and in order to reduce it to a negligible level, a complex modelling effort is required. The developed approach in this thesis concentrates on those of process inherent and external uncertainties.

2.1.2 Uncertainty analysis and sampling

Uncertainty analysis describes the propagation of uncertainty in model parameters and model structure to obtain reliable information for the risk. Such analysis also offers quantitative measures of the strengths of certain relationships between the uncertain

parameter and the predicted output result. The sampling approach is usually used to obtain a representative values from the parameter space frequently. This is especially used when performing uncertainty analysis of regression models. The main objective is to acquire a reliable result for the output distribution of the parameter analyzed. A number of works have been well discussed on the properties of uncertainty analysis and sampling. A comprehensive review has been presented below.

Maranas [68] studied a systematic method that quantitatively assesses the property prediction of uncertainty on optimal molecular design problems. Accordingly, the uncertainty has been explicitly quantified using multivariate probability distribution functions for modeling the different realizations of the group contribution of the parameters. The author has indicated the property predictions of the uncertainty which have a profound effect in optimal molecular design problems. Furthermore, the performance of the objectives, probability of meeting the objectives as well as the chances of satisfying design specifications offers a systematic guideline for optimal molecular design problems with respect to the property prediction of uncertainty.

Vasquez and Whiting [69] used a Monte Carlo sampling (MCS) technique to separate and study the effects of systematic and random errors in thermodynamic data for chemical process design and simulation. Accordingly, the authors pointed out the presence of systematic errors in thermodynamic data. Based on this, for the systematic error analysis, the data were perturbed systematically with a rectangular probability distribution. For analyzing the random errors, the perturbation was carried out randomly with normal probability distributions. Later, thermodynamic models were obtained from the appropriate regression methods. These parameters were used to simulate for a given unit operation as well as to obtain cumulative frequency distributions. In addition, the parameters provide a quantitative risk assessment and better understanding of the role uncertainty in process design and simulation. Even though Monte Carlo sampling techniques is most commonly used and easy to employ, it requires numerous model evaluations for accurate results. As a result, it may not be efficient for sampling a large number of input uncertainty factors.

Vasquez and Whiting [70] also introduced a new approach called equality probability sampling (EPS) for analyzing uncertainty and sensitivity analysis in thermodynamic models. Accordingly, the EPS method produces more realistic results in uncertainty analysis than methods based on other sampling techniques such as Latin hypercube sampling (LHS) or shifted Hammersley sampling (SHS). This is especially when the parameters are highly correlated. However, when the parameters are uncorrelated, EPS will reduce to the LHS method. The developed EPS can be extended to any regression model for various physical applications. It can be used also as a better tool for estimating more reliable safety factors in design and simulation of chemical process. Even if the EPS method performs better than LHS and SHS, there is no explanation presented for which distribution that the method is more efficient. For example, there are times where the Hammersley sequence sampling (HSS) proposed by Diwekar and Kalagnanam [71] exhibits a high efficiency for uncertainty analysis and optimization under uncertainty.

Tayal and Diwekar [72] presented a novel sampling approach for stochastic optimization which incorporates property-prediction uncertainty effects in a robust generalized optimization framework. Accordingly, the authors have addressed a detailed analysis of uncertainty using a number of case studies for various issues in computer-aided molecular design under uncertainty. Sensitivity analysis of uncertainties for the model parameters was also made to identify the uncertainty effect. In addition, the wider applications of solving problems involving various forms of uncertainties have been discussed. The results from the case studies indicate how the property-prediction uncertainty can significantly impact the optimal molecular designs.

Ulas and Diwekar [73] studied the unsteady state nature of a batch distillation unit. The authors addressed the importance of optimal control in batch distillation which allows optimizing the column operating policy by selecting a trajectory for the reflux ratio. However, due to the uncertainties in thermodynamic models, the reflux ratio obtained is often suboptimal. Hence, the authors have proposed a general approach to handle both dynamic and static uncertainties in thermodynamics for more complex non-ideal systems. Based on this, the unsteady state nature of batch distillation translates these static uncertainties into time-dependent uncertainties.

Moreover, the authors pointed out the uncertainty effect of the relative volatility which was previously considered as a deterministic parameter. However, more work is required to address on how these time-dependent uncertainties can be handled during optimization. Other related works on uncertainty analysis can be found in Diwekar and Rubin [74, 75], TØrvi and Hetzberg [76], Phenix et al. [77], Terwiesch et al. [78], Whiting [79], Saltelli et al. [80] and Diwekar [16].

2.1.3 Uncertainty and optimization

A number of works have discussed on how to incorporate uncertainties during optimization. The techniques mainly differ in a way of handling the sources of uncertainty or solving the resulting problem. A comprehensive review of uncertainties and optimization has been presented below.

Grossmann et al. [81] developed optimization strategies for flexible chemical processes. The optimization strategies are mainly used for designing chemical processes. Accordingly, for steady state operations, the feasible region ensures the existence of optimal solution exposed to parameter variations. Based on this, two major areas were considered. The first area discusses on optimal design with fixed degree flexibility whereas the second area presents for design with optimal degree flexibility. However, the major challenge in this problem still lies in the development of efficient solution procedures for large scale nonlinear programs. Moreover, for attaining the feasible solution, the economic performance may significantly be affected and hence the solution leads to a conservative decision.

Pistikopoulos and Grossmann [36] addressed on determining minimum cost modifications for redesigning existing process flowsheet. Accordingly, the authors developed a novel computational strategy for nonlinear models. The proposed method relies on the iterative solution of an optimal design formulation which features as a relaxed constraint of the feasibility function for the specified region of flexibility. The method has been applied for models that are bilinear in the uncertain parameters and control variables. On the other hand, Pistikopoulos and Grossmann [37] reported on establishing trade-off between investment costs for retrofit and expected revenue that

results from increasing flexibility in systems described by nonlinear models. Based on this, a procedure has been proposed for cost vs flexibility curve. Later, a stochastic optimization has been presented for evaluating the expected optimal revenue with the specified degree of flexibility. This can allow one to identify the level of flexibility that maximizes the expected profit in a retrofit design. However, in both of the flexibility works, the uncertain parameters are not considered as a continuous variable, still defined with a certain specific bound. Flexibility may be achieved, but it does not show to how much extent that this flexibility affect the economic performance. Hence, such kind of solution approach may also leads to a conservative decision.

Pistikopoulos and Ierapetritou [44] presented theoretical developments on a novel approach for optimization of design models under uncertain parameters. Based on this, the authors studied the general probability distribution functions which describe process uncertainty and variations. Later, the problem was formulated with two-stage programming in which the objective was to determine the design that maximizes profit by simultaneously measuring design feasibility. Uncertainty in process design and operations has been addressed also by Pistikopoulos [82]. The work here mainly focuses on process formulating process optimization problems by linking together various components such as characterization and quantification of uncertainty. Similarly, other works can be found related to process design and operations under uncertainty such as Dantzig [83], Wellons and Reklaitis [84], Shah and Pantelides [85], Straub and Grossmann [86], Ierapetritou and Pistikopoulos [87], Petkov and Maranas [88].

On the other hand, some works have also been reported on process planning problems under demand uncertainties. Ahmed and Sahinidis [45] have used two-stage programming approach for robust planning problems under uncertainty. Accordingly, the authors introduced a robustness measure that penalizes second-stage costs that are above the expected cost. Gupta and Maranas [46] have also used a two-stage programming for incorporating demand uncertainty for a multisite midterm supply-chain planning problems. The authors have developed a bi-level decision-making framework. Based on this, the first production decisions are made ‘here and now’ prior to realization of the uncertainty. However, the uncertain supply-chain decisions

are postponed in a ‘wait and see’ mode. Even though two-stage programming approach is more suitable for planning problems under uncertain product demand, one of the disadvantages is that it requires a penalty function to describe the relation between the constraint violation and the achievable profit. Moreover, some of these penalty functions are not usually available in practice. Hence, in such situations, it is usually not preferred to compensate for violation of constraints using additional cost; however, to maintain a high level of reliability to satisfy the constraints with a probability exceeding some pre-selected value [67].

Based on this, some other methods have been developed to keep the reliability of the constraints. Prékopa [52] proposed an efficient approach for linear systems which consists of stochastic variables with correlated multivariate normal distribution. The proposed approach combines both numerical integration and sampling techniques. The chance constraints during optimization are computed using sampling techniques. However, the disadvantage of the sampling approach is that it requires a lot of effort on optimizing when the approximation is not accurate [89]. In most stochastic optimization problems also, the main bottleneck is the computational time spent on evaluating the objective function and the probabilistic constraints especially for correlated uncertain variables. In addition, the accuracy of estimate for the mean and standard deviation is important to obtain a realistic value for the economic performance criteria. However, such accuracy also depends on the number of samples and uncertain parameters taken. For optimization problems, the number of samples by itself depends on the location of a trial point in the solution space [67]. Kim and Diwekar [90] have developed a combinatorial optimization algorithm that can automatically select the number of samples and provides a trade-off between accuracy and efficiency.

Sahinidis [40] provided an extensive review for optimization problems under demand uncertainty. The author has discussed on a large number of problems in production planning, scheduling and other applications for decision making in the presence of uncertainty. Accordingly, the author argued that a key difficulty in optimization under uncertainty is in dealing with an uncertainty space which is huge and frequently leads to a very large-scale optimization models. Furthermore, the authors have also discussed and contrast the different types of optimization used

under uncertainty. Applications and state-of-the-art in computations have also been presented. Another review on process scheduling under uncertainty has also been presented by Li and Ierapetritou [41]. The authors here described uncertainty as a major concern which can cause infeasibilities and production disturbances. Based on this, the uncertainties have been analyzed and discussed with the different mathematical approaches that exist to describe the process uncertainties.

Verderame et al. [91] recently presented a review for planning and scheduling problems with specific emphasis on the effect of uncertainty. Here, the authors argued that even if the objectives and physical constraints present in the problem formulation may vary greatly from one sector to another; however, all the problems share a common attribute for modeling parameter uncertainty in an explicit manner. Other related works regarding process planning under uncertainties have been presented in the works of Subrahmanyam et al. [92], Ierapetritou and Pistikopoulos [93], Ierapetritou et al. [94], Liu and Sahinidis [42], Clay and Grossmann [95], Acevedo and Pistikopoulos [96], Gupta and Maranas [97], Chufu et al. [98], Papageorgiou [99], Verderame and Floudas [100], Verderame et al. [101].

2.2 Process scheme options and optimization algorithms in GPP

Uncertainties are major issues in chemical process plant as discussed earlier. In gas processing industries, a number of process scheme options have also been proposed to improve the overall plant performance. Most of these process scheme options have arisen to allow more rigorous optimization variables such as operational flexibility, CO₂ tolerance and capital and operating cost. Based on this, the selection of the optimum process scheme depends on conditions and compositions of the inlet gas, cost of fuel and energy, product specifications and relative product values [102]. On the other hand, a number of optimization algorithms have also been developed for gas process plant. However, most of these optimizations concentrate on improving the existing plant performance rather than incorporating the uncertainty effect. In the following sections, a comprehensive review for the different process scheme alternatives and optimization algorithms applied in gas processing plant has been discussed below.

2.2.1 Gas plant process scheme options

Technology trends in gas processing industries have emerged since early 1900's. During those times, heavier hydrocarbons from natural gas streams are removed by compression and cooling methods. However, a number of changes have been made after that to improve the process efficiency which contributes to the incentive for high recoveries of the desired products from the plant such as refrigerated oil-absorption [103]. A major leap in gas processing technologies was the recovery of NGL in 1970 using a turbo-expander plant as shown in Fig. 2.1. Accordingly, the inlet gas is first treated to remove water and contaminants. The stream is then cooled and flashed before it enters to the demethanizer column. The top vapor from the demethanizer column is then compressed to sales gas after cooling using the inlet gas. Even though turbo-expander process scheme has a major break-through in gas processing industries, it has certain limitation in terms of the operational flexibility and overall recovery performance. As a result, a number process schemes have emerged after that and the comprehensive review of these process schemes has been presented below.

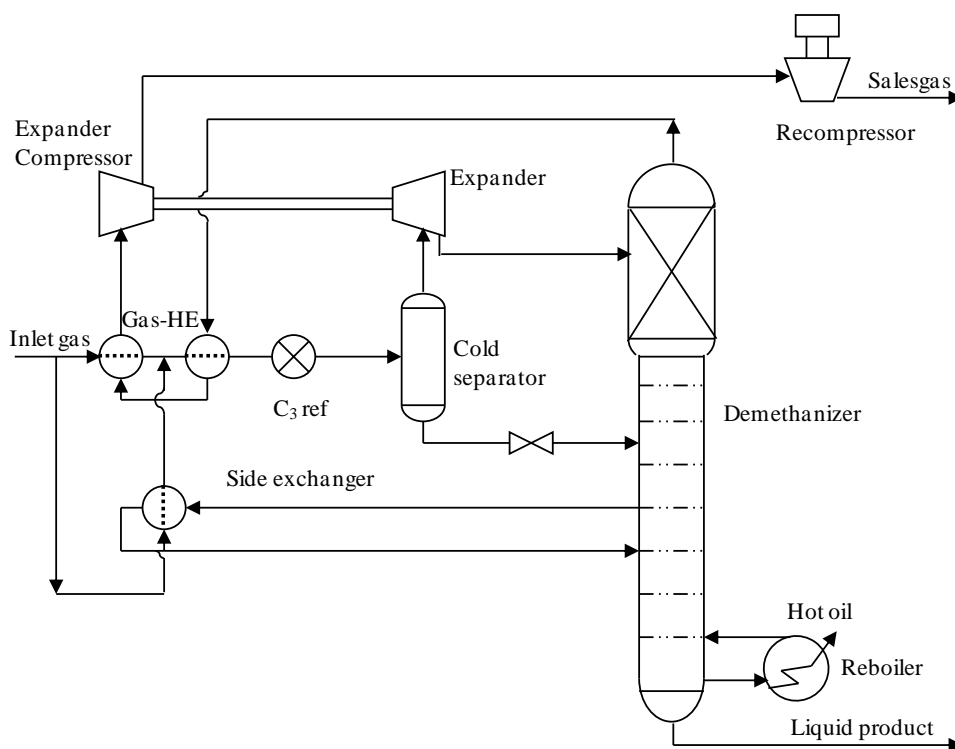


Fig 2.1: The 1970-vintage turbo-expander process scheme

Campbell and Wilkinson [104] introduced the gas sub-cooled process (GSP) scheme for high NGL recovery as shown in Fig. 2.2. Such process scheme has also been implemented at the PETRONAS gas GPP-A facilities in Malaysia by Ortloff Company [105]. The process uses the novel-split-vapor concept where a small portion of the non-condensed vapor as top reflux is introduced to the demethanizer after a substantial condensation and sub-cooling. As a result, it reduces the compression horsepower requirements and the risk of CO₂ freezing. Even though the GSP can be operated to reject ethane, propane recovery efficiency suffers significantly when operated in this mode. This is mainly due to the higher concentration of propane present in the top feed.

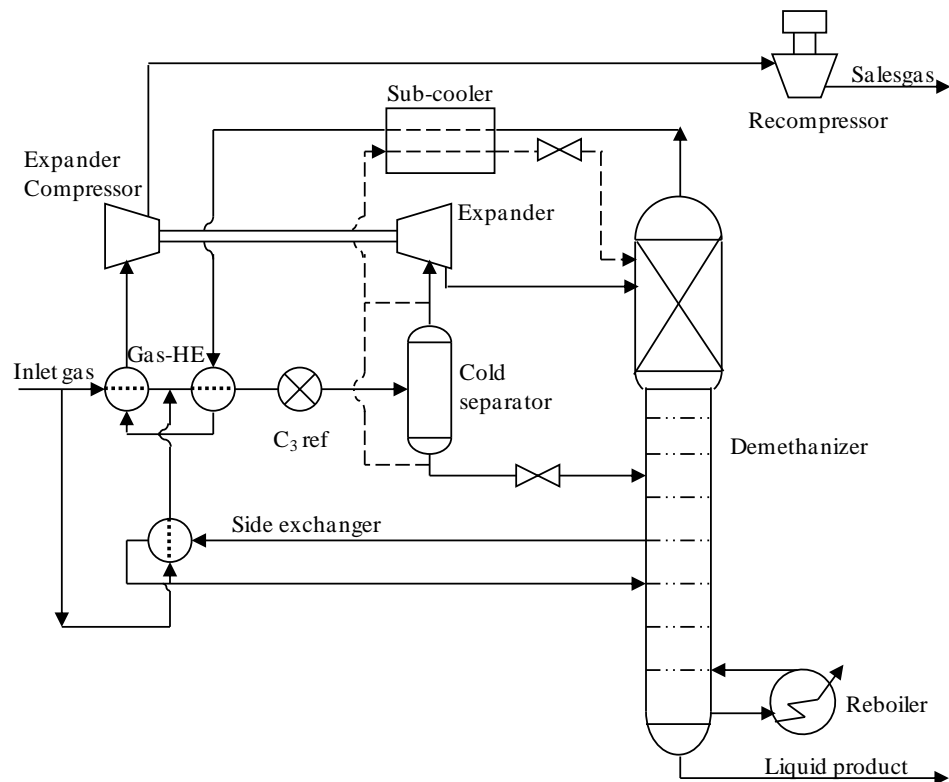


Fig 2.2: The gas sub-cooled process scheme

Buck [106] proposed an overhead-recycle process (OHR) scheme to improve propane recovery as shown in Fig. 2.3. In this process, the overhead vapor from the de-ethanizer column is condensed and recycled to the top of the demethanizer. This scheme is typically employed in a two-column arrangement with the de-methanizer comprising only the rectification section like an absorber. The absorber bottoms liquid

is pumped to the top the de-ethanizer. This process provides more efficient recovery of propane and heavier hydrocarbons than the GSP scheme. However, this process scheme is not suitable for high ethane recovery.

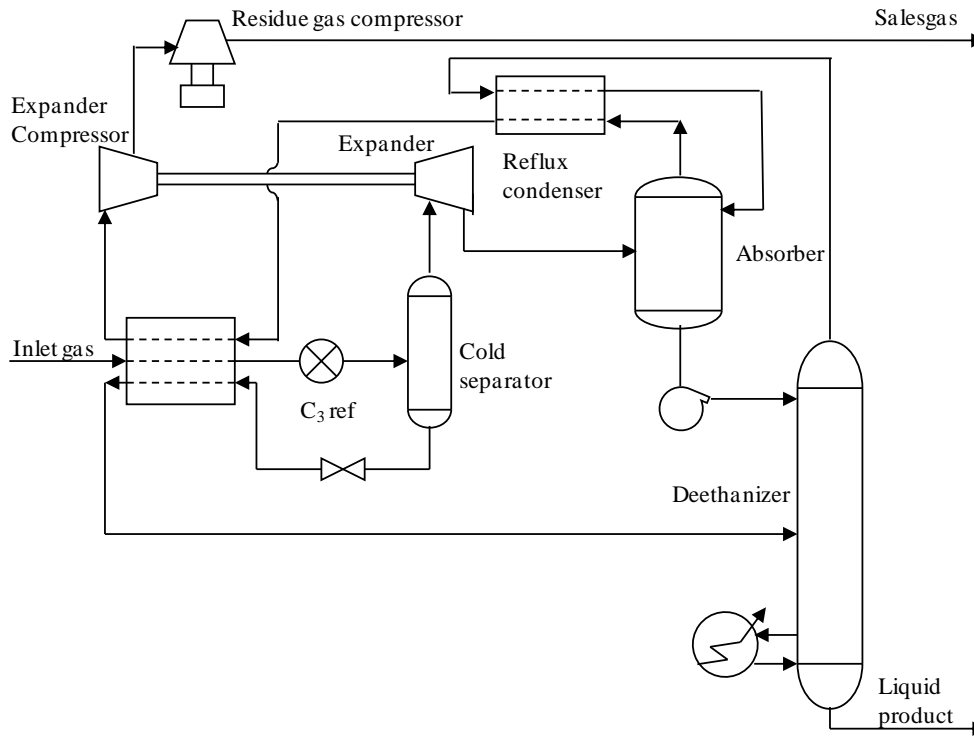


Fig 2.3: Deethanizer overhead recycle process scheme

Montgomery [107] introduced a cold residue gas-recycle (CRR) process scheme as shown in Fig. 2.4. Both the previous GSP and OHR process are limited by the capability of the split vapor concept to overcome the equilibrium limitations. Based on this, the CRR scheme uses recycling a portion of residue gas as a top reflux to the demethanizer column. As a result, a very high ethane recovery, in excess of 98%, is economically achievable with the CRR process. However, the cryogenic compressor can be very expensive. Later, a recycle split-vapor process (RSV) which requires less capital investment has been stated by Campbell et al. [108]. A modification of the RSV process, which is the recycle split-vapor with enrichment process (RSVE), has also been introduced by Campbell et al. [109]. In this scheme, the recycle stream is withdrawn from the recompressed residue gas and mixed with a split vapor feed before being condensed. As a result, it can avoid a separate exchanger or exchanger passage.

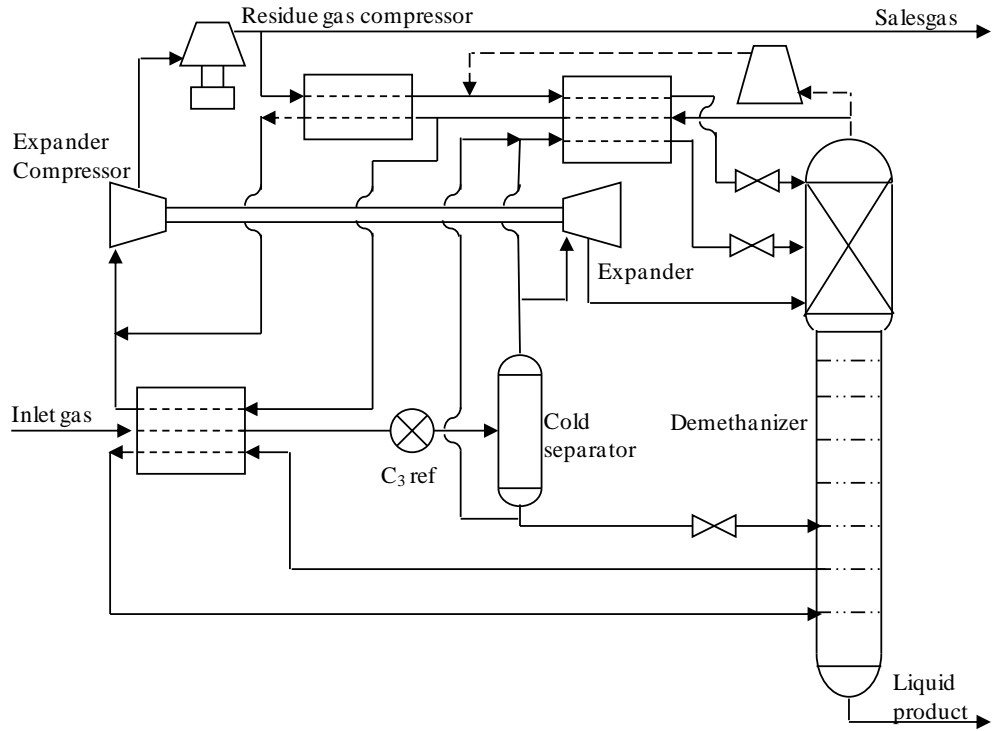


Fig 2.4: Cold residue recycles process scheme

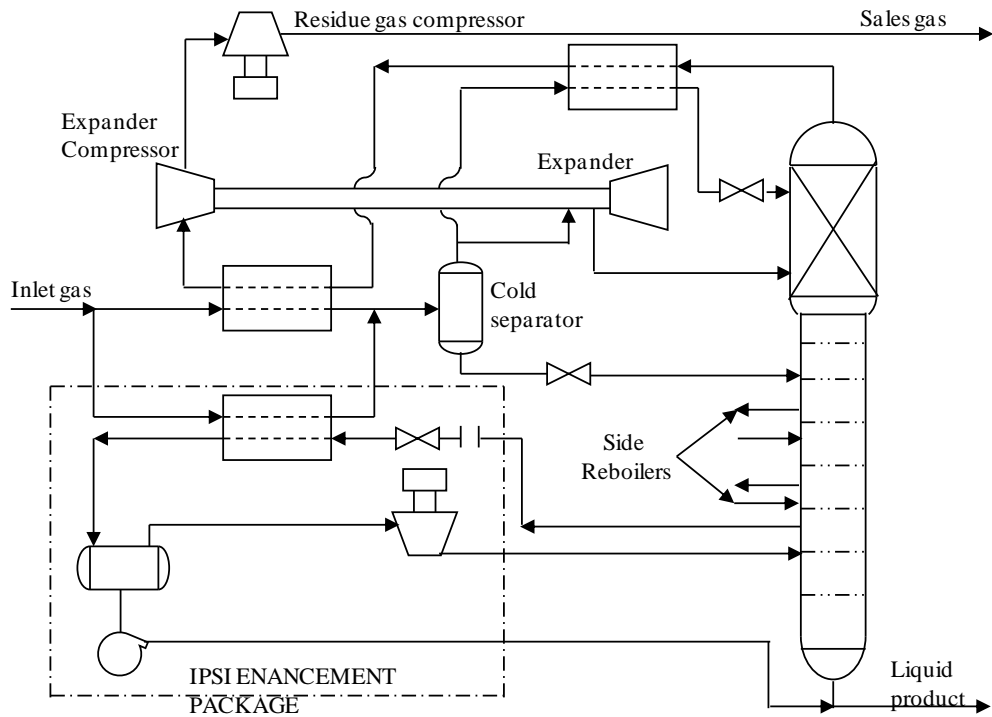


Fig 2.5: Enhanced NGL recovery process scheme

Yao et al. [110] introduced an enhanced NGL recovery process (IPSI scheme) a shown in Fig. 2.5. The GSP, OHR, CRR, RSV and RSVE process schemes mainly focus on improving the reflux stream to the demethanizer column. However, IPSI scheme gives a process enhancement that focuses on the bottom of the demethanizer column. It utilizes a slipstream from or near the bottom of the tower as a mixed refrigerant stream. The stream is used to cool the inlet gas, thereby reducing or eliminating the need for propane refrigeration. The vapor portion is then recycled back to the bottom of the tower where it serves as stripping gas. One of the limitations with the IPSI process scheme package is that when the plant capacity increases, it requires additional refrigeration to maintain NGL recovery level. Hence, more recompression and additional reboiler duty are also required to retrofit the existing process scheme. However, this can be achieved using a stripping gas refrigeration system which replaces the conventional refrigeration system with a self refrigeration system as reported in the works of Bai et al. [111].

Aggarwal and Singh [11] studied on how processing conditions and product specification affect the best method to recover NGLs. Accordingly, the authors pointed out important factors that can influence the selection of processing scheme used for NGLs. These factors includes: product recovery and separation requirements, amount of heavier components in the feed, flexibility to process feed with varying composition, feed gas availability at NGL plant battery limit, pressure requirement for the sales gas, carbon dioxide content in the feed gas as well as in ethane product. The authors pointed out that whenever there is a frequent feed composition changes from the plant inlet, it is advantageous to use a combination of different process schemes such as turbo-compression/expansion and mechanical refrigeration. This combination helps to compensate the increase in the heavier component (C_{5+}) concentrations by raising the feed gas refrigeration duty and vice versa. However, such combination requires careful design specifications which should recognize the temperature limits achievable by refrigeration.

Mehrpooya et al. [112] proposed a new process configuration for recovery of hydrocarbon liquids from natural gas. The refrigeration required in this configuration is achieved by a self-refrigeration system, which is open-closed cycle. The authors have pointed out the most important characteristic of the proposed configuration.

Accordingly, high performance of multi-stream heat exchangers, high recovery levels of the hydrocarbon liquids and low required compression power. The authors have also investigated for various feed composition and argued that the process can work efficiently with different feeds. Furthermore, in order to analyze the need of external refrigeration by a close or open cycle related to the composition of the inlet gas, another configuration with external refrigeration has been designed. In fact, it may be possible to overcome the variation of feed composition by employing different process scheme or configuration. However, from operational aspect, the implementation such process scheme has to be considered carefully. In addition, it should also be studied for the main parameters which can significantly affect the plant performance. Furthermore, such types of configuration may also require additional equipment to be installed, which may also increases the capital cost of the plant. Other related works on process scheme options can be found in the works of Campbell and Wilkinson [113], Wilkinson and Hudson [114], Pitman et al. [115], Lee et al. [116, 117], Hudson et al. [118], and Jibril et al. [10].

2.2.2 Gas plant optimizations algorithms

While most of the previous works focus to improve the overall plant performance using various process schemes, there were also some efforts put to overcome those problems using different optimization techniques. During the 1980's, many optimization projects were implemented successfully in non-gas processing industries such as Rhemann et al. [119], Sourander et al. [120] and White [121]. These projects simulated a variety of processes using correlation-based models with the objective to reduce computational time. Early plant optimization techniques reduced large problems into a series of smaller and more manageable problems that were solved using graphical or slide techniques [122]. As computer speed increased, the trend shifted to using large models based upon the fundamental underlying chemical and physical phenomena to predict the plant performance [123].

In gas processing plant, different optimization approaches have also been implemented since 1985. The different types optimization algorithms used in gas processing plant can be categorized into seven. These are statistical method, equation-

based method, model predictive control, sequential modular simulation technique, simulator response modeling technique and Genetic algorithm, and Taguchi method. A comprehensive review of these approaches has been presented below.

2.2.2.1 Statistical method

In statistical method, a large quantity of plant data are usually employed for plant optimization, inventory management, advanced process control and regulatory control purposes. Sometimes, an adaptation of factorial statistics is used to analyze data and compute a set of operating parameters based on the variance from the controlled sampling set [124]. Later, the controlled samples set are used to reference economic conditions and determine the current plant profitability. The technique includes also both primary and cross term interactions in the variance calculations. Based on this, the factorial approach is capable of evaluating the dependencies and interdependencies parameters.

The advantage of statistical approach is that it can adapt and build with the history database [122]. However, difficulties may arise in distinguishing interactive effects between control variables and the fact that majority of the plant data also may appear within a narrow range of operating point. Furthermore, it may be difficult also on screening large sets of data to identify measurement errors and unsteady state operations.

2.2.2.2 Equation based method

In case of equation based approach, the process models which represent the fundamental chemical and physical phenomena of thermodynamics and unit operations is rearranged with the plant economics as follows:

$$H(Y) = 0 \quad (2-1)$$

In the above equation, H is an m dimensional vector of equations, while Y is an n dimensional vector of variable. It should be noted that during optimization $m \neq n$.

Equation (2.1) can be alternatively expressed using the known general mass balance equation as follows:

$$\text{mass flow out} - \text{mass flow in} - \text{generation} + \text{consumption} + \text{accumulation} = 0 \quad (2-2)$$

Equation (2.2) can be solved using Newton's method, which is usually used for solution of equation-based models [123, 125]. Accordingly, a first order Taylor's series expansion is developed around the current value of Y and the resulting linear system is solved as:

$$Y_{n+1} = Y_n - \lambda_s J_n^{-1} H(Y_n) \quad (2-2)$$

where Y_n is the current value of Y , Y_{n+1} is the new value of Y , and J_n is the Jacobian matrix of the first derivatives of the function H with respect to the variable Y evaluated at Y_n . The parameter λ_s is the line search parameter. Equation based approach may have several advantages. One of the unique advantages of this method is that the ability to solve the entire system of process equations at one time by eliminating the need for repeated convergence loops. The other advantage is that its high accuracy and capable of representing any process or economic scenario. However, the main disadvantage is the complexity associated with large scale optimization problem in which the iteration may take longer time and may not give also an optimal solution. Some of the works have been discussed below.

Wang [126] presented the application of equation based approach in which a systematic search is carried out on optimum processing conditions for a turbo-expansion plant. The simulation result showed that a combination of turbo-expansion and refrigeration leads to minimum energy requirements. Moreover, the author argued that the processing should be carried out at highest practical pressure. However, working at high pressure reduces the expansion ratio in the expander and results the temperature profile to rise in the de-methanizer column by making the heat integration to be difficult. In addition, the definition of the proper process scheme requires a detailed study for each particular case.

In another work, Bandoni et al. [17] simplify the selection process alternatives for extracting ethane and NGL from natural gas based on energy analysis over the cold

section of a gas processing plant. Accordingly, a large number of variables characterize each particular ethane and NGL recovery problem. Some of the key design variables are: inlet pressure, residual gas pressure, liquid gaseous state of the products, recovery levels, feed flow rate, feed composition and average ambient temperature. The simulation of the entire plant was carried out using SIPREQ (process simulator owned by the plant) and the Soave-Redlich-Kwong (SRK) equation of state has been applied for the calculation of thermodynamic properties. However, this may raise a question on the capabilities of the process simulator used. For a reliable simulation, the process simulator should enable the user good flexibility in order to vary the different independent parameters and observe their effects of on the dependent parameters. Process simulator such as, HYSYS and ASPEN PLUS offers a high degree of flexibility since they have multiple ways to accomplish specific tasks. Furthermore, the selection of the fluid package is also another factor which highly contributes on the results of the entire simulation. For instance, effects of pressure and temperature may drastically alter the accuracy of the simulation. However, HYSYS can quickly view and change the particular parameter associated with any of the property package.

Gomes and Wolf-Maciel [22] developed a methodology to make a simulation to be possible to reproduce and optimize the operating conditions of natural gas processing unit. The unit process used was refrigerated absorption, which is studied for its energetic optimization and the reduction of absorption oil molecular weight. The simulation was built with the help of commercial software HYSIM [127]. The methodology developed was based up on O'Connell correlation [128] which helps to incorporate column stage efficiencies and to bring near the column internal flows and temperatures to the real values. Thus using optimization, the authors proposed to reduce the molecular weight of the absorption oil to approach to the molecular weight of natural gasoline (C_{5+}). The possible reduction of the fuel gas was found to be 30.7% and 5.8% savings in total power consumption. It was also argued that using Pinch technology it is possible to economize fuel gas consumption by 16.4%. However, the use of oil absorption may not successfully recover the required ethane and propane amounts and it is one of the early technologies used before. In addition,

using the empirical O'Connell correlations requires a repetitive iteration in order to calculate the tower efficiency.

2.2.2.3 Model predictive control

The application of computer-based multivariable control was first applied to natural gas processing plant by Cutler and Ramaker [129]. Perino and Moran [130] has also discussed the most popular multivariable control approaches based on dynamic linear models, matrix mathematics and linear programming. The method developed incorporates the dynamic behavioral models of the plant based upon plant reactions to a series of step or impulse perturbations of significant control variables. This was achieved by setting all the process controlled variables to a particular value and allowing the plant to reach steady state. After the steady state condition has been achieved, one of the control variables at a time is perturbed and the output response is recorded as a function of time.

Most of the time, model predictive control methods include economics on three levels (lowest, intermediate and top). The lowest economic model uses only linear economic terms with respect to the manipulated variables in the objective function. The objective function is also constrained with maximum and minimum value of the controlled and manipulated variables. Thus, the technique may give the multivariable controller a high degree of robustness and permits the multivariable controllers to handle a large combination of process conditions. It also provides the economic solution when the feed costs, utility costs, and product flow rates are known [122, 131]. The intermediate level of economic modeling rests up on top of the lower level based up on reduced order process modeling and reduced-order economics. This level of modeling may have nonlinear parameters. As a result, it is slightly more sophisticated than linear equations compared to the lower level. However, it still retains the simplicity, speed and robustness of reduced order model. The top level of economic modeling resides above all the other levels and is based upon rigorous and first-principles modeling of both the process and economics.

Some of the drawbacks of the first-principle model include difficulties associated with equation-based models, such as poor convergence, slow execution and distinguishing infeasible or trivial solutions. In addition, plants with simple economics can realize the majority of the optimization benefits using only a low level economic modeling. It is obvious that gas plant with complex economic conditions may receive increased revenue with each level modeling. However, the increased revenue is offset by the rising implementation and software costs due to the complexity of the model and by other unexpected problems associated with the solution of more difficult problems.

2.2.2.4 Sequential modular simulation technique

The sequential modular simulation technique uses first principles modeling approach to predict the behavior of the process units. It combines the material and energy balances, complex thermodynamic relationships between components, and equipment specific information in order to predict plant performance. The method begins from the plant inlet and follows the material flows throughout the plant in such a way that when a unit operation is encountered, the sequential modular approach simulates its performance and predicts the conditions of the stream(s) leaving the unit. This procedure continues until the entire plant is simulated.

Economic optimization using sequential modular simulation techniques provides advantages of high model accuracy and flexibility for extrapolating to new scenarios. The main advantage of this method over equation based approach is that it can avoid the problems associated with solving large systems. In addition, caution must be taken with online-steady-state simulation models since it has got convergence problems. As a result, it may not yield a sensible answer. Furthermore, operating in the gas processor's time frame of a few minutes requires steady state operation to be reached and adding considerable expense as well as complexity [130]. Some of the works which uses this optimization algorithm have been presented below (most of the works have been made by Diaz et al. [9, 19-21]).

In the works of Diaz et al. [19], mixed integer nonlinear programming (MINLP) model was used for debottlenecking problem in an ethane extraction plant from natural gas. The plant is based on a turbo-expansion process at cryogenic temperatures. Accordingly, the low temperatures associated to the process require proper consideration of CO₂ contents in natural gas. Equipment capacities and the conditions of CO₂ precipitation in the demethanizer are handled as constraints for the optimization problem, while the main continuous optimization variables are directly related to actual plant's manipulated variables. The optimization program used was an extension of the outer approximation algorithm [132, 133] to directly interface a simulator. They found out that ethane recovery can be increased from 80% to 92% in the structural and operative optimum. The algorithm they used normally requires successive solutions of NLP sub-problems followed by MILP problems. However, the feasible region and the objective function for a maximization problem are overestimated. Even though the algorithm guarantees convergence to global optimum for convex problem, outer approximations may cut off parts of the feasible region and converge to locally optimal solutions for non-convex problems.

Some improvements have been made also by Diaz et al. [20]. The authors have extended their previous model Diaz et al. [19] to rigorously represent the compression and separation areas. In the improved work, a superstructure model is proposed which includes the cryogenic sector of turbo-expansion processes. The model was formulated as MINLP problem where continuous optimization variables are related to operating conditions and binary variables represent discrete decisions. The plant mathematical model constitute the set of nonlinear equation and solved using "ad-hoc" simulator. The process specifications and bounds on equipment capacities were handled as nonlinear constraints. Unlike their previous work [19] which mainly focuses on the cryogenic sector to maximize production, a rigorous simulation model for turbo-expander together with the introduction of new optimization and process variables has been presented. Even if they used the algorithm for a real plant application and reached convergence in small number of iteration, it still has go a limitation to achieve global optimum convergence for non-convex problem.

In a later work, Diaz et al. [21] presented a strategy for process configuration design and debottlenecking of natural gas processing plant based on turbo-expansion.

The approach they used combines a rigorous process simulation model for the cryogenic sector and a mixed-integer nonlinear programming (MINLP) optimization methodology that embeds different expansion alternatives within a superstructure. A wide range of natural gas mixtures with 6-25% of condensable components (C_{5+}) has been studied in order to determine the optimal plant topology and operating parameters under different process conditions. The inlet feed gases by varying CO_2 content are also be analyzed to evaluate the impact on plant design and operation. Accordingly, they stated that proper design and operating conditions for different inlet feed compositions can be automatically determined by means of the proposed design strategy. The implementation of the outer approximation algorithms performs better than the previous algorithm especially when the current operating point is selected as initial point for the MINLP problem. At this time, the first MILP problem of the outer approximation algorithm already determines the best configuration and the entire MINLP problem converges in two major iterations. It should be highlighted that with the limitation of the outer approximation, optimization algorithm built with rigorous simulations packages may also have solution difficulty when the plant conditions changes automatically.

In their next work, Diaz et al. [9] addressed a flexibility study on natural gas processing plant through the integration of a process simulator to a “worst-case” flexibility strategy. The plant consists of a gas sub-cooled turbo-expansion design, which is suitable for working in dual operation mode. The two modes of operations are ethane production or ethane rejection for propane production. Four uncertain parameters comprising feed flow rate, condensable hydrocarbons content, carbon dioxide content, and ambient temperature based on the impact which brings to the process operating conditions. The authors assumed that well-defined upper, lower and nominal values for the uncertain parameters are available.

The solution strategy in Diaz et al. [9] comprises of two-level of optimizations. The first level is the outer optimization where a fixed value of the uncertain parameters usually assigned to nominal or average value. The second level is the inner optimization which assumes the optimization variables to be fixed at the optimal value of the outer level optimization. In the inner optimization level, the largest violation of constraint is obtained by maximizing each single inequality constraint

over the uncertain parameters. Thus, the constraints that are violated at this level are added as a new constraint at the outer level problem, and the sequence of outer and inner sub-problems is repeated in an iterative way. The algorithm stops when no constraint violation is determined at the inner level, and the current solution of the previous outer loop represents a point that remains feasible if the uncertain parameter realization lies inside the specified bounds. In terms of performance, the algorithm is robust but requires large computational time. The computational time may be reduced to great extent by using KS aggregation function [134]. However, the problem needs to be solved several times. Moreover, fixing the uncertain parameter at their nominal value may result to aggressive decision. As a result, there will be a high possibility for violation of constraint to occur.

2.2.2.5 Simulator response surface modeling technique

Response surface modeling technique explores the relationships between several explanatory variables and one or more response variables. Several statistical designs are available to minimize the number of data points required to solve models of a given order. Response surface modeling techniques are usually preferred to identify the detailed dependence of different factors on a response using a full quadratic model. Accordingly, the full quadratic model for two factors x_1 and x_2 can be represented as:

$$Response = \ell_0 + \ell_1 x_1 + \ell_2 x_2 + \ell_3 x_1 x_2 + \ell_4 x_1^2 + \ell_5 x_2^2 + error \quad (2-4)$$

where ℓ represents constants and x is a continuous optimization variable. This modeling technique has been used by Bullin [122] for gas processing plant optimization by correlating the key process variables with the residue composition using a rigorous process simulator. Accordingly, the two types of modeling designs which are effective for residue stream modeling are: central composite designs and Box-Behnken designs as shown in Fig. 2.6 and 2.7.

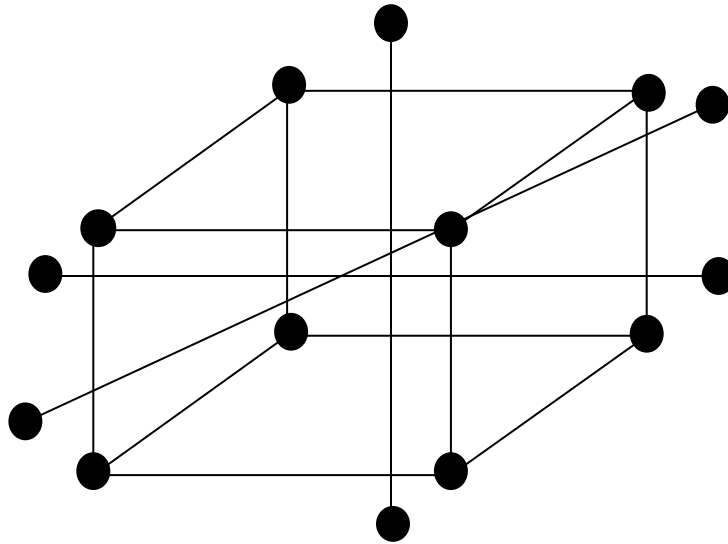


Fig 2.6: Three factor inscribed central composite design [122]

According to the significant adjustable process variables, one of the response modeling designs is selected. A central composite design is selected if the plant operation of the adjustable variables is near the corners of the constraints on normal operation. The box-Behnken design is chosen if the process variables are predominantly in the middle of normal operating ranges.

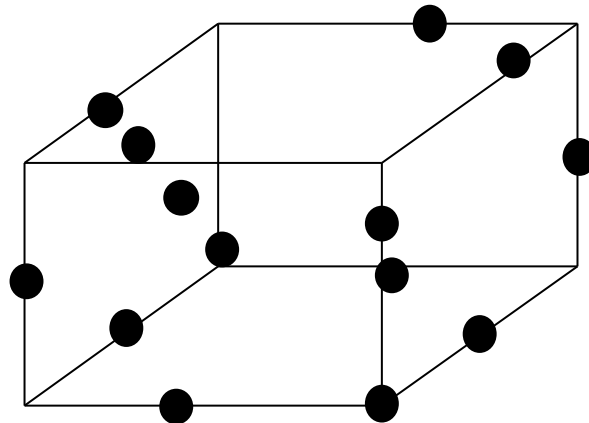


Fig 2.7: Three factor box-Behnken design [122]

Upon selection of the modeling design, rigorous simulation of the plant is performed for each set of the process variables. Parameters are suggested by response surface modeling design. The mole fraction of carbon dioxide, ethane, and propane in the residue stream are the desired outputs of the simulation run. The simulation results are correlated to relate the mole fractions to the process using coefficient of multiple

determination of R^2 . The value of R^2 is always increases with the additions of coefficients. However, for a given number of variables, the R^2 statistic can identify the best fit. The adjusted R^2 value is related to the standard R^2 as follows:

$$R_{ADJ}^2 = 1 - \frac{(n_d - 1)}{(n_d - p_m)} (1 - R^2) \quad (2-5)$$

where n_d is the number of data points and p_m is the number of parameter in the model. The adjusted R^2 value is equivalent to searching for the model with lowest mean square error. Even though the methodology developed by Bullin [122] yields a fast and reliable model of gas processing plant by maintaining simplicity, small errors are incorporated into the process model because of the absence of purely rigorous model. Furthermore, the process model also requires a moderate amount of work initially for model creation and verification.

2.2.2.6 Metaheuristic algorithms

Metaheuristic algorithms are based on nature-inspired or bio-inspired since the algorithms are developed based on the successful evolutionary behavior of natural systems [135]. Modern metaheuristic algorithms used in engineering application includes genetic algorithms (GA), simulated annealing (SA), particle swarm optimization (PSO), ant colony algorithm, bee algorithm, tabu search (TS), harmony search (HS), firefly algorithm (FA) and many others. Some of the optimization algorithms among these have also been applied for gas processing plant. These works are discussed below.

The genetic algorithm is based on the process of Darwin's theory of evolution. By starting with a set of potential solutions and changing them during several iterations, the GA hopes to converge on the most 'fit' solution. The process begins with a set of potential solutions or chromosomes (usually in the form of bit strings) that are randomly generated or selected. The entire set of these chromosomes comprises a population. The chromosomes evolve during several iterations or generations. New

generations or offspring are generated using techniques such as crossover and mutation.

Mehrpooya et al. [136] applied the genetic algorithm method to perform a parametric optimization for NGL recovery plant. Accordingly, they determined the optimum operating conditions, in which the objective function was based on cost analysis. In addition, different turbo-expansion processes were analyzed and the best flow sheet was selected based on capital analysis and operating limitations. The authors found that the best revamping alternative was the turbo-expander exchanger process, which was selected among external refrigeration, Joule-Thompson expansion, and absorption processes. The profit for the optimum solution has increased by 28%. The GA developed uses HYSYS simulation program to evaluate the objective function. The MATLAB program is also linked with HYSYS for optimization purpose as shown in Fig. 2.8. During the optimization process, the data switch between these two softwares (HYSYS and MATLAB). Eventually, the information is transferred to the GA. Once, the ranges of values of the independent variables are defined, the values of parameters of the genetic algorithm were varied to achieve optimum fitness value or to verify to a good approximation. Consequently, the value obtained is a global maximum in the defined fields of variables.

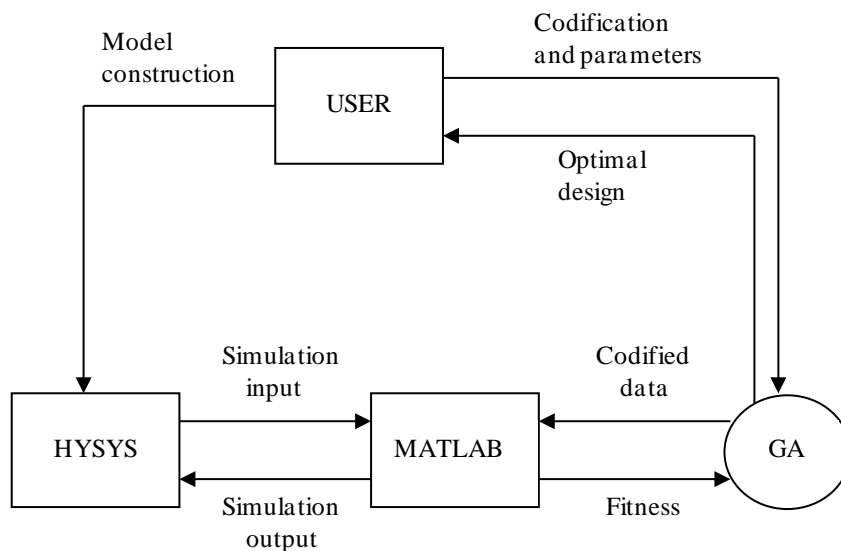


Fig 2.8: Implemented architecture GA algorithm [133]

The advantage of GA is that it works well during global optimization especially with poorly behaved objective functions such as those with discontinuous or multiple extreme points. The disadvantages of GA includes computational problem in which it takes longer time by comparing the results to get the best one. In addition, it is also difficult to predict the required number of generations for obtaining a solution within a certain level of accuracy. This may result to an excessive computational burden. Other related works can also be found in Wang et al. [137, 138] and Jang et al. [139].

The other metaheuristic approach which is recently applied to GPP is tabu search (TS). Tabu search uses a local search procedure to iteratively move from one solution to another in the local area until some stopping criteria has been satisfied. Hence, it modifies the local structure of each solution as the search progresses. The works by Aspelund et al. [140] used a tabu search technique together with the Nelder-Mead Downhill simplex (NMDS) method. The authors argued that the local search usually converges faster to the best solution in the area when the TS is used with NMDS than by itself. The developed approach has been applied to find the total refrigerant flow rate, composition, refrigerant suction and condenser pressures that minimize the energy requirements of a Prico process (a simple LNG process).

The optimization tool used consists of a combined TS and NMDS which are connected to a process simulator Aspen HYSYS via Microsoft Excel using Visual basic for applications (VBA). It is observed that the majority of the time spent during computation is in running the simulation compared to running the search algorithm. Hence, the Visual basic (VBA) is very important in terms of the surrounding layer since it can provide the necessary means to get access to the component object model (COM) functionality of HYSYS. The Microsoft Excel is used in such a way that it can include the input data, the TS and NMDS settings and numerical as well as graphical results. The VBA routine consists of the HYSYS simulation and the error handling which helps to calculate the objective value. On each cycle run, all the corresponding values are given to HYSYS and this continues until it converges. Later, some of the calculated values are retrieved and the feasibility status is checked to utilize the information for obtaining a single objective value.

The advantage of TS relative to other metaheuristic approaches such as GA and SA is that it can escape the local minima. The GA and SA depend on random numbers to go from one local minimum to another. However, the TS uses history or memory for such kind of moves and hence can be considered as a learning process. One of the shortcomings of this approach is that the algorithm does not guarantee to find optimum solution. This is due to the fact that the search uses only one solution which can easily miss some promising areas in the search space, and hence a larger set of parallel solutions does not exchange information [141].

2.2.2.7 Taguchi method

Taguchi method is a systematic parametric design approach used for optimization of various parameters with respect to performance, quality and cost. In most recent works, it is commonly used for design of experiment, signal-to-noise ratio (SNR), analysis of means (ANOM) and analysis of variance (ANOVA) for accomplishing different objectives such as to identify and rate optimization variables under various disturbances. In addition, it is also used to determine optimum configuration of optimization and disturbance variables. Furthermore, it can also be used to estimate and validate the maximum profit with the specified constraints [142, 143]. The most recent work applied to a refrigerated gas plant (RGP) has been discussed below.

Yusoff et al. [143] presented a systematic procedure for selecting optimization variables in a refrigerated gas plant using Taguchi method. Accordingly, a dynamic RGP model has been developed under HYSYS environment, which can be used as a test bed. Based on this, nine variables with three levels each are employed for optimizing RGP profit. The optimization variables are selected due to their significance as manipulated variables to control the process. The optimal configuration of the optimization and manipulated variables were then validated. The results obtained from HYSYS simulations shows a good agreement with analysis of means (ANOM).

The advantage of Taguchi method is that it can allow for analysis of many different parameters without prohibiting a large number of experimentation. Thus,

the key parameters that have the most effect on the performance characteristic value can be identified. As a result, further experimentation on those variables can be performed and those parameters which have little effect can be ignored [144]. The main disadvantage of Taguchi method is that the results obtained from experimentation are relative. Hence, it does not exactly signify which parameter has the highest effect on the performance characteristic value. Taguchi method has also been criticized in literatures for its difficulty to describe interactions between parameters. In addition, it may be applied at the early stage of process development, but after the design variables are specified, it will be less cost effective to use it.

2.3 Summary

As it has been discussed in this chapter, uncertainty is an inherent characteristic of any chemical process plant. However, handling of such uncertainties especially in the presence of operational constraints using more advanced approaches have not been addressed well. Thus, uncertainty is usually considered as the main bottleneck in applying optimization techniques for a real chemical process plant.

A number of different process schemes in gas process plant have been employed in order to tackle the variation of main process parameters such as feed composition and flow rates. Based on this, there have been a number of significant achievements made in improving the overall plant efficiency. However, handling the variation in process condition by altering different process schemes may not be preferred as the best option to overcome those uncertainties. This is due to some of the process scheme options may require the plant to be shut down for revamping stage. In addition, it may also require additional equipments to be installed, which also increases the capital cost of the plant.

The optimization algorithms developed in gas processing plant mostly based on deterministic approach as shown in Table 2.1, which mainly targets the economic objective function rather than considering the uncertainty effect. However, question might be raised also about the operability and reliability of the process which are more crucial than the economic objective function. Moreover, the process engineers

need to control the whole plant by implementing a systematic approach to handle any variations that arise from both external and internal factors. Thus, implementing such a solution technique substantially helps to avoid any conservative and aggressive decision for the plant performance.

Table 2.1: Classification of all gas plant optimization algorithms

Gas plant optimization algorithm types	Optimization classification
Statistical method	Deterministic programming
Equation-based method	Deterministic programming
Model predictive control	Deterministic programming
Sequential modular simulation technique	Deterministic Programming /“worst case”/
Simulator response modeling technique	Deterministic Programming
Genetic algorithm	Stochastic Programming
Taguchi method	Deterministic Programming

CHAPTER 3

DEVELOPMENT OF CHANCE-CONSTRAINED OPTIMIZATION METHOD FOR GPP

This chapter presents a detailed discussion of the solution method proposed for gas processing plant optimization. The chapter starts by defining some of the preliminary terms in chance constrained optimizations. Later, identifying and representing all the inflows and outflows in a gas processing plant. Based on this, a deterministic formulation is initially established as a basis. The corresponding probabilistic model is then formulated by incorporating the stochastic formulation of the uncertain variables. The developed probabilistic model is then relaxed to their equivalent deterministic form so as to be solved with the available commercial optimization routines. Finally, a summary of the developed approach is provided at the end of the chapter.

3.1 Preliminary terms

The term chance-constrained or probabilistic programming represents optimization of a function subject to certain conditions where at least one is formulated so that a condition, involving a random variable, should hold with a prescribed probability [52]. The generic representation of an optimization problem under uncertainty can be given as:

$$\min f(s, w, x, \xi)$$

Subject to

$$h(s, w, x, \xi) = 0$$

$$g(s, w, x, \xi) \geq 0$$

$$x_{\min} \leq x \leq x_{\max} \tag{3-1}$$

where the term f represents for the objective function, which is a performance criterion to be optimized. The expressions $(s, w, x, \xi) \subseteq \mathfrak{R}$ represent for differential state, constrained output, optimization and uncertain variables, respectively. The vectors h and g represent for the equality model equation and inequality constraints, respectively. x_{\min} and x_{\max} are the lower and upper bounds for the optimization variable, respectively. In order to convert the above optimization problem in to a general chance constrained problem, it requires a certain steps. Based on equation (3.1), the inequality constraint g can be described using a user-predefined probability level or confidence level α as:

$$\Pr\{g(x, \xi) \geq 0\} \geq \alpha \quad (3-2)$$

where \Pr represent the probability operator. The probability operator \Pr defines the reliability of complying with the inequality constraint g . Here, x and ξ are the decision and uncertain variables, respectively. The value of α is in the range of $0 \leq \alpha \leq 1$. It is possible to choose different levels of α and make a compromise between the objective function value and the constraints. For the output variable w , it is usually a common practice in engineering to restrict using inequality constraint between its maximum and minimum value as:

$$w_j^{\min} \leq w \leq w_j^{\max}, \quad j = 1, \dots, J \quad (3-3)$$

where w_j^{\min} and w_j^{\max} represent the lower and upper bounds for the output variable w , respectively. Such constraints are also employed to ensure safe production operation. Thus, the output constraints in equation (3.3) can be converted to the corresponding single and joint chance constraints as follows:

$$\Pr_j \{w_j^{\min} \leq w(x, \xi) \leq w_j^{\max}\} \geq \alpha_j, \quad j = 1, \dots, J \quad (3-4)$$

$$\Pr \{w_j^{\min} \leq w(x, \xi) \leq w_j^{\max}, j = 1, \dots, J\} \geq \alpha \quad (3-5)$$

In equation (3.4) above, the chance constraint represent single probabilities of ensuring the inequality output variable w . In this constraint, different confidence

levels can be assigned for the different output variable w based on the requirement. For the joint chance constraint shown in equation (3.5), all the inequalities constraints are included in the probability computation and satisfied simultaneously with a certain confidence or probability level. For evaluating the objective function, the expected value and the variance of the objective function have been used [24, 145]:

$$\min E[f(s, w, \xi)] + \omega Var[f(s, w, \xi)] \quad (3-6)$$

where E and Var are operators of expectation and variation, respectively. The letter ω represents a weight factor between the two terms. Based on this, the objective function in equation (3.6) is converted to a deterministic function using the two operators E and Var . Thus, the general single chance constrained problem can be represented as:

$$\min E[f(s, w, \xi)] + \omega Var[f(s, w, \xi)]$$

Subject to

$$h(s, w, x, \xi) = 0$$

$$\Pr_j \{w_j^{\min} \leq w(x, \xi) \leq w_j^{\max}\} \geq \alpha_j, \quad j = 1, \dots, J$$

$$x_{\min} \leq x \leq x_{\max} \quad (3-7)$$

Similarly, the general joint chance constrained problem representation is then given as:

$$\min E[f(s, w, \xi)] + \omega Var[f(s, w, \xi)]$$

Subject to

$$h(s, w, x, \xi) = 0$$

$$\Pr \{w_j^{\min} \leq w(x, \xi) \leq w_j^{\max}, \quad j = 1, \dots, J\} \geq \alpha$$

$$x_{\min} \leq x \leq x_{\max} \quad (3-8)$$

The two types of chance constraints described in equation (3.4) and (3.5) are usually used to classify the different chance constrained problems that appear in

process system engineering [24]. The classification is based on the properties of the process, uncertainty and constraints. Initial letters can be used to denote each problem. For example, Linear Steady-state process with Constant uncertainties under Single chance constraint (LSCS). Alternatively, for a linear Dynamic process with Time- dependent uncertainties under Joint chance constraints (LDTJ). Based on this, the different linear chance constrained problems have been shown in Fig. 3.1.

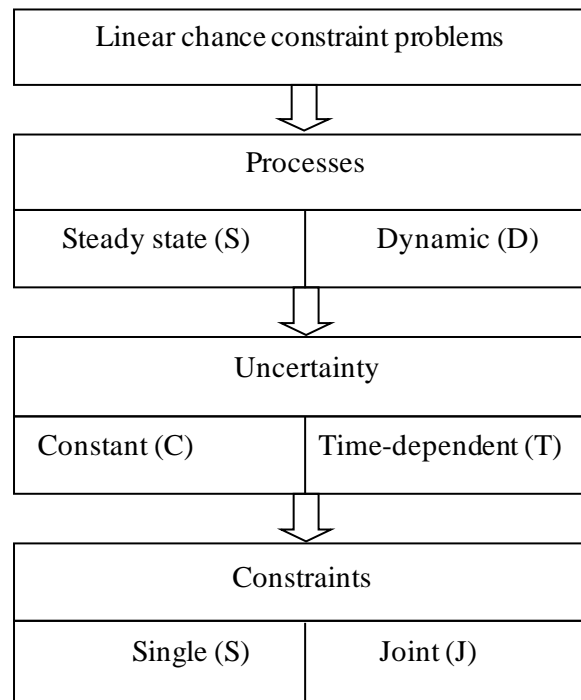


Fig 3.1: Classification of linear chance constrained problems

3.2 Inflows and outflows

A gas processing plant (GPP) produces outflows by processing some inflows as shown in Fig. 3.2. On the plant inlet side, the inflows consist of certain raw materials R as feed streams which may be brought from upstream suppliers. In addition, the inflow also consists of certain utilities U which may be supplied from the nearby cogeneration plant such as, electrical power, heating steam and cooling water. Some of the inflows may be supplied as much as demanded by the GPP. In this case, the inflows are certain and can be decided. However, the supply of other inflows may be

fluctuating due to some degree of uncertainty. These uncertain raw material and utilities inflows are represented as \hat{R} and \hat{U} , respectively.

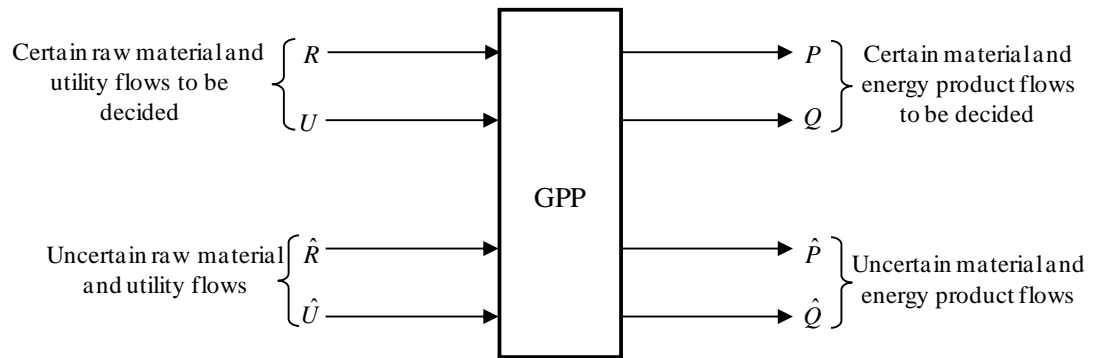


Fig 3.2: A schematic representation for inflows and outflows of GPP

On the plant outlet side, the amount of certain material product P and energy products Q outflows can be treated as decision variables. Additionally, the amount of uncertain material \hat{P} and energy products \hat{Q} outflows may depend on the random demands of the customers. As a result, the demands of those products will become unknown in the future time period. Thus, the material and energy flows are the basic factors that determine the performance of the plant. Moreover, the analysis of both material and energy balances significantly help to optimize the consumption of raw material and energy by pursuing systematically internal flows in the production process. Furthermore, Li et al. [27] argued that a linear mass and energy balance is usually preferred in industrial practice in order to model the internal mass and energy flows. Hence, it is important first to model the inflows and outflows from the plant.

3.3 Modeling material inflow and outflow

The feeds entering to a gas processing plant involve multiple inlet streams that are combined and processed to produce the desired products as shown in Fig. 3.3. The separation of the raw gas into different products is based on the difference in boiling point. Hence, during separations, some of the components are not affected by the variation in process conditions. For instance, the separation in deethanizer column is mainly between ethane and propane. The other components such as methane and

carbon dioxide may exist at some quantities. However, butanes and heavier hydrocarbons possess a small quantity. Based on this, the overall material balance for the whole plant can be reduced into a linear form using the volatility of components and product specifications [23].

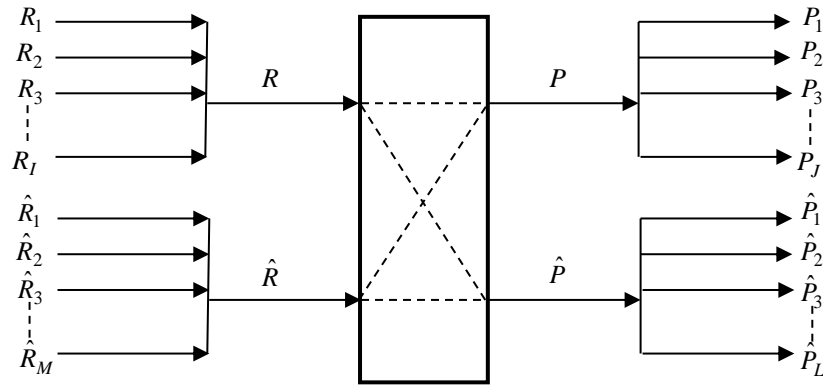


Fig 3.3: A schematic representation for material inflows and outflows of GPP

During steady state operation, the flow rate of component k into the process as a raw material stream is equal to the amount of component k leaving in the product streams:

$$\sum_{j=1}^J a_{k,j} P_j + \sum_{l=1}^L \hat{a}_{k,l} \hat{P}_l = \sum_{i=1}^I b_{k,i} R_i + \sum_{m=1}^M \hat{b}_{k,m} \hat{R}_m \quad (3-9)$$

In equation (3-9), k is the index for components in the raw materials and products. The indices i and j represent for certain raw material and product flows to be decided, respectively. m and l are indices for uncertain raw material and product flows, respectively. The terms $b_{k,i} R_i$ and $\hat{b}_{k,m} \hat{R}_m$ are the mass flow rate of component k for certain and uncertain inlet streams, respectively. Similarly, $a_{k,j} P_j$ and $\hat{a}_{k,l} \hat{P}_l$ are the mass flow rate of component k for certain and uncertain out streams, respectively. The feed and product streams in gas processing plant are expressed in terms of the following components C_1 , C_2 , C_3 , C_{4s} , C_{5+} , N_2 and CO_2 . The material balance equations for these main seven components are shown below:

For $k = 1$, C_1 or methane balance:

$$\underbrace{a_{1,1}P_1 + a_{1,2}P_2 + a_{1,3}P_3 + \dots + a_{1,J}P_J}_{j\text{-index}} + \underbrace{\hat{a}_{1,1}\hat{P}_1 + \hat{a}_{1,2}\hat{P}_2 + \hat{a}_{1,3}\hat{P}_3 + \dots + \hat{a}_{1,L}\hat{P}_L}_{l\text{-index}} = \underbrace{b_{1,1}R_1 + b_{1,2}R_2 + b_{1,3}R_3 + \dots + b_{1,I}R_I}_{i\text{-index}} + \underbrace{\hat{b}_{1,1}\hat{R}_1 + \hat{b}_{1,2}\hat{R}_2 + \hat{b}_{1,3}\hat{R}_3 + \dots + \hat{b}_{1,M}\hat{R}_M}_{m\text{-index}} \quad (3-10)$$

For $k = 2$, C_2 or ethane balance:

$$\underbrace{a_{2,1}P_1 + a_{2,2}P_2 + a_{2,3}P_3 + \dots + a_{2,J}P_J}_{j\text{-index}} + \underbrace{\hat{a}_{2,1}\hat{P}_1 + \hat{a}_{2,2}\hat{P}_2 + \hat{a}_{2,3}\hat{P}_3 + \dots + \hat{a}_{2,L}\hat{P}_L}_{l\text{-index}} = \underbrace{b_{2,1}R_1 + b_{2,2}R_2 + b_{2,3}R_3 + \dots + b_{2,I}R_I}_{i\text{-index}} + \underbrace{\hat{b}_{2,1}\hat{R}_1 + \hat{b}_{2,2}\hat{R}_2 + \hat{b}_{2,3}\hat{R}_3 + \dots + \hat{b}_{2,M}\hat{R}_M}_{m\text{-index}} \quad (3-11)$$

For $k = 3$, C_3 or propane balance:

$$\underbrace{a_{3,1}P_1 + a_{3,2}P_2 + a_{3,3}P_3 + \dots + a_{3,J}P_J}_{j\text{-index}} + \underbrace{\hat{a}_{3,1}\hat{P}_1 + \hat{a}_{3,2}\hat{P}_2 + \hat{a}_{3,3}\hat{P}_3 + \dots + \hat{a}_{3,L}\hat{P}_L}_{l\text{-index}} = \underbrace{b_{3,1}R_1 + b_{3,2}R_2 + b_{3,3}R_3 + \dots + b_{3,I}R_I}_{i\text{-index}} + \underbrace{\hat{b}_{3,1}\hat{R}_1 + \hat{b}_{3,2}\hat{R}_2 + \hat{b}_{3,3}\hat{R}_3 + \dots + \hat{b}_{3,M}\hat{R}_M}_{m\text{-index}} \quad (3-12)$$

For $k = 4$, C_4 or butanes balance:

$$\underbrace{a_{4,1}P_1 + a_{4,2}P_2 + a_{4,3}P_3 + \dots + a_{4,J}P_J}_{j\text{-index}} + \underbrace{\hat{a}_{4,1}\hat{P}_1 + \hat{a}_{4,2}\hat{P}_2 + \hat{a}_{4,3}\hat{P}_3 + \dots + \hat{a}_{4,L}\hat{P}_L}_{l\text{-index}} = \underbrace{b_{4,1}R_1 + b_{4,2}R_2 + b_{4,3}R_3 + \dots + b_{4,I}R_I}_{i\text{-index}} + \underbrace{\hat{b}_{4,1}\hat{R}_1 + \hat{b}_{4,2}\hat{R}_2 + \hat{b}_{4,3}\hat{R}_3 + \dots + \hat{b}_{4,M}\hat{R}_M}_{m\text{-index}} \quad (3-13)$$

For $k = 5$, C_5+ or heavier hydrocarbons balance:

$$\underbrace{a_{5,1}P_1 + a_{5,2}P_2 + a_{5,3}P_3 + \dots + a_{5,J}P_J}_{j\text{-index}} + \underbrace{\hat{a}_{5,1}\hat{P}_1 + \hat{a}_{5,2}\hat{P}_2 + \hat{a}_{5,3}\hat{P}_3 + \dots + \hat{a}_{5,L}\hat{P}_L}_{l\text{-index}} = \underbrace{b_{5,1}R_1 + b_{5,2}R_2 + b_{5,3}R_3 + \dots + b_{5,I}R_I}_{i\text{-index}} + \underbrace{\hat{b}_{5,1}\hat{R}_1 + \hat{b}_{5,2}\hat{R}_2 + \hat{b}_{5,3}\hat{R}_3 + \dots + \hat{b}_{5,M}\hat{R}_M}_{m\text{-index}} \quad (3-14)$$

For $k = 6$, N_2 or nitrogen balance:

$$\underbrace{a_{6,1}P_1 + a_{6,2}P_2 + a_{6,3}P_3 + \dots + a_{6,J}P_J}_{j\text{-index}} + \underbrace{\hat{a}_{6,1}\hat{P}_1 + \hat{a}_{6,2}\hat{P}_2 + \hat{a}_{6,3}\hat{P}_3 + \dots + \hat{a}_{6,L}\hat{P}_L}_{l\text{-index}} = \underbrace{b_{6,1}R_1 + b_{6,2}R_2 + b_{6,3}R_3 + \dots + b_{6,I}R_I}_{i\text{-index}} + \underbrace{\hat{b}_{6,1}\hat{R}_1 + \hat{b}_{6,2}\hat{R}_2 + \hat{b}_{6,3}\hat{R}_3 + \dots + \hat{b}_{6,M}\hat{R}_M}_{m\text{-index}} \quad (3-15)$$

For $k = 7$, CO_2 or carbon dioxide balance:

$$\underbrace{a_{7,1}P_1 + a_{7,2}P_2 + a_{7,3}P_3 + \dots + a_{7,J}P_J}_{j\text{-index}} + \underbrace{\hat{a}_{7,1}\hat{P}_1 + \hat{a}_{7,2}\hat{P}_2 + \hat{a}_{7,3}\hat{P}_3 + \dots + \hat{a}_{7,L}\hat{P}_L}_{l\text{-index}} = \underbrace{b_{7,1}R_1 + b_{7,2}R_2 + b_{7,3}R_3 + \dots + b_{7,I}R_I}_{i\text{-index}} + \underbrace{\hat{b}_{7,1}\hat{R}_1 + \hat{b}_{7,2}\hat{R}_2 + \hat{b}_{7,3}\hat{R}_3 + \dots + \hat{b}_{7,M}\hat{R}_M}_{m\text{-index}} \quad (3-16)$$

Thus, the steady state component material balance equations for each component can be represented in such a way. Here, the uncertain variables are incorporated in order to obtain a more robust as well as profitable production. Moreover, such kind of linear representation of mass flows also significantly helps for modeling and simulation in current industrial practice [27].

3.4 Modeling energy inflow and outflow

The utility inflows to a gas processing plant and energy product outflows from the plant are represented in Fig. 3.4. The general energy balance equation which involves all energy inflows to the plant and outflows from the plant is given as:

$$\sum_{j=1}^J Q_j + \sum_{l=1}^L \hat{Q}_l = \sum_{i=1}^{i'} U_i + \sum_{m=1}^{m'} \hat{U}_m \quad (3-17)$$

where the prime indices i' and j' represent for certain utility and energy product flows, which can be decided, respectively. m' and l' are indices for uncertain utility and energy product flows, respectively.

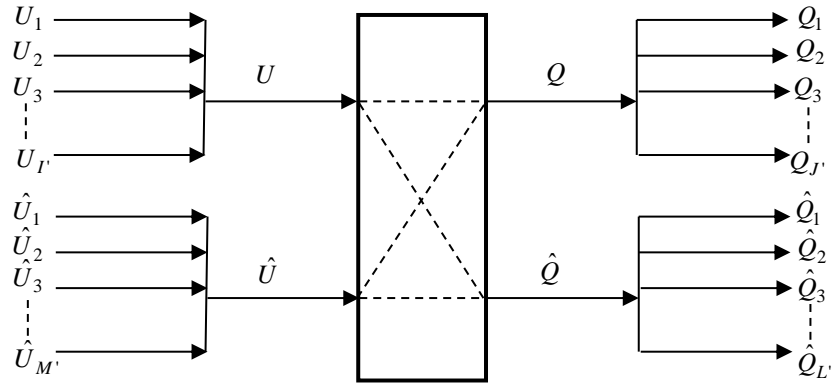


Fig 3.4: A schematic representation for energy inflow and outflow of GPP

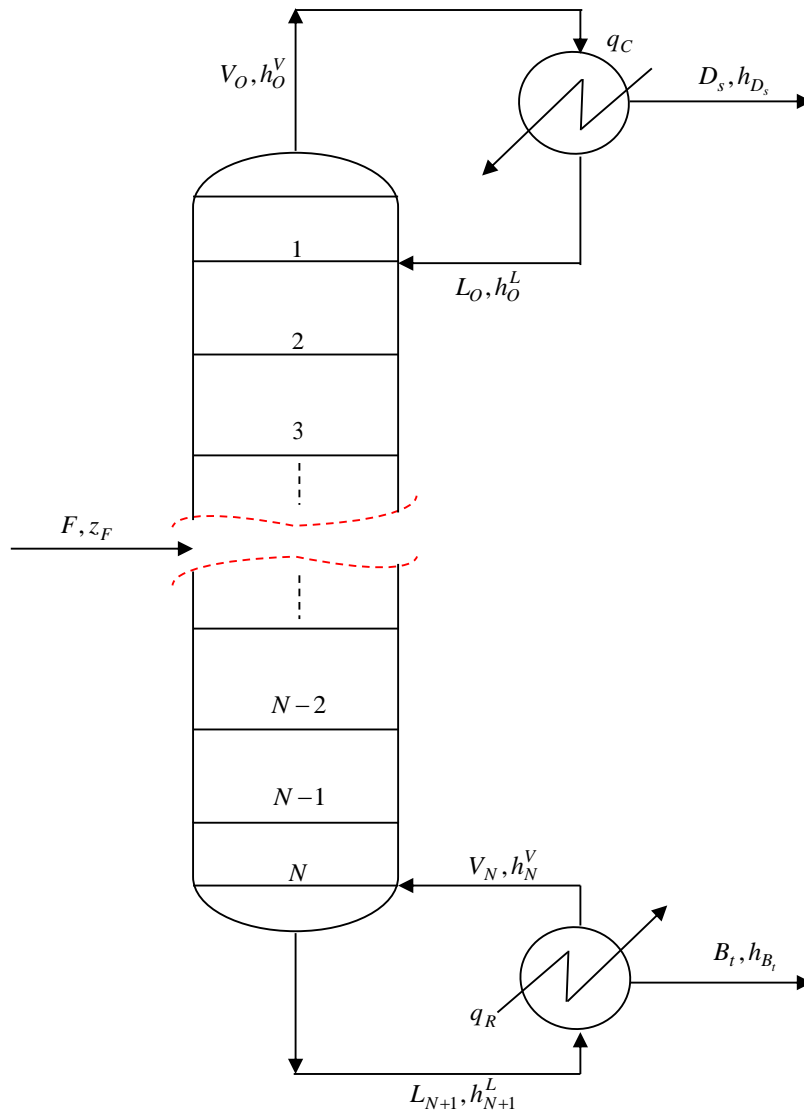


Fig 3.5: A typical conventional distillation column used in gas processing plant

Since most of the energy consumed and produced rely on the distillation columns, it is important first to calculate the amount of energy consumed by the columns in order to represent the utility and energy products flows. A conventional distillation column which consists of the rectifying and stripping section is shown in Fig. 3.5. The energy requirement for each distillation column is obtained using the Underwood equation [23]. Accordingly, the Underwood method calculates the minimum reflux ratio for a distillation column based upon constant volatility and constant mass overflow (CMO). The CMO approximation is the basis for the application of the shortcut distillation approach in which the mass flows and relative volatility are assumed to be constant at each column stages. In addition to Underwood equation, other correlation can also be used such as Edmister, Hengstebeck-Geddes, Fenske, Gilliland and Kirkbride. All these shortcut distillation correlations are shown in Appendix A. In order to estimate the energy consumption by a distillation column, the reflux ratio should be obtained. The reflux ratio is defined in the following equation:

$$R_{flx} = L_o / D_s = \eta_c \left(L_o / D_s \right)_{\min} \quad (3-18)$$

where L_o and D_s represent the reflux and distillate flow rates, respectively. R_{flx} is the reflux ratio and η_c is a constant value, usually in the range of 1.2 to 1.5. A typical one is to use $\eta_c = 1.2$. However, it is usually preferred to overestimate than underestimate the reflux ratio. For instance, using $\eta_c = 1.5$ gives a more sensible and good choice especially for optimization purpose [146]. The Underwood method consists of two parts. The first is to evaluate the correlating parameter ϕ using the following equation:

$$1 - q_f = \sum_{k=1}^K \frac{(z_{F,k})(F)}{(\partial_k - \phi) / \partial_k} \quad (3-19)$$

where ∂ is the relative volatility of each component k . The letter q_f represent for the feed quality, which is the mass or mole fraction of the feed that is liquid. Usually for saturated liquid feed, the value of q_f is equal to one. Hence, the parameter ϕ is

used for adjusting the left hand side of the equation (3-19) to be zero. Based on this, the minimum reflux ratio R_{flx}^{\min} is obtained using the following equation:

$$R_{flx}^{\min} + 1 = \sum_{k=1}^K \frac{(a_{k,D_s})(D_s)}{(\partial_k - \varphi)/\partial_k} \quad (3-20)$$

Thus, the minimum reflux ratio can be used to perform an energy balance on the condenser. The energy balance for the condenser and reboiler gives the heat duty as a function of the specific enthalpy of the mixture and the vapor flow. This is shown in the following equations:

$$q_C = \left[(h_o^V - h_{D_s}) + (h_o^L - h_{D_s}) \frac{R_{flx}}{R_{flx} + 1} \right] V_o \quad (3-21)$$

$$q_R = \left[(h_N^V - h_{N+1}^L) + \tau (h_{B_t} - h_{N+1}^L) \right] V_N \quad (3-22)$$

where q_C and q_R represent the heat removed in the condenser and the heat supplied to the reboiler, respectively. h^V and h^L are the specific mass enthalpies for the vapor and liquid flows, respectively. The top and bottom vapor flow rates are represented by V_o and V_N , respectively. The Greek letter τ is for the boil up ratio. For the equations (3-21) and (3-22), some special forms of total condensers and partial reboilers can be considered. When the CMO approximation is applied, the condenser and reboiler duty becomes:

$$q_C = \lambda_o V_o = (R_{flx} + 1) D_s \quad (3-23)$$

$$q_R = \lambda_N V_N = \lambda_N \tau B_t \quad (3-24)$$

where D_s and B_t are the distillate and bottom flow rates, respectively. λ_o and λ_N are heats of vaporization evaluated at the condenser and reboiler conditions. The latent heat is approximated to account for the small heat effects on the condenser and reboiler based on CMO approximation. Thus, equation (3-21) and (3-22) are now replaced using equation (3-23) and (3-24), respectively.

The utility demand for the condenser and reboiler can be determined from the heat loads q_C and q_R . For instance, when cooling water is used as utility for the condenser, the heat load can be calculated easily from the inlet and outlet temperature. The range of this temperature usually lies between 30 to 50°C. However, when condensing steam is used to provide heating in the reboiler, there are often several pressure levels available which correspond to different temperatures and heats of vaporization. This time, the cooling and heating utilities flow are obtained from equation (3-23) and (3-24):

$$\dot{M}_{cool} = \frac{q_C}{c_p \Delta T_C} = \frac{\lambda_o}{c_p \Delta T_C} V_o \quad (3-25)$$

$$\dot{M}_{heat} = \frac{q_R}{\Delta H_{stm}} = \frac{\lambda_N}{\Delta H_{stm}} V_N \quad (3-26)$$

where \dot{M} is the mass flow rate, T is the saturation temperature in Kelvin and ΔH_{stm} represents the latent heat of the steam in kJ/kg . From equation (3-25) and (3-26), it can be seen that the heat duties and utility flows increase linearly with the vapor rates. Hence, it also increases linearly with the reflux and boil up ratios. Here, it should be noted that the energy outflow produced from the distillation column is actually the condenser duty. This energy can be recovered and used as heat source for the process or may also be exported to next door plant to generate revenue.

The remaining plant's energy consumption for compressors, pump and heaters are either calculated based on stream flow rates or correlated with process parameters using equations formulated from rigorous steady state simulation. The energy transfer in cross-exchangers, in the LTSU section, is neglected since it is not a direct plant cost. In addition, the energy product from the expanders can be used as a potential energy option for some of the compressors.

3.5 Deterministic model formulation

Deterministic model formulation largely emphasize on ensuring the feasibility of a solution over a given range of uncertain variable. Thus, one of the main optimization tasks in deterministic formulation may be to find the optimal stream flow rate that maximize the overall profit of the existing plant subject to a certain constraints. However, the optimal solutions of a deterministic programming problem may become infeasible even if the nominal data is slightly perturbed [147]. Moreover, Sen and Hignle [148] reported that deterministic formulations in which uncertain variable are mathematically and statistically replaced by their expected values may not provide a feasible solution. However, developing the deterministic formulation initially helps to convert to the corresponding probabilistic problem. For clarity of the problem formulation, in the next sections, the uncertain parameters have been included in the deterministic formulation. Thus, the formulations for uncertainty from the plant inlet and outlet as well as utilities and operating conditions are presented below.

3.5.1 Uncertain feed inflow

In order to represent the uncertainty from the plant inlet, all the plant outlet material flows are considered to be decided. Based on this, equation (3-9) can be re-defined as:

$$\sum_{j=1}^J a_{k,j} P_j - \sum_{i=1}^I b_{k,i} R_i = \sum_{m=1}^M \hat{b}_{k,m} \hat{R}_m = r_k^{\xi} \quad , \quad k=1, \dots, K \quad (3-27)$$

where $\xi_k \subseteq \mathfrak{R}^K$ is a vector of the total uncertain feed component inflows and r_k^{ξ} represent the total actual uncertain feed component flow rate which enter to the plant. Accordingly, the objective function from the deterministic formulation becomes:

$$\max \text{Profit} = \sum_{j=1}^J \bar{C}_j^P P_j - \sum_{i=1}^I \bar{C}_i^R R_i - \bar{C}^{\hat{R}} \left[\sum_{k=1}^K r_k^{\xi} \right] \quad (3-28)$$

where \bar{C}^R and \bar{C}^P are the expected price factors for certain raw material and product flows which can be decided, respectively. The expression $\bar{C}^{\hat{R}}$ represent expected price factor for the uncertain raw material flow. The constraints from the plant material flows are described below:

Inlet material flow distribution to the plant:

$$R = \sum_{i=1}^I R_i, \quad \hat{R} = \sum_{k=1}^K r_k^{\xi} \quad (3-29)$$

Outlet material flow distribution from the plant:

$$P = \sum_{j=1}^J P_j \quad (3-30)$$

Availability of material flow constraint:

$$r_k^{\xi} = \sum_{j=1}^J a_{k,j} P_j - \sum_{i=1}^I b_{k,i} R_i \leq \xi_k, \quad k = 1, \dots, K \quad (3-31)$$

Total material balance:

$$P = R + \hat{R} \quad (3-32)$$

Material flow capacity restriction:

$$P_{j,\min} \leq P_j \leq P_{j,\max}, \quad j = 1, \dots, J; \quad R_{i,\min} \leq R_i \leq R_{i,\max}, \quad i = 1, \dots, I \quad (3-33)$$

In equation (3-31), the inequality constraint describes the resource availability of the total uncertain feed flows. During deterministic optimization, the expected or average value of the uncertain feed component flow ξ is usually employed. However, the decision from the deterministic optimization may violate the constraints by 50% [24]. Thus, such kinds of decision are usually referred as aggressive decision due to expecting a higher profit. On the other hand, the restriction for the uncertain feed component flow ξ may also be specified other than the expected value to make sure that there is no violation of constraint. This may also leads to a conservative decision

and thereby deteriorates the objective function. Such decisions are also called “worst case”, as discussed in the introduction section. Hence, it is important to know the optimum trade-off between profitability and reliability of holding the process constraints. This also requires studying the uncertainty effect of ξ to make decision under uncertain conditions. A similar approach can be adopted for the uncertain material outflow, utility inflow and energy product outflow, which are all presented in the following sections.

3.5.2 Uncertain product outflow

For representing the uncertainty from the plant outlet, all the plant inlet material flows are taken as a decision variable. Based on this, equation (3-9) can be re-written as:

$$p_k^\zeta = \sum_{l=1}^L \hat{a}_{k,l} \hat{P}_l = \sum_{i=1}^I b_{k,i} R_i - \sum_{j=1}^J a_{k,j} P_j, \quad k=1, \dots, K \quad (3-34)$$

where $\zeta_k \subseteq \mathfrak{R}^K$ is a vector of the total actual uncertain product component outflows and p_k^ζ represent for the total uncertain product component flow rate which is produced from the plant. Thus, the objective function for the deterministic formulation is given as:

$$\max \text{Profit} = \sum_{j=1}^J \bar{C}_j^P P_j + \bar{C}^{\hat{p}} \left[\sum_{k=1}^K p_k^\zeta \right] - \sum_{i=1}^I \bar{C}_i^R R_i \quad (3-35)$$

where $\bar{C}^{\hat{p}}$ is the expected price factor for the uncertain product flow. The constraints are described below. The capacity restriction defined in equation (3-33) remains the same:

Inlet material flow distribution to the plant:

$$R = \sum_{i=1}^I R_i \quad (3-36)$$

Outlet material flow distribution from the plant:

$$P = \sum_{j=1}^J P_j, \quad \hat{P} = \sum_{k=1}^K p_k^{\zeta} \quad (3-37)$$

Availability of material flow constraint:

$$p_k^{\zeta} = \sum_{i=1}^I b_{k,i} R_i - \sum_{j=1}^J a_{k,j} P_j \geq \zeta_k, \quad k=1, \dots, K \quad (3-38)$$

Total material balance:

$$P + \hat{P} = R \quad (3-39)$$

3.5.3 Uncertain utility inflow

For uncertain utility inflow, all the outflows from the plant are considered as decision variables. Based on this, equation (3-17) can be re-defined as:

$$\sum_{j=1}^J Q_{e,j} - \sum_{i=1}^I U_{e,i} = \sum_{m=1}^M \hat{U}_{e,m} = u_e^{\varepsilon}, \quad e=1, \dots, E \quad (3-40)$$

where $\varepsilon \subseteq \mathfrak{R}^{M,M}$ is a vector of the total uncertain energy inflows. The subscript e represents index for energy flow types. u_e^{ε} is for the total actual uncertain energy flow which enter to the plant. The objective function for the deterministic formulation is given as:

$$\max \text{Profit} = \sum_{j=1}^J \bar{C}_j^Q Q_j - \sum_{m=1}^M \bar{C}_m^U U_m - \left[\sum_{e=1}^E \bar{C}_e^u u_e^{\varepsilon} \right] \quad (3-41)$$

where \bar{C}^u is the expected price factor of the uncertain energy inflow. The constraints from the deterministic formulations are shown below:

Inlet energy flow distribution to the plant:

$$U = \sum_{m=1}^M U_m, \quad \hat{U} = \sum_{e=1}^E u_e^{\varepsilon} \quad (3-42)$$

Outlet energy flow distribution from the plant:

$$Q = \sum_{l=1}^L Q_l \quad (3-43)$$

Availability of utility flow constraint:

$$u_e^\varepsilon = \sum_{j=1}^J Q_j - \sum_{i=1}^I U_i \leq \varepsilon_e, \quad e=1, \dots, E \quad (3-44)$$

Total energy balance:

$$Q = U + \hat{U} \quad (3-45)$$

Energy flow capacity restriction:

$$Q_{l,\min} \leq Q_l \leq Q_{l,\max}, \quad l=1, \dots, L; \quad U_{m,\min} \leq U_m \leq U_{m,\max}, \quad m=1, \dots, M \quad (3-46)$$

3.5.4 Uncertain energy product outflow

For representing the uncertain energy outflow, all the utility flows are considered as a decision variable. Based on this equation (3-17) can be re-written as:

$$q_e^\zeta = \sum_{l=1}^L \hat{Q}_{e,l} = \sum_{i=1}^I U_{e,i} - \sum_{j=1}^J Q_{e,j}, \quad e=1, \dots, E \quad (3-47)$$

where $\zeta \subseteq \mathfrak{R}^{L,L}$ is a vector of the total uncertain energy outflows and q_e^ζ represent for the total actual uncertain energy product flow which is produced from the plant. The objective function for the deterministic formulation is given as:

$$\max \text{Profit} = \sum_{j=1}^J \bar{C}_j^Q Q_j + \left[\sum_{e=1}^E \bar{C}_e^q q_e^\zeta \right] - \sum_{m=1}^M \bar{C}_m^U U_m \quad (3-48)$$

where \bar{C}^q is the expected price factor for the uncertain energy outflow. The constraints for the deterministic formulation are given below; only the energy capacity restriction defined in equation (3-46) remain the same:

Inlet energy flow distribution to the plant:

$$U = \sum_{m=1}^M U_m \quad (3-49)$$

Outlet energy flow distribution from the plant:

$$Q = \sum_{l=1}^L Q_l, \quad \sum_{e=1}^E q_e^\zeta \quad (3-50)$$

Availability of energy flow constraint:

$$q_e^\zeta = \sum_{i=1}^I U_i - \sum_{j=1}^J Q_j \geq \zeta_e, \quad e=1, \dots, E \quad (3-51)$$

Total energy balance:

$$Q + \hat{Q} = U \quad (3-52)$$

Thus, in such a way the deterministic formulation for all the uncertain material inflows and outflows as well as utility inflows and energy product outflows are represented. The formulation of such models significantly helps to develop the corresponding chance constrained model which is presented in the following section.

3.6 Chance constrained model formulation

The chance constrained model formulation mostly relies on deterministic model which is developed in the previous section. During deterministic optimization, the implementation of the result will violate the inequality constraint described in equation (3-31), (3-38), (3-44) and (3-51) with a probability of 50%. Thus, it is important to take the probability measurements of the uncertain variables ξ, ζ, ε and ς in between 50% to 100%. The probabilistic measurement is expressed in terms of a unit called confidence level (α), which is assigned by the user for each or the whole constraint(s). The constraints can be represented in terms of single or joint chance constraints as described in the following sections.

3.6.1 Single chance constrained

An important instance of optimization problems with uncertain data occurs if the constraints depend on a stochastic parameter. In such circumstances, emphasis is shifted towards the reliability of a system by requiring a decision to be feasible at high probability level for each constraint. Thus, the higher the probability the more reliable is the modeled system [12]. The single chance constraint is used when some outputs are more critical than others. For example, considering propane and butane products, when the market for propane is high, while for butane is depressed, the plant may want to produce more amount of propane to satisfy the customer demand. As a result, more emphasis is given to individual constraints or single chance constraints to meet the required production level.

The basic formulation for single chance constrained optimization can be developed from the deterministic formulation developed in Section 3.5. Most of the formulations remains the same except for the constraints defined in equation (3-31), (3-38), (3-44) and (3-51). These constraints are defined for single chance constrained optimization as follows:

$$\Pr_k \left\{ r_k^\xi = \sum_{j=1}^J a_{k,j} P_j - \sum_{i=1}^I b_{k,i} R_i \leq \xi_k \right\} \geq \alpha_k, \quad k=1, \dots, K \quad (3-53)$$

$$\Pr_k \left\{ p_k^\zeta = \sum_{i=1}^I b_{k,i} R_i - \sum_{j=1}^J a_{k,j} P_j \geq \zeta_k \right\} \geq \alpha_k, \quad k=1, \dots, K \quad (3-54)$$

$$\Pr_e \left\{ u_e^\varepsilon = \sum_{j=1}^J Q_j - \sum_{i=1}^I U_i \leq \varepsilon_e \right\} \geq \alpha_e, \quad e=1, \dots, E \quad (3-55)$$

$$\Pr_e \left\{ q_e^\varsigma = \sum_{i=1}^I U_i - \sum_{j=1}^J Q_j \geq \varsigma_e \right\} \geq \alpha_e, \quad e=1, \dots, E \quad (3-56)$$

where Pr is the probability operator holding the constraints and α is the user-defined confidence level for holding the individual constraints. Thus, in such a way the single chance constrained model can be formulated based on the previous

developed deterministic formulations. The joint chance constrained model formulation is presented in the next section.

3.6.2 Joint chance constrained

Joint chance constraints express the condition that at minimum confidence level (α), certain trajectories satisfy the given constraints over the whole interval [12]. Basically, passing from individual probabilistic constraints to joint chance constraints involves a number of inequality constraints to be turned to a single inequality. As a result, the problem may become more complex. However, by introducing one-dimensional uncertain variables, the joint chance constraint will hold all the individual constraints into one inequality constraint at certain confidence level.

The joint chance constrained mostly used for the safe production of the planned operation. For example, when the market for LPG (liquefied petroleum gas) is high, both propane and butane products are highly required to be produced. At this time, the production of these two products can be held jointly at a certain confidence level to acquire the planned production level. For joint chance constrained formulation, most of the formulations from the deterministic model remain the same. However, the only change is on the probabilistic constraint in equation (3-31), (3-38), (3-44) and (3-51). These constraints are now defined as follows:

$$\Pr \left\{ r_k^\xi = \sum_{j=1}^J a_{k,j} P_j - \sum_{i=1}^I b_{k,i} R_i \leq \xi_k, k = 1, \dots, K \right\} \geq \alpha \quad (3-57)$$

$$\Pr \left\{ p_k^\zeta = \sum_{i=1}^I b_{k,i} R_i - \sum_{j=1}^J a_{k,j} P_j \geq \zeta_k, k = 1, \dots, K \right\} \geq \alpha \quad (3-58)$$

$$\Pr_e \left\{ u_e^\varepsilon = \sum_{j=1}^J Q_j - \sum_{i=1}^I U_i \leq \varepsilon_e, e = 1, \dots, E \right\} \geq \alpha \quad (3-59)$$

$$\Pr_e \left\{ q_e^\varsigma = \sum_{i=1}^I U_i - \sum_{j=1}^J Q_j \geq \varsigma_e, e = 1, \dots, E \right\} \geq \alpha \quad (3-60)$$

In order to solve both the single and joint chance constrained models, it requires evaluating the probabilistic constraints defined in equation (3-53) to (3-60). However, this needs also to relax all the probabilistic constraints to their corresponding equivalent deterministic form. On the other hand, the objective function in equation (3-28) and (3-34), (3-41) and (3-48) have now been defined as a continuous variable for the uncertain flow cases. However, in the recent works of Li et al. [24], the evaluations for such uncertain variables in the objective function have not been considered. The objective function was defined similar to a deterministic optimization approach. However, this significantly affects the economic performance of the plant since the cost of such uncertain variables should be included. The relaxations of the probabilistic constraints defined in equation (3-53) to (3-60) are presented in the following section.

3.7 Relaxed deterministic model formulation

The relaxation of a probabilistic problem into deterministic equivalent has to be formulated such that the problem could be solved using the available commercial software routines. The chance constraints defined in equation (3-53) to (3-60) have to be treated carefully. These constraints can not be solved unless they are relaxed to their equivalent deterministic form. The relaxation starts from the probability computation for both single and joint chance constrained. The probability computation allows in quantifying the uncertain inflows and outflows using a known probability density function. Based on this, the probability computation for the uncertain variables for r_k^ξ , p_k^ζ , u_e^ε and q_e^ς becomes:

$$\Phi(r_k^\xi) = \Pr_k \{ \xi_k \leq r_k^\xi \} = \int_{-\infty}^{r_k^\xi} \rho_k(\xi_k) d\xi_k, \quad k=1, \dots, K \quad (3-61)$$

$$\Phi(p_k^\zeta) = \Pr_k \{ \zeta_k \leq p_k^\zeta \} = \int_{-\infty}^{p_k^\zeta} \rho_k(\zeta_k) d\zeta_k, \quad k=1, \dots, K \quad (3-62)$$

$$\Phi(u_e^\varepsilon) = \Pr_e \{ \varepsilon_e \leq u_e^\varepsilon \} = \int_{-\infty}^{u_e^\varepsilon} \rho_e(\varepsilon_e) d\varepsilon_e, \quad e=1, \dots, E \quad (3-63)$$

$$\Phi(q_e^\zeta) = \Pr_e \{ \varepsilon_e \leq q_e^\zeta \} = \int_{-\infty}^{q_e^\zeta} \rho_e(\zeta_e) d\zeta_e, \quad e = 1, \dots, E \quad (3-64)$$

In the above equations (3-61) to (3-64), ρ refers to the probability density function for the uncertain variables ξ, ζ, ε and ζ . The symbol Φ is the probability distribution function with $\Phi(\infty)=1$. The probability distribution of different uncertain variables can be different and their distribution is usually obtained in three ways [24, 149]: (i) contractual formulation provided by suppliers and customers; (ii) statistical regression from previous data if a large amount of data is available; or (iii) creation through interpolation or extrapolation if few data are available. Usually, the normal distribution is used since it comprises the basic properties of the uncertain variables [150].

In many instances the uncertain variables are independent of each other as shown in equation (3-61) to (3-64). However, if the uncertain variables have correlations, a unified density function has to be formulated [24]. For example, considering the uncertain variable ζ , there are times in which the demand of propane product is low in the market; and due to the low demand of propane in the market, the demand for butane product may be high. In such cases, the uncertain variables are considered to be correlated to each other since the market of one of the product influences the other. For such cases, the probability computation becomes:

$$\Phi(r_k^\xi) = \int_{-\infty}^{\infty} d\xi_1 \dots \int_{-\infty}^{r_k^\xi} d\xi_k \dots \int_{-\infty}^{\infty} d(\xi_1, \dots, \xi_k) d\xi_k, \quad k = 1, \dots, K \quad (3-65)$$

$$\Phi(p_k^\zeta) = \int_{-\infty}^{\infty} d\zeta_1 \dots \int_{-\infty}^{p_k^\zeta} d\zeta_k \dots \int_{-\infty}^{\infty} d(\zeta_1, \dots, \zeta_k) d\zeta_k, \quad k = 1, \dots, K \quad (3-66)$$

$$\Phi(u_e^\varepsilon) = \int_{-\infty}^{\infty} d\varepsilon_1 \dots \int_{-\infty}^{u_e^\varepsilon} d\varepsilon_e \dots \int_{-\infty}^{\infty} d(\varepsilon_1, \dots, \varepsilon_e) d\varepsilon_e, \quad e = 1, \dots, E \quad (3-67)$$

$$\Phi(q_e^\zeta) = \int_{-\infty}^{\infty} d\zeta_1 \dots \int_{-\infty}^{q_e^\zeta} d\zeta_e \dots \int_{-\infty}^{\infty} d(\zeta_1, \dots, \zeta_e) d\zeta_e, \quad e = 1, \dots, E \quad (3-68)$$

Thus, based on equations (3-61) to (3-68), the probabilistic single chance constraints in equations (3-53) to (3-56) are converted in to the corresponding equivalent deterministic form as follows:

$$\sum_{j=1}^J a_{k,j} P_j - \sum_{i=1}^I b_{k,i} R_i \leq \Phi_k^{-1}(1 - \alpha_k), \quad k = 1, \dots, K \quad (3-69)$$

$$\sum_{i=1}^I b_{k,i} R_i - \sum_{j=1}^J a_{k,j} P_j \geq \Phi_k^{-1}(\alpha_k), \quad k = 1, \dots, K \quad (3-70)$$

$$\sum_{j=1}^J Q_j - \sum_{i=1}^I U_i \leq \Phi_e^{-1}(1 - \alpha_e), \quad e = 1, \dots, E \quad (3-71)$$

$$\sum_{i=1}^I U_i - \sum_{j=1}^J Q_j \geq \Phi_e^{-1}(\alpha_e), \quad e = 1, \dots, E \quad (3-72)$$

where Φ^{-1} is a parameter for the inverse value of the probability distribution function. The inverse value Φ^{-1} is a known value at the specified confidence levels α . The relaxations of the single chance constraints result to a convex solution [52, 151]. This is due to the fact that for linear chance constrained problems, the input uncertain variable will have the same distribution with the output variable. Hence, the resulting problem gives a global solution. Thus, such models can be solved with the available commercial LP solvers. Similarly, using equations (3-61) to (3-68), the probabilistic joint chance constraints in equations (3-57) to (3-60) are converted into the corresponding equivalent form as follows:

$$\prod_{k=1}^K \left[1 - \Phi_k \left(\sum_{j=1}^J a_{k,j} P_j - \sum_{i=1}^I b_{k,i} R_i \right) \right] \geq \alpha \quad (3-73)$$

$$\prod_{k=1}^K \left[\Phi_k \left(\sum_{i=1}^I b_{k,i} R_i - \sum_{j=1}^J a_{k,j} P_j \right) \right] \geq \alpha \quad (3-74)$$

$$\prod_{e=1}^E \left[1 - \Phi_e \left(\sum_{j=1}^J Q_j - \sum_{i=1}^I U_i \right) \right] \geq \alpha \quad (3-75)$$

$$\prod_{e=1}^E \left[\Phi_e \left(\sum_{i=1}^i U_i - \sum_{j=1}^j Q_j \right) \right] \geq \alpha \quad (3-76)$$

The relaxation of the joint chance constrained described in equation (3-73) to (3-76) results the model to an NLP problem. This is due to the presence of the non-linear term Φ . Thus, such kinds of models can be solved with available commercial NLP solvers. The relaxation for correlated uncertain variables defined in equations (3-65) to (3-68) becomes:

$$\prod_{k=1}^K \left[\int_{-\infty}^{r_1^\xi} d\xi_1 \dots \int_{-\infty}^{r_k^\xi} d\xi_k \dots \int_{-\infty}^{\infty} d(\xi_1, \dots, \xi_k) d\xi_k \right] \quad (3-37)$$

$$\prod_{k=1}^K \left[\int_{-\infty}^{p_1^\zeta} d\zeta_1 \dots \int_{-\infty}^{p_k^\zeta} d\zeta_k \dots \int_{-\infty}^{\infty} d(\zeta_1, \dots, \zeta_k) d\zeta_k \right] \quad (3-78)$$

$$\prod_{e=1}^E \left[\int_{-\infty}^{u_1^\varepsilon} d\varepsilon_1 \dots \int_{-\infty}^{u_E^\varepsilon} d\varepsilon_e \dots \int_{-\infty}^{\infty} d(\varepsilon_1, \dots, \varepsilon_E) d\varepsilon_E \right] \quad (3-79)$$

$$\prod_{e=1}^E \left[\int_{-\infty}^{q_1^\zeta} d\zeta_1 \dots \int_{-\infty}^{q_E^\zeta} d\zeta_e \dots \int_{-\infty}^{\infty} d(\zeta_1, \dots, \zeta_e) d\zeta_e \right] \quad (3-80)$$

In equation (3-77) to (3-80), it is difficult to find an explicit solution since it involves multivariate integral. An integration method was presented by Li et al. [56]. This was initially developed by Szántai [152] based on simulation scheme for correlated variables with normal distribution. In order to prevent the multivariate integration, marginal distribution can be used in equations (3-69) to (3-76). However, such kind of formulation may not reflect the real-world problem due to the complexity associated with the uncertain correlated variables and may lead to wrong solution [24]. On the other hand, the unintegrable term $\Phi(\cdot)$ in equations (3-73) to (3-76) needs to be evaluated carefully for the model to be solved. In the following sections, evaluations techniques for cumulative distribution function (cdf) based on computer program and numerical approximation are presented.

3.8 Evaluation of probability distribution function

The probability distribution $\Phi(\cdot)$ is also referred as cumulative distribution function (cdf). The probability computation for $\Phi(r_k^\xi)$, $\Phi(p_k^\zeta)$, $\Phi(u_e^\varepsilon)$ and $\Phi(q_e^\varsigma)$ defined in equation (3-73) to (3-76) can be alternatively expressed using a standard form. This is done by converting the uncertain flows r_k^ξ , p_k^ζ , u_e^ε and q_e^ς to their corresponding standardized form. Accordingly, for normal distribution, the standardized form for r_k^ξ , p_k^ζ , u_e^ε and q_e^ς becomes:

$$Z_k^\xi = \frac{r_k^\xi - \theta_k}{\sigma_k} \quad (3-81)$$

$$Z_k^\zeta = \frac{p_k^\zeta - \theta_k}{\sigma_k} \quad (3-82)$$

$$Z_e^\varepsilon = \frac{u_e^\varepsilon - \theta_e}{\sigma_e} \quad (3-83)$$

$$Z_e^\varsigma = \frac{q_e^\varsigma - \theta_e}{\sigma_e} \quad (3-84)$$

where Z represent the standardized parameter. The symbols θ and σ represent mean and standard deviation, respectively. Thus, the standard normal cumulative distribution functions are now represented as $\Phi(Z_k^\xi)$, $\Phi(Z_k^\zeta)$, $\Phi(Z_e^\varepsilon)$ and $\Phi(Z_e^\varsigma)$. The standard normal cumulative distribution function $\Phi(Z)$ is shown in Fig. 3.6. The values of $\Phi(Z)$ is also usually available in most standard tables for some range of Z as shown in Appendix B. The formula used to evaluate $\Phi(Z)$ is given as:

$$\Phi(Z) = \int_{-\infty}^Z \frac{1}{\sqrt{2\pi}} e^{-\frac{z^2}{2}} \quad (3-85)$$

In order to evaluate $\Phi(Z)$ using the above expression, it requires a computer program to be developed. For example, in GAMS programming language, there is an available function called *errorf* for evaluating the standard normal cumulative

distribution function [153]. However, this may not be supplied in other optimization routines softwares and hence the numerical representation of the function is essential to evaluate $\Phi(Z)$. Moreover, developing a one-term-to-calculate $\Phi(Z)$ significantly helps to avoid computer programming [154].

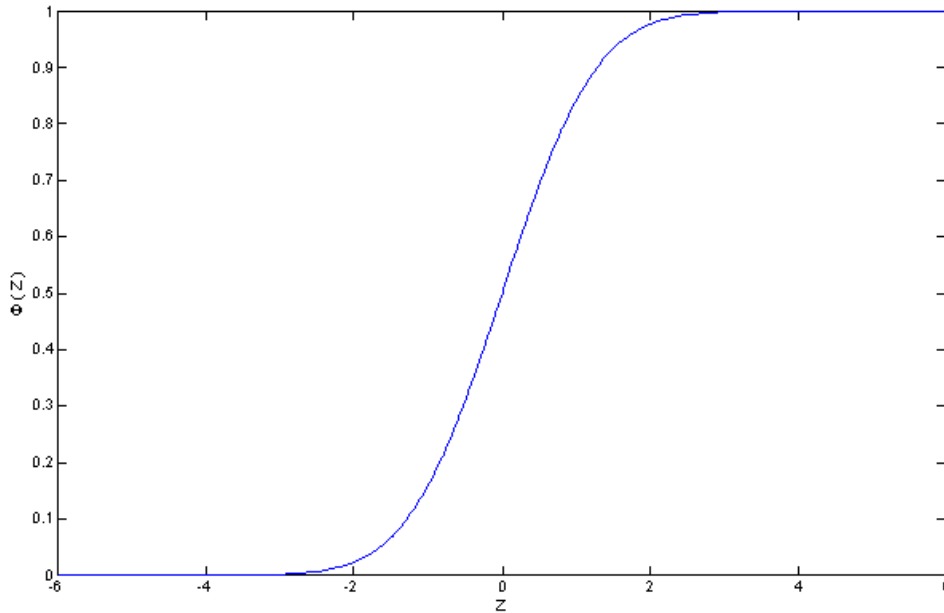


Fig 3.6: The standard normal cumulative distribution function

A number of mathematicians have tried to approximate the standard normal cumulative distribution function such as Bailey [155], Johnson [156], Chokri [157] and Aludatt & Alodat [154]. These approximations are described below:

$$\Phi(Z) \approx 1 - 0.5(a_0 + a_1Z + a_2Z^2 + a_3Z^3 + a_4Z^4 + a_5Z^5)^{-16} \quad (3-86)$$

$$\Phi(Z) \approx \exp(2t)/(1 + \exp(2t)), \quad t = 0.7988Z(1 + 0.04417Z^2) \quad (3-87)$$

$$\Phi(Z) \approx 1 - 0.5 \exp[-((83Z + 351)Z + 562)/(703/Z + 165)] \quad (3-88)$$

$$\Phi(Z) \approx 0.5 \left[1 + \sqrt{\left(1 - \exp\left(-\sqrt{\frac{\pi}{8}} Z^2 \right) \right)} \right] \quad (3-89)$$

where the coefficients in equation (3-86) are: $a_0, 0.9999998582$; $a_1, 0.487385796$; $a_2, 0.02109811045$; $a_3, 0.003372948927$; $a_4, 0.00005172897742$; $a_5, 0.0000856957942$. The approximations shown in equation (3-86), (3-87) and (3-88) give a high accuracy. However, computer program are needed to obtain their values. In addition, their inverse function can not be easily obtained. Only the approximation proposed by Aludatt & Alodat [154] can represent $\Phi(Z)$ using a one term to calculate both the standard normal cumulative distribution function and its inverse. The calculation involves algebraic equation followed by finding the roots of the first derivatives of $\Phi(Z)$ using mathematical software to avoid a computer program code.

3.9 Feasibility analysis

For an efficient treatment of probabilistic constraints, it is important to study the property of the feasible set in which the solution lies. Increasing the confidence level (α) in the probabilistic constraints shrinks the feasible set. Accordingly, the feasible set becomes empty starting from a critical value (α_c) which may be less than one. Some implemented solution techniques dealing with probabilistic constraints might unintentionally choose a value of α above the critical value. As a result, convergence may be possible by enforcing feasibility with a number of iteration. However, this will consume a lot of computing time due to operating on an empty constraint set [12].

On the other hand, a maximization step can be used to find the reachable maximum value of the confidence level. This can be done by defining the confidence levels as variables after relaxation and replace the objective function with summation of them. However, this may have sometimes a convergence problem and it may not give optimal solution. The simple way to find the reachable maximum value of confidence level is to increase it by stepwise. This can clearly help to see the performance both the objective function and the constraint for each stepwise increment.

The feasible region of single chance constrained is formed by half-spaces, while joint chance constraint is built by curvature due to the nonlinearity of the problem associated with this formulation. Thus, for both cases, their frame is determined by the value of the specified confidence level. Based on this, the whole probable operating region is outstretched between $\alpha = 0$ and $\alpha = 1$ as shown in Fig. 3.7[24]. x_1 and x_2 are the decision variables. As it can be observed from the Fig. 3.7, the 50% solution space (s_1, s_2, s_4 , and s_3) for single chance constrained problems is much wider than that of the 50% joint chance constrained solution space (s_3, s_4 and s_5). Moreover, the joint chance constrained solution space is part of the solution space of single chance constrained. In other word, the joint chance constrained solution space is a subset of the single chance constrained solution space.

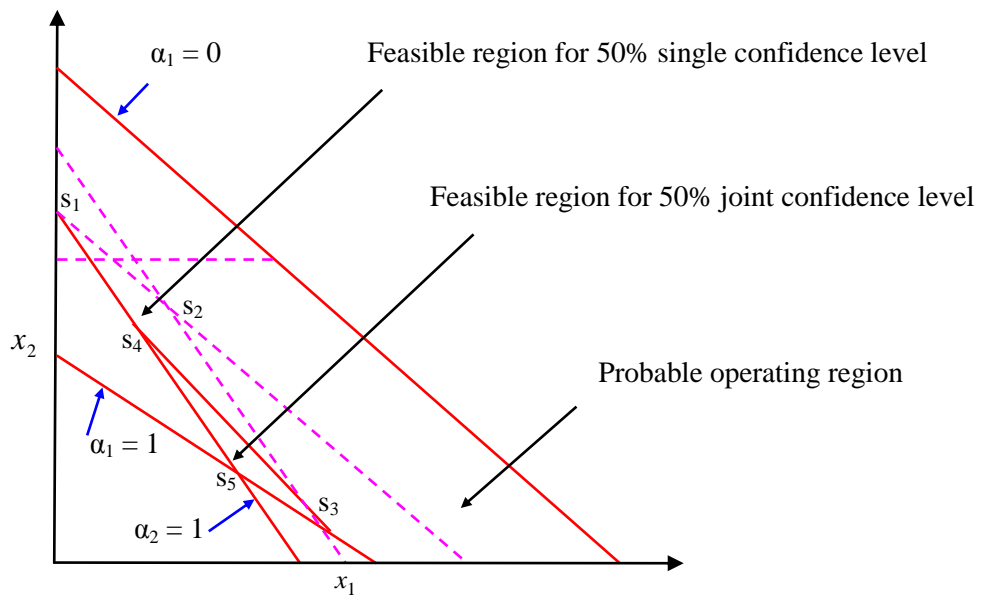


Fig. 3.7: Probable and feasible operating region with specified confidence level

3.10 Reliability vs profitability analysis

The reliability of the process is defined as to how much extent that a process can be held so that violation of constraint is reduced by a certain level. The profitability of the plant is the corresponding economic performance of the plant at the specified reliability of the process. Thus, the relation between reliability of the process and

profitability of the plant can be gained by solving the optimization problem at different confidence level.

The possible expected profit profiles with respect to confidence level are well discussed in the works of Li et al. [27] as well as Li et al. [24]. Accordingly, there are three types of profit profiles that were encountered when analyzing the reliability of the process and profitability of the plant as shown in Fig 3.8. For a slow decreasing profit profile (PR), such as profile PR1, point **a** should be chosen as the decision for the operating point. This is because increasing the confidence level from this point will lead to a considerable reduction in profit. For profit profile like PR2, it is difficult to determine the solution point. Thus, the decision is based on the specific requirement or priority between the profit and reliability of the problem. For profile like PR3, the optimal value is determined in the higher confidence region at point **b** since profit is not much sensitive.

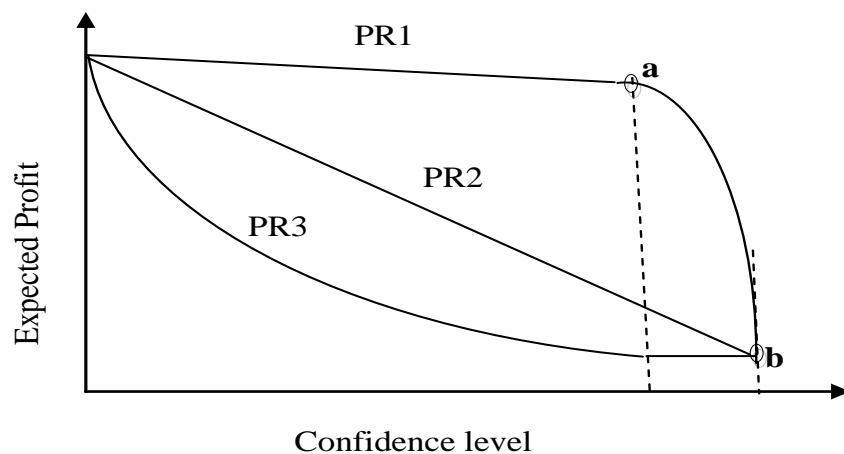


Fig 3.8: Possible profit profiles with respect to confidence level

Thus, in such a way, the relation between reliability of the process and profitability of the plant are described. The following two sections give a short briefing about the basic principles of HYSYS and GAMS softwares which are used in this thesis.

3.11 ASPEN HYSYS process simulator

HYSYS is a powerful engineering process simulator that has been uniquely built with respect to program architecture, interface design, engineering capabilities, and interactive operations [62]. The different components that exist in HYSYS provide an extremely powerful approach for steady state modeling. The comprehensive selection of operations and property methods significantly helps to model a wide range of process. In addition, the built-in property packages in HYSYS provide accurate thermodynamic, physical and transport property predictions for hydrocarbon, non-hydrocarbon, petrochemical and chemical fluids. Furthermore, the inherent flexibility contributed through its design as well as its robustness leads to a more realistic model.

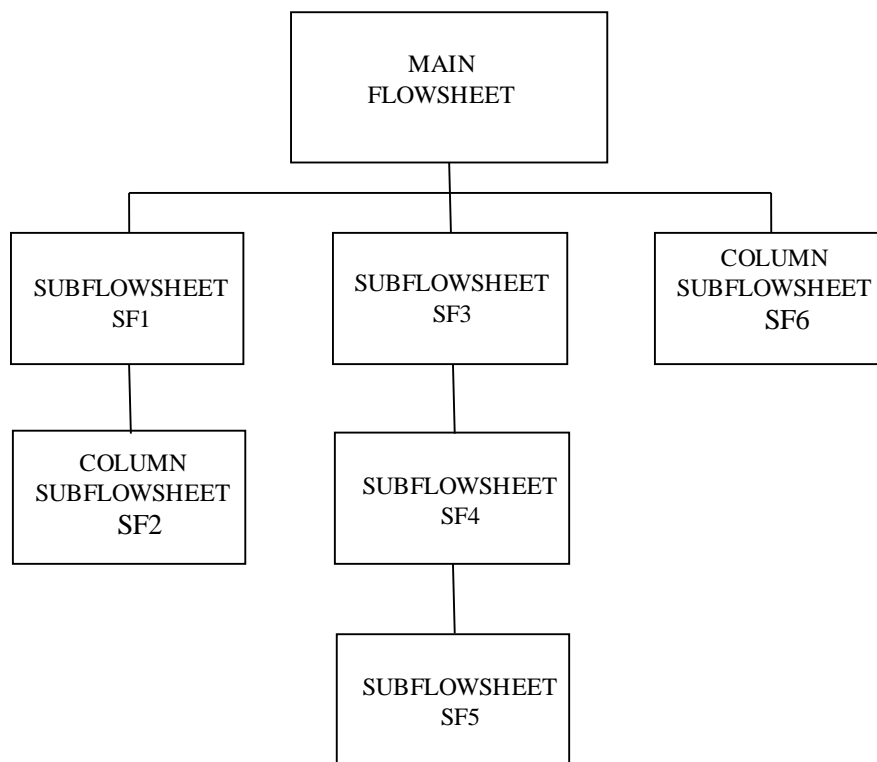


Fig 3.9: Hierarchical tree for simulation environment in HYSYS

The majority of the work in HYSYS is performed at the main flowsheet environment. However, it is also possible to create a sub-flowsheets under the main environment. Fig. 3.9 shows the hierarchical tree for the main flowsheet environment and sub-flowsheets. In the main flowsheet, the basic tasks include installing and defining streams, unit operations and columns. Thus, the main flowsheet is considered

as a base level for the whole simulation case. One can generate any number of sub-flowsheets in the main flowsheet. In addition, each sub-flowsheets may have also its own corresponding sub-flowsheets. However, there is only one main flowsheet environment for all the sub-flowsheet.

If one wants to change the number of trays for a column in sub-flowsheet SF6 shown in Fig. 3.9, it needs to enter the environment for this sub-flowsheet and make the changes. HYSYS then re-calculate the column. Here, it should be noted that there are no other sub-flowsheets below SF6. Hence, all other flowsheets remain on hold status when modifying this column. The changes continue until a satisfactory solution is obtained for SF6. After that, it needs to be returned to the main flowsheet to automatically calculate all the flowsheet based on the new sub-flowsheet solution.

In order to modify the sub-flowsheet SF4, all the flowsheets remain on hold status except SF4 and SF5, which will be solved based on the modifications. Once, a new solution has been reached for SF4, the sub-flowsheet SF3 is entered which then resumes the calculations. When returning to the main flowsheet, all the other flowsheets (MAIN, SF1, SF2 and SF6) will resume calculations. If someone wants to move from sub-flowsheet SF4 to sub-flowsheet SF1, HYSYS automatically check the main flowsheet and updates all the calculations. Hence, the sub-flowsheet A will have the most up-to-date information. Thus, any movement to a sub-flowsheet other than the one shown not on the “branch” of the tree results a full recalculation by HYSYS.

3.12 General algebraic modeling system (GAMS)

General algebraic modeling system or GAMS is a high-level modeling system for mathematical programming, particularly for optimization models. It comprises of a language compiler called IDE (integrated development environment) and a stable of high-performance solvers. The IDE facilitates the selection of default solvers and also manages GAMS parameters on a file by file basis. GAMS can be tailored for complex, large scale modeling applications. It also allows building large models which can be adapted quickly to new situations. The general structure of GAMS

which describes the basic level steps towards optimization problem formulation is shown in Fig. 3.10.

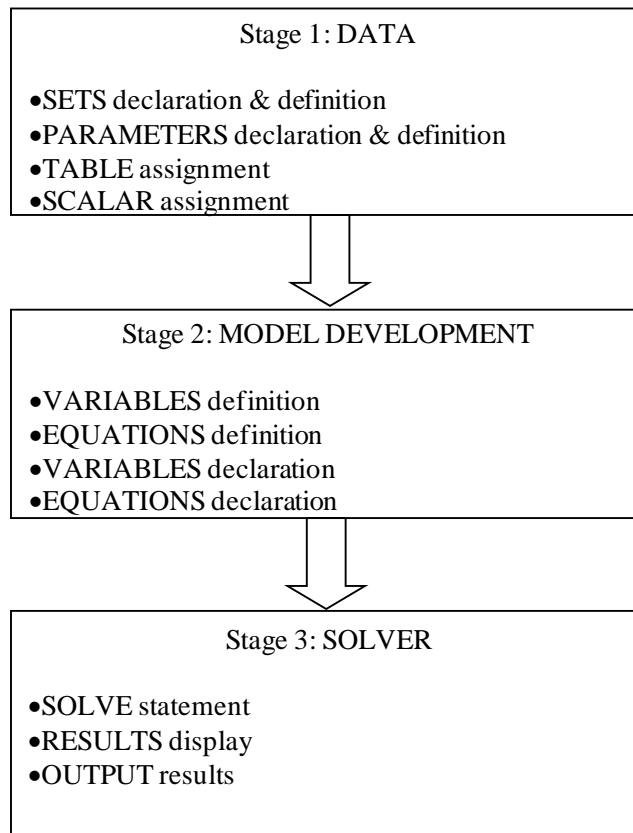


Fig 3.10: General structure of GAMS representation

One of the main features of GAMS is that the optimization problem can be expressed independently of the data it uses. The data can be represented in the form of Sets, Parameters, Table and Scalar. Such separation of data from logic statement significantly helps for a problem to be increased in size without causing any complexity. All the data in GAMS can be entered in their most elemental form. As a result, all the transformations made in constructing the model and reporting are available for inspection.

The model representation is concise and makes a full use of elegance of the mathematical expressions that are found in GAMS. The model developed should be more accessible, understandable, verifiable and also credible. After all the information has been entered and the model developed, the last step is to solve the model by choosing the appropriate solver. The GAMS statement contains all the data and

logical specifications needed to solve the model. It is also possible to alternatively shift the sequence for DATA and MODEL, while the SOLVER remains at the end in both cases [63]. GAMS contain different types of solvers based on the problem formulation whether is a linear or nonlinear problem. The main solvers used for LP and NLP problems are discussed in the following sections.

3.12.1 GAMS LP solvers

The majority of LP problems solve best using CPLEX's algorithm. GAMS/CPLEX solver allows users to combine the high level modeling capabilities of GAMS with the power of CPLEX optimizers [63]. Basically, the CPLEX optimizers are designed to quickly solve large and difficult problems with minimal user intervention. In addition, compared to other solvers, GAMS/CPLEX can automatically calculate and set options at the best values for specific problems.

Solving LP problems is a memory intensive by itself. Even though CPLEX can manage memory very efficiently; however, insufficient physical memory is one of the most common problems when running large LPs. If the memory is limited, CPLEX will automatically make algorithmic adjustments to compensate. In GAMS, the default setting option is usually used to solve the majority of LP problems. However, there are option settings to improve performance, avoid numerical difficulties and control output options. The GAMS/CPLEX solver can also provide access to the infeasibility finder. Based on this, the infeasibility finder takes an infeasible linear program and produces an irreducibly inconsistent set of constraints (IIS). GAMS/CPLEX reports the IIS in terms of GAMS equation and variable names. It also includes the IIS report as part of the normal solution listing.

3.12.2 GAMS NLP solvers

NLP problems in GAMS must be solved with a nonlinear programming algorithm. There are three standard NLP algorithms available in GAMS: CONOPT, MINOS and SNOPT. CONOPT solver is available in three versions namely, the old CONOPT, CONOPT2 and CONOPT3. The similarity among all the NLP solvers is that their

developed algorithm attempts to find a local optimum. However, the algorithms in CONOPT, MINOS and SNOPT are based on fairly different mathematical algorithms and behave differently on most models. This means that CONOPT may perform much better for some models, while MINOS or SNOPT may also be superior for some other models. As a result, it is almost difficult to choose which solver is best for a particular model especially for NLP problems [63]. However, there are some few rules of thumb used to choose the appropriate solvers. For example, GAMS/ CONOPT2 is well preferred for models with very nonlinear constraints. Besides, CONOPT2 solver can quickly find a first solution that is particularly with few degrees of freedom. On the other hand, if the model contains little nonlinearity outside the objective function, then either MINOS or SNOPT are probably the best solver.

The new version of CONOPT2 is known as CONOPT3. This solver has many new features and possibilities compared to the old versions. One of the most important new features of CONOPT3 is that it can use exact second derivatives to compute better search directions using sequential quadratic programming (SQP). There are two main consequences of the new SQP components developed in CONOPT3. The first one is that models that take much iteration can now be solved more quickly. In addition, many models with a large number of superbasic variables, which could be solved slowly, can now be solved faster and more reliably. The second important feature in CONOPT3 is a new scaling algorithm which can work better than the algorithm in CONOPT2. Furthermore, the new version CONOPT3 can solve large models than any of the old CONOPT and CONOPT2.

Thus, the overall solution strategy developed by linking HYSYS and GAMS softwares is shown in Fig. 3.11. The HYSYS model ensures the performance of the existing plant including the material and energy balance and other operating parameters too. Later, the main data are transferred from HYSYS to GAMS. The GAMS model performs the optimization task based on the information obtained from HYSYS and historical plant data. It is also possible to update the historical plant data from time to time and GAMS will solve as per the given data provided.

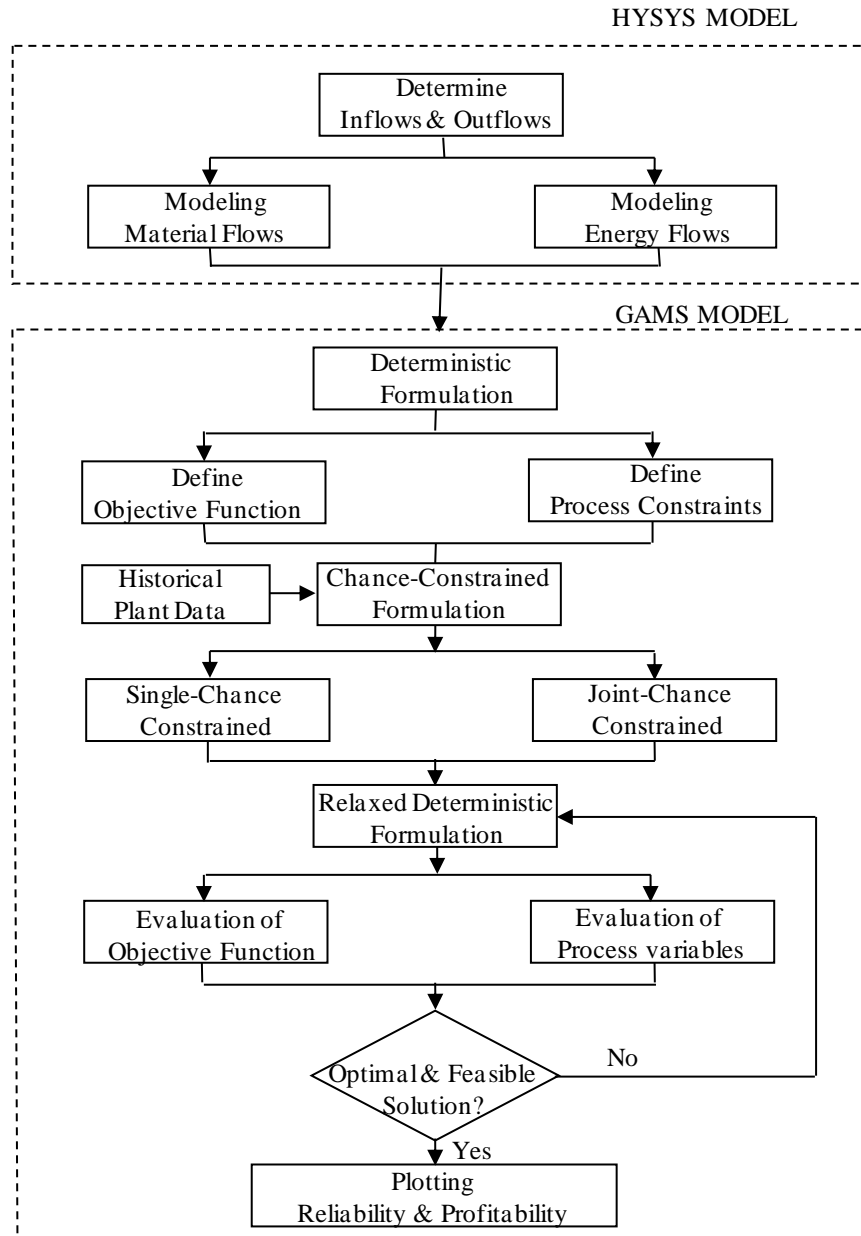


Fig. 3.11: The overall methodology developed

3.13 Summary

Determining the internal mass and energy flows is an important step for problem formulation during optimization. Formulating a deterministic problem formulation initially significantly helps to convert it to the corresponding probabilistic model. The objective function and constraints, which are the main body of the optimization problem, should be defined clearly to solve the whole optimization problem.

The relaxation of a probabilistic model mainly concentrates on evaluating the chance constraints. The evaluation technique consists of studying the property of the function that appears in the constraints. Alternative approximation methods can be used for evaluating the probability distribution to avoid computer programming. For example, there are optimization softwares which may not a built-in function to evaluate the probability distribution function. In such cases, approximation techniques with high accuracy can be used for the calculating the probability distributions function.

Once the relaxation has been made, feasibility study is performed to find the feasible set where the optimal solution lies. The feasibility study requires a step-by-step evaluation for the inverse probability distribution function. The value for inverse probability distribution function is evaluated by defining a user confidence or probability level. Based on this, the reliability of the process and the profitability can simultaneously be checked until an optimal solution for the optimization problem is found.

CHAPTER 4

RESULTS AND DISCUSSIONS

This chapter presents the main features and performance of the proposed approach which is developed in this thesis. The first case study focuses on uncertainty of feed flows from the plant inlet. The second case study considers the uncertainty of products from the plant outlet. The third case study deals with uncertain utilities, energy products flow. Based on this, a rigorous ASPEN HYSYS process model for the whole plant operation has initially been built as shown in Appendix C. The optimization models are formulated using GAMS IDE (Integrated Development Environment) version 2.0.20.0 (Module GAMS Rev 133). The solvers CPLEX 7.5 and CONOPT 3 are used for single chance constrained (LP) and joint chance constrained optimizations (NLP), respectively. The solvers are selected based on their efficient performance for the type of the LP and NLP problems as discussed in the previous chapter. For the three case studies, a historical plant data from a real plant operation is taken based on an hourly basis for a period of one year. The target in all optimization problems is to maximize the overall plant profit by taking into account the reliability of holding the process constraints.

4.1 Case study 1: Optimal operation of gas processing plant with uncertain feed flows

The simplified plant configuration involving the main processes (PTU, AGRU, LTSU and PRU) is shown in Fig. 4.1. The flows of the two feeds \hat{R}_1 and \hat{R}_2 which supplied from the upstream plant are highly uncertain. The flows of the remaining two feed R_3 and R_4 are usually known and hence can be decided. The products from the plant include sales gas (P_1), ethane (P_2), Propane product (P_3), butane (P_4), condensate (P_5) and carbon dioxide (P_6). In this case study, all the products from the plant outlet

are considered to be decided. The product recovery unit (PRU) consists of three conventional distillation columns as shown in Fig. 4.2. The arrangement of the columns follows with deethanizer as first, depropanizer second and finally debutanizer.

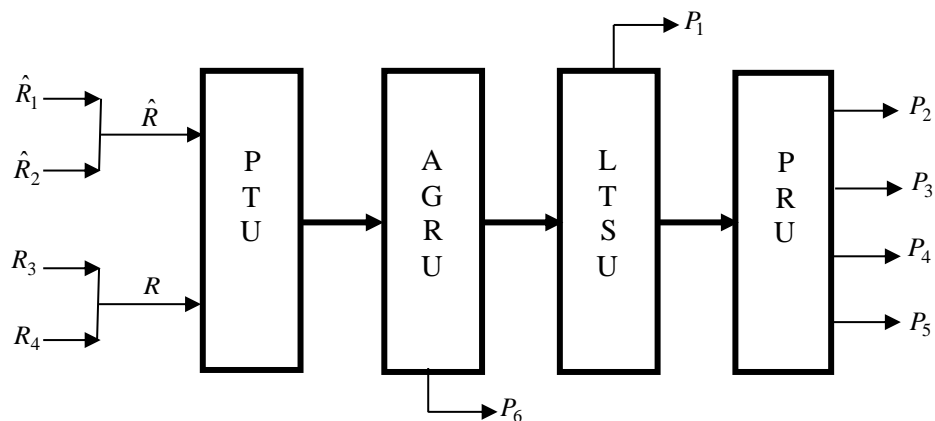


Fig 4.1: Simplified block diagram of GPP with uncertain feed flow

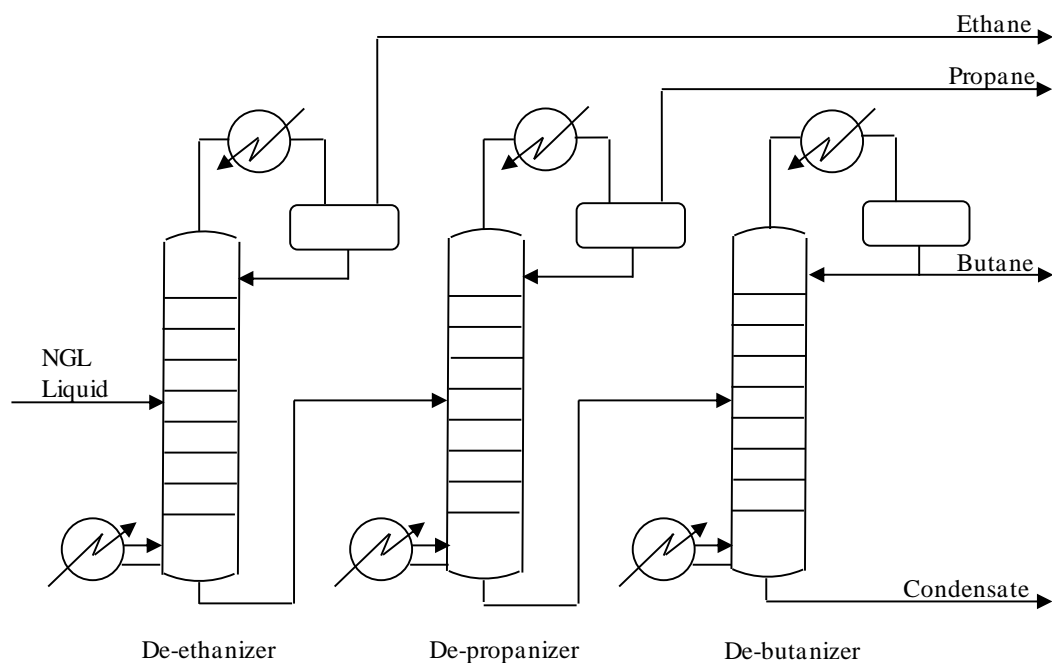


Fig 4.2: The three column arrangements in the PRU section

4.1.1 Data analysis

A large set of data for the uncertain feed flows \hat{R}_1 and \hat{R}_2 with each of around 8,785 data points on hourly basis is taken. The seven feed components ($k = 1, \dots, 7$) involved in the total uncertain feed flows \hat{R} include C_1 , C_2 , C_3 , C_{4s} , C_{5+} , N_2 and CO_2 , respectively. The normal distribution for these seven uncertain feed component inflows ($\xi_1, \xi_2, \dots, \xi_7$) is shown in Appendix D (Fig. D1 to Fig. D7). Table 4.1 shows the mean and standard deviations of the uncertain feed component inflows ($\xi_1, \xi_2, \dots, \xi_7$).

Table 4.1: Mean and standard deviations of the uncertain feed component inflows

Components (k)	Uncertain feed component inflows (ξ_k)	Mean (ton/h)	Standard deviation (ton/h)
C_1	ξ_1	190.0522	31.360
C_2	ξ_2	32.2608	5.788
C_3	ξ_3	20.782	4.289
C_{4s}	ξ_4	13.082	3.173
C_{5+}	ξ_5	9.060	3.348
N_2	ξ_6	2.439	0.656
CO_2	ξ_7	47.224	9.742

Table 4.2 shows the maximum values for the raw material and products flows which are considered as decision variables. The minimum values are set zero for all the decision variables. The expected price factor for each raw material and products is given in Table 4.3. The expected price factor for the condensate product is assumed to be nil since the plant currently does not generate revenue from this product. The price values for all the products and raw materials have been modified to keep confidentiality. The evaluation for the utilities, capital cost as well as other costs is not considered for this case study.

Table 4.2: Maximum and minimum values of decision variables for uncertain feed flow case

Raw material and products	Maximum value (ton/h)
R_3	10.706
R_4	35.586
P_1	298.518
P_2	37.311
P_3	47.706
P_4	29.586
P_5	43.111
P_6	57.659

Table 4.3: Expected price value for products and raw material

Raw material and product	Expected value (\$/ton)
\hat{R}_1	35.631
\hat{R}_2	28.871
R_3	15.132
R_4	21.441
P_1	101.941
P_2	61.031
P_3	166.712
P_4	212.013
P_5	-
P_6	-

4.1.2 Optimization

The formulations of the optimization problems follows degree of freedom analysis in which the number of variables should be greater than or equal to the number of equations and inequalities by one. The problem formulation for this case study starts by looking to the equation (3-10) to (3-16). Accordingly, for single chance constrained optimization, the total uncertain feed component flows which are held probabilistically based on equation (3-53):

For $k = 1$; C_1 component:

$$\Pr_1 \left\{ r_1^\xi = a_{1,1}P_1 + a_{1,2}P_2 + a_{1,3}P_3 + a_{1,4}P_4 + a_{1,5}P_5 + a_{1,6}P_6 - b_{1,3}R_3 - b_{1,3}R_4 \leq \xi_1 \right\} \geq a_1 \quad (4-1)$$

For $k = 2$; C_2 component:

$$\Pr_2 \left\{ r_2^\xi = a_{2,1}P_1 + a_{2,2}P_2 + a_{2,3}P_3 + a_{2,4}P_4 + a_{2,5}P_5 + a_{2,6}P_6 - b_{2,3}R_3 - b_{2,3}R_4 \leq \xi_2 \right\} \geq a_2 \quad (4-2)$$

For $k = 3$; C_3 component:

$$\Pr_3 \left\{ r_3^\xi = a_{3,1}P_1 + a_{3,2}P_2 + a_{3,3}P_3 + a_{3,4}P_4 + a_{3,5}P_5 + a_{3,6}P_6 - b_{3,3}R_3 - b_{3,3}R_4 \leq \xi_3 \right\} \geq a_3 \quad (4-3)$$

For $k = 4$; C_{4s} component:

$$\Pr_4 \left\{ r_4^\xi = a_{4,1}P_1 + a_{4,2}P_2 + a_{4,3}P_3 + a_{4,4}P_4 + a_{4,5}P_5 + a_{4,6}P_6 - b_{4,3}R_3 - b_{4,3}R_4 \leq \xi_4 \right\} \geq a_4 \quad (4-4)$$

For $k = 5$; C_{5+} component:

$$\Pr_5 \left\{ r_5^\xi = a_{5,1}P_1 + a_{5,2}P_2 + a_{5,3}P_3 + a_{5,4}P_4 + a_{5,5}P_5 + a_{5,6}P_6 - b_{5,3}R_3 - b_{5,3}R_4 \leq \xi_5 \right\} \geq a_5 \quad (4-5)$$

For $k = 6$; N_2 component:

$$\Pr_6 \left\{ r_6^\xi = a_{6,1}P_1 + a_{6,2}P_2 + a_{6,3}P_3 + a_{6,4}P_4 + a_{6,5}P_5 + a_{6,6}P_6 - b_{6,3}R_3 - b_{6,3}R_4 \leq \xi_6 \right\} \geq a_6 \quad (4-6)$$

For $k = 7$; CO₂ component:

$$\Pr_7 \left\{ r_7^\xi = a_{7,1}P_1 + a_{7,2}P_2 + a_{7,3}P_3 + a_{7,4}P_4 + a_{7,5}P_5 + a_{7,6}P_6 - b_{7,3}R_3 - b_{7,3}R_4 \leq \xi_7 \right\} \geq a_7 \quad (4-7)$$

Similarly, for joint chance constrained optimization, the probabilistic constraints in the above are held based on equation (3-57):

$$\Pr \left\{ \begin{array}{l} r_1^\xi = a_{1,1}P_1 + a_{1,2}P_2 + a_{1,3}P_3 + a_{1,4}P_4 + a_{1,5}P_5 + a_{1,6}P_6 - b_{1,3}R_3 - b_{1,3}R_4 \leq \xi_1 \\ r_2^\xi = a_{2,1}P_1 + a_{2,2}P_2 + a_{2,3}P_3 + a_{2,4}P_4 + a_{2,5}P_5 + a_{2,6}P_6 - b_{2,3}R_3 - b_{2,3}R_4 \leq \xi_2 \\ r_3^\xi = a_{3,1}P_1 + a_{3,2}P_2 + a_{3,3}P_3 + a_{3,4}P_4 + a_{3,5}P_5 + a_{3,6}P_6 - b_{3,3}R_3 - b_{3,3}R_4 \leq \xi_3 \\ r_4^\xi = a_{4,1}P_1 + a_{4,2}P_2 + a_{4,3}P_3 + a_{4,4}P_4 + a_{4,5}P_5 + a_{4,6}P_6 - b_{4,3}R_3 - b_{4,3}R_4 \leq \xi_4 \\ r_5^\xi = a_{5,1}P_1 + a_{5,2}P_2 + a_{5,3}P_3 + a_{5,4}P_4 + a_{5,5}P_5 + a_{5,6}P_6 - b_{5,3}R_3 - b_{5,3}R_4 \leq \xi_5 \\ r_6^\xi = a_{6,1}P_1 + a_{6,2}P_2 + a_{6,3}P_3 + a_{6,4}P_4 + a_{6,5}P_5 + a_{6,6}P_6 - b_{6,3}R_3 - b_{6,3}R_4 \leq \xi_6 \\ r_7^\xi = a_{7,1}P_1 + a_{7,2}P_2 + a_{7,3}P_3 + a_{7,4}P_4 + a_{7,5}P_5 + a_{7,6}P_6 - b_{7,3}R_3 - b_{7,3}R_4 \leq \xi_7 \end{array} \right\} \geq a \quad (4-8)$$

The objective functions in equation (3-28) and other constraints for single and joint chance constrained remains the same as discussed in section 3.6.1 and 3.6.2. The corresponding relaxation, equivalent deterministic formulation, for the single chance constrained optimization based on equation (3-69) becomes:

$$a_{1,1}P_1 + a_{1,2}P_2 + a_{1,3}P_3 + a_{1,4}P_4 + a_{1,5}P_5 + a_{1,6}P_6 - b_{1,3}R_3 - b_{1,3}R_4 \leq \Phi^{-1}(1-a_1) \quad (4-9)$$

$$a_{2,1}P_1 + a_{2,2}P_2 + a_{2,3}P_3 + a_{2,4}P_4 + a_{2,5}P_5 + a_{2,6}P_6 - b_{2,3}R_3 - b_{2,3}R_4 \leq \Phi^{-1}(1-a_2) \quad (4-10)$$

$$a_{3,1}P_1 + a_{3,2}P_2 + a_{3,3}P_3 + a_{3,4}P_4 + a_{3,5}P_5 + a_{3,6}P_6 - b_{3,3}R_3 - b_{3,3}R_4 \leq \Phi^{-1}(1-a_3) \quad (4-11)$$

$$a_{4,1}P_1 + a_{4,2}P_2 + a_{4,3}P_3 + a_{4,4}P_4 + a_{4,5}P_5 + a_{4,6}P_6 - b_{4,3}R_3 - b_{4,3}R_4 \leq \Phi^{-1}(1-a_4) \quad (4-12)$$

$$a_{5,1}P_1 + a_{5,2}P_2 + a_{5,3}P_3 + a_{5,4}P_4 + a_{5,5}P_5 + a_{5,6}P_6 - b_{5,3}R_3 - b_{5,3}R_4 \leq \Phi^{-1}(1-a_5) \quad (4-13)$$

$$a_{6,1}P_1 + a_{6,2}P_2 + a_{6,3}P_3 + a_{6,4}P_4 + a_{6,5}P_5 + a_{6,6}P_6 - b_{6,3}R_3 - b_{6,3}R_4 \leq \Phi^{-1}(1-a_6) \quad (4-14)$$

$$a_{7,1}P_1 + a_{7,2}P_2 + a_{7,3}P_3 + a_{7,4}P_4 + a_{7,5}P_5 + a_{7,6}P_6 - b_{7,3}R_3 - b_{7,3}R_4 \leq \Phi^{-1}(1-a_7) \quad (4-15)$$

The relaxation from the joint chance constrained optimization is given below based on equation (3-73):

$$\left[\begin{array}{l} \left(1 - \Phi(a_{1,1}P_1 + a_{1,2}P_2 + a_{1,3}P_3 + a_{1,4}P_4 + a_{1,5}P_5 + a_{1,6}P_6 - b_{1,3}R_3 - b_{1,3}R_4)\right) \\ \left(1 - \Phi(a_{2,1}P_1 + a_{2,2}P_2 + a_{2,3}P_3 + a_{2,4}P_4 + a_{2,5}P_5 + a_{2,6}P_6 - b_{2,3}R_3 - b_{2,3}R_4)\right) \\ \left(1 - \Phi(a_{3,1}P_1 + a_{3,2}P_2 + a_{3,3}P_3 + a_{3,4}P_4 + a_{3,5}P_5 + a_{3,6}P_6 - b_{3,3}R_3 - b_{3,3}R_4)\right) \\ \left(1 - \Phi(a_{4,1}P_1 + a_{4,2}P_2 + a_{4,3}P_3 + a_{4,4}P_4 + a_{4,5}P_5 + a_{4,6}P_6 - b_{4,3}R_3 - b_{4,3}R_4)\right) \\ \left(1 - \Phi(a_{5,1}P_1 + a_{5,2}P_2 + a_{5,3}P_3 + a_{5,4}P_4 + a_{5,5}P_5 + a_{5,6}P_6 - b_{5,3}R_3 - b_{5,3}R_4)\right) \\ \left(1 - \Phi(a_{6,1}P_1 + a_{6,2}P_2 + a_{6,3}P_3 + a_{6,4}P_4 + a_{6,5}P_5 + a_{6,6}P_6 - b_{6,3}R_3 - b_{6,3}R_4)\right) \\ \left(1 - \Phi(a_{7,1}P_1 + a_{7,2}P_2 + a_{7,3}P_3 + a_{7,4}P_4 + a_{7,5}P_5 + a_{7,6}P_6 - b_{7,3}R_3 - b_{7,3}R_4)\right) \end{array} \right] \geq a \quad (4-16)$$

The GAMS models developed for both single and joint chance constrained optimizations is shown in Appendix E. The model consists of sets of the raw material and products flows. In addition, parameters for the composition each raw materials and products are given at the normal plant operating conditions. The values for the total uncertain feed component flow starting from 50% to 100% confidence level is given in the developed GAMS model (case study 1). The evaluation at 100% confidence level is approximated to 0.999999, which is almost close to the value of 1.

The relation between the achievable profit and reliability to hold the constraints has been quantified for decision making purpose. The optimal profit profile under

seven single and joint chance constraints with confidence level starting from 50% to 100% is shown in Fig. 4.3. The profit profiles in Fig. 4.3 resembles to profit profile ‘PR1’ shown in Fig. 3.8 and decreases rapidly after reaching to a critical confidence level $\alpha_c = 0.95$. Accordingly, moving further from this point α_c to the right direction guarantees the reliability of the process; however, the profit decreases dramatically. On the other hand, moving from α_c to the left direction improves the profitability, but at the expense of losing the reliability of the process. This also supports the concept of Pareto optimality in which the actual choice of the optimal value depends on the relative values of reliability and expected profit. Hence, according to Pareto principle, the reliability of holding the process constraints is better only by reducing the expected profit to a certain level.

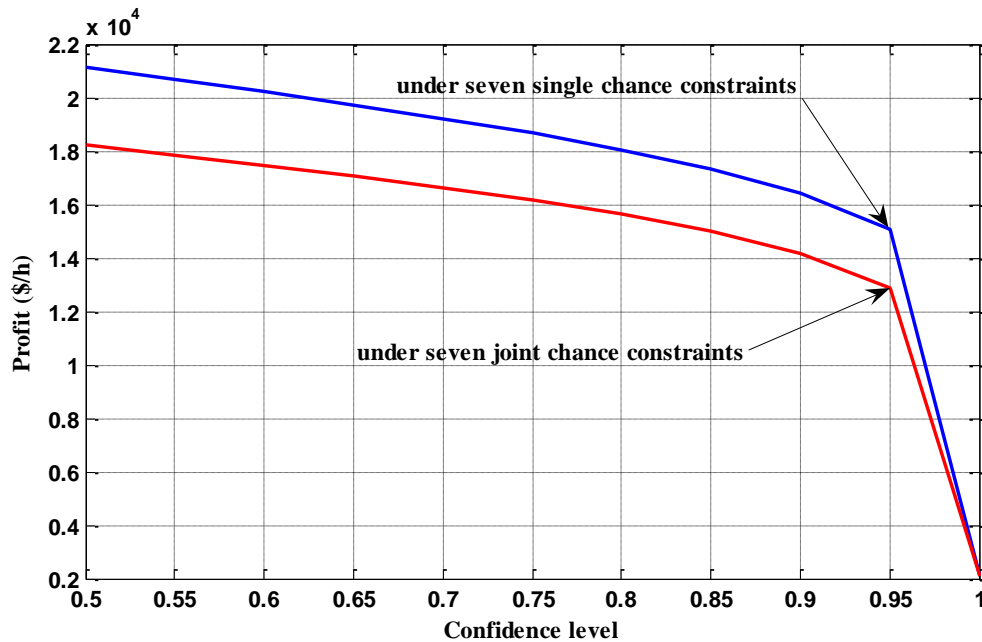


Fig 4.3: Optimal profit profiles for uncertain feed flows case

Consider an example; if someone wants to decide at 50% confidence level using single chance constrained optimization, the corresponding profit at this point is high as shown in Fig. 4.3. However, there is also a 50% probability for the violation constraints to occur. Similarly, if someone wants to decide at 75% confidence level, there is still exist 25% probability for possible violation of constraint to occur. Accordingly, there should be a trade-off for the reliability of the process and

profitability of the plant. Hence, the 95% confidence level will be a suitable choice that can compromise both reliability of the process and profitability of the plant. Thus, with this decision, there is only a 5% risk of violation of constraint. Here, it should be noted that all the seven single and joint chance constraints are measured at same the confidence level. However, it is also possible to hold each single chance constraints at different confidence level so that the optimal solution and risk of violation of constraints may also differ.

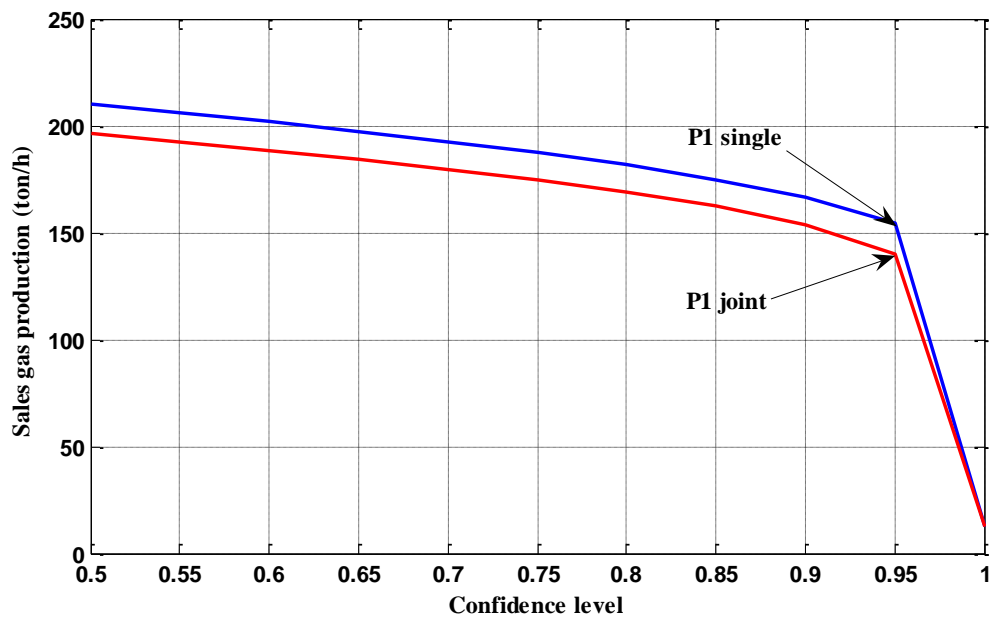


Fig 4.4: Optimal sales gas product profiles for uncertain feed flow case

The corresponding product profiles for main products: sales gas, ethane, propane and butane are shown in Fig. 4.4, 4.5, 4.6 and 4.7, respectively. The product profile for sales gas shows that the optimal decision under single and joint chance constrained optimization is not much sensitive compared to the other product profiles. This indicates that the optimal range of flow rate for sales gas under single and joint chance constrained optimization is close to each other. However, the product profile for ethane, propane and butane show that the optimal decision has relatively a significant difference under single and joint chance constrained optimization. Similarly, the product profile for condensate P_5 and carbon dioxide P_6 as well as raw material R_3 and R_4 can be plotted in same way for decision making purpose.

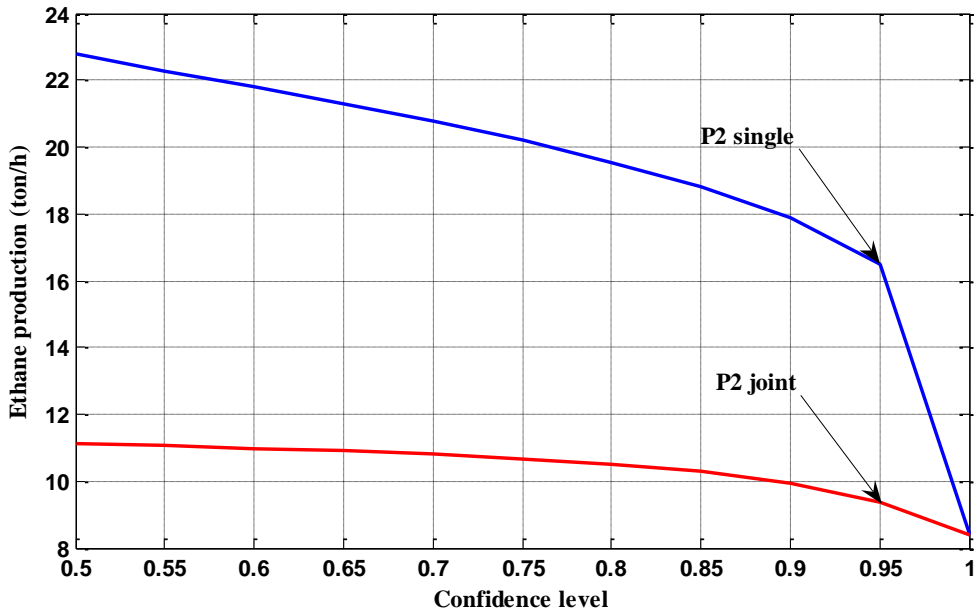


Fig 4.5: Optimal ethane product profiles for uncertain feed flow case

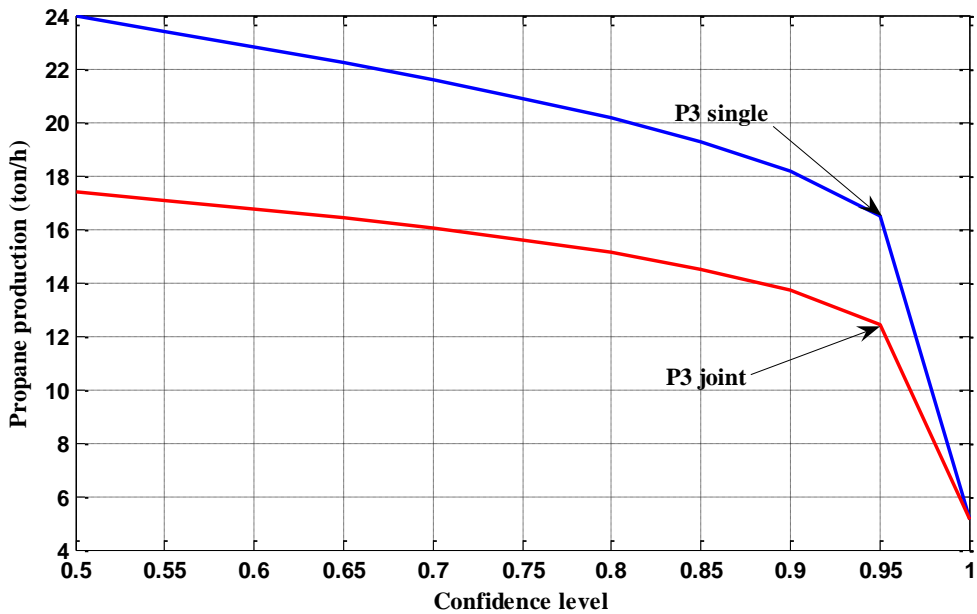


Fig 4.6: Optimal propane product profiles for uncertain feed flow case

Using the product profiles shown in Fig.4.4 to 4.7 for single chance constrained optimization, if the plant had decided to produce P_1 (sales gas) = 154 ton/h, P_2 (ethane) = 16 ton/h, P_3 (Propane) = 17 ton/h and P_4 (butane) = 10 ton/h, then with this decision, the production is satisfied with a probability of 95%. Accordingly, there

is a 5% risk that the amount of the uncertain feed component flows may not be enough to produce the desired amount of products. The corresponding profit value in Fig. 4.3 using the above decision gives \$15,095 per hour. Again using the same product profiles for joint chance constrained optimization, if the plant had decided to produce P_1 (sales gas) = 140 ton/h, P_2 (ethane) = 10 ton/h, P_3 (Propane) = 12 ton/h and P_4 (butane) = 7 ton/h, then with this decision, the production is achieved with a probability of 95%. The optimal profit value from Fig. 4.3 gives \$12,840 per hour.

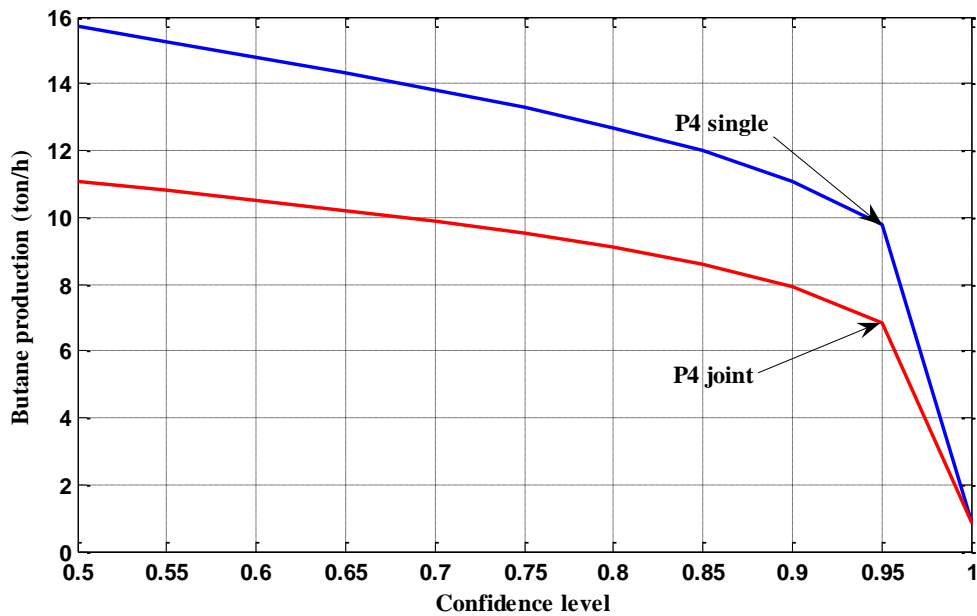


Fig 4.7: Optimal butane product profiles for uncertain feed flow case

Consider again the profit profile for single chance constrained optimization in Fig. 4. 3, if the optimal decision is to be made at 50% and 100% confidence level, the corresponding profit values result to \$21,138 per hour and \$2,088 per hour, respectively. However joint chance constrained optimization, the corresponding profit values becomes \$18,203 per hour and \$2,088 per hour, respectively. The difference in profit at 50% and 100% confidence level for single and joint chance constrained optimization give 19,050 and 16,115, respectively. The difference in profit at 50% confidence level for single and joint chance constrained optimization gives \$2,935 per hour. Such profit differences results because the single chance constrained

optimization has a more solution space than the joint chance constrained optimization as discussed in section 3.8 (Fig. 3.7).

4.1.3 Sensitivity analysis

Sensitivity analysis is performed on the profit for each uncertain feed component flows ($\xi_1, \xi_2, \dots, \xi_7$). Fig. 4.8 shows the single confidence level values assigned by the optimizer for the specified joint confidence level. From the optimization result, the optimal decision will lead to almost a 100% confidence level for ξ_2 (C_2 inflow), ξ_3 (C_3 inflow), ξ_4 (C_{4s} inflow), ξ_5 (C_{5+} inflow), ξ_6 (N_2 inflow), and ξ_7 (CO_2 inflow). However, for ξ_1 (C_1 inflow) indicates that there is a possibility for the violation of constraints to occur. Hence, there will be 11.6 % risk of violation constraint for ξ_1 .

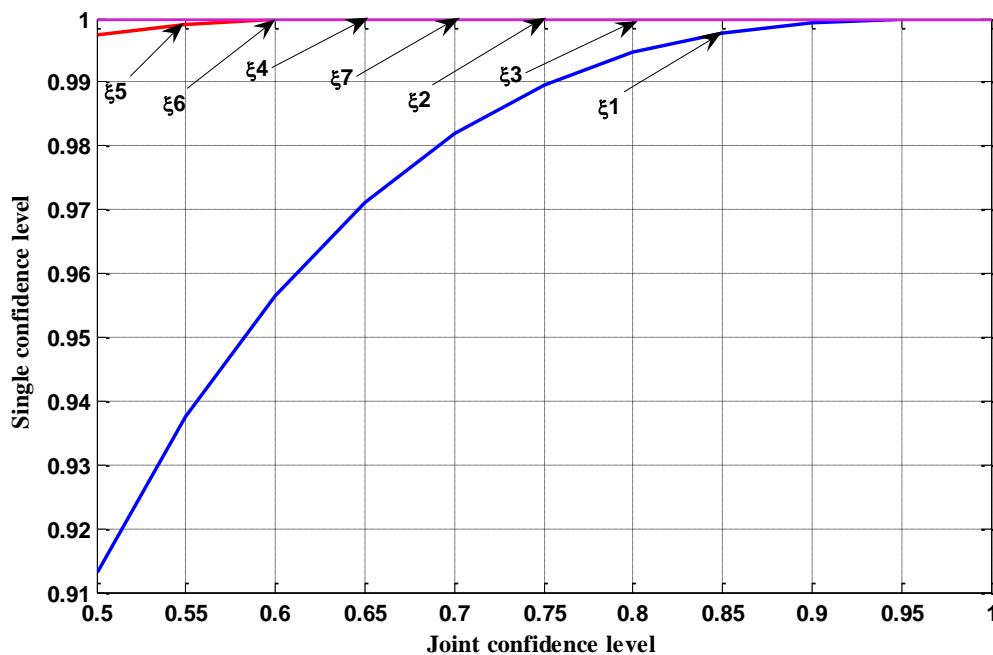


Fig 4.8: Joint vs single confidence level for uncertain feed flow case

The sensitivity analysis on profit profile for each uncertain feed component flows with respect to the specified single confidence level is shown in Fig. 4.9. The optimal result shows that the profit will not be affected if the optimal decision has to be made at 95% confidence level for ξ_1, ξ_2, ξ_3 and ξ_4 cases. However, the optimal profit

decision for ξ_5 , ξ_6 and ξ_7 show that it is not affected at different single confidence level. Such sensitivity analysis helps to identify the most critical feed with uncertainty inflow which have significant impact on the performance of the plant during the plant operation. For example, the N_2 content in the feed affects the production of sales gas by reducing its BTU value. This is because the N_2 rich gases cannot be burned due to the environmental constraint [158]. Hence, it is important to determine the optimal value of N_2 in the feed so that its effect can be minimized from environmental perspective. In addition, the optimal N_2 value also indicates the possible revenue that the plant can generate based on this decision.

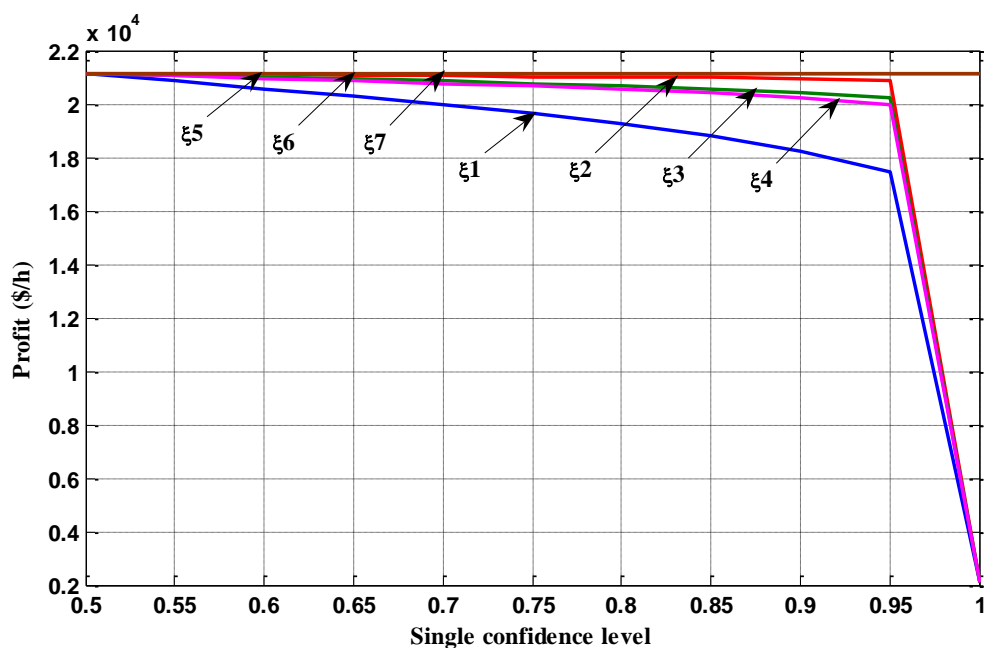


Fig 4.9: Single confidence level vs profit for uncertain feed flow case

The amount of C_{5+} in the feed also affects the performance of the plant. As the C_{5+} content in the feed increases, the LTSU section will require more compression energy. This means, the feed gas must expand to lower pressures to meet higher compressor requirements [11]. In addition, when the feed gas is rich in C_{5+} content, ethane recovery may also be halted. In such cases, the feed gas cannot produce the sufficient low temperatures required for the process and hence mechanical refrigeration is needed to maintain acceptable levels for ethane recovery [9].

The CO₂ content in the feed gas is another factor which significantly affects the plant performance by increasing the risk of plugging in the demethanizer column and reducing the BTU value of sales gas [11]. In addition, it influences ethane recovery since higher pressures are required to process more acidic gas mixtures [9]. Propane recovery has also an upper limit, which depends mainly upon the CO₂ content in the feed gas. The reason is that high CO₂ content will lower the CO₂ freeze-out temperature in the expanded vapor and continually cause plugging. The effects of this all feed component inflows have been discussed in the literature review section 2.2.1. Accordingly, different process scheme was used as an option to overcome the variation that results from feed composition.

4.1.4 Computational results

The final optimization results from deterministic, “worst case”, Two-stage programming, LSTS and LSTJ are shown in Table 4.4. The abbreviation DT represents for deterministic approach, WC is for Worst case approach and TS for two-stage programming approach. LSTS is for linear steady state with time-dependent uncertainty under single chance constraint and LSTJ is for linear steady state with time-dependent uncertainty under joint chance constraint. The superscript 1 and 2 refer to the corresponding LSTS and LSTJ cases, respectively. For example, the DT¹ represent when the deterministic optimization is compared to LSTS, while DT² represent when it is compared with LSTJ.

The optimal result for single and joint chance constrained optimization were evaluated at 98% confidence level. The corresponding optimal profit value from LSTS and LSTJ give \$15,095 per hour and \$12,840 per hour. For the deterministic case, the expected value of the uncertain feed component flow is employed. The two deterministic optimizations DT¹ and DT² show that the profit value results to \$21,138 per hour and \$18,203 per hour, respectively. However, the solution from the deterministic optimization indicates that there is a 50% probability that violation of constraints may occur.

Table 4.4: Final computational result for uncertain feed flow case

	DT ¹	DT ²	WC ¹	WC ²	TS ¹	TS ²	LSTS	LSTJ
α	0.5	0.5	0.995	0.995	0.95	0.95	0.95	0.95
Profit	21137.577	18202.923	7361.750	6318.140	15127.672	12899.138	15095.009	12840.102
r_1^{ξ}	190.055	177.763	57.620	57.184	138.472	125.154	138.472	125.181
r_2^{ξ}	32.265	20.041	14.897	8.977	22.740	14.847	138.472	22.740
r_3^{ξ}	20.782	14.631	7.915	4.921	13.727	9.861	13.727	9.853
r_4^{ξ}	13.082	8.960	3.562	1.491	7.862	5.258	7.862	5.249
r_5^{ξ}	-	-	-	-	-	-	-	-
r_6^{ξ}	1.533	1.432	0.472	0.476	1.119	1.011	1.119	1.011
r_7^{ξ}	-	-	-	-	-	-	-	-
R_3	10.706	10.706	10.706	10.706	10.706	10.706	10.706	10.706
R_4	14.059	9.957	3.847	1.785	8.509	5.909	8.509	5.897
P_1	210.291	196.626	66.480	65.800	154.114	139.495	154.114	139.523
P_2	22.771	11.123	13.889	7.847	16.487	9.326	16.487	9.369
P_3	23.939	17.140	10.497	7.295	16.504	12.417	16.504	12.408
P_4	15.727	11.068	4.879	2.537	9.782	6.839	9.782	6.827
P_5	9.203	6.548	2.591	1.225	5.609	3.926	5.609	3.918
P_6	0.547	0.716	0.684	0.770	0.639	0.744	0.639	0.743

The “worst case” strategy was evaluated by taking the nominal or expected value to be displaced by -3σ (statistical data analysis). As can be seen from Table 4.4, the ‘worst case’ strategy has resulted the optimal profit to drop drastically from \$15,095 per hour to \$ 7,362 per hour (compared with single chance constrained case) and from \$12,840 to \$ 6,318 per hour (compared with joint chance constrained case). However, the reliability of the process has reached to 99.5 % as compared to 95% single chance and joint chance constrained case. Thus, the optimization result of WC¹ and WC² prove the argument made by Li et al. [27] that the worst case strategy may seem good in holding the constraint, but the achievable profit will drop drastically.

For two-stage programming approach, the evaluation has been made based on the corresponding data from the probabilistic approach at 95% confidence level. It has been assumed that the penalty term is \$1 per ton for both TS¹ and TS² cases. The corresponding optimal profit from this decision has resulted \$15,128 per hour (compared to single chance constrained case) and \$12,899 per hour (compared to joint

chance constrained case). As discussed earlier, the solution from the two-stage programming approach does not quantify the relation between reliability and profitability. In addition, the exact values of the penalty terms are difficult to determine since they may include also some intangible components. Furthermore, it may not give a uniform measurement for the probability occurrence of the uncertain variables. This means that probability value may differ for each uncertain variable. As a result, sometimes it will be difficult to hold the constraint at a certain probability decision.

4.2 Case study 2: Optimal operation of gas processing plant with uncertain product flows

The previous case study discussed about the uncertainty of the feed supply from the plant inlet. However, on the plant outlet, there are some products such as propane and butane in which their product requirement or specifications may vary as per the demand of the customers. These two products are mostly used as feed stock for petrochemical plants. Due to seasonal variation of the products demand or for some special order which they obtain from their customers, the petrochemical plants may change the specification of their feed stock. As a result, the composition of C_2 , C_3 , C_{4s} , and C_{5+} in the products should meet the requirement in order to satisfy the customer demand.

On the other hand, during conditions such as the demand for propane is high and butane is depressed, the plant may need to shift its production mode and produce more amount of propane. This ensures the plant to continue generating high revenue under the particular demand conditions. Similarly, if the demand for LPG is high, both propane and butane will be highly required to take advantage in favor of the market condition. Moreover, it is also advantageous to use the depropanizer column as LPG column and so that the debutanizer column can be shut down for energy saving purpose. The plant configuration for this case study is shown in Fig. 4.10. The four feeds which enter the plant are represented as: R_1 , R_2 , R_3 and R_4 . The products from the plant outlet are: P_1 (sales gas), P_2 (ethane), $\hat{P}_{3,4}$ (uncertain LPG product),

P_5 (condensate) and P_6 (carbon dioxide). The product recovery unit (PRU) consists of only two conventional distillation columns as shown in Fig. 4.11. The arrangement of the columns follows with deethanizer as a first and LPG column.

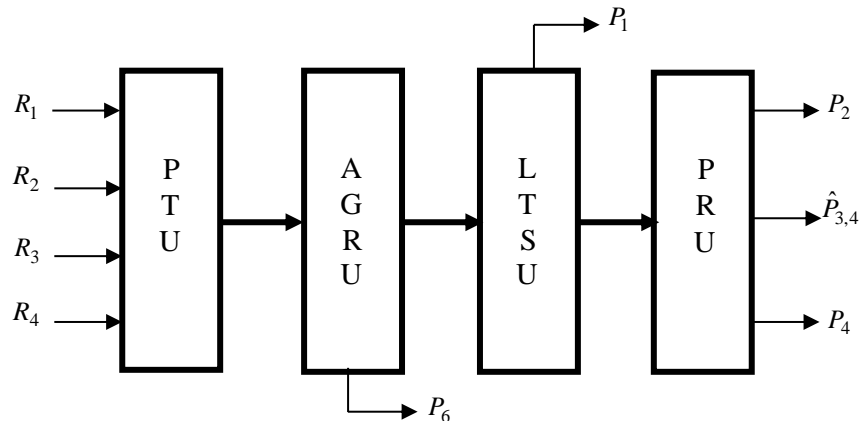


Fig 4.10: Simplified block diagram of GPP with uncertain product flow

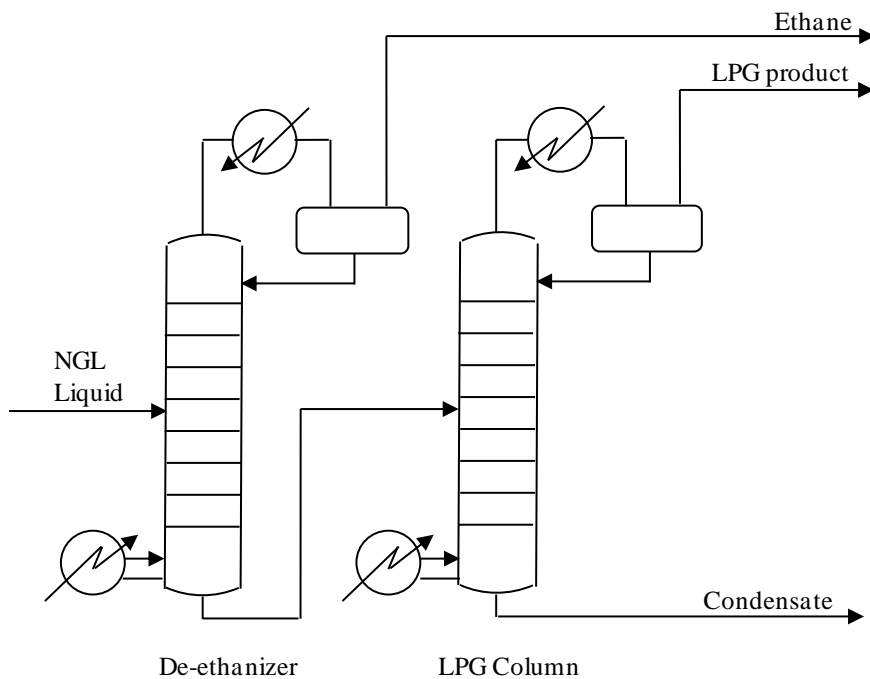


Fig 4.11: The two column arrangements in the PRU section

4.2.1 Data analysis

Similar to the previous case study, a large set of data with 8,785 data points on hourly basis for the uncertain LPG product $\hat{P}_{3,4}$ has been taken. The seven feed components ($k=1,\dots,7$) in the LPG product $\hat{P}_{3,4}$ include C_1 , C_2 , C_3 , C_{4s} , C_{5+} , N_2 and CO_2 , respectively. Here, it should be noted that the composition of C_1 , N_2 and CO_2 are all zero in the LPG product $\hat{P}_{3,4}$. Based on this, the normal distribution for the remaining uncertain product component outflows ($\zeta_2, \zeta_3, \zeta_4, \zeta_5$) is shown in Appendix D (Fig. D8 to Fig. D11). Moreover, the values of ζ_2 and ζ_5 in the LPG product $\hat{P}_{3,4}$ are usually known and sometimes can be considered as deterministic parameter. The mean and standard deviations of all the product component outflows is given in Table 4.5. The maximum values for the raw material and products flows which are taken as decision variables is given in Table 4.6, while their minimum value is set zero. The expected price factor shown in Table 4.3 remains the same except for LPG product $\hat{P}_{3,4}$ which is \$ 189.362 per ton. The cost evaluations for utilities, capital as well as others are not considered for this case study.

Table 4.5: Mean and standard deviations of the uncertain product component outflow

Components (k)	Uncertain product component outflows (ζ_k)	Mean (ton/h)	Standard deviation (ton/h)
C_1	ζ_1	-	-
C_2	ζ_2	0.291	0.153
C_3	ζ_3	24.486	5.027
C_{4s}	ζ_4	15.66	2.780
C_{5+}	ζ_5	0.156	0.136
N_2	ζ_6	-	-
CO_2	ζ_7	-	-

Table 4.6: Maximum and minimum values of decision variables for uncertain product flow case

Raw material and products	Maximum value (ton/h)
R_1	334.582
R_2	220.314
R_3	10.706
R_4	35.586
P_1	298.518
P_2	37.311
P_5	43.111
P_6	57.659

4.2.2 Optimization

The problem formulation for this case study starts from the basic equations (3-10) to (3-16). For the single chance constrained optimization, the probabilistic constraints can be described based on equation (3-54):

For $k = 1$; C_1 component:

$$\Pr_1 \left\{ p_1^\zeta = b_{1,1}R_1 + b_{1,2}R_2 + b_{1,3}R_3 + b_{1,4}R_4 - a_{1,1}P_1 - a_{1,2}P_2 - a_{1,5}P_5 - a_{1,6}P_6 \geq \zeta_1 \right\} \geq a_1 \quad (4-17)$$

For $k = 2$; C_2 component:

$$\Pr_2 \left\{ p_2^\zeta = b_{2,1}R_1 + b_{2,2}R_2 + b_{2,3}R_3 + b_{2,4}R_4 - a_{2,1}P_1 - a_{2,2}P_2 - a_{2,5}P_5 - a_{2,6}P_6 \geq \zeta_2 \right\} \geq a_2 \quad (4-18)$$

For $k = 3$; C_3 component:

$$\Pr_3 \left\{ p_3^\zeta = b_{3,1}R_1 + b_{3,2}R_2 + b_{3,3}R_3 + b_{3,4}R_4 - a_{3,1}P_1 - a_{3,2}P_2 - a_{3,5}P_5 - a_{3,6}P_6 \geq \zeta_3 \right\} \geq a_3 \quad (4-19)$$

For $k = 4$; C_{4s} component:

$$\Pr_4 \left\{ p_4^\zeta = b_{4,1}R_1 + b_{4,2}R_2 + b_{4,3}R_3 + b_{4,4}R_4 - a_{4,1}P_1 - a_{4,2}P_2 - a_{4,5}P_5 - a_{4,6}P_6 \geq \zeta_4 \right\} \geq a_4 \quad (4-20)$$

For $k = 5$; C_{5+} component:

$$\Pr_5 \left\{ p_5^\zeta = b_{5,1}R_1 + b_{5,2}R_2 + b_{5,3}R_3 + b_{5,3}R_4 - a_{5,1}P_1 - a_{5,2}P_2 - a_{5,5}P_5 - a_{5,6}P_6 \geq \zeta_5 \right\} \geq a_5 \quad (4-21)$$

For $k = 6$; N_2 component:

$$\Pr_6 \left\{ p_6^\zeta = b_{6,1}R_1 + b_{6,2}R_2 + b_{6,3}R_3 + b_{6,3}R_4 - a_{6,1}P_1 - a_{6,2}P_2 - a_{6,5}P_5 - a_{6,6}P_6 \geq \zeta_6 \right\} \geq a_6 \quad (4-22)$$

For $k = 7$; CO_2 component:

$$\Pr_7 \left\{ p_7^\zeta = b_{7,1}R_1 + b_{7,2}R_2 + b_{7,3}R_3 + b_{7,3}R_4 - a_{7,1}P_1 - a_{7,2}P_2 - a_{7,5}P_5 - a_{7,6}P_6 \geq \zeta_7 \right\} \geq a_7 \quad (4-23)$$

The joint chance constrained formulation based on equation (3-58) becomes:

$$\Pr \left\{ \begin{array}{l} p_1^\zeta = b_{1,1}R_1 + b_{1,2}R_2 + b_{1,3}R_3 + b_{1,4}R_4 - a_{1,1}P_1 - a_{1,2}P_2 - a_{1,5}P_5 - a_{1,6}P_6 \geq \zeta_1 \\ p_2^\zeta = b_{2,1}R_1 + b_{2,2}R_2 + b_{2,3}R_3 + b_{2,4}R_4 - a_{2,1}P_1 - a_{2,2}P_2 - a_{2,5}P_5 - a_{2,6}P_6 \geq \zeta_2 \\ p_3^\zeta = b_{3,1}R_1 + b_{3,2}R_2 + b_{3,3}R_3 + b_{3,4}R_4 - a_{3,1}P_1 - a_{3,2}P_2 - a_{3,5}P_5 - a_{3,6}P_6 \geq \zeta_3 \\ p_4^\zeta = b_{4,1}R_1 + b_{4,2}R_2 + b_{4,3}R_3 + b_{4,4}R_4 - a_{4,1}P_1 - a_{4,2}P_2 - a_{4,5}P_5 - a_{4,6}P_6 \geq \zeta_4 \\ p_5^\zeta = b_{5,1}R_1 + b_{5,2}R_2 + b_{5,3}R_3 + b_{5,3}R_4 - a_{5,1}P_1 - a_{5,2}P_2 - a_{5,5}P_5 - a_{5,6}P_6 \geq \zeta_5 \\ p_6^\zeta = b_{6,1}R_1 + b_{6,2}R_2 + b_{6,3}R_3 + b_{6,3}R_4 - a_{6,1}P_1 - a_{6,2}P_2 - a_{6,5}P_5 - a_{6,6}P_6 \geq \zeta_6 \\ p_7^\zeta = b_{7,1}R_1 + b_{7,2}R_2 + b_{7,3}R_3 + b_{7,3}R_4 - a_{7,1}P_1 - a_{7,2}P_2 - a_{7,5}P_5 - a_{7,6}P_6 \geq \zeta_7 \end{array} \right\} \geq a \quad (4-24)$$

The objective function follows the one described in equation (3-35). The corresponding relaxation for the single chance constrained case based on equation (3-70) becomes:

$$b_{1,1}R_1 + b_{1,2}R_2 + b_{1,3}R_3 + b_{1,4}R_4 - a_{1,1}P_1 - a_{1,2}P_2 - a_{1,5}P_5 - a_{1,6}P_6 \geq \Phi^{-1}(a_1) \quad (4-25)$$

$$b_{2,1}R_1 + b_{2,2}R_2 + b_{2,3}R_3 + b_{2,4}R_4 - a_{2,1}P_1 - a_{2,2}P_2 - a_{2,5}P_5 - a_{2,6}P_6 \geq \Phi^{-1}(a_2) \quad (4-26)$$

$$b_{3,1}R_1 + b_{3,2}R_2 + b_{3,3}R_3 + b_{3,4}R_4 - a_{3,1}P_1 - a_{3,2}P_2 - a_{3,5}P_5 + a_{3,6}P_6 \geq \Phi^{-1}(a_3) \quad (4-27)$$

$$b_{4,1}R_1 + b_{4,2}R_2 + b_{4,3}R_3 + b_{4,4}R_4 - a_{4,1}P_1 - a_{4,2}P_2 - a_{4,5}P_5 - a_{4,6}P_6 \geq \Phi^{-1}(a_4) \quad (4-28)$$

$$b_{5,1}R_1 + b_{5,2}R_2 + b_{5,3}R_3 + b_{5,3}R_4 - a_{5,1}P_1 - a_{5,2}P_2 - a_{5,5}P_5 - a_{5,6}P_6 \geq \Phi^{-1}(a_5) \quad (4-29)$$

$$b_{6,1}R_1 + b_{6,2}R_2 + b_{6,3}R_3 + b_{6,3}R_4 - a_{6,1}P_1 - a_{6,2}P_2 - a_{6,5}P_5 - a_{6,6}P_6 \geq \Phi^{-1}(a_6) \quad (4-30)$$

$$b_{7,1}R_1 + b_{7,2}R_2 + b_{7,3}R_3 + b_{7,3}R_4 - a_{7,1}P_1 - a_{7,2}P_2 - a_{7,5}P_5 - a_{7,6}P_6 \geq \Phi^{-1}(a_7) \quad (4-31)$$

The relaxation for the joint chance constrained optimization based on equation (3-74) is given as:

$$\left[\begin{array}{l} \left(\Phi(b_{1,1}R_1 + b_{1,2}R_2 + b_{1,3}R_3 + b_{1,4}R_4 - a_{1,1}P_1 - a_{1,2}P_2 - a_{1,5}P_5 - a_{1,6}P_6) \right) \\ \left(\Phi(b_{2,1}R_1 + b_{2,2}R_2 + b_{2,3}R_3 + b_{2,4}R_4 - a_{2,1}P_1 - a_{2,2}P_2 - a_{2,5}P_5 - a_{2,6}P_6) \right) \\ \left(\Phi(b_{3,1}R_1 + b_{3,2}R_2 + b_{3,3}R_3 + b_{3,4}R_4 - a_{3,1}P_1 - a_{3,2}P_2 - a_{3,5}P_5 - a_{3,6}P_6) \right) \\ \left(\Phi(b_{4,1}R_1 + b_{4,2}R_2 + b_{4,3}R_3 + b_{4,4}R_4 - a_{4,1}P_1 - a_{4,2}P_2 - a_{4,5}P_5 - a_{4,6}P_6) \right) \\ \left(\Phi(b_{6,1}R_1 + b_{6,2}R_2 + b_{6,3}R_3 + b_{6,3}R_4 - a_{6,1}P_1 - a_{6,2}P_2 - a_{6,5}P_5 - a_{6,6}P_6) \right) \\ \left(\Phi(b_{5,1}R_1 + b_{5,2}R_2 + b_{5,3}R_3 + b_{5,3}R_4 - a_{5,1}P_1 - a_{5,2}P_2 - a_{5,5}P_5 - a_{5,6}P_6) \right) \\ \left(\Phi(b_{7,1}R_1 + b_{7,2}R_2 + b_{7,3}R_3 + b_{7,3}R_4 - a_{7,1}P_1 - a_{7,2}P_2 - a_{7,5}P_5 - a_{7,6}P_6) \right) \end{array} \right] \geq a \quad (4-32)$$

The GAMS optimization model developed for both single and joint chance constrained optimization is shown in Appendix E. The model consists of the set of raw materials flows and products. The values for the uncertain LPG product component outflows starting from 50% to 100 % confidence level (0.999999) is also given for evaluation purpose. The optimal profit profiles starting from 96% to 100% confidence level for the single and joint chance constrained optimization cases are shown in Fig. 4.12. The profit is taken at 96% confidence level because it starts to show a significant change within this range. Comparing this profit profile with the one shown in Fig. 4.3, the change in profit for uncertainty from the plant inlet is much more significant than that of the plant outlet.

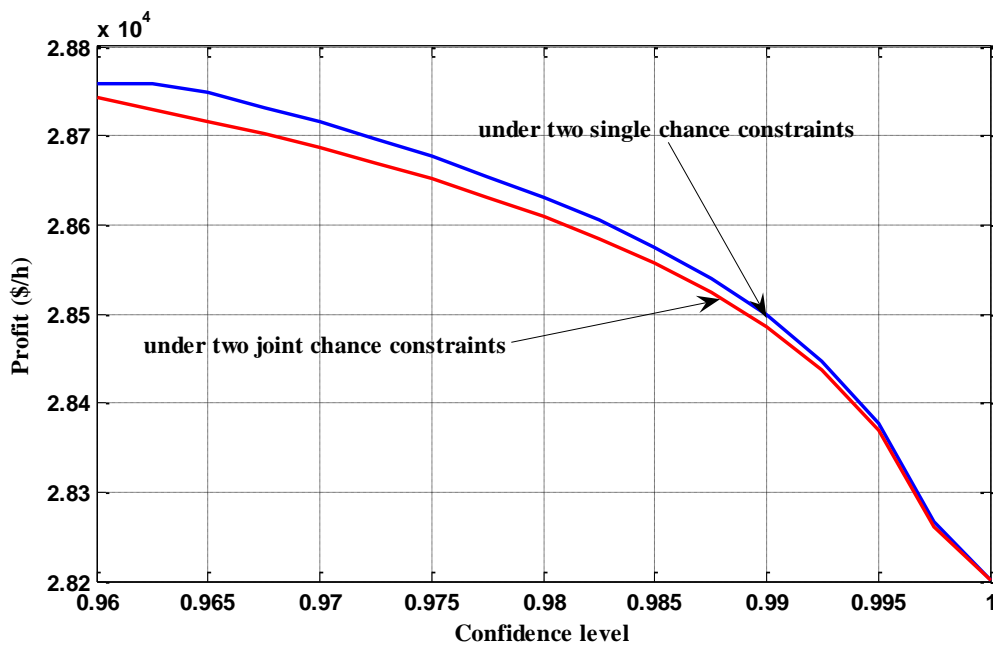


Fig 4.12: Optimal profit profiles for uncertain product flows case

For further explanation, consider the single chance constrained profile shown in Fig. 4.3, the profit values at 96% and 100% confidence level are \$14,706 per hour and \$2,088 per hour, respectively. Accordingly, the profit has been changed by 85.8% as moving from 96% to 100% confidence level. However, if we take the same data at 96% and 100% confidence level for single chance constrained optimization case from Fig. 4.12; the corresponding profit values become \$28,758 per hour and \$ 28,201 per

hour, respectively. The profit has been changed this time only by 1.93% as moving from 96% to 100% confidence level.

The corresponding product profiles for sales gas, ethane and LPG product are shown in Fig. 4.13, 4.14 and 4.15, respectively. The sales gas product profile shows that the production decision remains the same for both single and joint chance constrained optimizations. Moreover, the decision can be made at any of the confidence level in between 96% to 100%. The product profile for ethane production shows that the production is increasing, for both single and joint chance constrained optimization, as the confidence level reaches to 100%. Thus, the decision can be made in the higher confidence region around 99.75% with 0.25% risk.

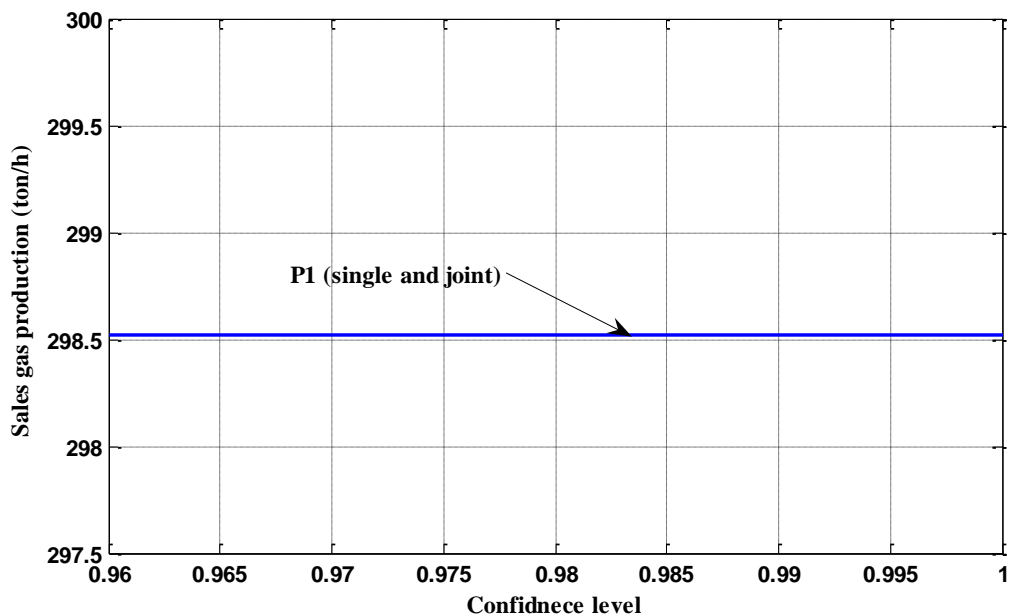


Fig 4.13: Optimal sales gas product profiles for uncertain product flows case

The resulting optimal product profile for LPG product from both single and joint optimization is shown in Fig. 4.14. The optimal LPG product produced from this case study has been compared with that of propane and butane products produced in case study one. Consider Table 4.4 again, the optimal decision from LSTS for propane and butane products evaluated at 95% confidence level give 16 ton per hour and 10 ton per hour, respectively. Based on this, the total propane and butane product produced at the specified confidence level becomes 26 ton per hour. However, the optimal

decision for LPG product from single chance constrained optimization gives 136 ton per hour. Accordingly, the LPG production has increased by 81% increment compared with the combined production of propane and butane in case study one.

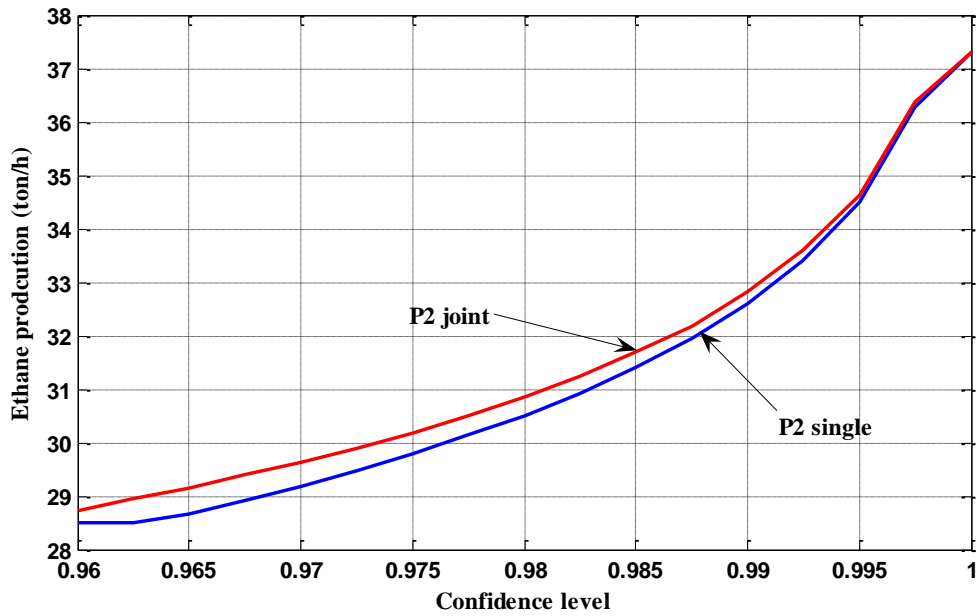


Fig 4.14: Optimal ethane product profiles for uncertain product flows case

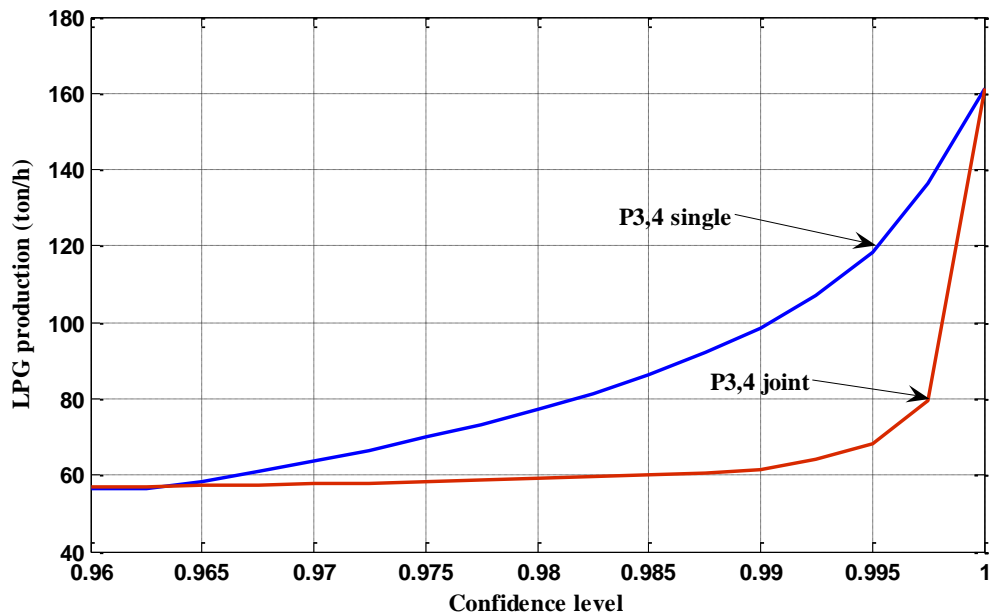


Fig 4.15: Optimal LPG product profile for uncertain product flow case

This is due to the fact that in the previous case study, the propane and butane products were considered as decision variable in which their upper and lower limit are known. However, the LPG product in this case study is taken as uncertain variable where there is no upper and lower limit specified. Hence, the optimizer gives the maximum possible production of LPG by considering all the other constraints.

4.2.3 Sensitivity analysis

The sensitivity analysis has been made for the uncertain product components ζ_1 and ζ_7 as shown in Fig. 4.16. Such sensitivity analysis is made by varying the joint chance confidence level starting from 96% to 100%. The corresponding single confidence level is obtained based on the specified joint confidence level. For example, at 96% confidence level, the profit value from the joint chance constrained optimization is \$28,743 per hour. This profit value is depicted in the single chance constrained optimization and the corresponding single confidence level is then taken.

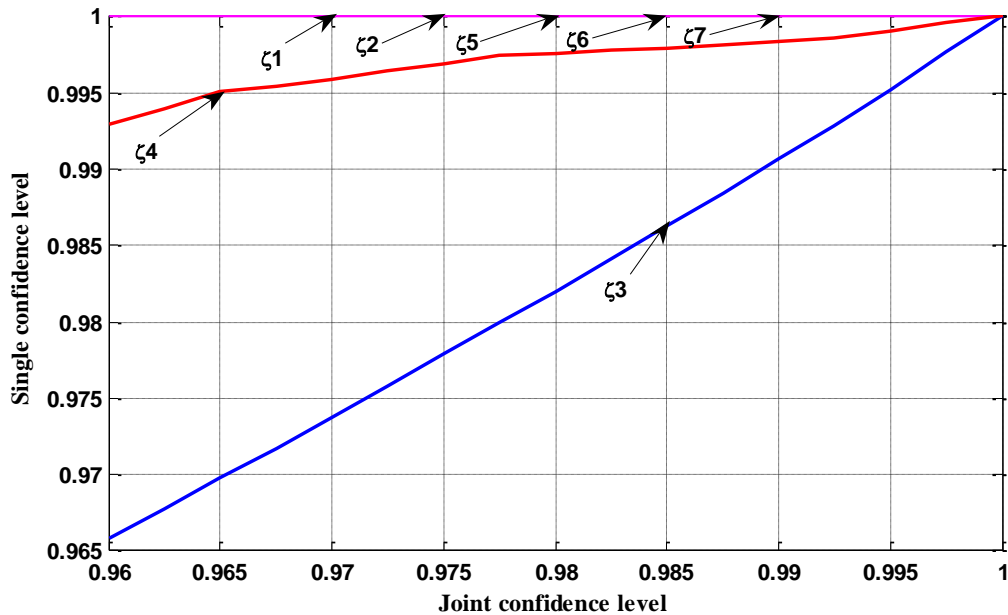


Fig 4.16: Joint vs single confidence level for uncertain product flow case

Based on this, the sensitivity analysis result from ζ_3 and ζ_4 show that the corresponding single confidence level increases linearly as the joint chance

constrained varies. As a result, the decision from ζ_3 and ζ_4 may violate the constraint by 0.035% and 0.0069%, respectively. The sensitivity analysis result for the remaining product components ($\zeta_1, \zeta_2, \zeta_5, \zeta_6$ and ζ_7) are constant since their values are very small and usually known.

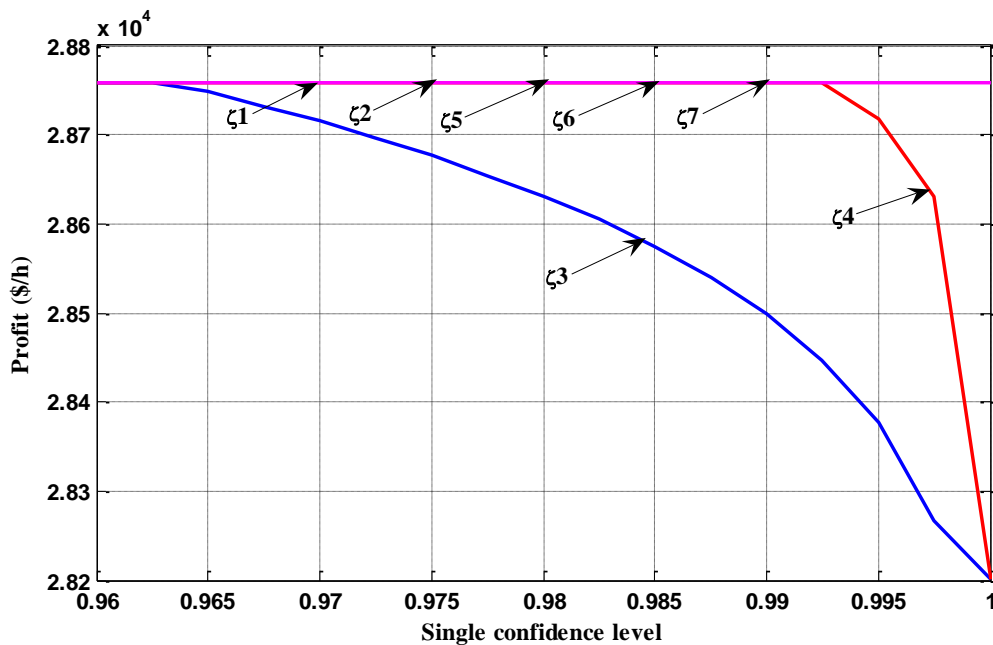


Fig 4.17: Single confidence level vs profit for uncertain product flow case

The sensitivity analysis for profit by varying the single confidence level is shown in Fig. 4.17. Such sensitivity analysis is made by varying each individual constraint separately starting from 96% to 10% confidence level. The profit profile for ζ_3 and ζ_4 show that how these two uncertain variables can affect the profit value. Sensitivity result from the remaining product components ($\zeta_1, \zeta_2, \zeta_5, \zeta_6$ and ζ_7) show that the profit value remains constant since the value of these components are usually small and their content in LPG product is almost negligible.

4.2.4 Computational results

The final computational results for the uncertain product flows case are shown in Table 4.7. The optimization is performed for deterministic, “worst case”, two-stage

programming, single and joint chance constrained cases. The optimal decision from the deterministic (DT^1 and DT^2), “worst case” (WC^1 and WC^2), two stage programming (TW^1 and TW^2) are all compared with LSTS and LSTJ. The indices 1 and 2 represent when each of the optimization compared to the single and joint chance constrained optimization cases, respectively. The decision for deterministic optimization is based on considering the expected or nominal values of the uncertain variables, while for the “worst case” approach, the nominal values are taken to be displaced by $+3\sigma$ (statistical data analysis). The two-stage optimization is evaluated by assuming 1\$/ton penalty term and taking the same data at the specified confidence level from the corresponding LSTS and LSTJ. It should be noted that the profit value in Table 4.7 is given in \$ per hour and all the flow rates are in ton per hour.

Table 4-7: Final optimization result for uncertain product flow case

	DT ¹	DT ²	WC ¹	WC ²	TS ¹	TS ²	LSTS	LSTJ
α	0.5	0.5	0.9978	0.9978	0.9975	0.9975	0.9975	0.9975
Profit	28758.780	28742.954	28208.061	28203.131	28263.226	28258.320	28265.908	28261.088
p_1^ζ	-	-	-	-	-	-	-	-
p_2^ζ	0.291	0.291	0.291	0.291	0.291	0.291	0.291	0.291
p_3^ζ	33.485	33.650	39.198	39.249	38.598	38.648	38.598	38.648
p_4^ζ	22.528	22.645	26.586	26.622	26.160	26.195	26.160	26.195
p_5^ζ	0.156	0.156	0.156	0.156	0.156	0.156	0.156	0.156
p_6^ζ	-	-	-	-	-	-	-	-
p_7^ζ	-	-	-	-	-	-	-	-
P_1	298.518	298.518	298.518	298.518	298.518	298.518	298.518	298.518
P_2	28.488	28.739	37.202	37.280	36.287	36.363	36.287	36.363
P_5	31.571	31.625	33.468	33.485	33.268	33.285	33.268	33.285
P_6	-	2.287	79.580	80.293	71.221	71.918	71.221	71.918
R_1	334.582	334.582	334.582	334.582	334.582	334.582	334.582	334.582
R_2	34.163	37.036	134.124	135.019	123.624	124.499	123.624	124.499
R_3	10.706	10.706	10.706	10.706	10.706	10.706	10.706	10.706
R_4	35.586	35.586	35.586	35.586	35.586	35.586	35.586	35.586

The optimal LPG product component flow rates (p_1^ζ to p_2^ζ) have been shown also in Table 4.7 together with the remaining product and raw material flow rates. The flow rate of p_1^ζ (C₁ flow in LPG), p_6^ζ (N₂ flow in LPG), p_7^ζ (CO₂ flow in LPG) are all zero. It can be seen from Table 4.7 that the component flow rates p_3^ζ (C₃ flow in LPG) and p_4^ζ (C_{4s} flow in LPG) vary for each of the cases. Thus, the optimal profit values at 99.75 % confidence level from LSTS and LSTJ optimization gives \$28,266 per hour and \$ 28,261 per hour, respectively. The optimal decision ensures the reliability of holding all the constraints by 99.75% with only having a 0.25% risk of violation of constraints.

4.3 Case study 3: Optimal operation of gas processing plant with uncertain utility and energy product flows

The utility and energy product flows are other factors that are uncertain in the future time period. The utility flow which is supplied from the nearby cogeneration plant varies from time to time. As a result, the energy product produced from the plant will also vary. In addition, problem may result also during the plant operation due to the continuous variation of the operating points [12, 13]. Sometimes, the planned operating point has to be changed; hence an adjustment of the planned operating point has to be made. This time, a conservative decision by specifying a higher confidence level has the advantage of keeping a more stable operation [24]. Hence, it is important to make a decision in such situations so that the optimal decision will be implemented in the future time period.

In this case study, a large scale optimization model has been developed using GAMS. The developed model consists of a number of operating parameters, utility and energy product flows. The inflow and outflow variables are related using equation obtained from rigorous HYSYS simulation as shown in Appendix C. The costs for utilities such as steam, cooling water, compression, refrigeration, electricity and fuel have been incorporated in the model. A short cut design approach for the distillation columns, in the product recovery unit, has also been included to calculate the energy

requirement. The model developed using GAMS consists of 175 equations and 170 variables. The GAMS code is shown in Appendix E.

4.3.1 Optimization

The optimization in this case study is performed by taking both the uncertain utility and energy product flows simultaneously. Accordingly, the heat inflows resulted from the uncertain utility are represented as $\varepsilon_1, \varepsilon_2, \varepsilon_3, \varepsilon_4, \varepsilon_5$ and ε_6 . These uncertain heat inflows are from raw material, steam, refrigerant, compression, electricity and fuel, respectively. Similarly, the heat outflows from the energy product include $\zeta_1, \zeta_2, \zeta_3$ and ζ_4 . These uncertain heat outflows are due to using cooling water, refrigeration process, using sales gas as a cooler and heat resulted from material product produced, respectively.

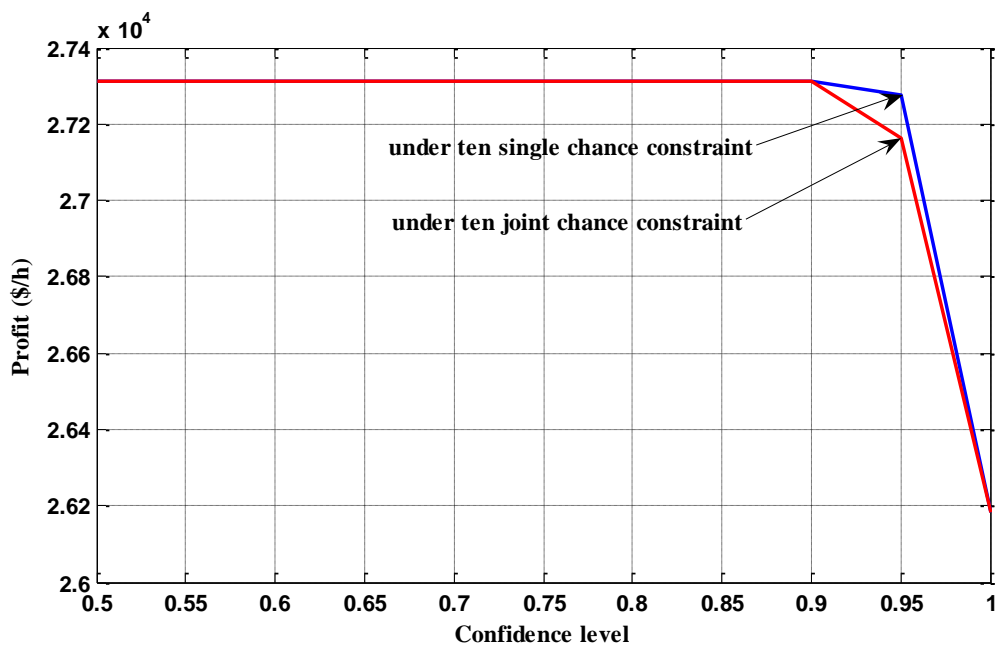


Fig 4.18: Optimal Profit profile with specified confidence level

The optimal profit profile for both single and joint chance constrained optimization is shown in Fig. 4.18. The profit profile for both cases is constant until it reaches to a certain confidence level. The decision maker may have the option to decide starting from 50% confidence level until to 90% confidence level. All the

decision made in this range is constant and does not affect the profit. Here, it should be noted that the decision for both the single and joint chance constrained optimization remains the same until 90% confidence level. However, the profit starts to decrease slightly after 90% confidence level until it reaches to 95% confidence level for both cases. After 95% confidence level, the profit drastically drops and this point is considered as an optimal value. Thus, comparing this profit profile to those obtained in case study one and two, the profit change in this case study appears to be less sensitive. This shows that the material flows have a more significant effect on the performance measured against the objective function.

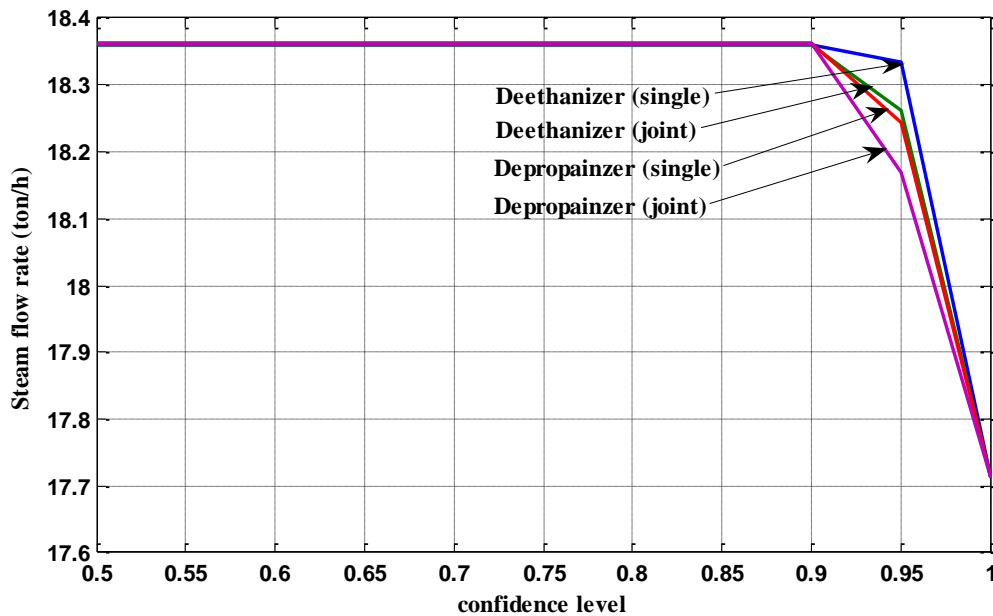


Fig 4.19: Optimal steam flow rate with specified confidence level

The optimal steam flow rate for the deethanizer and depropanizer columns under single and joint chance constrained optimization is shown in Fig. 4.19. The deethanizer first process the NGL liquid product that comes from the demethanizer column as shown in Appendix C (product recovery unit). As a result, the steam consumption rate for deethanizer column is usually high compared to the other columns. The bottom feed from the deethanizer column is combined with another feed coming from the condensate treatment unit to be processed in the depropanizer column. It can be seen from Fig. 4.19 that the steam requirement for both deethanizer and depropanizer column is same up to 90% confidence level. The steam flow rate

starts to slightly decrease from 90% to 95% confidence level. From 95% to 100% confidence level, the steam flow rate drops significantly and the optimal decision is made at 95% confidence level. Furthermore, the temperature required for the steam supply should also be considered carefully. This is because the thermal stability of the components in the mixtures to be separated. Some components are not stable at their normal boiling point. Hence, a maximum allowable temperature should be specified to make the separation ease.

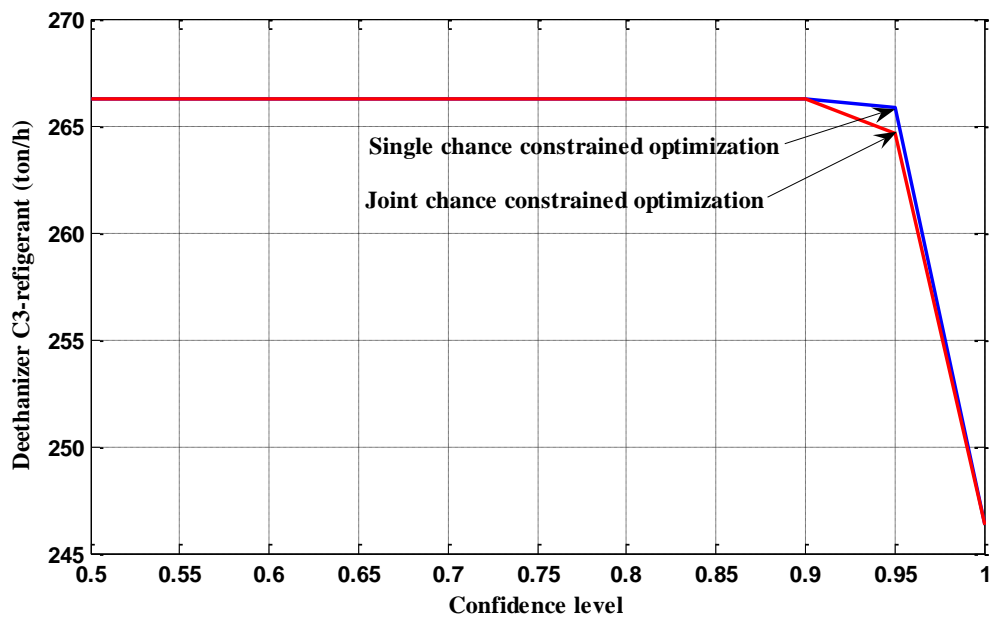


Fig 4.20: Optimal C₃-refrigerant flow rate with specified confidence level

The corresponding C₃-refrigerant and cooling water consumption rate for deethanizer and depropanizer condensers are shown in Fig. 4.20 and 4.21, respectively. The C₃-refrigerant is used for deethanizer column to cool the ethane product. Such refrigerant is used because cooling water could not sufficiently condense the ethane product. However, for the depropanizer column, the propane product produced can be condensed with the supplied cooling water. Sometimes, the depropanizer condenser duty becomes high and as a result it requires more cooling water. This is due to the additional feed coming from the condensate treatment unit. This feed normally contains C₃₊ and usually affects the operation of the depropanizer column. In industrial practice, it is common to estimate and adjust the reflux ratio in order to keep the stable operation of the column. However, the reflux ratio should be

estimated based on certain knowledge than a common practice which involves trial approach. For example, the reflux ratio sometimes goes higher and as a result the reflux rate increases. This in turn may halt the amount of propane product produced. Hence, it is important to estimate the minimum reflux ratio based on CMO approximation and obtain the possible optimal reflux ratio to overcome such problems.

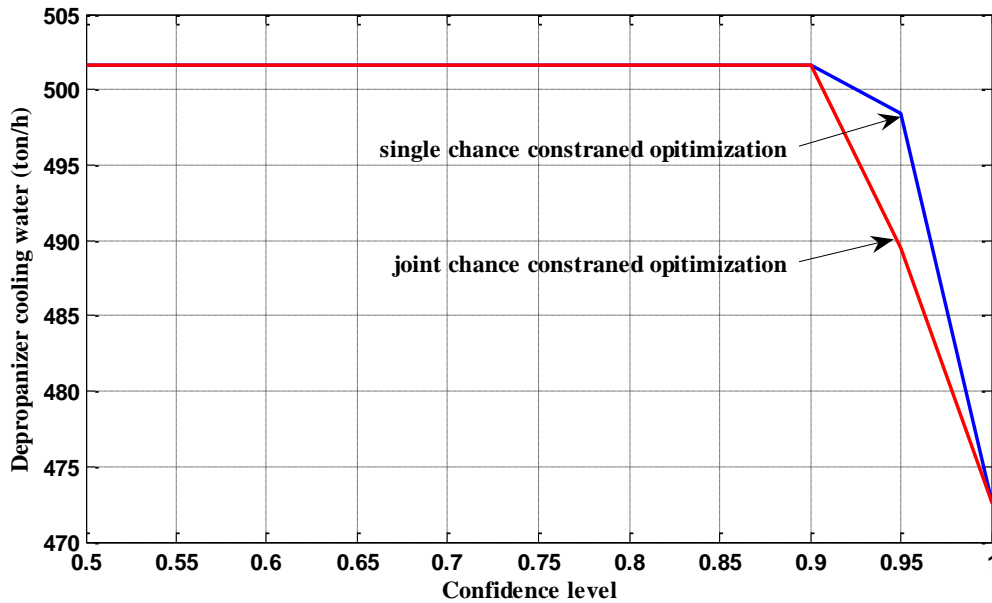


Fig 4.21: Optimal cooling water flow rate with specified confidence level

Beside this, the idea of introducing a new flash drum before the depropanizer column may also help to maintain the stable of operation of the depropanizer column. In this case, the C_{3+} feed which is coming from the condensate treatment unit may be separately flashed before it combines with the deethanizer bottom feed. The top feed from the flash drum which mainly contains C_3 is introduced to the depropanizer column, while the bottom feed (mainly C_{5+}) is directly sent to the debutanizer column. However, this also should be considered together with the capital cost of the plant for introducing additional equipment. Thus, the optimal decision from the single and joint chance constrained optimization can be made at 95% confidence level for both C_3 -refrigerant and cooling water consumption rate.

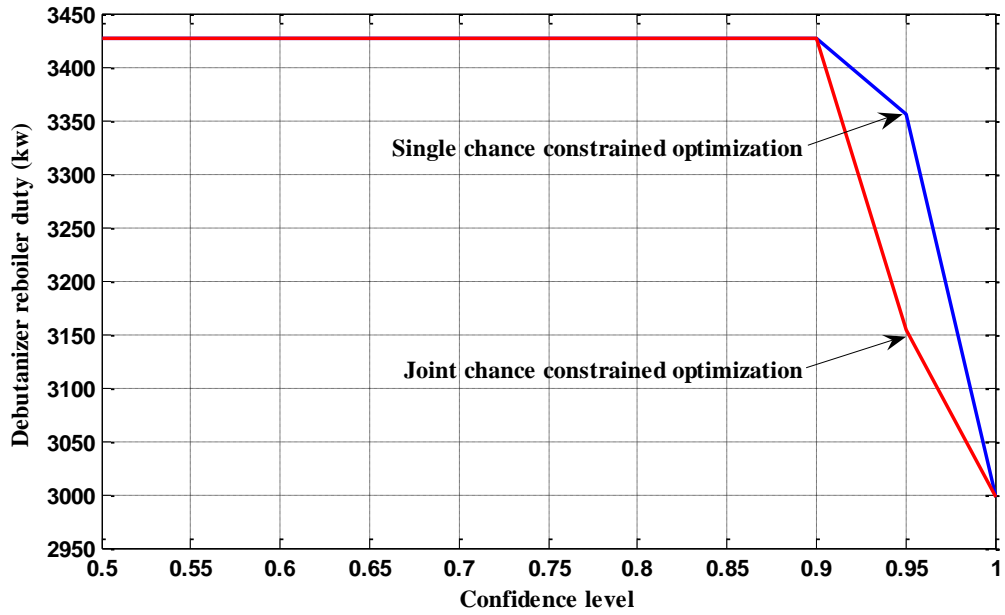


Fig 4.22: Optimal reboiler duty with specified confidence level

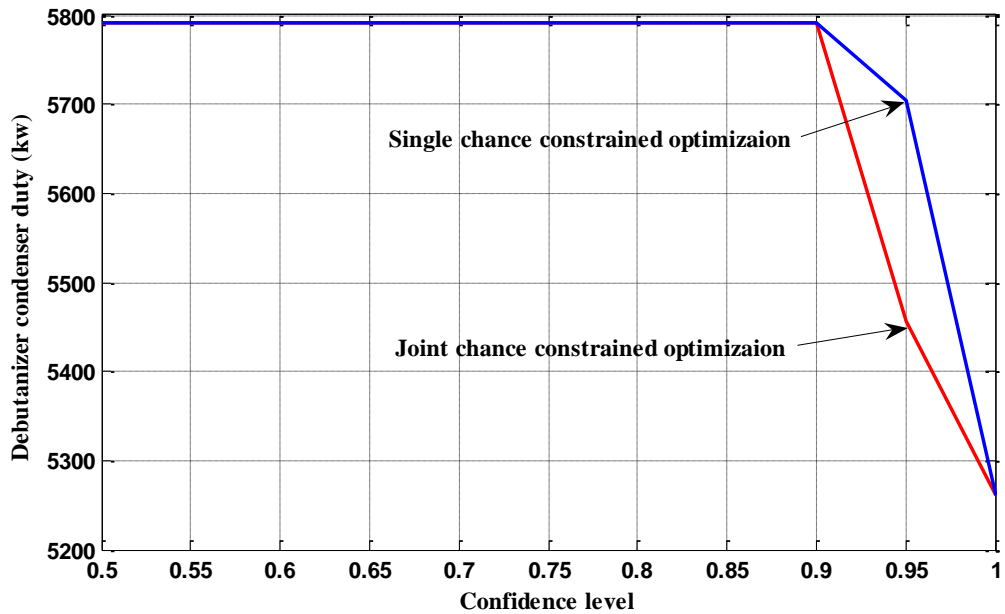


Fig 4.23: Optimal condenser duty with specified confidence level

The reboiler and condenser duties for debutanizer column are shown in Fig. 4.22 and 23, respectively. The debutanizer column processes heavier hydrocarbons (C_{4+}) as a feed which is coming from depropanizer bottom to separate into butane (C_{4s}) and condensates (C_{5+}). The condenser and reboiler duties for debutanizer column are

usually less than that of the deethanizer and depropanizer columns. The close range of the relative volatility of C_{4s} and C_{5+} gives more advantages to facilitate the separation in debutanizer column. The optimal decision from single chance constrained optimization for the debutanizer reboiler and condenser duties is made at 95% confidence level. However, for the joint chance constrained optimization the optimal decision is made at 90% confidence level for both duties.

4.3.2 Computational results

The final computational result for deterministic (DT^1 and DT^2), “worst case”(WC^1 and WC^2), two-stage programming (TW^1 and TW^2) are all compared with the LSTS and LSTJ as shown in Table 4.8. The total heat inflow entering to the plant are u_1^ε (raw material), u_2^ε (steam), u_3^ε (refrigerant), u_4^ε (compression), u_5^ε (electricity) and u_6^ε (fuel). The total heat outflows from the plant are q_1^ζ (cooling water), q_2^ζ (refrigeration process), q_3^ζ (sales gas as cooling agent) and q_4^ζ (material product). The optimal steam flow rate in deethanizer, depropanizer and debutanizer are represented as F_{stm}^{De} , F_{stm}^{Dp} and F_{stm}^{Db} , respectively. The corresponding optimal refrigerant for the deethanizer column and cooling water for the depropanizer and debutanizer column are shown as F_{ref}^{De} , F_{cool}^{Dp} and F_{cool}^{Db} , respectively. It should be noted that the unit for the total heat inflows (u_1^ε to u_6^ε) and total heat outflows (q_1^ζ to q_4^ζ) are all given in kW. The units for the steam flows, refrigerant and cooling water are given in ton per hour. The unit for the profit is given in \$ per hour.

The deterministic optimization for all cases is performed at 50% confidence level. The “worst case” are evaluated by displacing the mean value of each uncertain heat inflows ($\varepsilon_1, \dots, \varepsilon_6$) by -3σ and the uncertain heat outflows (ζ_1, \dots, ζ_4) by $+3\sigma$. For two-stage programming, similar to the other previous case study, a penalty term 1\$ per unit has been assumed. The reliability of the process for deterministic, “worst case” and two-stage programming have been included for comparison purpose. Thus, unlike the deterministic, “worst case” and two-stage programming, the LSTS and LSTJ give optimal solutions by taking into consideration of the reliability and

profitability of the plant. Accordingly, the optimal profit value at 95% confidence level from the LSTS and LSTJ gives \$ 27,273 per hour and 27,162 per hour, respectively.

Table 4-8: Final optimization result for uncertain utility and energy product flows

	DT ¹	DT ²	WC ¹	WC ²	TS ¹	TS ²	LSTS	LSTJ
α	0.5	0.5	0.9987	0.99787	0.95	0.95	0.95	0.95
Profit	27313.909	27313.909	26786.605	26754.856	27308.074	27195.925	27273.968	27161.820
u_1^ε	-512087.1	-512087.1	-499971.9	-499988.1	-510928.8	-507676.1	-510928.8	-507676.1
u_2^ε	35992.138	35992.138	34451.110	34657.579	35778.790	35179.728	35778.790	35179.728
u_3^ε	4502.288	4502.288	4423.377	4432.504	4491.829	4462.464	4491.829	4462.464
u_4^ε	4455.741	4455.741	4290.190	4309.339	4433.801	4372.193	4433.801	4372.193
u_5^ε	72.988	72.988	69.434	69.845	72.517	71.195	72.517	71.195
u_6^ε	3698.253	3698.253	3554.532	3571.155	3679.205	3625.722	3679.205	3625.722
q_1^ζ	19342.340	19342.340	18287.970	18479.941	19179.996	18724.148	19179.996	18724.148
q_2^ζ	14522.135	14522.135	14323.053	14346.080	14495.750	14421.665	14495.750	14421.665
q_3^ζ	4634.916	4634.916	4459.737	4479.999	4611.699	4546.509	4611.699	4546.509
q_4^ζ	-501865.1	-501865.1	-490254.0	-490253.6	-500760.1	-497657.2	-500760.1	-497657.2
F_{stm}^{De}	18.360	18.360	18.045	18.033	18.334	18.261	18.334	18.261
F_{stm}^{Dp}	18.362	18.362	17.529	17.650	18.243	17.911	18.243	17.911
F_{stm}^{Db}	5.527	5.527	4.830	4.982	5.411	5.087	5.411	5.087
F_{ref}^{De}	266.233	266.233	261.094	260.889	265.810	264.623	265.810	264.623
F_{cool}^{Dp}	501.664	501.664	479.220	482.484	498.473	489.515	498.473	489.515
F_{cool}^{Db}	249.054	249.054	226.159	231.149	245.263	234.620	245.263	234.620

4.4 Summary

The results from the three case studies show that the decisions using LSTS and LSTJ give a reliable solution which can guarantee profitability with respect to the reliability of the process. It should be noted that any of the other approaches such as deterministic, “worst case” and two-stage programming lack systematic analysis both the profitability and reliability of the process at the same time. Those approaches are mainly focus on the profitability of the plant. Sometimes, compensation is applied to the objective function like the case of two-stage programming to eliminate the constraint violation. However, the LSTS and LSTJ methods significantly help to closely analyze and adjust both the profitability and reliability of the process. Thus, the solution approach using LSTS and LSTJ can clearly shows for the decision maker to how much percent that the risk to be taken if the decision has to be implemented. Moreover, the solution from LSTS and LSTJ also helps as a guideline for the decision maker to make a flexible decision based on the market conditions.

CHAPTER 5

CONCLUSIONS AND FUTURE WORKS

This chapter presents the conclusion and future works based on the results obtained from this thesis. The chapter initially discusses the conclusion section by first addressing the main issues about the research and interpreting the results to reach at some basic conclusions. The next section addresses about the future works which helps for other interested researchers to give a direction by discussing about the central idea so as to expand the research work.

5.1 Conclusions

Uncertainty is an inherent characteristic of any chemical process plant and the operation of the plant is usually subject to uncertain conditions from both internal and external factors. In order to handle such uncertainties, it requires a good understanding about the sources of the uncertainty, quantification and characterization as well as analysis. From industrial aspect, these uncertainties have been usually overestimated due to lack of systematic analysis of the objective function and constraints. Sometimes, aggressive decision may be preferred by expecting a higher profit. This however significantly affects the economic performance of the plant. In order to reduce such effects, a systematic solution approach has been introduced in this work. The overall conclusions made from this work are discussed below.

- In this work, a first effort has been made to apply chance constrained programming for gas processing plant. The main challenge was developing a solution strategy that can incorporate for any variation of the feed conditions that resulted from the upstream plant before it propagates and affects the overall plant's performance. In addition, the solution approach developed in this thesis also deals with conditions where there is uncertain product

requirement, operating parameters and utility and energy product flows. Based on this, a single and joint chance constrained optimization models have been developed. In order to handle the uncertainty effect, all the uncertain variables have been explicitly incorporated in the formulation of both single and joint chance constrained models so that their impact can be taken into account in the solution. Based on the stochastic distribution of the uncertain variables, the single and joint chance constrained probabilistic problems are converted to their corresponding equivalent deterministic form so that it can be solved using the available commercial optimization software routines.

- The performance of the solution approach developed in this thesis has been implemented by taking three case studies for an existing gas processing plant. Based on the results obtained from case studies, the uncertainty from the plant inlet has a significant impact in the overall plant performance. This is due to the continuous variation of the feed conditions from the upstream plants. As a result, such variation propagates throughout the plant and results the plant operation to be unstable. The uncertainty from the plant outlet can also affect the economic performance of the plant. However, the profit change is far less compared to the uncertainty from the plant inlet. This has been supported from results in the two case studies. Accordingly, the profit has been changed by 85.8% for inlet uncertainty case and 1.93% for outlet uncertainty case. For each of the cases, the profit has been measured starting from 50% confidence level to 100% confidence level.
- On the other hand, for uncertain utility and energy product flows, the profit change is less than from any of the results obtained in case study one and two. There may be two reasons for this. First, the unit price factor for each utility and energy products flows are quite small compared to the price value of the raw material purchased and products sold. Second, the variations from the supply of some of the utilities which enter to the plant are different from one another. For example, the electricity supply is usually does not significantly vary compared to the supply of steam to the plant. This is due to the majority of the steam consumption is applied on the distillation columns. Hence, the steam consumption rate relies on mainly on the performance of the distillation

columns. Furthermore, the energy products produced from the plant can generate income or used to the plant itself as a potential energy source. Hence, this may have also a significant contribution to the economic performance of the plant.

- Using the solution strategy developed in this thesis, the optimum trade-off has been found for the reliability of the process and profitability of the plant. The reliability of the process can now be measured just like other measurements with the “unit” known as confidence level. However, such kind of analysis has not been used in deterministic, “worst case” and two-stage programming approaches. The solution from this approaches mainly focus on the performance of the objective function than handling the constraints. An equivalent confidence level has been assigned based on the basic definition of these approaches to compare their solution performance with LSTS and LSTJ. Based on this, decisions from deterministic optimizations are usually aggressive. This is due to the optimal solution from the deterministic may deviate with a probability of 50%.
- The decision from the “worst case” approach is considered as conservative. The solution from the “worst case” approach has shown how it can significantly handle the constraints. However, the profit value also significantly drops. The solution performances from the two-stage programming approaches give a closer solution to LSTS and LSTJ. The two-stage programming approach is better than deterministic and worst case approach since it can at least make a compensation in the objective function by expecting for any violation of constraint that may occur. However, the compensation is based on a scenario measurement for the uncertain variables and hence it may not be effective for a continuous case. In addition, it still lacks in holding the constraint in a reliable way since the focus is given more to the objective function. Furthermore, there are still terms which are not tangible to represent as a compensation measurement.
- Flexible decision can be made also using the solution method developed in this work. This is based on the market condition by shifting the production line

as discussed in the case studies. Based on this, the decision maker can make a prior-decision for the in-operating plant to produce the desired products by satisfying all the process constraints at certain confidence level. The decision maker also has the option to update the data and make a robust decision. Generally, using the systematic approach developed in this thesis, process engineer will have significantly reduces the burden to operate the plant as compared to the common practice of using trial and error approaches. The method can also be applied to other chemical process plant for decision making purpose

5.2 Future works

This work mainly addresses on introducing a new solution strategy for a real gas plant by taking into consideration the relation between profitability and reliability of holding the process constraints. However, the work can fully extended and more inputs can also be put on top of the existing method by other researchers. Some of the future directions from this work are discussed below.

- The method introduced in this thesis is based on linear chance constrained optimization. During linear chance constrained optimization, the inlet uncertain variable propagates linearly and the distribution of the resulting output variables are usually known. Based on this, the whole material balance equation was reduced into a linear form using volatility of components and product specifications. However, if the concepts of rigorous equilibrium method for the distillation columns have used, then the inlet uncertain variables are correlated to the output uncertain variables nonlinearly. These uncertainties can arise from tray efficiency, tray column temperature, pressure and flows. Hence, linear chance constrained optimization may not be efficient as an option to solve such problems unless they are approximated to a linear form. Thus, such problems are solved using nonlinear chance constrained optimizations which are usually known with the presence of multivariate numerical integration. The nonlinear chance constrained optimization uses collocation method based on finite element for evaluating the multivariate

numerical integration [59]. However, nonlinear chance constrained optimization is more efficient to optimize the performance of a single equipment (such as the distillation columns) than the whole plant optimization [57].

- On the other hand, the solution developed in this work is based on a single objective function from the operational aspect. However, the decision maker may need to coordinate decisions from the design as well as operational aspect due to the interconnection between them [159]. In such cases, a multi-objective function is required to obtain the optimal decision from both. Multi-objective optimization is defined as a process of simultaneously optimizing two or more conflicting objectives subject to certain constraints. The multi-objective function can be formulated in such a way that it can maximize the profit and at the same time minimizes the energy consumption. If a multi-objective problem is well formed, there should not be a single solution that simultaneously maximizes or minimizes each objective function to its fullest. Thus, the optimal solutions obtained from the multi-objective optimization represent ultimately for the condition that was set as objectives during the optimization.
- In addition, the correlation for the prices factors with supply of raw material or utility as well as demand of material or energy products are all considered to be independent. However, recent works show that there exists a possible correlation of these price factors with supply or demand the aforementioned flows [160]. The authors argue that such correlation to be incorporated in the objective function to avoid any sub-optimal solution. Such approach should be investigated carefully by studying the historical trend of the prices factors as well as supply and demand. This also may need to closely see the correlation coefficient among those parameters. This correlation coefficient may also vary from time to time. Hence, it is also important to update the data at certain time interval.

- Finally, the distillation columns in this thesis are all regarded to be conventional. Process integration has proven to be very successful in reducing the energy costs of conventional distillation columns. However, the scope of integrating a conventional distillation column into an overall process is limited for energy saving purpose. Due to this, more attention has been turned to heat integrated distillation columns or non-conventional distillation column. Even though such kind of applications have not been yet implemented in real plant operation due to the complexity of the models as well as high investment; however, there are still a research going on to improve those models. Interested researchers can refer to the works by Halvorsen and Skogestad [161-163].

REFERENCES

- [1] V. Chandra, *Fundamentals of natural gas: an international perspective*, Pennwell Corp: Tulsa, pp.1, 2006.
- [2] EIA, "Short term energy outlook", *U.S department of energy: Energy information administration*, pp. 6-8, 2010.
- [3] George, *North American natural gas supply dynamics: A focus on U.S*, 1999.
- [4] EIA, "International energy outlook", *U.S department of energy: Energy information administration*, pp. 3-5, 2008.
- [5] A. J. Kidnay and R. W. Parish, *Fundamentals of natural gas processing*, 2006.
- [6] R. Parthasarathy, "Duke Energy's Gulf Plains plant fractionation and its analysis", A Master thesis, Texas A&M University - Kingsville: United States -- Texas, pp. 11-12, 2004.
- [7] A.M. Eliceche, N.C. Petracci, P. Hoch, and E.A. Brignole, "Optimal operation of an ethylene plant at variable feed conditions", *Computers & Chemical Engineering*, vol. 19., no.1, pp. 223-228, 1995.
- [8] J. Fleshman, P. Alderton, E. Bahnassi, and A. R. Khouri, "Achieving Product Specifications for Ethane through to Pentane Plus from NGL Fractionation Plants," *Presented on AIChE annual meeting*: Cincinnati, OH, 2005.
- [9] S. Diaz, E. A. Brignole, and A. Bandoni, "Flexibility study on a dual mode natural gas plant in operation," *Chemical Engineering Communications*, vol. 189., no.5, pp. 623-641, 2002.

- [10] K.L. Jibril, A.I. Al-Humaizi, A.A. Idriss, and A.A. Ibrahim, "Simulation study determines optimum turboexpander process for NGL recovery," *Oil and Gas Journal*, vol. 104, pp. 58-62, 2006.
- [11] V. Aggarwal and S. Singh, "Improve NGL recovery Processing conditions and product specifications determine the best method to recover NGLs," *Hydrocarbon Processing*, vol., 80, no.5, pp. 41-46, 2001.
- [12] R. Henrion, P. Li, A. Möller, M. Steinbach, M. Wendt, and G. Wozny, "Stochastic optimization for chemical processes under uncertainty," *Online optimization of large scale systems*, pp. 455–476, 2001.
- [13] A.E.S. Konukman and U. Akman, "Flexibility and operability analysis of a HEN-integrated natural gas expander plant," *Chemical Engineering Science.*, vol. 60, no. 24, pp. 7057-7074, 2005.
- [14] V. Bansal, J.D. Perkins, and E.N. Pistikopoulos, "Flexibility analysis and design using a parametric programming framework," *AIChE Journal.*, vol. 48, no.12, pp. 2851-2868, 2002.
- [15] T.F. Edgar, D.M. Himmelblau, and L.S. Lasdon, *Optimization of chemical processes*, McGraw-Hill: New-York, 2001.
- [16] U.M. Diwaker, *Introduction to applied optimization*, Springer Optimization and Applications, pp. 1-36, 2008.
- [17] J.A. Bandoni, A.M. Eliceche, G.D.B. Mabe, and E.A. Brignole, "Synthesis and optimization of ethane recovery process," *Computers & Chemical Engineering.*, vol. 13, no. 4-5, pp. 587-594, 1989.
- [18] L. Fernández, A.M. Eliceche, and E.A. Brignole, "Optimization of ethane extraction plants from natural gas containing carbon dioxide," *Gas separation & purification.*, vol. 5, no. 4, pp. 229-233, 1991.

- [19] S. Diaz, A. Serrani, R.D. Beistegui, and E.A. Brignole, "A MINLP strategy for the debottlenecking problem in an ethane extraction plant," *Computers & Chemical Engineering.*, vol. 19, pp. 175-180, 1995.
- [20] S. Diaz, A. Serrani, A. Bandoni, and E.A. Brignole, "A study on the capital and operating alternatives in an ethane extraction plant," *Computers & Chemical Engineering.*, vol. 20, pp. S1499-S1504, 1996.
- [21] M.S. Diaz, A. Serrani, A. Bandoni, and E.A. Brignole, "Automatic design and optimization of natural gas processing plants," *Industrial & Engineering Chemistry Research.*, vol. 36, no. 7, pp. 2715-2724, 1997.
- [22] L.G. Gomes and M.R. Wolf-Maciel, "Development of a methodology to reproduce and to optimize the operating conditions of a natural gas processing plant," *Computers & Chemical Engineering.*, vol. 20, pp. S1511-S1516, 1996.
- [23] K. A. Bullin and K. R. Hall, "Optimization of Natural Gas Processing Plants Including Business Aspects," *Presented on the 79th GPA annual convention: Atlanta, Gas processors association, Bryan research and engineering, Inc*, 2000.
- [24] P. Li, H. Arellano-Garcia, and G. Wozny, "Chance constrained programming approach to process optimization under uncertainty," *Computers & Chemical Engineering*, vol. 32., no. 1-2, pp. 25-45, 2008.
- [25] A. Shapiro, "Stochastic programming approach to optimization under uncertainty," *Mathematical Programming*, vol. 112., no. 1, pp. 183-220, 2008.
- [26] A.M. Eliceche, M. Sanchez, and L. Fernandez, "Feasible operating region of natural gas plants under feed perturbations," *Computers & Chemical Engineering*, vol. 22, pp. S879-S882, 1998.
- [27] P. Li, M. Wendt and G. Wozny, "Optimal production planning for chemical processes under uncertain market conditions," *Chemical Engineering & Technology*, vol. 27., no. 26, pp. 641-651, 2004.
- [28] I. E. Grossmann and R. W. H. Sargent, "Optimum design of chemical plants with uncertain parameters," *AIChE Journal*, vol. 24., no.6, pp. 1021-1028, 1978.

- [29] I. E. Grossmann and K. P. Halemane, "Decomposition strategy for designing flexible chemical plants," *AIChE Journal*, vol. 28., no.4, pp. 686-694, 1982.
- [30] D. K. Varvarezos, I. E. Grossmann, and L. T. Biegler, "An outer-approximation method for multiperiod design optimization," *Industrial & Engineering Chemistry Research*, vol. 31., no.6, pp. 1466-1477, 1992.
- [31] I. E. Grossmann, K. P. Halemane, and R. E. Swaney, "Optimization strategies for flexible chemical processes," *Computers & Chemical Engineering*, vol. 7., no. 3, pp. 439-462, 1983.
- [32] R. E. Swaney and I. E. Grossmann, "An index for operational flexibility in chemical process design. Part I: Formulation and theory," *AIChE Journal*, vol. 31., no.4, pp. 621-630, 1985.
- [33] R. E. Swaney and I. E. Grossmann, "An index for operational flexibility in chemical process design. Part II: Computational algorithms," *AIChE Journal*, vol. 31., no. 4, pp. 631-641, 1985.
- [34] I. E. Grossmann and C. A. Floudas, "Active constraint strategy for flexibility analysis in chemical processes," *Computers & Chemical Engineering*, vol. 11., no.6, pp. 675-693, 1987.
- [35] E. N. Pistikopoulos and I. E. Grossmann, "Stochastic optimization of flexibility in retrofit design of linear systems," *Computers & Chemical Engineering*, vol. 12., no. 12, pp. 1215-1227, 1988.
- [36] E. N. Pistikopoulos and I. E. Grossmann, "Optimal retrofit design for improving process flexibility in nonlinear systems--I. Fixed degree of flexibility," *Computers & Chemical Engineering*, vol. 13., no. 9, pp. 1003-1016, 1989.
- [37] E. N. Pistikopoulos and I. E. Grossmann, "Optimal retrofit design for improving process flexibility in nonlinear systems--II. Optimal level of flexibility," *Computers & Chemical Engineering*, vol. 13., no. 10, pp. 1087-1096, 1989.

- [38] D. K. Varvarezos, I. E. Grossmann, and L. T. Biegler, "A sensitivity based approach for flexibility analysis and design of linear process systems," *Computers & Chemical Engineering*, vol. 19., no. 12, pp. 1301-1316, 1995.
- [39] W. Li, "Modeling oil refinery for production planning, scheduling and economic analysis," *Hong Kong University of Science and Technology: Hong Kong*, pp. 155-200, 2004.
- [40] N.V. Sahinidis, "Optimization under uncertainty: state-of-the-art and opportunities," *Computers & Chemical Engineering*, vol. 28., no. 6-7, pp. 971-983, 2004.
- [41] Z. Li and M. Ierapetritou, "Process scheduling under uncertainty: Review and challenges," *Computers & Chemical Engineering*, vol. 32, no. 4-5, pp. 715-727, 2008.
- [42] M. L. Liu and N. V. Sahinidis, "Optimization in process planning under uncertainty," *Ind. Eng. Chem. Res*, vol. 35., no. 11, pp. 4154-4165, 1996.
- [43] G. E. Paules, "Stochastic programming in process synthesis: a two-stage model with MINLP recourse for multi-period heat-integrated distillation sequences," *Computers & Chemical Engineering*, vol. 16., no. 3, pp. 189-210, 1992.
- [44] E. N. Pistikopoulos and M. G. Ierapetritou, "Novel approach for optimal process design under uncertainty," *Computers and Chemical Engineering*, vol. 19., no. 10, pp. 1089-1110, 1995.
- [45] S. Ahmed and N. V. Sahinidis, "Robust process planning under uncertainty," *Industrial & Engineering Chemistry Research*, vol. 37., no. 5, pp. 1883-1892, 1998.
- [46] A. Gupta and Maranas, C.D, "A Two-stage modeling and solution framework for multitude midterm planning under demand uncertainty," *Industrial & Engineering Chemistry Research*, vol. 39., no. 10, pp. 3799-3813, 2000.

- [47] W. C. Rooney and L. T. Biegler, "Optimal process design with model parameter uncertainty and process variability," *AIChE Journal*, vol. 49., no.2, pp. 438-449, 2003.
- [48] C. S. Khor, A. Elkamel, K. Ponnambalam, and P. L. Douglas, "Two-stage stochastic programming with fixed recourse via scenario planning with economic and operational risk management for petroleum refinery planning under uncertainty," *Chemical Engineering and Processing: Process Intensification*, vol. 47., no. 9-10, pp. 1744-1764, 2008.
- [49] A. Charnes and W. W. Cooper, "Chance-constrained programming," *Management Science*, vol. 6, pp. 73-79, 1959.
- [50] B. L. Miller and H. M. Wagner, "Chance constrained programming with joint constraints," *Operations Research*, vol. 13, no. 6, pp. 930-945, 1965.
- [51] A. Prékopa, *On probabilistic constrained programming*, pp. 113-138, 1970.
- [52] A. Prekopa, *Stochastic programming*, Kluwer Academic Publishers: Dordrecht, 1995.
- [53] P. Kall and S. W. Wallace, *Stochastic programming*: Citeseer, 1994.
- [54] S. Uryasev, *Probabilistic constrained optimization: methodology and applications*: Kluwer Academic Pub, 2000.
- [55] A. T. Schwarm and M. Nikolaou, "Chance-constrained model predictive control," *AIChE Journal*, vol. 45., no. 8, pp. 1743-1752, 1999.
- [56] P. Li, M. Wendt and G. Wozny, "Robust model predictive control under chance constraints," *Computers & Chemical Engineering*, vol. 24., no. 2-7, pp. 829-834, 2000.
- [57] P. Li, M. Wendt, H. Arellano-Garcia, and G. Wozny, "Optimal operation of distillation processes under uncertain inflow streams accumulated in a feed tank" *AIChE Journal.*, vol. 48, pp. 1198–1211, 2002.

- [58] P. Li, M. Wendt and G. Wozny, "A probabilistically constrained model predictive controller", *Automatica.*, vol. 38, pp. 1171–1176, 2002.
- [59] M. Wendt, P. Li, and G. Wozny, "Nonlinear chance-constrained process optimization under uncertainty," *Industrial & Engineering Chemistry Research*, vol. 41., no. 15, pp. 3621-3629, 2002.
- [60] R. Henrion and A. Möller, "Optimization of a continuous distillation process under random inflow rate," *Computers & Mathematics with Applications*, vol. 45., no. 1-3, pp. 247-262, 2003.
- [61] H. Arellano-Garcia and G. Wozny, "Chance constrained optimization of process systems under uncertainty: I. Strict monotonicity," *Computers & Chemical Engineering*, vol. 33., no. 10, pp. 1568-1583, 2009.
- [62] ASPEN HYSYS, "A user guide manual," Aspen technology, 2006.
- [63] GAMS IDE, "General algebraic modeling system: integrated development environment: user manual," *Module: GAMS Rev 133, Build: VIS 20.7 133*, , 2002.
- [64] M. G. Ierapetritou, J. Acevedo, and E. N. Pistikopoulos, "An optimization approach for process engineering problems under uncertainty," *Computers & Chemical Engineering*, vol. 20., no. 6-7, pp. 703-709, 1996.
- [65] W. B. Whiting, "Effects of Uncertainties in Thermodynamic Data and Models on Process Calculations," *Journal of Chemical Engineering Data*, vol. 41., no. 5, pp. 935-944, 1996.
- [66] J. Mula, R. Poler, J. P. Garcia-Sabater, and F. C. Lario, "Models for production planning under uncertainty: A review," *International Journal of Production Economics*, vol. 103., no. 1, pp. 271-285, 2006.
- [67] H. Arellano-Garcia, "Chance constrained optimization of process systems under uncertainty," *PhD thesis: Berlin University of technology: Berlin, Germany*, 2006.

- [68] C.D. Maranas, "Optimal molecular design under property prediction uncertainty," *AIChE Journal*, vol. 43., no. 5, pp. 1250-1264, 1997.
- [69] V.R. Vasquez and W. B. Whiting, "Effect of systematic and random errors in thermodynamic models on chemical process design and simulation: A Monte Carlo approach," *Ind. Eng. Chem. Res*, vol. 38., no. 8, pp. 3036-3045, 1999.
- [70] V.R. Vasquez and W. B. Whiting, "Uncertainty and sensitivity analysis of thermodynamic models using equal probability sampling (EPS)," *Computers & Chemical Engineering*, vol. 23., no. 11-12, pp. 1825-1838, 2000.
- [71] U.M. Diwaker and J.R. Kalagnanam, "An efficient sampling technique for optimization under uncertainty," *AIChE Journal*, vol. 43., no. 2, pp. 440-447, 1997.
- [72] M. C. Tayal and U. M. Diwekar, "Novel sampling approach to optimal molecular design under uncertainty," *AIChE Journal*, vol. 47., no. 3, pp. 609-628, 2001.
- [73] S. Ulsa and U. Diwekar, "Thermodynamic uncertainties in batch processing and optimal control," *Computers & Chemical Engineering*, vol. 28., no. 11, pp. 2245-2258, 2004.
- [74] U.M. Diwaker and E.S. Rubin, "Stochastic modeling of chemical processes," *Computer & Chemical Engineering*, vol. 15., no. 2, pp. 105-114, 1991.
- [75] U.M. Diwaker and E.S. Rubin, "Parameter design methodology for chemical processes using a simulator," *Industrial & Engineering Chemistry Research*, vol. 33, pp. 22-298, 1994.
- [76] H. Tørvi and T. Hertzberg, "Estimation of uncertainty in dynamic simulation results," *Computers & Chemical Engineering*, vol. 21(suppl), pp. S181-S185, 1997.
- [77] B. D. Phenix, J. L. Dinero, M. A. Tatang, J. W. Tester, J. B. Howard, and G. J. McRae, "Incorporation of parametric uncertainty into complex kinetic mechanisms: application to hydrogen oxidation in supercritical water," *Combustion and flame*, vol. 112., no. 1-2, pp. 132-146, 1998.

- [78] D. R. P. Terwish, B. Schenker, D.W.T. Rippin, "Semi-Batch optimization under uncertainty: Theory and experiment," *Computer & Chemical Engineering*, vol. 22., no. 1-2, pp. 201-213, 1998.
- [79] W. B. Whiting, V. R. Vasquez, and M. M. Meerschaert, "Techniques for assessing the effects of uncertainties in thermodynamic models and data," *Fluid Phase Equilibria*, vol. 158, pp. 627-641, 1999.
- [80] A. Saltelli, K. Chan, and E. M. Scott, *Sensitivity analysis*, Wiley: New York, 2000.
- [81] I.E. Grossmann, K.P. Halemane, and R.E. Swaney, "Optimization strategy for flexible chemical processes," *Computers & Chemical Engineering*, vol. 7., no. 4, pp. 439-462, 1983.
- [82] E. N. Pistikopoulos, "Uncertainty in process design and operations," *Computers & Chemical Engineering*, vol. 19, pp. 553-563, 1995.
- [83] G. B. Dantzig, "Linear programming under uncertainty," *Management Science*, vol. 1.,no. 3, pp. 197-206, 1955.
- [84] H. S. Wellons and G. V. Reklaitis, "The design of multiproduct batch plants under uncertainty with staged expansion," *Computers & Chemical Engineering*, vol. 13., no. 1-2, pp. 115-126, 1989.
- [85] N. Shah and C. C. Pantelides, "Design of multipurpose batch plants with uncertain production requirements," *Industrial & Engineering Chemistry Research*, vol. 31., no. 5, pp. 1325-1337, 1992.
- [86] D. A. Straub and I. E. Grossmann, "Design optimization of stochastic flexibility," *Computers & Chemical Engineering*, vol. 17., no. 4, pp. 339-354, 1993.
- [87] M. G. Ierapetritou and E. N. Pistikopoulos, "Batch plant design and operations under uncertainty," *Ind. Eng. Chem. Res*, vol. 35., no. 3, pp. 772-787, 1996.

- [88] S. B. Petkov and C. D. Maranas, "Design of single product campaign batch plants under demand uncertainty," *AIChE Journal*, vol. 44., no. 4, pp. 896-911, 1998.
- [89] J.R. Birge and F. Louveaux, *Introduction to stochastic programming*, Springer: New York, 1997.
- [90] K. J. Kim and U. M. Diwekar, "Efficient combinatorial optimization under uncertainty.1. Algorithmic development," *Industrial & Engineering Chemistry Research*, vol. 41, pp. 1276-1284, 2002.
- [91] P. M. Verderame, J. A. Elia, J. Li, and C. A. Floudas, "Planning and scheduling under uncertainty: A review across multiple sectors," *Industrial & Engineering Chemistry Research*, vol. 49., no. 9, pp. 3993-4017, 2010.
- [92] S. Subrahmanyam, J. F. Pekny, and G. V. Reklaitis, "Design of batch chemical plants under market uncertainty," *Industrial & Engineering Chemistry Research*, vol. 33., no. 11, pp. 2688-2701, 1994.
- [93] M. G. Ierapetritou and E. N. Pistikopoulos, "Novel optimization approach of stochastic planning models," *Industrial & Engineering Chemistry Research*, vol. 33., no. 8, pp. 1930-1942, 1994.
- [94] M. G. Ierapetritou and E. N. Pistikopoulos, "Simultaneous incorporation of flexibility and economic risk in operational planning under uncertainty," *Computers & Chemical Engineering*, vol. 18., no. 3, pp. 163-189, 1994.
- [95] R.L. Clay and I.E. Grossmann "A disaggregation algorithm for the optimization of stochastic planning models," *Computers & Chemical Engineering*, vol. 21., no. 7, pp. 751-774, 1997.
- [96] J. Acevedo and E. N. Pistikopoulos, "A hybrid parametric/stochastic programming approach for mixed-integer linear problems under uncertainty," *Ind. Eng. Chem. Res*, vol. 36., no. 6, pp. 2262-2270, 1997.

- [97] A. Gupta and C. D. Maranas, "A hierarchical Lagrangean relaxation procedure for solving midterm planning problems," *Ind. Eng. Chem. Res.*, vol. 38., no. 5, pp. 1937-1947, 1999.
- [98] L. X. Chufu, H. Bingzhen, C. Qiang, X, "A hybrid programming model for optimal production planning under demand uncertainty in refinery," *Chinese journal of chemical engineering*, vol. 16., no. 2, pp. 241-246, 2008.
- [99] L. G. Papageorgiou, "Supply chain optimisation for the process industries: Advances and opportunities," *Computers & Chemical Engineering*, vol. 33., no. 12, pp. 1931-1938, 2009.
- [100] P. M. Verderame and C. A. Floudas, "Operational planning of large-scale industrial batch plants under demand due date and amount uncertainty: I. Robust optimization framework," *Industrial & Engineering Chemistry Research*, vol. 48., no. 15, pp. 7214-7231, 2009.
- [101] P. M. Verderame and J., C. A. Floudas, "Operational planning of large-scale industrial batch plants under demand due date and amount uncertainty: II. Conditional value-at-risk framework," *Industrial & Engineering Chemistry Research*, vol. 49., no. 1, pp. 260-275, 2010.
- [102] R. J. Lee, J. Yao, and D.G. Elliot, "Flexibility, efficiency to characterize gas-processing technologies in the next century," *Oil & gas journal*, vol. 97., no. 15, pp. 90-94, 1999.
- [103] D.G. Elliot, J.J. Chen, T.S. Brown, E.D. Sloan, and A.J. Kidnay, "The economic impact of fluid properties research on expander plants", *Fluid Phase Equilibria*, vol. 116, no. 1- 2, pp. 27-38, 1996.
- [104] R. E. Campbell, (Midland, TX) and J.D. Wilkinson, (Midland, TX), "Hydrocarbon gas processing," *Untied states*, Ortloff Corporation (Midland, TX), 42579041979, 1979.
- [105] A. A. Rahaman, A.A. Yusof, J.D. Wilkinson, and L.D. Tyler, "Improving ethane extraction at the PETRONAS gas GPP-A facilities in Malaysia," in

Presented at the 83rd annual convention of the gas processors association New Orleans, Louisiana, 2004.

- [106] L. L. Buck (Tulsa, OK), "Separating hydrocarbon gases," *United States: Pro-Quip Corporation* (Tulsa, OK), 4617039, 1986.
- [107] G.J. Montgomery (Huston, TX), "Ethane recovery system", *United States: McDermott International, inc* (New Orleans, LA), 4851020, 1989.
- [108] R.E. Campbell (Midland, TX), J.D. Wilkinson (Midland, TX), and H.M. Hudson (Midland, TX), "Hydrocarbon gas processing", *United States: Elcor Corporation* (Dallas, TX), 5568737, 1996.
- [109] R.E. Campbell (Late of Midland, TX), J.D. Wilkinson (Midland, TX), H.M. Hudson (Midland, TX), and M.C. Pierce (Odessa, TX) , "Hydrocarbon gas processing", *United States: Elcor Corporation* (Dallas, TX), 5983664, 1999.
- [110] G. Yao, J.J. Chen, S. Land, D.G. Elliot, "Enhanced NGL recovery processes", *United states patent number: 5992175*, 1999.
- [111] L. Bai, R. Chen, J. Yao, and D. Elliot, "Retrofit for NGL recovery performance using a novel stripping gas refrigeration scheme", *Presented at the 85th Annual Gas Processors Association Convention: Dallas, TX*, 2006.
- [112] M. Mehrpooya, A. Vatani, and S.M. Ali Mousavian, "Introducing a novel integrated NGL recovery process configuration (with a self-refrigeration system (open-closed cycle)) with minimum energy requirement", *Chemical Engineering and Process Intensification.*, vol. 49, no. 4, pp. 376-388, 2010.
- [113] R.E. Campbell (Midland, TX) and J.D. Wilkinson (Midland, TX), "Hydrocarbon gas processing", *United States: Ortloff Corporation* (Midland, TX), 4278457, 1981.
- [114] J.D. Wilkinson and H.M. Hudson, "Improved NGL recovery designs maximize operating flexibility and product recoveries", *Presented at the 71st annual convention of gas processors association, Anaheim: California*, pp. 318-325, 1992.

- [115] R.N. Pitman, H.M. Hudson, J.D. Wilkinson, "Next generation processes for NGL/LPG recovery", *Presented at the 77th annual convention of the gas processors association, Dallas, TX, 1998.*
- [116] R.J. Lee (Sugar land, TX), J. Yao (Sugar land, TX), R.J.J. Chen (Sugar land, TX), and D.G. Elliot (Huston, TX), "Lean reflux process for high recovery of ethane and heavier components", *United States: IPSI, L.L.C. (Houston, TX), 6244070, 2001.*
- [117] R.J. Lee (Sugar land, TX), J. Yao (Sugar land, TX), R.J.J. Chen (Sugar land, TX), and D.G. Elliot (Huston, TX) , "Enhanced NGL recovery processes", *United States Patent: 6401486, 2002.*
- [118] H.M. Hudson, J.D. Wilkinson, J.T. Lynch, R.N. Pitman, and M.C. Pierce, "Reducing treating requirements for cryogenic NGL recovery plants", *Presented at the 80th annual convention of the gas Processors association, San Antonio, TX, 2001.*
- [119] H. Rhemann, G. Schwartz, T. Badgwell, and D. White, "On-line FCCU advanced control and optimization," *Hydrocarbon Processing*, 1989.
- [120] M.L. Sourander, J.C. Cugini, M. Kolari, J.B. Poje, and D.C White, "Control and optimization of olefin-cracking heaters", *Hydrocarbon process.*, vol. 63, no. 6, pp. 63-69, 1984.
- [121] D. C. White, "Application of advanced controls and on-line optimization on the chemical industry," in *Proceedings second Seoul international chemical plant exhibition*, 1990.
- [122] K.A. Bullin, "Economic optimization of natural gas processing plant including business aspects", *A PhD thesis: Texas A & M University, United States, Texas*, pp.34-35, 1999.
- [123] S.E. Gallun, R.H. Luecke, D.E. Scott, and A.M. Morshedi, "Use open equations for better models", *Hydrocarbon processing*, pp. 71-78, 1992.

- [124] Q.K. Williams and M. Rameshni, "Real-time economic control", *Hydrocarbon processing*, pp. 77-99, 1998.
- [125] A. Lucia and S. Macchietto, "New approach to approximation of quantities involving physical properties derivatives in equation-oriented process design", *AIChE Journal*, vol. 29, no. 5, 705-712, 1983.
- [126] W. B. Wang, "Optimization of expander plants," *United States, Oklahoma: Tulsa University*, 1985.
- [127] Hyprotech, "HYSIM User's Guide," Hyprotech, Ltd 1991.
- [128] C. J. King, *Separation processes*, Second ed. New-York: Mc-Graw-Hill, 1980.
- [129] C.B. Cutler and B.L, "Dynamic matrix control-a computer control algorithm," in *Proceedings fifty-eighth AIChE national meeting*, San Antonio, TX, 1979.
- [130] J.O. Perino and M.K. Moran, "Process model-based multivariable control alternatives," *Hydrocarbon processing*, vol. 73., no. 65, p. 65, 1994.
- [131] R.C. Sorensen and C.R. Cutler, "integrates economics into dynamic matrix control," *Hydrocarbon carbon processing*, vol. 77, p. 57, 1998.
- [132] S. Diaz, A. Bandoni, N. Petracci, L. Aparicio and E.A. Brignole, "Structural and parameter optimization of an ethylene plant," in *European symposium on computer aided process engineering* Elsinore, Denmark: ESCAPE-1, 1992.
- [133] M. Duran and I.E. Grossmann, "A mixed-integer nonlinear programming approach for process synthesis," *AIChE Journal*, vol. 32., no. 4, pp. 592-606, 1986.
- [134] G. Kreisselmeier and R. Steinhauser, "Application of vector performance optimization to a robust control loop design for a fighter aircraft," *Int.J. of control*, vol. 37, pp. 251-284, 1983.
- [135] X-S, Yang, *Engineering optimization: An introduction to metaheuristic approaches*, Wiley: Cambridge, UK, 2010.

- [136] M. Mehrpooya, F. Gharagheizi, and A. Vatani, "An optimization of capital and operating alternatives in a NGL recovery unit," *Chemical Engineering & Technology*, vol. 29, pp. 1469-1480, 2006.
- [137] K. Wang, T. Löhl, M. Stobbe, and S. Engell, "A genetic algorithm for online-scheduling of a multiproduct polymer batch plant," *Computers & Chemical Engineering*, vol. 24., no. 2-7, pp. 393–400, 2000.
- [138] K. Wang, A. Salhi and E.S. Fraga, "Process design optimization using embedded hybrid visualization and data analysis techniques within a genetic algorithm optimization framework," *Chemical Engineering and Processing: Process Intensification*, vol. 43., no. 5, pp. 657–669, 2004.
- [139] W-H. Jang, J. Hahn, K.R. Hall, "Genetic/quadratic search algorithm for plant economic optimizations using a process simulator," *Computers & Chemical Engineering*, vol. 30., no. 2, pp. 285-294, 2005.
- [140] A. Aspelund, T. Gundersen, J. Myklebust, M.P. Nowak and A. Tomasgard, "An optimization-simulation model for a simple LNG process," *Computers & Chemical Engineering*, vol. 34., no. 10, pp. 1606-1617, 2010.
- [141] M. ŽDĀNSKÝ and J. POŽIVIL, "Combination of Genetic/Tabu search for hybrid flowshops optimization," *Proceeding of Algoritmy: Conference on scientific computing*, pp. 230-236, 2002.
- [142] R. K. Roy, *A Primer of Taguchi method*. New York: Van Nostrand Reinhold, 1990.
- [143] N. Yusoff, M. Ramasamy, and S. Yusup, "Taguchi's parametric design approach for the selection of optimization variables in a refrigerated gas plant," *Chemical Engineering Research and Design*, vol. 89, pp. 665-675, 2011.
- [144] S. Fraley, M. Oom, B. Terrien, J. Zaekwski, "The Michigan chemical process dynamics and controls open text book," 2007.
https://controls.engin.umich.edu/wiki/index.php/Main_Page

- [145] J. Darlington, C.C. Pantelides, B. Rustem, and B.A. Tanyi, "An algorithm for constrained nonlinear optimization under uncertainty," *Automatica*, vol. 35, pp. 217-228, 1999.
- [146] M.F. Doherty and M.F. Malone, *Conceptual design of distillation systems*: McGraw-Hill, 2001.
- [147] A. Ben-Tal and A. Nemirovski, "Robust solutions of linear programming problems contaminated with uncertain data," *Mathematical programming*, vol. 88, pp. 411-424, 2000.
- [148] S. Sen and J.L. Hige, "An introductory tutorial on stochastic linear programming," *Interfaces*, vol. 29, pp. 33-61, 1999.
- [149] R. J.-B. Wets, *Challenges in stochastic programming*. Laxenburg: IIASA, 1994.
- [150] W. Li, C.W. Hui, P. Li and A.X. Li, "Refinery planning under uncertainty," *Industrial Engineering & Chemical Research*, vol. 43, pp. 6742-6755, 2004.
- [151] P. Li, A.G. Harvey, and G, "Chance constrained programming approach to process optimization under uncertainty," in *Presented in 16th European symposium on computer aided process engineering and 9th international symposium on process system engineering*, 2006, pp. 1245-1250.
- [152] T. Szántai, *A Computer code for solution of probabilistic-constrained stochastic programming problems*. New York: Springer, 1988.
- [153] R.E. Rosenthal, "A User's Guide: tutorial," Washington, DC, USA: GAMS Development Corporation, 2006.
- [154] K.M. Aludaat and M.T. Alodat, "A note on approximating the normal distribution function," *Applied mathematical sciences*, vol. 2., no. 9, pp. 425-429, 2008.

- [155] B.J.R. Baily, "Alternatives to hastings's approximation to the inverse of the normal cumulative distribution function," *Applied statistics*, vol. 30., no. 3, pp. 275-276, 1981.
- [156] N.I. Johnson, S. Kotz, and N. Balakrishnan, *Continuous univariate distributions*: John Wily & sons, 1994.
- [157] Chokri, "A short note on the numerical approximation of the standard normal cumulative distribution and its inverse", *Real 03-T-7, online manuscript*, 2003.
- [158] Y. R. Mehra, "New process flexibility improves gas processing margins," *Energy Progress*, pp. 7,150-7156, 1987.
- [159] L. Cheng, E. Subrahmanian, and A.W. Westerberg, "Multiobjective decision processes under uncertainty: Applications, problem formulations and solution strategies," *Industrial & Engineering Chemistry Research*, vol. 44, pp. 2405-2415, 2005.
- [160] W. Li, I.A. Karimi, and R. Srinivasan, "Refinery planning under correlated and truncated price and demand uncertainties," in *16th European symposium on computer aided process engineering and 9th international symposium on process system engineering*, 2006.
- [161] J.I. Halvorsen and S. Skogestad, "Minimum energy consumption in multicomponent distillation.1.Vmin diagram for a two-product column," *Industrial & Engineering Chemistry Research*, vol. 42, pp. 595-604, 2003.
- [162] J.I. Halvorsen and S. Skogestad, "Minimum energy consumption in multicomponent distillation.2.Three-product petlyuk arrangement," *Industrial & Engineering Chemistry Research*, vol. 42, pp. 605-615, 2003.
- [163] J.I. Halvorsen and S. Skogestad, "Minimum energy consumption in multicomponent distillation.3.More than three-product and generalized petlyuk arrangements," *Industrial & Engineering Chemistry Research*, vol. 42, pp. 616-629, 2003.

PUBLICATION LISTS

- Mesfin, G., & Shuhaimi, M.(2010).A chance constrained approach for a gas processing plant with uncertain feed conditions. *Computers & Chemical Engineering*, 34(8), 1256-1267.
- Mesfin, G., & Shuhaimi, M.(2010). A probabilistic optimization approach for gas processing plant under uncertain feed conditions and product requirements. Selected paper from *World Academy of Science, Engineering and Technology Conference (WASET' 10)*. ISSN: 1307-6892, Issue 62, pp 585-590.
- Mesfin, G., & Shuhaimi, M.(2008).Achieving flexibility for optimizing the profit of an existing gas processing plant. *The 15th regional symposium on chemical engineering (RSCE) in conjunction with the 22nd symposium of Malaysian Chemical Engineers (SOMChE)*.
- Mesfin, G., & Shuhaimi, M.(2009). Optimal operational planning model for gas processing plant under uncertain conditions. *The 3rd International Conference on Chemical and Bioprocess Engineering in conjunction with 23rd symposium of Malaysian Chemical Engineers (SOMChE)*.
- Mesfin, G., & Shuhaimi, M.(2009). Flexible and optimal operations of gas processing plant under uncertain conditions. *Environmental Science and Technology Conference 2009 (ESTEC' 09)*.
- Mesfin, G., & Shuhaimi, M.(2009). Optimal operation of gas processing plant under uncertain conditions. *National Postgraduate Conference on Engineering, Science and Technology (NPC)*.

APPENDIX A

SHORTCUT DISTILLATION CORRELATIONS

A.1 Fenske method

Fenske equation used to estimate the minimum number of stages, N_{\min} . For total reflux, the flows of component k and a reference component k_r are related by:

$$\frac{d_{t,k}}{d_{t,k_r}} = \left(\hat{\alpha}_{k,k_r}^{N_{\min}} \right) \left(\frac{b_{t,k}}{b_{t,k_r}} \right) \quad \text{or} \quad \frac{x_{Dt,k}}{x_{Dt,k_r}} = \left(\hat{\alpha}_{k,k_r}^{N_{\min}} \right) \left(\frac{x_{Bt,k}}{x_{Bt,k_r}} \right) \quad (\text{A-1})$$

where the symbols d_t and b_t are column distillate and bottom flow rates, respectively. x_{dt} and x_{bt} are compositions for the distillate and bottom flows, respectively. Given the light key component k_L and heavy key components k_H , then the minimum number of theoretical stage becomes:

$$N_{\min} = \frac{\log \left[\left(\frac{x_{dt,k_L}}{x_{dt,k_H}} \right) \left(\frac{x_{bt,k_H}}{x_{bt,k_L}} \right) \right]}{\log \hat{\alpha}_{k_L,k_H}} \quad (\text{A-2})$$

$$N_{\min} = \frac{\log \left[\left(\frac{d_{t,k_L}}{d_{t,k_H}} \right) \left(\frac{b_{t,k_H}}{b_{t,k_L}} \right) \right]}{\log \hat{\alpha}_{k_L,k_H}} \quad (\text{A-3})$$

A.2 Hengstebeck-Geddes method

This method is used to estimate the composition of the products. It is based on total reflux conditions. The basic assumption here is that component distributions do not depend on reflux ratio. Based on this, the Fenske equation can also be written in the following form:

$$\log \left[\frac{d_{t,k_L}}{d_{t,k_H}} \right] = A + C \log \hat{\alpha}_{k_L,k_H} \quad (\text{A-4})$$

where parameter A and C are obtained by applying the relation to the light and heavy key components. The composition of non-key components can be estimated

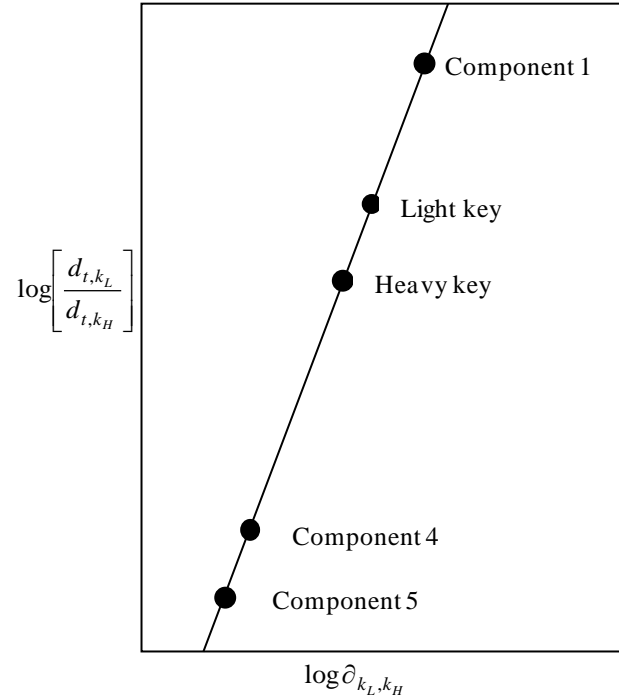


Fig A.1: A logarithmic plot for component distribution

A.3 Gilliland method

The Gilliland correlation used to calculate the number of stages, given reflux ratio R_{flx} and minimum number of stages N_{min} . The correlation can be evaluated using graphical method or equation based approach:

$$\text{Let } Y_e = \frac{N - N_{min}}{N + 1} \text{ and } X_e = \frac{R_{flx} - R_{flx}^{min}}{R_{flx} + 1} \quad (\text{A-5})$$

Based on this, several equations have been developed to relate X_e and Y_e :

$$\text{Liddle (1940): } Y_e = 0.545827 - 0.591422X_e + 0.002743 \cdot \frac{1}{X_e} \quad (\text{A-6})$$

$$\text{Molokonov (1972): } Y_e = 1 - \exp\left[\frac{1 + 54.4X_e}{11 + 117.2X_e} \cdot \frac{X_e - 1}{X_e^{0.5}}\right] \quad (\text{A-7})$$

$$\text{Eduljee (1975): } Y_e = 0.75(1 - X_e^{0.5668}) \quad (\text{A-8})$$

$$\text{Rusche (1999): } Y_e = 0.2788 - 1.3154X_e + 0.4114X_e^{0.2910} + 0.8268 \ln X_e + 0.9020\left(X_e + \frac{1}{X_e}\right) \quad (\text{A-9})$$

A.4 Kirkbride method

The Kirkbride equation is used to estimate the most appropriate feed point location:

$$\log \frac{N_r}{N_s} = 0.206 \log \left[\frac{Z_{k_H}}{Z_{k_L}} \cdot \frac{B_t}{D_s} \cdot \left(\frac{x_{bt,k_L}}{x_{dt,k_H}} \right)^2 \right] \quad (\text{A-10})$$

where N_r and N_s are number of rectification and stripping stages above and below the feed location, respectively. Z_{k_H} and Z_{k_L} are composition for heavy and light key. D_s and B_t are distillate and bottom flow rates, respectively.

A.5 Edmister Method

This method is used to find the product distribution ratio $d_{t,k}/b_{t,k}$ for each component in a column with a known number of trays above and below the feed and also with known reflux ratio. An absorption factor for each component k on each tray $n = 1, \dots, N$ is defined as:

$$A_{k,n} = L_n / V_n K_n \quad (\text{A-11})$$

Usually it is understood to apply to a specific component so the subscript k is dropped and the absorption factors on tray N becomes:

$$A_n = L_n / V_n K_n \quad (\text{A-12})$$

Similarly a stripping factor for each component is defined as:

$$S_n = K_n V_n / L_n \quad (\text{A-13})$$

The ratio of bottom and overhead flow rates for each component is :

$$\frac{b_i}{d_i} = \frac{\varphi_1 + (L_o / D_s K_o) \varphi_2 - (1 - q_F) F}{\psi_1 + \left(\frac{V_b}{B_t} \right) \psi_2 - 1} \quad (\text{A-14})$$

The individual flow rates of each component are found:

$$b_k = \frac{f_k}{1 + \left(\frac{b_k}{d_k} \right)}, \quad d_k = f_k - b_k \quad (\text{A-15})$$

The functions are defined as:

$$\varphi_1 = \frac{A_e^{N_r+1} - 1}{A_e - 1} \quad (\text{A-16})$$

$$\varphi_2 = \left(A_1 A_{N_r} \right)^{N_r/2} \quad (\text{A-17})$$

$$\psi_1 = \frac{S_e^{N_s+1} - 1}{S_e - 1} \quad (\text{A-18})$$

$$\psi_2 = \left(S_1 S_{N_s} \right)^{N_s/2} \quad (\text{A-19})$$

The approximate effective absorption and stripping factors in each zone are:

$$A_e = -0.5 + \sqrt{A_{N_r} (A_1 + 1)} + 0.25 \quad (\text{A-20})$$

$$S_e = -0.5 + \sqrt{S_{N_{sr}} (S_1 + 1)} + 0.25 \quad (\text{A-21})$$

Initial estimate is required when applying Edmister's methods which are improved by iteration. The initial estimates at the top and bottom temperatures so that A_1 and S_1 can be estimated. These estimates are then later adjusted using a bubble point calculations after b_k and d_k are found by first iteration. The temperature at the feed zone can be found by taking a linear temperature gradient.

APPENDIX B

STANDARD NORMAL DISTRIBUTION FUNCTION

Table B1 Standard loss function and standard normal cumulative distribution function

z (-3, 3)

z	$\Phi(z)$	z	$\Phi(z)$
-3.00	1.349898E-03	0.00	5.000000E-01
-2.96	1.538195E-03	0.04	5.159534E-01
-2.92	1.750157E-03	0.08	5.318814E-01
-2.88	1.988376E-03	0.12	5.477584E-01
-2.84	2.255677E-03	0.16	5.635595E-01
-2.80	2.555130E-03	0.20	5.792597E-01
-2.76	2.890068E-03	0.24	5.948349E-01
-2.72	3.264096E-03	0.28	6.102612E-01
-2.68	3.681108E-03	0.32	6.255158E-01
-2.64	4.145301E-03	0.36	6.405764E-01
-2.60	4.661188E-03	0.40	6.554217E-01
-2.56	5.233608E-03	0.44	6.700314E-01
-2.52	5.867742E-03	0.48	6.843863E-01
-2.48	6.569119E-03	0.52	6.984682E-01
-2.44	7.343631E-03	0.56	7.122603E-01
-2.40	8.197536E-03	0.60	7.257469E-01
-2.36	9.137468E-03	0.64	7.389137E-01
-2.32	1.017044E-02	0.68	7.517478E-01
-2.28	1.130384E-02	0.72	7.642375E-01
-2.24	1.254546E-02	0.76	7.763727E-01
-2.20	1.390345E-02	0.80	7.881446E-01
-2.16	1.538633E-02	0.84	7.995458E-01
-2.12	1.700302E-02	0.88	8.105703E-01
-2.08	1.876277E-02	0.92	8.212136E-01
-2.04	2.067516E-02	0.96	8.314724E-01
-2.00	2.275013E-02	1.00	8.413447E-01
-1.96	2.499790E-02	1.04	8.508300E-01
-1.92	2.742895E-02	1.08	8.599289E-01
-1.88	3.005404E-02	1.12	8.686431E-01
-1.84	3.288412E-02	1.16	8.769756E-01
-1.80	3.593032E-02	1.20	8.849303E-01
-1.76	3.920390E-02	1.24	8.925123E-01
-1.72	4.271622E-02	1.28	8.997274E-01
-1.68	4.647866E-02	1.32	9.065825E-01

Z	$\Phi(Z)$	Z	$\Phi(Z)$
-1.64	5.050258E-02	1.36	9.130850E-01
-1.60	5.479929E-02	1.40	9.192433E-01
-1.56	5.937994E-02	1.44	9.250663E-01
-1.52	6.425549E-02	1.48	9.305634E-01
-1.48	6.943662E-02	1.52	9.357445E-01
-1.44	7.493370E-02	1.56	9.406201E-01
-1.40	8.075666E-02	1.60	9.452007E-01
-1.36	8.691496E-02	1.64	9.494974E-01
-1.32	9.341751E-02	1.68	9.535213E-01
-1.28	1.002726E-01	1.72	9.572838E-01
-1.24	1.074877E-01	1.76	9.607961E-01
-1.20	1.150697E-01	1.80	9.640697E-01
-1.16	1.230244E-01	1.84	9.671159E-01
-1.12	1.313569E-01	1.88	9.699460E-01
-1.08	1.400711E-01	1.92	9.725711E-01
-1.04	1.491700E-01	1.96	9.750021E-01
-1.00	1.586553E-01	2.00	9.772499E-01
-0.96	1.685276E-01	2.04	9.793248E-01
-0.92	1.787864E-01	2.08	9.812372E-01
-0.88	1.894297E-01	2.12	9.829970E-01
-0.84	2.004542E-01	2.16	9.846137E-01
-0.80	2.118554E-01	2.20	9.860966E-01
-0.76	2.236273E-01	2.24	9.874545E-01
-0.72	2.357625E-01	2.28	9.886962E-01
-0.68	2.482522E-01	2.32	9.898296E-01
-0.64	2.610863E-01	2.36	9.908625E-01
-0.60	2.742531E-01	2.40	9.918025E-01
-0.56	2.877397E-01	2.44	9.926564E-01
-0.52	3.015318E-01	2.48	9.934309E-01
-0.48	3.156137E-01	2.52	9.941323E-01
-0.44	3.299686E-01	2.56	9.947664E-01
-0.40	3.445783E-01	2.60	9.953388E-01
-0.36	3.594236E-01	2.64	9.958547E-01
-0.32	3.744842E-01	2.68	9.963189E-01
-0.28	3.897388E-01	2.72	9.967359E-01
-0.24	4.051651E-01	2.76	9.971099E-01
-0.20	4.207403E-01	2.80	9.974449E-01
-0.16	4.364405E-01	2.84	9.977443E-01
-0.12	4.522416E-01	2.88	9.980116E-01
-0.08	4.681186E-01	2.92	9.982498E-01
-0.04	4.840466E-01	2.96	9.984618E-01
0.00	5.000000E-01	3.00	9.986501E-01

APPENDIX C

HYSYS PROCESS MODEL AND STREAMS DATA TABLES

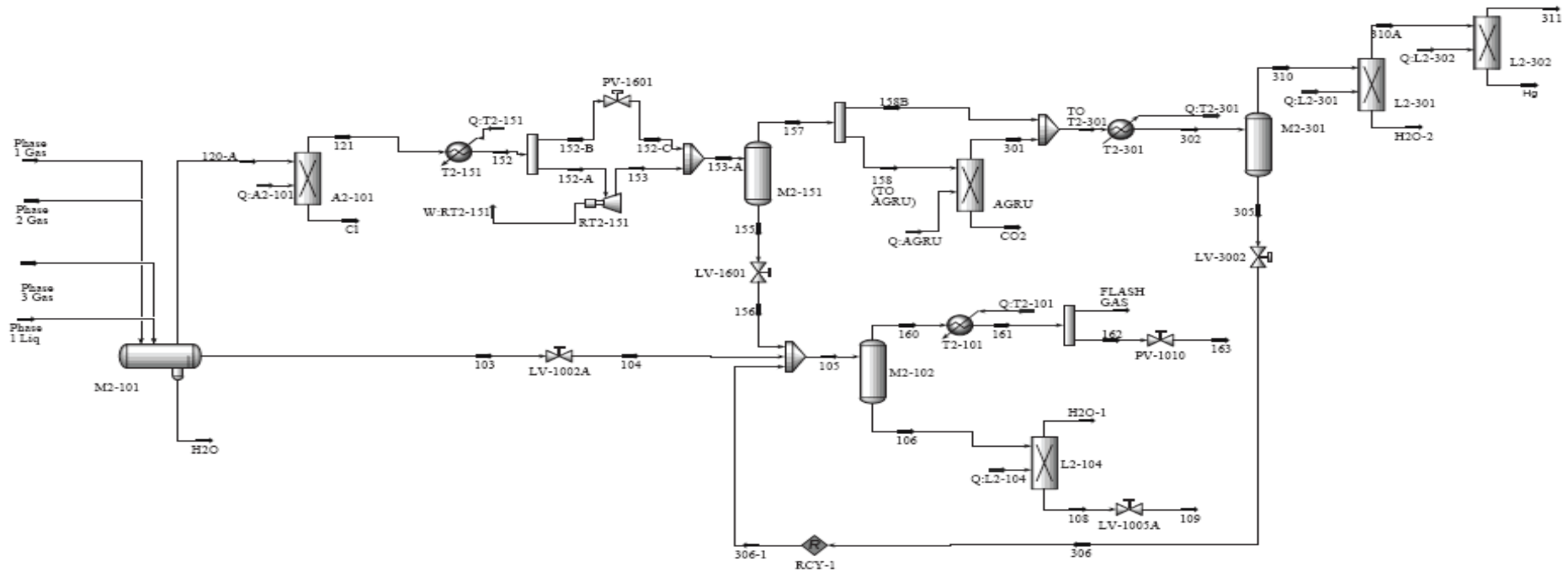


Fig. C.1. HYSYS process model for pretreatment unit (PTU), acid gas removal unit (AGRU) and Dehydration unit (DHU)

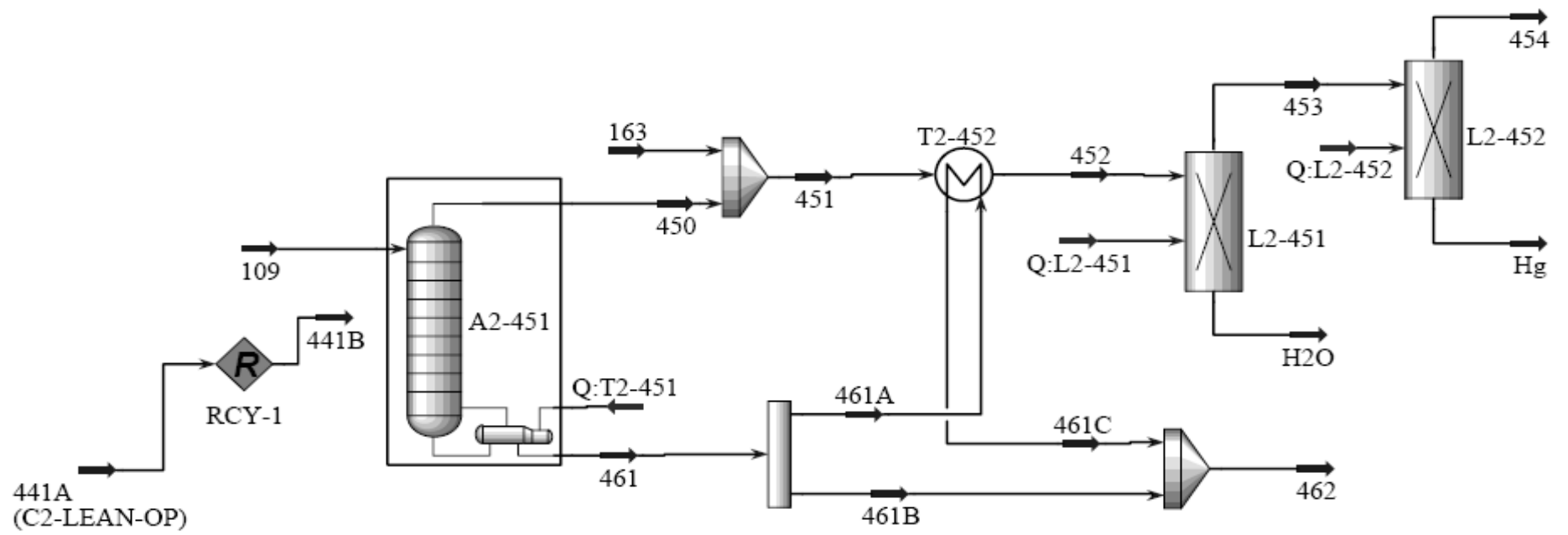


Fig. C.2. HYSYS process model for condensate treatment unit (CTU)

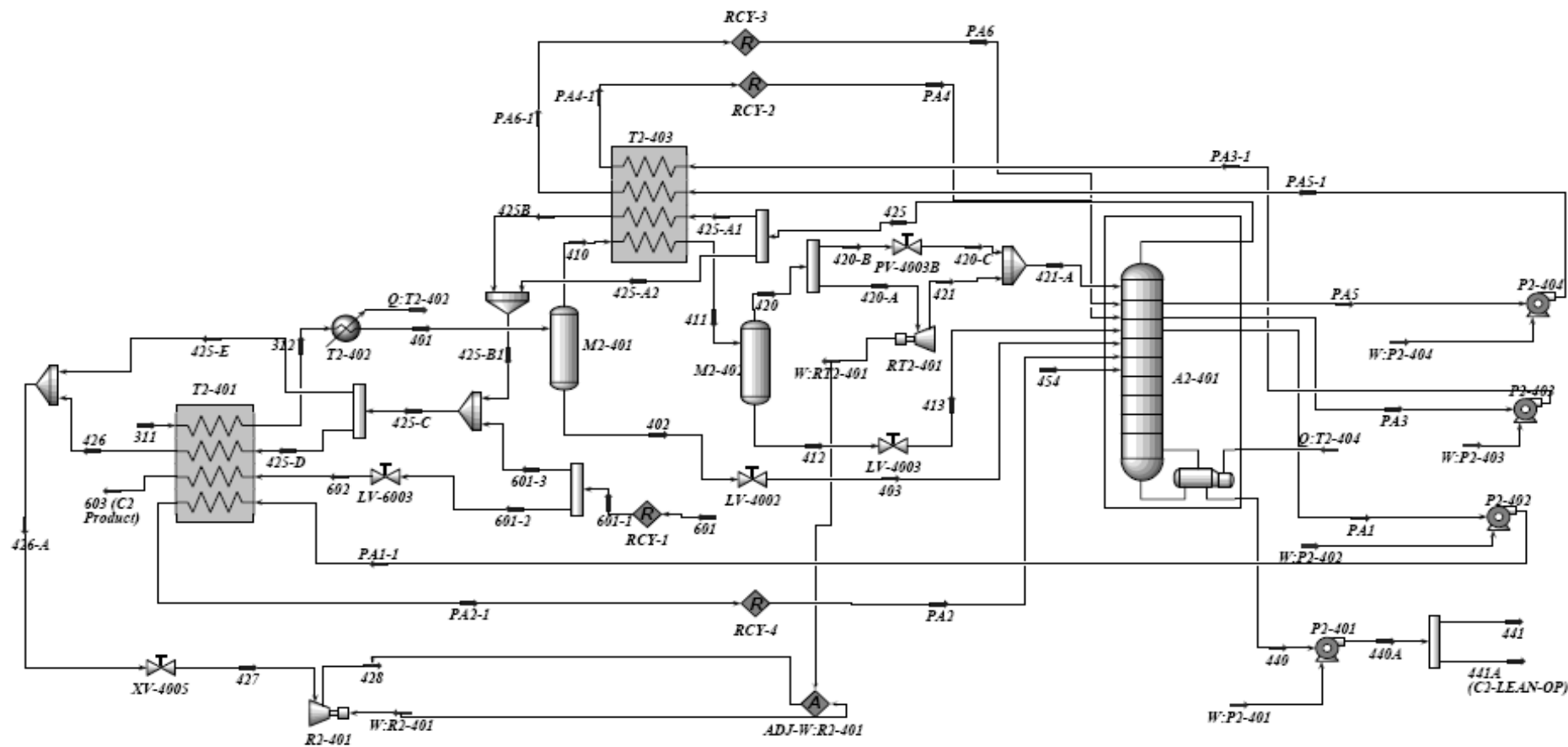


Fig. C.3. HYSYS process model for low temperature separation unit (LTSU)

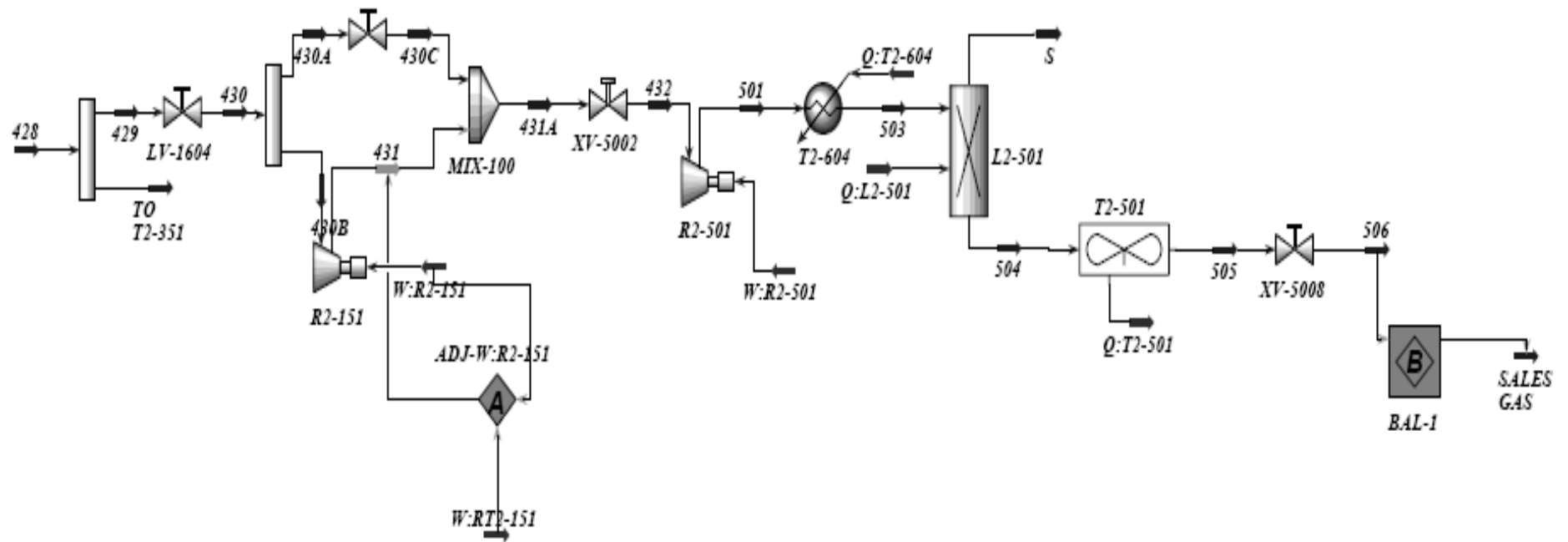


Fig. C.4. HYSYS process model for sales gas compression unit (SGCU)

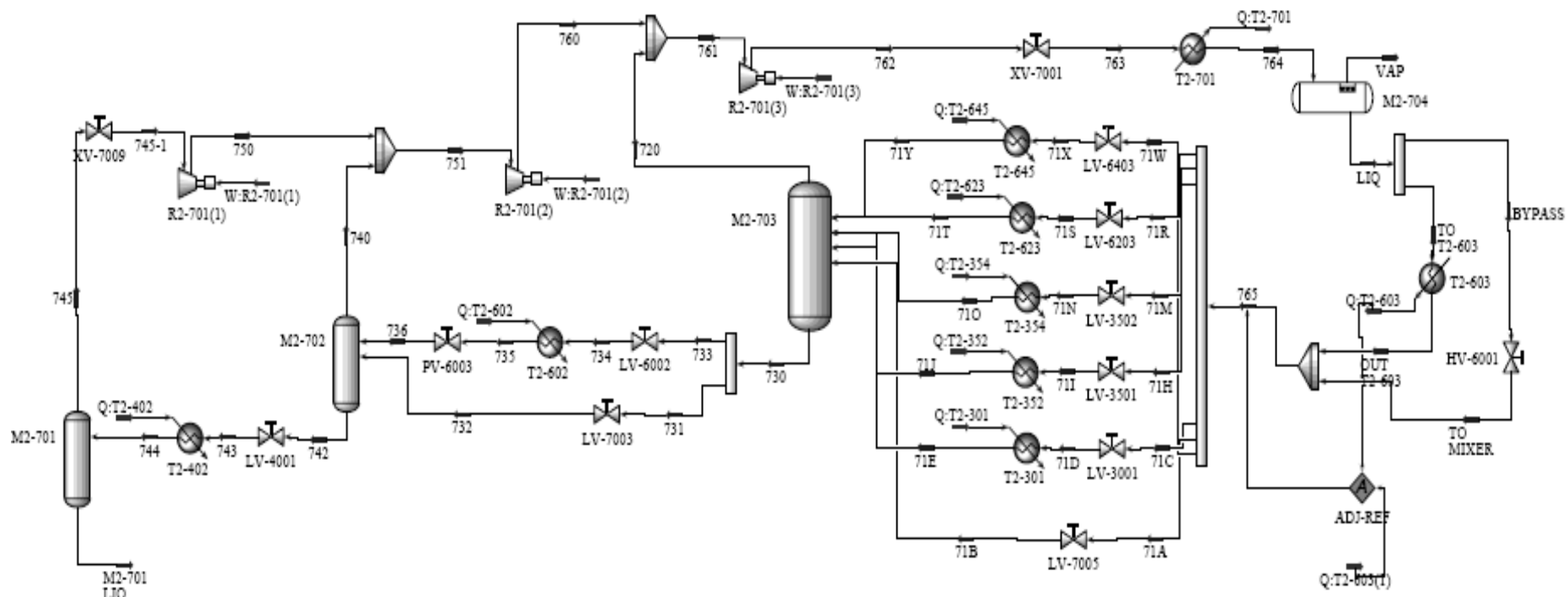


Fig. C.6. HYSYS process model for C₃ refrigeration unit (C₃RU)

Pretreatment unit (PTU) process stream data tables

Table C1: PTU process stream data table 1

	Streams												
		Phase 1 Gas	Phase 2 Gas	120-A	121	C1	103	152	153	157	155	156	104
Vapour Fraction		1.0000	1.0000	1.0000	1.0000	1.0000	0.0000	1.0000	1.0000	1.0000	0.0000	0.0824	0.0770
Temperature	C	25.00	18.00	20.42	28.82	26.82	20.42	28.54	28.73	25.08	25.08	23.05	18.62
Pressure	kPa	7262	7263	6514	6901	6900	6514	6721	6050	6050	6050	5322	5322
Molar Flow	kgmole/h	1.275e+004	2062	1.495e+004	1.495e+004	0.0000	492.0	1.495e+004	0.0000	1.495e+004	0.0000	0.0000	492.0
Mass Flow	tonne/h	254.5	40.10	298.9	298.9	0.0000	28.65	298.9	0.0000	298.9	0.0000	0.0000	28.65
Liquid Volume Flow	m ³ /h	744.2	117.7	871.5	871.5	0.0000	49.89	871.5	0.0000	871.5	0.0000	0.0000	49.89
Heat Flow	kW	-3.099e+005	-5.218e+004	-3.654e+005	-3.640e+005	0.0000	-2.124e+004	-3.639e+005	0.0000	-3.639e+005	0.0000	0.0000	-2.124e+004
Comp Mole Frac (Methane)		0.8341	0.8624	0.8367	0.8367	0.8367	0.2768	0.8367	0.8367	0.8367	0.2727	0.2727	0.2768
Comp Mole Frac (Ethane)		0.0787	0.0554	0.0749	0.0749	0.0749	0.0920	0.0749	0.0749	0.0749	0.0916	0.0916	0.0920
Comp Mole Frac (i-Butane)		0.0088	0.0094	0.0096	0.0096	0.0096	0.0605	0.0096	0.0096	0.0096	0.0609	0.0609	0.0605
Comp Mole Frac (n-Butane)		0.0075	0.0042	0.0071	0.0071	0.0071	0.0588	0.0071	0.0071	0.0071	0.0593	0.0593	0.0588
Comp Mole Frac (i-Pentane)		0.0029	0.0023	0.0031	0.0031	0.0031	0.0499	0.0031	0.0031	0.0031	0.0506	0.0506	0.0499
Comp Mole Frac (n-Pentane)		0.0016	0.0011	0.0016	0.0016	0.0016	0.0326	0.0016	0.0016	0.0016	0.0329	0.0329	0.0326
Comp Mole Frac (n-Hexane)		0.0009	0.0007	0.0011	0.0011	0.0011	0.0549	0.0011	0.0011	0.0011	0.0556	0.0556	0.0549
Comp Mole Frac (n-Heptane)		0.0004	0.0004	0.0007	0.0007	0.0007	0.0738	0.0007	0.0007	0.0007	0.0748	0.0748	0.0738
Comp Mole Frac (n-Octane)		0.0002	0.0002	0.0004	0.0004	0.0004	0.1041	0.0004	0.0004	0.0004	0.1053	0.1053	0.1041
Comp Mole Frac (n-Nonane)		0.0000	0.0000	0.0001	0.0001	0.0001	0.0642	0.0001	0.0001	0.0001	0.0650	0.0650	0.0642
Comp Mole Frac (n-Decane)		0.0000	0.0000	0.0000	0.0000	0.0000	0.0005	0.0000	0.0000	0.0000	0.0005	0.0005	0.0005
Comp Mole Frac (Nitrogen)		0.0042	0.0019	0.0038	0.0038	0.0038	0.0005	0.0038	0.0038	0.0038	0.0005	0.0005	0.0005
Comp Mole Frac (CO2)		0.0242	0.0368	0.0255	0.0255	0.0255	0.0175	0.0255	0.0255	0.0255	0.0162	0.0162	0.0175
Comp Mole Frac (H2S)		0.0000	0.0000	0.0000	0.0000	0.0000	0.0000	0.0000	0.0000	0.0000	0.0000	0.0000	0.0000
Comp Mole Frac (M-Mercaptan)		0.0000	0.0000	0.0000	0.0000	0.0000	0.0000	0.0000	0.0000	0.0000	0.0000	0.0000	0.0000
Comp Mole Frac (E-Mercaptan)		0.0000	0.0000	0.0000	0.0000	0.0000	0.0000	0.0000	0.0000	0.0000	0.0000	0.0000	0.0000
Comp Mole Frac (Propane)		0.0365	0.0252	0.0355	0.0355	0.0355	0.1139	0.0355	0.0355	0.0355	0.1143	0.1143	0.1139

Table C2: PTU process stream data table 2

		306-1	105	158B	158 (TO AGRU)	301	CO2	TO T2-301	302	310	305	306	310A
Vapour Fraction		0.0225	0.0769	1.0000	1.0000	1.0000	1.0000	1.0000	1.0000	1.0000	0.0000	0.0225	1.0000
Temperature	C	22.85	18.63	25.08	25.08	30.04	43.00	30.04	23.31	23.31	23.31	22.85	26.00
Pressure	kPa	5322	5322	6050	6050	5782	5781	5782	5681	5681	5681	5322	2127
Molar Flow	kgmole/h	0.6532	492.7	0.0000	1.495e+004	1.457e+004	380.6	1.457e+004	1.457e+004	1.456e+004	0.6582	0.6582	1.456e+004
Mass Flow	tonne/h	4.112e-002	28.69	0.0000	298.9	282.2	16.75	282.2	282.2	282.1	4.144e-002	4.144e-002	282.1
Liquid Volume Flow	m ³ /h	6.993e-002	49.96	0.0000	871.5	851.2	20.30	851.2	851.2	851.1	7.048e-002	7.048e-002	851.1
Heat Flow	kW	-28.77	-2.127e+004	0.0000	-3.639e+005	-3.207e+005	-4.186e+004	-3.207e+005	-3.220e+005	-3.219e+005	-28.99	-28.99	-3.176e+005
Comp Mole Frac (Methane)		0.2440	0.2768	0.8367	0.8367	0.8585	0.0000	0.8585	0.8585	0.8586	0.2440	0.2440	0.8586
Comp Mole Frac (Ethane)		0.0858	0.0920	0.0749	0.0749	0.0768	0.0000	0.0768	0.0768	0.0768	0.0858	0.0858	0.0768
Comp Mole Frac (i-Butane)		0.0611	0.0605	0.0096	0.0096	0.0098	0.0000	0.0098	0.0098	0.0098	0.0611	0.0611	0.0098
Comp Mole Frac (n-Butane)		0.0600	0.0588	0.0071	0.0071	0.0073	0.0000	0.0073	0.0073	0.0073	0.0600	0.0600	0.0073
Comp Mole Frac (i-Pentane)		0.0527	0.0499	0.0031	0.0031	0.0032	0.0000	0.0032	0.0032	0.0031	0.0527	0.0527	0.0031
Comp Mole Frac (n-Pentane)		0.0347	0.0326	0.0016	0.0016	0.0016	0.0000	0.0016	0.0016	0.0016	0.0347	0.0347	0.0016
Comp Mole Frac (n-Hexane)		0.0610	0.0549	0.0011	0.0011	0.0012	0.0000	0.0012	0.0012	0.0012	0.0610	0.0610	0.0012
Comp Mole Frac (n-Heptane)		0.0853	0.0738	0.0007	0.0007	0.0007	0.0000	0.0007	0.0007	0.0007	0.0853	0.0853	0.0007
Comp Mole Frac (n-Octane)		0.1246	0.1042	0.0004	0.0004	0.0004	0.0000	0.0004	0.0004	0.0004	0.1246	0.1246	0.0004
Comp Mole Frac (n-Nonane)		0.0787	0.0643	0.0001	0.0001	0.0001	0.0000	0.0001	0.0001	0.0001	0.0787	0.0787	0.0001
Comp Mole Frac (n-Decane)		0.0006	0.0005	0.0000	0.0000	0.0000	0.0000	0.0000	0.0000	0.0000	0.0006	0.0006	0.0000
Comp Mole Frac (Nitrogen)		0.0004	0.0005	0.0038	0.0038	0.0039	0.0000	0.0039	0.0039	0.0039	0.0004	0.0004	0.0039
Comp Mole Frac (CO2)		0.0000	0.0175	0.0255	0.0255	0.0000	1.0000	0.0000	0.0000	0.0000	0.0000	0.0000	0.0000
Comp Mole Frac (H2S)		0.0000	0.0000	0.0000	0.0000	0.0000	0.0000	0.0000	0.0000	0.0000	0.0000	0.0000	0.0000
Comp Mole Frac (M-Mercaptan)		0.0000	0.0000	0.0000	0.0000	0.0000	0.0000	0.0000	0.0000	0.0000	0.0000	0.0000	0.0000
Comp Mole Frac (E-Mercaptan)		0.0000	0.0000	0.0000	0.0000	0.0000	0.0000	0.0000	0.0000	0.0000	0.0000	0.0000	0.0000
Comp Mole Frac (Propane)		0.1111	0.1139	0.0355	0.0355	0.0364	0.0000	0.0364	0.0364	0.0364	0.1111	0.1111	0.0364

Table C3: PTU process stream data table 3

		H2O-2	311	Hg	160	106	161	FLASH GAS	162	163	H2O-1	108	109
Vapour Fraction		1.0000	0.9998	1.0000	1.0000	0.0000	1.0000	1.0000	1.0000	0.9994	0.0159	0.0158	0.2019
Temperature	C	25.00	22.00	25.00	18.63	18.63	29.37	29.37	29.37	12.04	27.10	27.10	20.81
Pressure	kPa	2126	5683	5630	5322	5322	5451	5451	5451	2500	5450	5452	2502
Molar Flow	kgmole/h	0.0000	1.456e+004	0.0000	37.88	454.8	37.88	0.0000	37.88	37.88	0.0000	454.8	454.8
Mass Flow	tonne/h	0.0000	282.1	0.0000	0.7618	27.93	0.7618	0.0000	0.7618	0.7618	0.0000	27.93	27.93
Liquid Volume Flow	m ³ /h	0.0000	851.1	0.0000	2.216	47.74	2.216	0.0000	2.216	2.216	0.0000	47.74	47.74
Heat Flow	kW	0.0000	-3.222e+005	0.0000	-930.9	-2.034e+004	-925.5	0.0000	-925.5	-925.5	0.0000	-2.018e+004	-2.018e+004
Comp Mole Frac (Methane)		0.8586	0.8586	0.8586	0.8288	0.2308	0.8288	0.8288	0.8288	0.8288	0.2308	0.2308	0.2308
Comp Mole Frac (Ethane)		0.0768	0.0768	0.0768	0.0811	0.0929	0.0811	0.0811	0.0811	0.0811	0.0929	0.0929	0.0929
Comp Mole Frac (i-Butane)		0.0098	0.0098	0.0098	0.0096	0.0647	0.0096	0.0096	0.0096	0.0096	0.0647	0.0647	0.0647
Comp Mole Frac (n-Butane)		0.0073	0.0073	0.0073	0.0070	0.0631	0.0070	0.0070	0.0070	0.0070	0.0631	0.0631	0.0631
Comp Mole Frac (i-Pentane)		0.0031	0.0031	0.0031	0.0029	0.0538	0.0029	0.0029	0.0029	0.0029	0.0538	0.0538	0.0538
Comp Mole Frac (n-Pentane)		0.0016	0.0016	0.0016	0.0015	0.0352	0.0015	0.0015	0.0015	0.0015	0.0352	0.0352	0.0352
Comp Mole Frac (n-Hexane)		0.0012	0.0012	0.0012	0.0010	0.0594	0.0010	0.0010	0.0010	0.0010	0.0594	0.0594	0.0594
Comp Mole Frac (n-Heptane)		0.0007	0.0007	0.0007	0.0005	0.0799	0.0005	0.0005	0.0005	0.0005	0.0799	0.0799	0.0799
Comp Mole Frac (n-Octane)		0.0004	0.0004	0.0004	0.0003	0.1128	0.0003	0.0003	0.0003	0.0003	0.1128	0.1128	0.1128
Comp Mole Frac (n-Nonane)		0.0001	0.0001	0.0001	0.0001	0.0696	0.0001	0.0001	0.0001	0.0001	0.0696	0.0696	0.0696
Comp Mole Frac (n-Decane)		0.0000	0.0000	0.0000	0.0000	0.0005	0.0000	0.0000	0.0000	0.0000	0.0005	0.0005	0.0005
Comp Mole Frac (Nitrogen)		0.0039	0.0039	0.0039	0.0029	0.0003	0.0029	0.0029	0.0029	0.0029	0.0003	0.0003	0.0003
Comp Mole Frac (CO2)		0.0000	0.0000	0.0000	0.0273	0.0166	0.0273	0.0273	0.0273	0.0273	0.0166	0.0166	0.0166
Comp Mole Frac (H2S)		0.0000	0.0000	0.0000	0.0000	0.0000	0.0000	0.0000	0.0000	0.0000	0.0000	0.0000	0.0000
Comp Mole Frac (M-Mercaptan)		0.0000	0.0000	0.0000	0.0000	0.0000	0.0000	0.0000	0.0000	0.0000	0.0000	0.0000	0.0000
Comp Mole Frac (E-Mercaptan)		0.0000	0.0000	0.0000	0.0000	0.0000	0.0000	0.0000	0.0000	0.0000	0.0000	0.0000	0.0000
Comp Mole Frac (Propane)		0.0364	0.0364	0.0364	0.0372	0.1203	0.0372	0.0372	0.0372	0.0372	0.1203	0.1203	0.1203

Table C4: PTU process stream data table 4

		H2O	462	441	601	428	152-B	152-A	152-C	153-A	Phase 2 Liq	441A (C2-LEAN-OP)	TCOT Gas
Vapour Fraction		0.0000	0.0000	0.0000	0.0000	1.0000	1.0000	1.0000	1.0000	1.0000	0.1048	0.0000	1.0000
Temperature	C	20.42	166.3	30.96	4.631	36.18	28.54	28.54	25.08	25.08	27.44	30.96	29.64
Pressure	kPa	6514	2396	3009	2771	2579	6721	6721	6050	6050	6662	3009	6514
Molar Flow	kgmole/h	-2.998e-013	282.0	1726	825.3	1.316e+004	1.495e+004	0.0000	1.495e+004	1.495e+004	572.3	0.0000	48.58
Mass Flow	tonne/h	-1.745e-014	23.70	71.89	24.90	218.5	298.9	0.0000	298.9	298.9	31.70	0.0000	1.255
Liquid Volume Flow	m ³ /h	-3.039e-014	36.44	155.5	69.42	718.4	871.5	0.0000	871.5	871.5	56.23	0.0000	3.239
Heat Flow	kW	1.294e-011	-1.285e+004	-5.647e+004	-2.286e+004	-2.742e+005	-3.639e+005	0.0000	-3.639e+005	-3.639e+005	-2.319e+004	0.0000	-1370
Comp Mole Frac (Methane)		0.2768	0.0000	0.0016	0.0034	0.9605	0.8367	0.8367	0.8367	0.8367	0.3438	0.0016	0.5575
Comp Mole Frac (Ethane)		0.0920	0.0050	0.4773	0.9860	0.0339	0.0749	0.0749	0.0749	0.0749	0.0615	0.4773	0.2264
Comp Mole Frac (i-Butane)		0.0605	0.0937	0.0845	0.0000	0.0000	0.0096	0.0096	0.0096	0.0096	0.0700	0.0845	0.0204
Comp Mole Frac (n-Butane)		0.0588	0.0942	0.0626	0.0000	0.0000	0.0071	0.0071	0.0071	0.0071	0.0520	0.0626	0.0144
Comp Mole Frac (i-Pentane)		0.0499	0.0839	0.0270	0.0000	0.0000	0.0031	0.0031	0.0031	0.0031	0.0500	0.0270	0.0021
Comp Mole Frac (n-Pentane)		0.0326	0.0553	0.0140	0.0000	0.0000	0.0016	0.0016	0.0016	0.0016	0.0300	0.0140	0.0010
Comp Mole Frac (n-Hexane)		0.0549	0.0949	0.0099	0.0000	0.0000	0.0011	0.0011	0.0011	0.0011	0.0550	0.0099	0.0001
Comp Mole Frac (n-Heptane)		0.0738	0.1285	0.0058	0.0000	0.0000	0.0007	0.0007	0.0007	0.0007	0.0700	0.0058	0.0001
Comp Mole Frac (n-Octane)		0.1041	0.1817	0.0036	0.0000	0.0000	0.0004	0.0004	0.0004	0.0004	0.0950	0.0036	0.0000
Comp Mole Frac (n-Nonane)		0.0642	0.1122	0.0010	0.0000	0.0000	0.0001	0.0001	0.0001	0.0001	0.0383	0.0010	0.0000
Comp Mole Frac (n-Decane)		0.0005	0.0008	0.0000	0.0000	0.0000	0.0000	0.0000	0.0000	0.0000	0.0004	0.0000	0.0000
Comp Mole Frac (Nitrogen)		0.0005	0.0000	0.0000	0.0000	0.0044	0.0038	0.0038	0.0038	0.0038	0.0000	0.0000	0.0016
Comp Mole Frac (CO2)		0.0175	0.0000	0.0050	0.0105	0.0001	0.0255	0.0255	0.0255	0.0255	0.0040	0.0050	0.0494
Comp Mole Frac (H2S)		0.0000	0.0000	0.0000	0.0000	0.0000	0.0000	0.0000	0.0000	0.0000	0.0000	0.0000	0.0000
Comp Mole Frac (M-Mercaptan)		0.0000	0.0000	0.0000	0.0000	0.0000	0.0000	0.0000	0.0000	0.0000	0.0000	0.0000	0.0000
Comp Mole Frac (E-Mercaptan)		0.0000	0.0000	0.0000	0.0000	0.0000	0.0000	0.0000	0.0000	0.0000	0.0000	0.0000	0.0000
Comp Mole Frac (Propane)		0.1139	0.1498	0.3077	0.0001	0.0011	0.0355	0.0355	0.0355	0.0355	0.1100	0.3077	0.1270

Table C5: PTU process stream data table 5

		3	454	Q:A2-101	Q:T2-151	W:RT2-151	Q:T2-301	Q:L2-301	Q:T2-101	Q:L2-104	Q:AGRU	Q:L2-302	
Vapour Fraction		0.0000	1.0000										
Temperature	C	5.000	33.40										
Pressure	kPa	5000	2244										
Molar Flow	kgmole/h	430.1	210.7										
Mass Flow	tonne/h	31.13	4.993										
Liquid Volume Flow	m ³ /h	50.06	13.52										
Heat Flow	kW	-2.184e+004	-5331	1432	136.7	0.0000	1280	4360	5345	161.7	1334	-4647	
Comp Mole Frac (Methane)		0.2205	0.6471										
Comp Mole Frac (Ethane)		0.0550	0.2084										
Comp Mole Frac (i-Butane)		0.0542	0.0160										
Comp Mole Frac (n-Butane)		0.0339	0.0115										
Comp Mole Frac (i-Pentane)		0.0379	0.0044										
Comp Mole Frac (n-Pentane)		0.0219	0.0022										
Comp Mole Frac (n-Hexane)		0.0687	0.0013										
Comp Mole Frac (n-Heptane)		0.1145	0.0007										
Comp Mole Frac (n-Octane)		0.1866	0.0004										
Comp Mole Frac (n-Nonane)		0.1174	0.0001										
Comp Mole Frac (n-Decane)		0.0005	0.0000										
Comp Mole Frac (Nitrogen)		0.0000	0.0012										
Comp Mole Frac (CO2)		0.0158	0.0408										
Comp Mole Frac (H2S)		0.0000	0.0000										
Comp Mole Frac (M-Mercaptan)		0.0000	0.0000										
Comp Mole Frac (E-Mercaptan)		0.0000	0.0000										
Comp Mole Frac (Propane)		0.0732	0.0639										

Condensate treatment unit (CTU) process stream data tables

Table C6: CTU process stream data table 1

		Streams									
		109	163	441A (C2-LEAN-OP)	441B	450	451	452	453	454	461
Vapour Fraction		0.2019	0.9994	0.0000	0.0000	1.0000	0.9998	1.0000	1.0000	1.0000	0.0000
Temperature	C	20.81	12.04	30.96	30.96	26.37	23.88	46.36	32.40	33.40	169.3
Pressure	kPa	2502	2500	3009	3009	2375	2375	2450	2400	2244	2396
Molar Flow	kgmole/h	454.8	37.88	0.0000	0.0000	172.8	210.7	210.7	210.7	210.7	282.0
Mass Flow	tonne/h	27.93	0.7618	0.0000	0.0000	4.232	4.993	4.993	4.993	4.993	23.70
Liquid Volume Flow	m ³ /h	47.74	2.216	0.0000	0.0000	11.30	13.52	13.52	13.52	13.52	36.44
Heat Flow	kW	-2.018e+004	-925.5	0.0000	0.0000	-4636	-5561	-5497	-5537	-5531	-1.279e+004
Comp Mole Frac (Methane)		0.2308	0.8288	0.0016	0.0016	0.6072	0.6471	0.6471	0.6471	0.6471	0.0000
Comp Mole Frac (Ethane)		0.0929	0.0811	0.4773	0.4772	0.2364	0.2084	0.2084	0.2084	0.2084	0.0050
Comp Mole Frac (i-Butane)		0.0647	0.0096	0.0845	0.0846	0.0174	0.0160	0.0160	0.0160	0.0160	0.0937
Comp Mole Frac (n-Butane)		0.0631	0.0070	0.0626	0.0626	0.0125	0.0115	0.0115	0.0115	0.0115	0.0942
Comp Mole Frac (i-Pentane)		0.0538	0.0029	0.0270	0.0270	0.0047	0.0044	0.0044	0.0044	0.0044	0.0839
Comp Mole Frac (n-Pentane)		0.0352	0.0015	0.0140	0.0140	0.0024	0.0022	0.0022	0.0022	0.0022	0.0553
Comp Mole Frac (n-Hexane)		0.0594	0.0010	0.0099	0.0099	0.0014	0.0013	0.0013	0.0013	0.0013	0.0949
Comp Mole Frac (n-Heptane)		0.0799	0.0005	0.0058	0.0058	0.0007	0.0007	0.0007	0.0007	0.0007	0.1285
Comp Mole Frac (n-Octane)		0.1128	0.0003	0.0036	0.0036	0.0004	0.0004	0.0004	0.0004	0.0004	0.1817
Comp Mole Frac (n-Nonane)		0.0696	0.0001	0.0010	0.0010	0.0001	0.0001	0.0001	0.0001	0.0001	0.1122
Comp Mole Frac (n-Decane)		0.0005	0.0000	0.0000	0.0000	0.0000	0.0000	0.0000	0.0000	0.0000	0.0008
Comp Mole Frac (Nitrogen)		0.0003	0.0029	0.0000	0.0000	0.0008	0.0012	0.0012	0.0012	0.0012	0.0000
Comp Mole Frac (CO ₂)		0.0166	0.0273	0.0050	0.0050	0.0438	0.0408	0.0408	0.0408	0.0408	0.0000
Comp Mole Frac (H ₂ S)		0.0000	0.0000	0.0000	0.0000	0.0000	0.0000	0.0000	0.0000	0.0000	0.0000
Comp Mole Frac (M-Mercaptan)		0.0000	0.0000	0.0000	0.0000	0.0000	0.0000	0.0000	0.0000	0.0000	0.0000
Comp Mole Frac (E-Mercaptan)		0.0000	0.0000	0.0000	0.0000	0.0000	0.0000	0.0000	0.0000	0.0000	0.0000
Comp Mole Frac (Propane)		0.1203	0.0372	0.3077	0.3079	0.0722	0.0659	0.0659	0.0659	0.0659	0.1498

Table C7: CTU process stream data table 2

		461A	461B	461C	462	H2O	Hg	Q:L2-451	Q:L2-452	Q:T2-451	
Vapour Fraction		0.0000	0.0000	0.0000	0.0000	1.0000	1.0000				
Temperature	C	169.3	169.3	166.4	166.3	32.40	32.40				
Pressure	kPa	2396	2396	2471	2396	2400	2244				
Molar Flow	kgmole/h	282.0	0.0000	282.0	282.0	0.0000	0.0000				
Mass Flow	tonne/h	23.70	0.0000	23.70	23.70	0.0000	0.0000				
Liquid Volume Flow	m3/h	36.44	0.0000	36.44	36.44	0.0000	0.0000				
Heat Flow	kW	-1.279e+004	0.0000	-1.285e+004	-1.285e+004	0.0000	0.0000	-40.15	6.152	2757	
Comp Mole Frac (Methane)		0.0000	0.0000	0.0000	0.0000	0.6471	0.6471				
Comp Mole Frac (Ethane)		0.0050	0.0050	0.0050	0.0050	0.2084	0.2084				
Comp Mole Frac (i-Butane)		0.0937	0.0937	0.0937	0.0937	0.0160	0.0160				
Comp Mole Frac (n-Butane)		0.0942	0.0942	0.0942	0.0942	0.0115	0.0115				
Comp Mole Frac (i-Pentane)		0.0839	0.0839	0.0839	0.0839	0.0044	0.0044				
Comp Mole Frac (n-Pentane)		0.0553	0.0553	0.0553	0.0553	0.0022	0.0022				
Comp Mole Frac (n-Hexane)		0.0949	0.0949	0.0949	0.0949	0.0013	0.0013				
Comp Mole Frac (n-Heptane)		0.1285	0.1285	0.1285	0.1285	0.0007	0.0007				
Comp Mole Frac (n-Decane)		0.0005	0.0000	0.0000	0.0000	0.0000	0.0000	0.0000	0.0000	0.0000	0.0008
Comp Mole Frac (Nitrogen)		0.0003	0.0029	0.0000	0.0000	0.0008	0.0012	0.0012	0.0012	0.0012	0.0000
Comp Mole Frac (CO2)		0.0166	0.0273	0.0050	0.0050	0.0438	0.0408	0.0408	0.0408	0.0408	0.0000
Comp Mole Frac (H2S)		0.0000	0.0000	0.0000	0.0000	0.0000	0.0000	0.0000	0.0000	0.0000	0.0000
Comp Mole Frac (M-Mercaptan)		0.0000	0.0000	0.0000	0.0000	0.0000	0.0000	0.0000	0.0000	0.0000	0.0000
Comp Mole Frac (E-Mercaptan)		0.0000	0.0000	0.0000	0.0000	0.0000	0.0000	0.0000	0.0000	0.0000	0.0000
Comp Mole Frac (Propane)		0.1203	0.0372	0.3077	0.3079	0.0722	0.0659	0.0659	0.0659	0.0659	0.1498

Table C8: CTU process stream data table 3

		461A	461B	461C	462	H2O	Hg	Q:L2-451	Q:L2-452	Q:T2-451	
Vapour Fraction		0.0000	0.0000	0.0000	0.0000	1.0000	1.0000				
Temperature	C	169.3	169.3	166.4	166.3	32.40	32.40				
Pressure	kPa	2396	2396	2471	2396	2400	2244				
Molar Flow	kgmole/h	282.0	0.0000	282.0	282.0	0.0000	0.0000				
Mass Flow	tonne/h	23.70	0.0000	23.70	23.70	0.0000	0.0000				
Liquid Volume Flow	m3/h	36.44	0.0000	36.44	36.44	0.0000	0.0000				
Heat Flow	kW	-1.279e+004	0.0000	-1.285e+004	-1.285e+004	0.0000	0.0000	-40.15	6.152	2757	
Comp Mole Frac (Methane)		0.0000	0.0000	0.0000	0.0000	0.6471	0.6471				
Comp Mole Frac (Ethane)		0.0050	0.0050	0.0050	0.0050	0.2084	0.2084				
Comp Mole Frac (i-Butane)		0.0937	0.0937	0.0937	0.0937	0.0160	0.0160				
Comp Mole Frac (n-Butane)		0.0942	0.0942	0.0942	0.0942	0.0115	0.0115				
Comp Mole Frac (i-Pentane)		0.0839	0.0839	0.0839	0.0839	0.0044	0.0044				
Comp Mole Frac (n-Pentane)		0.0553	0.0553	0.0553	0.0553	0.0022	0.0022				
Comp Mole Frac (n-Hexane)		0.0949	0.0949	0.0949	0.0949	0.0013	0.0013				
Comp Mole Frac (n-Heptane)		0.1285	0.1285	0.1285	0.1285	0.0007	0.0007				
Comp Mole Frac (n-Octane)		0.1817	0.1817	0.1817	0.1817	0.0004	0.0004				
Comp Mole Frac (n-Nonane)		0.1122	0.1122	0.1122	0.1122	0.0001	0.0001				
Comp Mole Frac (n-Decane)		0.0008	0.0008	0.0008	0.0008	0.0000	0.0000				
Comp Mole Frac (Nitrogen)		0.0000	0.0000	0.0000	0.0000	0.0012	0.0012				
Comp Mole Frac (CO2)		0.0000	0.0000	0.0000	0.0000	0.0408	0.0408				
Comp Mole Frac (H2S)		0.0000	0.0000	0.0000	0.0000	0.0000	0.0000				
Comp Mole Frac (M-Mercaptan)		0.0000	0.0000	0.0000	0.0000	0.0000	0.0000				
Comp Mole Frac (E-Mercaptan)		0.0000	0.0000	0.0000	0.0000	0.0000	0.0000				
Comp Mole Frac (Propane)		0.1498	0.1498	0.1498	0.1498	0.0659	0.0659				

Low temperature separation unit (LTSU) process stream data tables

Table C9: LTSU process stream data table 1

		Streams											
		311	312	425B	426	602	603 (C2 Product)	PA1-1	PA2-1	401	410	402	411
Vapour Fraction		0.9998	0.9180	1.0000	1.0000	0.0985	1.0000	0.0000	0.0171	0.8906	1.0000	0.0000	0.8972
Temperature	C	22.00	-30.00	-58.29	20.00	-3.000	20.00	-20.23	-17.74	-36.00	-36.00	-36.00	-56.00
Pressure	kPa	5681	5581	2301	2231	2301	2271	2321	2321	5621	5621	5621	5541
Molar Flow	kgmole/h	1.455e+004	1.455e+004	1.304e+004	1.315e+004	715.6	715.6	4145	4145	1.455e+004	1.296e+004	1591	1.296e+004
Mass Flow	tonne/h	281.6	281.6	215.0	218.3	21.59	21.59	153.3	153.3	281.6	231.0	50.68	231.0
Liquid Volume Flow	m3/h	849.9	849.9	708.5	717.7	60.19	60.19	349.5	349.5	849.9	731.7	118.2	731.7
Heat Flow	kW	-3.218e+005	-3.356e+005	-2.845e+005	-2.760e+005	-1.982e+004	-1.786e+004	-1.355e+005	-1.351e+005	-3.378e+005	-2.898e+005	-4.796e+004	-2.963e+005
Comp Mole Frac (Methane)		0.8588	0.8588	0.9685	0.9605	0.0035	0.0035	0.1302	0.1302	0.8588	0.9047	0.4845	0.9047
Comp Mole Frac (Ethane)		0.0768	0.0768	0.0259	0.0339	0.9860	0.9860	0.4681	0.4681	0.0768	0.0650	0.1726	0.0650
Comp Mole Frac (i-Butane)		0.0098	0.0098	0.0000	0.0000	0.0000	0.0000	0.0622	0.0622	0.0098	0.0033	0.0625	0.0033
Comp Mole Frac (n-Butane)		0.0072	0.0072	0.0000	0.0000	0.0000	0.0000	0.0457	0.0457	0.0072	0.0019	0.0506	0.0019
Comp Mole Frac (i-Pentane)		0.0031	0.0031	0.0000	0.0000	0.0000	0.0000	0.0195	0.0195	0.0031	0.0004	0.0251	0.0004
Comp Mole Frac (n-Pentane)		0.0016	0.0016	0.0000	0.0000	0.0000	0.0000	0.0101	0.0101	0.0016	0.0002	0.0134	0.0002
Comp Mole Frac (n-Hexane)		0.0011	0.0011	0.0000	0.0000	0.0000	0.0000	0.0071	0.0071	0.0011	0.0000	0.0101	0.0000
Comp Mole Frac (n-Heptane)		0.0007	0.0007	0.0000	0.0000	0.0000	0.0000	0.0041	0.0041	0.0007	0.0000	0.0061	0.0000
Comp Mole Frac (n-Octane)		0.0004	0.0004	0.0000	0.0000	0.0000	0.0000	0.0025	0.0025	0.0004	0.0000	0.0038	0.0000
Comp Mole Frac (n-Nonane)		0.0001	0.0001	0.0000	0.0000	0.0000	0.0000	0.0007	0.0007	0.0001	0.0000	0.0011	0.0000
Comp Mole Frac (n-Decane)		0.0000	0.0000	0.0000	0.0000	0.0000	0.0000	0.0000	0.0000	0.0000	0.0000	0.0000	0.0000
Comp Mole Frac (Nitrogen)		0.0039	0.0039	0.0044	0.0044	0.0000	0.0000	0.0000	0.0000	0.0039	0.0043	0.0008	0.0043
Comp Mole Frac (CO2)		0.0000	0.0000	0.0000	0.0001	0.0105	0.0105	0.0131	0.0131	0.0000	0.0000	0.0000	0.0000
Comp Mole Frac (H2S)		0.0000	0.0000	0.0000	0.0000	0.0000	0.0000	0.0000	0.0000	0.0000	0.0000	0.0000	0.0000
Comp Mole Frac (M-Mercaptan)		0.0000	0.0000	0.0000	0.0000	0.0000	0.0000	0.0000	0.0000	0.0000	0.0000	0.0000	0.0000
Comp Mole Frac (E-Mercaptan)		0.0000	0.0000	0.0000	0.0000	0.0000	0.0000	0.0000	0.0000	0.0000	0.0000	0.0000	0.0000
Comp Mole Frac (Propane)		0.0364	0.0364	0.0011	0.0011	0.0000	0.0000	0.2367	0.2367	0.0364	0.0200	0.1695	0.0200

Table C10: LTSU process stream data table 2

		425	PA5-1	PA6-1	PA3-1	PA4-1	403	420	412	413	421	601	PA2
Vapour Fraction		1.0000	0.0000	0.0922	0.0000	0.0846	0.3223	1.0000	0.0000	0.3969	0.8823	0.0000	0.0178
Temperature	C	-88.92	-51.10	-41.13	-48.06	-36.17	-55.69	-56.00	-56.00	-82.75	-88.69	4.631	-17.69
Pressure	kPa	2301	2310	2310	2314	2314	2314	5541	5541	2306	2332	2771	2321
Molar Flow	kgmole/h	1.305e+004	2417	2417	1758	1758	1601	1.163e+004	1331	1331	1.163e+004	825.3	4145
Mass Flow	tonne/h	215.2	73.78	73.78	61.69	61.69	51.03	200.6	30.48	30.48	200.6	24.90	153.3
Liquid Volume Flow	m3/h	709.2	188.6	188.6	142.8	142.8	119.0	647.0	85.15	85.15	647.0	69.42	349.5
Heat Flow	kW	-2.896e+005	-7.060e+004	-6.967e+004	-5.563e+004	-5.487e+004	-4.827e+004	-2.618e+005	-3.464e+004	-3.464e+004	-2.639e+005	-2.286e+004	-1.351e+005
Comp Mole Frac (Methane)		0.9685	0.2556	0.2556	0.2408	0.2408	0.4845	0.9287	0.6960	0.6960	0.9287	0.0034	0.1304
Comp Mole Frac (Ethane)		0.0259	0.5150	0.5150	0.3820	0.3820	0.1725	0.0536	0.1649	0.1649	0.0536	0.9860	0.4679
Comp Mole Frac (i-Butane)		0.0000	0.0293	0.0293	0.0613	0.0613	0.0625	0.0012	0.0216	0.0216	0.0012	0.0000	0.0622
Comp Mole Frac (n-Butane)		0.0000	0.0169	0.0169	0.0453	0.0453	0.0506	0.0006	0.0136	0.0136	0.0006	0.0000	0.0457
Comp Mole Frac (i-Pentane)		0.0000	0.0038	0.0038	0.0195	0.0195	0.0251	0.0001	0.0036	0.0036	0.0001	0.0000	0.0195
Comp Mole Frac (n-Pentane)		0.0000	0.0015	0.0015	0.0101	0.0101	0.0135	0.0000	0.0015	0.0015	0.0000	0.0000	0.0101
Comp Mole Frac (n-Hexane)		0.0000	0.0004	0.0004	0.0072	0.0072	0.0102	0.0000	0.0004	0.0004	0.0000	0.0000	0.0071
Comp Mole Frac (n-Heptane)		0.0000	0.0001	0.0001	0.0042	0.0042	0.0061	0.0000	0.0001	0.0001	0.0000	0.0000	0.0041
Comp Mole Frac (n-Octane)		0.0000	0.0000	0.0000	0.0026	0.0026	0.0038	0.0000	0.0000	0.0000	0.0000	0.0000	0.0025
Comp Mole Frac (n-Nonane)		0.0000	0.0000	0.0000	0.0007	0.0007	0.0011	0.0000	0.0000	0.0000	0.0000	0.0000	0.0007
Comp Mole Frac (n-Decane)		0.0000	0.0000	0.0000	0.0000	0.0000	0.0000	0.0000	0.0000	0.0000	0.0000	0.0000	0.0000
Comp Mole Frac (Nitrogen)		0.0044	0.0001	0.0001	0.0001	0.0001	0.0008	0.0046	0.0015	0.0015	0.0046	0.0000	0.0000
Comp Mole Frac (CO2)		0.0000	0.0006	0.0006	0.0002	0.0002	0.0000	0.0000	0.0000	0.0000	0.0000	0.0105	0.0130
Comp Mole Frac (H2S)		0.0000	0.0000	0.0000	0.0000	0.0000	0.0000	0.0000	0.0000	0.0000	0.0000	0.0000	0.0000
Comp Mole Frac (M-Mercaptan)		0.0000	0.0000	0.0000	0.0000	0.0000	0.0000	0.0000	0.0000	0.0000	0.0000	0.0000	0.0000
Comp Mole Frac (E-Mercaptan)		0.0000	0.0000	0.0000	0.0000	0.0000	0.0000	0.0000	0.0000	0.0000	0.0000	0.0000	0.0000
Comp Mole Frac (Propane)		0.0011	0.1767	0.1767	0.2260	0.2260	0.1694	0.0112	0.0968	0.0968	0.0112	0.0001	0.2367

Table C11: LTSU process stream data table 3

		PA4	PA6	440	PA1	PA5	PA3	427	428	441	420-B	420-A	420-C
Vapour Fraction		0.0844	0.0921	0.0000	0.0000	0.0000	0.0000	1.0000	1.0000	0.0000	1.0000	1.0000	0.9340
Temperature	C	-36.17	-41.13	30.00	-20.24	-51.10	-48.06	19.59	36.18	30.96	-56.00	-56.00	-82.61
Pressure	kPa	2314	2310	2326	2321	2310	2314	2151	2579	3009	5541	5541	2332
Molar Flow	kgmole/h	1759	2417	1726	4145	2417	1758	1.316e+004	1.316e+004	1726	0.0000	1.163e+004	0.0000
Mass Flow	tonne/h	61.69	73.78	71.89	153.3	73.78	61.69	218.5	218.5	71.89	0.0000	200.6	0.0000
Liquid Volume Flow	m3/h	142.9	188.6	155.5	349.5	188.6	142.8	718.4	718.4	155.5	0.0000	647.0	0.0000
Heat Flow	kW	-2.639e+005	-2.896e+005	0.0000	-2.847e+005	-3038	-1.982e+004	-2.878e+005	-2.878e+005	0.0000	-2.763e+005	-5531	-5.647e+004
Comp Mole Frac (Methane)		0.9287	0.9685	0.9685	0.9685	0.0035	0.0035	0.9605	0.9605	0.9605	0.9605	0.6471	0.0016
Comp Mole Frac (Ethane)		0.0536	0.0259	0.0259	0.0259	0.9860	0.9860	0.0339	0.0339	0.0339	0.0339	0.2084	0.4773
Comp Mole Frac (i-Butane)		0.0012	0.0000	0.0000	0.0000	0.0000	0.0000	0.0000	0.0000	0.0000	0.0000	0.0160	0.0845
Comp Mole Frac (n-Butane)		0.0006	0.0000	0.0000	0.0000	0.0000	0.0000	0.0000	0.0000	0.0000	0.0000	0.0115	0.0626
Comp Mole Frac (i-Pentane)		0.0001	0.0000	0.0000	0.0000	0.0000	0.0000	0.0000	0.0000	0.0000	0.0000	0.0044	0.0270
Comp Mole Frac (n-Pentane)		0.0000	0.0000	0.0000	0.0000	0.0000	0.0000	0.0000	0.0000	0.0000	0.0000	0.0022	0.0140
Comp Mole Frac (n-Hexane)		0.0000	0.0000	0.0000	0.0000	0.0000	0.0000	0.0000	0.0000	0.0000	0.0000	0.0013	0.0099
Comp Mole Frac (n-Heptane)		0.0000	0.0000	0.0000	0.0000	0.0000	0.0000	0.0000	0.0000	0.0000	0.0000	0.0007	0.0058
Comp Mole Frac (n-Octane)		0.0000	0.0000	0.0000	0.0000	0.0000	0.0000	0.0000	0.0000	0.0000	0.0000	0.0004	0.0036
Comp Mole Frac (n-Nonane)		0.0000	0.0000	0.0000	0.0000	0.0000	0.0000	0.0000	0.0000	0.0000	0.0000	0.0001	0.0010
Comp Mole Frac (n-Decane)		0.0000	0.0000	0.0000	0.0000	0.0000	0.0000	0.0000	0.0000	0.0000	0.0000	0.0000	0.0000
Comp Mole Frac (Nitrogen)		0.0046	0.0044	0.0044	0.0044	0.0000	0.0000	0.0044	0.0044	0.0044	0.0044	0.0012	0.0000
Comp Mole Frac (CO2)		0.0000	0.0000	0.0000	0.0000	0.0105	0.0105	0.0001	0.0001	0.0001	0.0001	0.0408	0.0050
Comp Mole Frac (H2S)		0.0000	0.0000	0.0000	0.0000	0.0000	0.0000	0.0000	0.0000	0.0000	0.0000	0.0000	0.0000
Comp Mole Frac (M-Mercaptan)		0.0000	0.0000	0.0000	0.0000	0.0000	0.0000	0.0000	0.0000	0.0000	0.0000	0.0000	0.0000
Comp Mole Frac (E-Mercaptan)		0.0000	0.0000	0.0000	0.0000	0.0000	0.0000	0.0000	0.0000	0.0000	0.0000	0.0000	0.0000
Comp Mole Frac (Propane)		0.0112	0.0011	0.0011	0.0011	0.0000	0.0000	0.0011	0.0011	0.0011	0.0011	0.0659	0.3077

Table C12: LTSU process stream data table 4

		441A (C2-LEAN-OP)	601-1	Q:T2-402	W:RT2-401	Q:T2-404	W:P2-403	W:P2-404	W:P2-402	W:P2-401	W:R2-401		
Vapour Fraction		0.0000	0.0000										
Temperature	C	30.96	4.607										
Pressure	kPa	3009	2771										
Molar Flow	kgmole/h	0.0000	825.3										
Mass Flow	tonne/h	0.0000	24.90										
Liquid Volume Flow	m3/h	0.0000	69.42										
Heat Flow	kW	0.0000	-2.286e+004	2159	2083	4206	0.0000	0.0000	0.0000	39.15	2083		
Comp Mole Frac (Methane)		0.0016	0.0035										
Comp Mole Frac (Ethane)		0.4773	0.9860										
Comp Mole Frac (i-Butane)		0.0845	0.0000										
Comp Mole Frac (n-Butane)		0.0626	0.0000										
Comp Mole Frac (i-Pentane)		0.0270	0.0000										
Comp Mole Frac (n-Pentane)		0.0140	0.0000										
Comp Mole Frac (n-Hexane)		0.0099	0.0000										
Comp Mole Frac (n-Heptane)		0.0058	0.0000										
Comp Mole Frac (n-Octane)		0.0036	0.0000										
Comp Mole Frac (n-Nonane)		0.0010	0.0000										
Comp Mole Frac (n-Decane)		0.0000	0.0000										
Comp Mole Frac (Nitrogen)		0.0000	0.0000										
Comp Mole Frac (CO2)		0.0050	0.0105										
Comp Mole Frac (H2S)		0.0000	0.0000										
Comp Mole Frac (M-Mercaptan)		0.0000	0.0000										
Comp Mole Frac (E-Mercaptan)		0.0000	0.0000										
Comp Mole Frac (Propane)		0.3077	0.0000										

Sales gas compression unit (SGCU) process stream data tables

Table C13: SGCU process stream data table 1

	Streams												
		428	429	430	430A	430B	430C	431	431A	432	501	503	504
Vapour Fraction		1.0000	1.0000	1.0000	1.0000	1.0000	1.0000		1.0000	1.0000	1.0000	1.0000	1.0000
Temperature	C	36.18	36.18	35.55	35.55	35.55	35.55		35.55	35.55	66.23	61.89	62.03
Pressure	kPa	2578	2578	2440	2440	2440	2440	2440	2440	2440	3363	3363	3193
Molar Flow	kgmole/h	1.315e+004	1.315e+004	1.315e+004	1.315e+004	0.0000	1.315e+004	0.0000	1.315e+004	1.315e+004	1.315e+004	1.315e+004	1.315e+004
Mass Flow	tonne/h	218.3	218.3	218.3	218.3	0.0000	218.3	0.0000	218.3	218.3	218.3	218.3	218.3
Liquid Volume Flow	m ³ /h	717.7	717.7	717.7	717.7	0.0000	717.7	0.0000	717.7	717.7	717.7	717.7	717.7
Heat Flow	kW	-2.740e+005	-2.740e+005	-2.740e+005	-2.740e+005	0.0000	-2.740e+005		-2.740e+005	-2.740e+005	-2.700e+005	-2.707e+005	-2.705e+005
Comp Mole Frac (Methane)		0.9605	0.9605	0.9605	0.9605	0.9605	0.9605	0.9605	0.9605	0.9605	0.9605	0.9605	0.9605
Comp Mole Frac (Ethane)		0.0339	0.0339	0.0339	0.0339	0.0339	0.0339	0.0339	0.0339	0.0339	0.0339	0.0339	0.0339
Comp Mole Frac (i-Butane)		0.0000	0.0000	0.0000	0.0000	0.0000	0.0000	0.0000	0.0000	0.0000	0.0000	0.0000	0.0000
Comp Mole Frac (n-Butane)		0.0000	0.0000	0.0000	0.0000	0.0000	0.0000	0.0000	0.0000	0.0000	0.0000	0.0000	0.0000
Comp Mole Frac (i-Pentane)		0.0000	0.0000	0.0000	0.0000	0.0000	0.0000	0.0000	0.0000	0.0000	0.0000	0.0000	0.0000
Comp Mole Frac (n-Pentane)		0.0000	0.0000	0.0000	0.0000	0.0000	0.0000	0.0000	0.0000	0.0000	0.0000	0.0000	0.0000
Comp Mole Frac (n-Hexane)		0.0000	0.0000	0.0000	0.0000	0.0000	0.0000	0.0000	0.0000	0.0000	0.0000	0.0000	0.0000
Comp Mole Frac (n-Heptane)		0.0000	0.0000	0.0000	0.0000	0.0000	0.0000	0.0000	0.0000	0.0000	0.0000	0.0000	0.0000
Comp Mole Frac (n-Octane)		0.0000	0.0000	0.0000	0.0000	0.0000	0.0000	0.0000	0.0000	0.0000	0.0000	0.0000	0.0000
Comp Mole Frac (n-Nonane)		0.0000	0.0000	0.0000	0.0000	0.0000	0.0000	0.0000	0.0000	0.0000	0.0000	0.0000	0.0000
Comp Mole Frac (n-Decane)		0.0000	0.0000	0.0000	0.0000	0.0000	0.0000	0.0000	0.0000	0.0000	0.0000	0.0000	0.0000
Comp Mole Frac (Nitrogen)		0.0044	0.0044	0.0044	0.0044	0.0044	0.0044	0.0044	0.0044	0.0044	0.0044	0.0044	0.0044
Comp Mole Frac (CO ₂)		0.0001	0.0001	0.0001	0.0001	0.0001	0.0001	0.0001	0.0001	0.0001	0.0001	0.0001	0.0001
Comp Mole Frac (H ₂ S)		0.0000	0.0000	0.0000	0.0000	0.0000	0.0000	0.0000	0.0000	0.0000	0.0000	0.0000	0.0000
Comp Mole Frac (M-Mercaptan)		0.0000	0.0000	0.0000	0.0000	0.0000	0.0000	0.0000	0.0000	0.0000	0.0000	0.0000	0.0000
Comp Mole Frac (E-Mercaptan)		0.0000	0.0000	0.0000	0.0000	0.0000	0.0000	0.0000	0.0000	0.0000	0.0000	0.0000	0.0000
Comp Mole Frac (Propane)		0.0011	0.0011	0.0011	0.0011	0.0011	0.0011	0.0011	0.0011	0.0011	0.0011	0.0011	0.0011

Table C14: SGCU process stream data table 2

		505	506	Q:L2-501	Q:T2-501	Q:T2-604	S	SALES GAS	TO T2-351	W:R2-151	W:R2-501	W:RT2-151	
Vapour Fraction		1.0000	1.0000				1.0000	1.0000	1.0000				
Temperature	C	38.12	38.12				62.03	-79.20	36.18				
Pressure	kPa	3193	3193				3193	3600	2578				
Molar Flow	kgmole/h	1.315e+004	1.315e+004				6.497e-014	1.315e+004	0.0000				
Mass Flow	tonne/h	218.3	218.3				2.214e-015	218.3	0.0000				
Liquid Volume Flow	m3/h	717.7	717.7				2.808e-015	717.7	0.0000				
Heat Flow	kW	-2.741e+005	-2.741e+005	116.5	3542	-650.0	-3.706e-013	-2.936e+005	0.0000	0.0000	3957	0.0000	
Comp Mole Frac (Methane)		0.9605	0.9605				0.0000	0.9605	0.9605				
Comp Mole Frac (Ethane)		0.0339	0.0339				0.0000	0.0339	0.0339				
Comp Mole Frac (i-Butane)		0.0000	0.0000				0.0000	0.0000	0.0000				
Comp Mole Frac (n-Butane)		0.0000	0.0000				0.0000	0.0000	0.0000				
Comp Mole Frac (i-Pentane)		0.0000	0.0000				0.0000	0.0000	0.0000				
Comp Mole Frac (n-Pentane)		0.0000	0.0000				0.0000	0.0000	0.0000				
Comp Mole Frac (n-Hexane)		0.0000	0.0000				0.0000	0.0000	0.0000				
Comp Mole Frac (n-Heptane)		0.0000	0.0000				0.0000	0.0000	0.0000				
Comp Mole Frac (n-Octane)		0.0000	0.0000				0.0000	0.0000	0.0000				
Comp Mole Frac (n-Nonane)		0.0000	0.0000				0.0000	0.0000	0.0000				
Comp Mole Frac (n-Decane)		0.0000	0.0000				0.0000	0.0000	0.0000				
Comp Mole Frac (Nitrogen)		0.0044	0.0044				0.0000	0.0044	0.0044				
Comp Mole Frac (CO2)		0.0001	0.0001				0.0000	0.0001	0.0001				
Comp Mole Frac (H2S)		0.0000	0.0000				1.0000	0.0000	0.0000				
Comp Mole Frac (M-Mercaptan)		0.0000	0.0000				0.0000	0.0000	0.0000				
Comp Mole Frac (E-Mercaptan)		0.0000	0.0000				0.0000	0.0000	0.0000				
Comp Mole Frac (Propane)		0.0011	0.0011				0.0000	0.0011	0.0011				

Product recovery unit (PRU) process stream data tables

Table C15: PRU process stream data table 1

Streams												
		441	441-1	442	462	462-1	601	610	610-1	621	621-1	622
Vapour Fraction		0.0000	0.0000	0.0000	0.0000	0.2083	0.0000	0.0000	0.3567	0.0000	0.0000	0.0000
Temperature	C	30.96	32.27	32.27	166.3	155.6	4.631	96.45	69.89	41.69	42.24	20.16
Pressure	kPa	3009	3009	2959	2396	1610	2771	2835	1600	1491	1860	1780
Molar Flow	kgmole/h	1726	1726	1726	282.0	282.0	825.3	901.0	901.0	581.9	581.9	581.9
Mass Flow	tonne/h	71.89	71.89	71.89	23.70	23.70	24.90	46.99	46.99	25.50	25.50	25.50
Liquid Volume Flow	m3/h	155.5	155.5	155.5	36.44	36.44	69.42	86.09	86.09	50.62	50.62	50.62
Heat Flow	kW	-5.647e+004	-5.639e+004	-5.639e+004	-1.285e+004	-1.285e+004	-2.286e+004	-3.151e+004	-3.151e+004	-1.897e+004	-1.896e+004	-1.942e+004
Comp Mole Frac (Methane)		0.0016	0.0016	0.0016	0.0000	0.0000	0.0034	0.0000	0.0000	0.0000	0.0000	0.0000
Comp Mole Frac (Ethane)		0.4773	0.4773	0.4773	0.0050	0.0050	0.9860	0.0113	0.0113	0.0199	0.0199	0.0199
Comp Mole Frac (i-Butane)		0.0845	0.0845	0.0845	0.0937	0.0937	0.0000	0.1620	0.1620	0.0001	0.0001	0.0001
Comp Mole Frac (n-Butane)		0.0626	0.0626	0.0626	0.0942	0.0942	0.0000	0.1199	0.1199	0.0000	0.0000	0.0000
Comp Mole Frac (i-Pentane)		0.0270	0.0270	0.0270	0.0839	0.0839	0.0000	0.0518	0.0518	0.0000	0.0000	0.0000
Comp Mole Frac (n-Pentane)		0.0140	0.0140	0.0140	0.0553	0.0553	0.0000	0.0269	0.0269	0.0000	0.0000	0.0000
Comp Mole Frac (n-Hexane)		0.0099	0.0099	0.0099	0.0949	0.0949	0.0000	0.0189	0.0189	0.0000	0.0000	0.0000
Comp Mole Frac (n-Heptane)		0.0058	0.0058	0.0058	0.1285	0.1285	0.0000	0.0111	0.0111	0.0000	0.0000	0.0000
Comp Mole Frac (n-Octane)		0.0036	0.0036	0.0036	0.1817	0.1817	0.0000	0.0068	0.0068	0.0000	0.0000	0.0000
Comp Mole Frac (n-Nonane)		0.0010	0.0010	0.0010	0.1122	0.1122	0.0000	0.0019	0.0019	0.0000	0.0000	0.0000
Comp Mole Frac (n-Decane)		0.0000	0.0000	0.0000	0.0008	0.0008	0.0000	0.0000	0.0000	0.0000	0.0000	0.0000
Comp Mole Frac (Nitrogen)		0.0000	0.0000	0.0000	0.0000	0.0000	0.0000	0.0000	0.0000	0.0000	0.0000	0.0000
Comp Mole Frac (CO2)		0.0050	0.0050	0.0050	0.0000	0.0000	0.0105	0.0000	0.0000	0.0000	0.0000	0.0000
Comp Mole Frac (H2S)		0.0000	0.0000	0.0000	0.0000	0.0000	0.0000	0.0000	0.0000	0.0000	0.0000	0.0000
Comp Mole Frac (M-Mercaptan)		0.0000	0.0000	0.0000	0.0000	0.0000	0.0000	0.0000	0.0000	0.0000	0.0000	0.0000
Comp Mole Frac (E-Mercaptan)		0.0000	0.0000	0.0000	0.0000	0.0000	0.0000	0.0000	0.0000	0.0000	0.0000	0.0000
Comp Mole Frac (Propane)		0.3077	0.3077	0.3077	0.1498	0.1498	0.0001	0.5894	0.5894	0.9800	0.9800	0.9800

Table C16: PRU process stream data table 2

		623	630	630-1	641	641-1	642	643	650	651	652	H2O-1
Vapour Fraction		0.0000	0.0000	0.4501	0.0000	0.0000	0.0000	0.0000	0.0000	0.0000	0.0000	0.0000
Temperature	C	20.16	128.9	89.76	43.18	43.51	20.61	20.61	130.9	34.94	30.00	20.16
Pressure	kPa	1760	1620	561.3	511.3	860.0	770.0	750.0	581.0	570.0	550.0	1760
Molar Flow	kgmole/h	581.9	601.0	601.0	308.5	308.5	308.5	308.5	292.5	292.5	292.5	0.0000
Mass Flow	tonne/h	25.50	45.19	45.19	17.89	17.89	17.89	17.89	27.30	27.30	27.30	0.0000
Liquid Volume Flow	m3/h	50.62	71.91	71.91	31.36	31.36	31.36	31.36	40.56	40.56	40.56	0.0000
Heat Flow	kW	-1.942e+004	-2.688e+004	-2.688e+004	-1.274e+004	-1.273e+004	-1.301e+004	-1.301e+004	-1.534e+004	-1.714e+004	-1.722e+004	0.0000
Comp Mole Frac (Methane)		0.0000	0.0000	0.0000	0.0000	0.0000	0.0000	0.0000	0.0000	0.0000	0.0000	0.0000
Comp Mole Frac (Ethane)		0.0199	0.0000	0.0000	0.0000	0.0000	0.0000	0.0000	0.0000	0.0000	0.0000	0.0199
Comp Mole Frac (i-Butane)		0.0001	0.2866	0.2866	0.5584	0.5584	0.5584	0.5584	0.0000	0.0000	0.0000	0.0001
Comp Mole Frac (n-Butane)		0.0000	0.2240	0.2240	0.4316	0.4316	0.4316	0.4316	0.0050	0.0050	0.0050	0.0000
Comp Mole Frac (i-Pentane)		0.0000	0.1169	0.1169	0.0002	0.0002	0.0002	0.0002	0.2401	0.2401	0.2401	0.0000
Comp Mole Frac (n-Pentane)		0.0000	0.0662	0.0662	0.0000	0.0000	0.0000	0.0000	0.1360	0.1360	0.1360	0.0000
Comp Mole Frac (n-Hexane)		0.0000	0.0729	0.0729	0.0000	0.0000	0.0000	0.0000	0.1499	0.1499	0.1499	0.0000
Comp Mole Frac (n-Heptane)		0.0000	0.0769	0.0769	0.0000	0.0000	0.0000	0.0000	0.1580	0.1580	0.1580	0.0000
Comp Mole Frac (n-Octane)		0.0000	0.0955	0.0955	0.0000	0.0000	0.0000	0.0000	0.1962	0.1962	0.1962	0.0000
Comp Mole Frac (n-Nonane)		0.0000	0.0555	0.0555	0.0000	0.0000	0.0000	0.0000	0.1141	0.1141	0.1141	0.0000
Comp Mole Frac (n-Decane)		0.0000	0.0004	0.0004	0.0000	0.0000	0.0000	0.0000	0.0008	0.0008	0.0008	0.0000
Comp Mole Frac (n-Nonane)		0.0000	0.0555	0.0555	0.0000	0.0000	0.0000	0.0000	0.1141	0.1141	0.1141	0.0000
Comp Mole Frac (n-Decane)		0.0000	0.0004	0.0004	0.0000	0.0000	0.0000	0.0000	0.0008	0.0008	0.0008	0.0000
Comp Mole Frac (Nitrogen)		0.0000	0.0000	0.0000	0.0000	0.0000	0.0000	0.0000	0.0000	0.0000	0.0000	0.0000
Comp Mole Frac (CO2)		0.0000	0.0000	0.0000	0.0000	0.0000	0.0000	0.0000	0.0000	0.0000	0.0000	0.0000
Comp Mole Frac (H2S)		0.0000	0.0000	0.0000	0.0000	0.0000	0.0000	0.0000	0.0000	0.0000	0.0000	0.0000
Comp Mole Frac (M-Mercaptan)		0.0000	0.0000	0.0000	0.0000	0.0000	0.0000	0.0000	0.0000	0.0000	0.0000	0.0000
Comp Mole Frac (E-Mercaptan)		0.0000	0.0000	0.0000	0.0000	0.0000	0.0000	0.0000	0.0000	0.0000	0.0000	0.0000
Comp Mole Frac (Propane)		0.9800	0.0050	0.0050	0.0098	0.0098	0.0098	0.0098	0.0000	0.0000	0.0000	0.9800

Table C17: PRU process stream data table 2

		H2O-2	Q:L2-661	Q:L2-662	Q:T2-601	Q:T2-602	Q:T2-603	Q:T2-604	Q:T2-621	Q:T2-622	Q:T2-623	Q:T2-641
Vapour Fraction		0.0000										
Temperature	C	20.61										
Pressure	kPa	750.0										
Molar Flow	kgmole/h	0.0000										
Mass Flow	tonne/h	0.0000										
Liquid Volume Flow	m3/h	0.0000										
Heat Flow	kW	0.0000	4.057e-002	-5.010e-002	8263	6247	80.52	1.496	8651	1.014e+004	458.1	3036
Comp Mole Frac (Methane)		0.0000										
Comp Mole Frac (Ethane)		0.0000										
Comp Mole Frac (i-Butane)		0.5584										
Comp Mole Frac (n-Butane)		0.4316										
Comp Mole Frac (i-Pentane)		0.0002										
Comp Mole Frac (n-Pentane)		0.0000										
Comp Mole Frac (n-Hexane)		0.0000										
Comp Mole Frac (n-Heptane)		0.0000										
Comp Mole Frac (n-Octane)		0.0000										
Comp Mole Frac (n-Nonane)		0.0000										
Comp Mole Frac (n-Decane)		0.0000										
Comp Mole Frac (Nitrogen)		0.0000										
Comp Mole Frac (CO2)		0.0000										
Comp Mole Frac (H2S)		0.0000										
Comp Mole Frac (M-Mercaptan)		0.0000										
Comp Mole Frac (E-Mercaptan)		0.0000										
Comp Mole Frac (Propane)		0.0098										

Table C18: PRU process stream data table 3

		Q:T2-642	Q:T2-643	Q:T2-644	Q:T2-645	TO FLARE	TO HPFLARE	TO R2-401	W:P2-621	W:P2-641		
Vapour Fraction						1.0000	1.0000	1.0000				
Temperature	C					43.18	41.69	4.631				
Pressure	kPa					511.3	1491	2771				
Molar Flow	kgmole/h					0.0000	0.0000	0.0000				
Mass Flow	tonne/h					0.0000	0.0000	0.0000				
Liquid Volume Flow	m3/h					0.0000	0.0000	0.0000				
Heat Flow	kW	4226	1802	82.16	281.6	0.0000	0.0000	0.0000	7.530	4.304		
Comp Mole Frac (Methane)						0.0000	0.0000	0.0114				
Comp Mole Frac (Ethane)						0.0000	0.0496	0.9684				
Comp Mole Frac (i-Butane)						0.6171	0.0001	0.0000				
Comp Mole Frac (n-Butane)						0.3590	0.0000	0.0000				
Comp Mole Frac (i-Pentane)						0.0001	0.0000	0.0000				
Comp Mole Frac (n-Pentane)						0.0000	0.0000	0.0000				
Comp Mole Frac (n-Hexane)						0.0000	0.0000	0.0000				
Comp Mole Frac (n-Heptane)						0.0000	0.0000	0.0000				
Comp Mole Frac (n-Octane)						0.0000	0.0000	0.0000				
Comp Mole Frac (n-Nonane)						0.0000	0.0000	0.0000				
Comp Mole Frac (n-Decane)						0.0000	0.0000	0.0000				
Comp Mole Frac (Nitrogen)						0.0000	0.0000	0.0000				
Comp Mole Frac (CO2)						0.0000	0.0000	0.0201				
Comp Mole Frac (H2S)						0.0000	0.0000	0.0000				
Comp Mole Frac (M-Mercaptan)						0.0000	0.0000	0.0000				
Comp Mole Frac (E-Mercaptan)						0.0000	0.0000	0.0000				
Comp Mole Frac (Propane)						0.0239	0.9503	0.0000				

C₃-refrigeration unit (C₃RU) process stream data tables

Table C19: C₃RU process stream data table 1

Streams													
		71A	71B	71C	71D	71E	71H	71I	71J	71M	71N	71O	71R
Vapour Fraction		0.0000	0.1949	0.0000	0.1258	1.0000	0.0000	0.1258	1.0000	0.0000	0.1258	1.0000	0.0000
Temperature	C	31.76	5.578	31.76	15.95	15.46	31.76	15.95	15.46	31.76	15.95	15.46	31.76
Pressure	kPa	1174	559.5	1174	750.0	740.0	1174	750.0	740.0	1174	750.0	740.0	1174
Molar Flow	kgmole/h	2527	2527	338.6	338.6	338.6	51.32	51.32	51.32	89.14	89.14	89.14	121.2
Mass Flow	tonne/h	111.5	111.5	14.93	14.93	14.93	2.263	2.263	2.263	3.931	3.931	3.931	5.343
Liquid Volume Flow	m ³ /h	220.0	220.0	29.47	29.47	29.47	4.466	4.466	4.466	7.758	7.758	7.758	10.55
Heat Flow	kW	-8.367e+004	-8.367e+004	-1.121e+004	-1.121e+004	-9929	-1699	-1699	-1505	-2951	-2951	-2614	-4011
Comp Mole Frac (Methane)													
Comp Mole Frac (Ethane)													
Comp Mole Frac (i-Butane)													
Comp Mole Frac (n-Butane)													
Comp Mole Frac (i-Pentane)													
Comp Mole Frac (n-Pentane)													
Comp Mole Frac (n-Hexane)													
Comp Mole Frac (n-Heptane)													
Comp Mole Frac (n-Octane)													
Comp Mole Frac (n-Nonane)													
Comp Mole Frac (n-Decane)													
Comp Mole Frac (Nitrogen)													
Comp Mole Frac (CO ₂)													
Comp Mole Frac (H ₂ S)													
Comp Mole Frac (M-Mercaptan)													
Comp Mole Frac (E-Mercaptan)													
Comp Mole Frac (Propane)		1.0000	1.0000	1.0000	1.0000	1.0000	1.0000	1.0000	1.0000	1.0000	1.0000	1.0000	1.0000

Table C20: C₃RU process stream data table 2

		71S	71T	71W	71X	71Y	720	730	731	732	733	734	735
Vapour Fraction		0.1258	1.0000	0.0000	0.1258	1.0000	1.0000	0.0000	0.0000	0.1401	0.0000	0.0686	1.0000
Temperature	C	15.95	15.46	31.76	15.95	15.46	5.575	5.575	5.575	-16.90	5.575	-4.782	-5.561
Pressure	kPa	750.0	740.0	1174	750.0	740.0	559.5	559.5	559.5	272.5	559.5	408.0	398.0
Molar Flow	kgmole/h	121.2	121.2	74.50	74.50	74.50	1188	2014	583.0	583.0	1431	1431	1431
Mass Flow	tonne/h	5.343	5.343	3.285	3.285	3.285	52.38	88.83	25.71	25.71	63.12	63.12	63.12
Liquid Volume Flow	m ³ /h	10.55	10.55	6.483	6.483	6.483	103.4	175.3	50.74	50.74	124.6	124.6	124.6
Heat Flow	kW	-4011	-3553	-2466	-2466	-2185	-3.499e+004	-6.846e+004	-1.982e+004	-1.982e+004	-4.865e+004	-4.865e+004	-4.240e+004
Comp Mole Frac (Methane)													
Comp Mole Frac (Ethane)													
Comp Mole Frac (i-Butane)													
Comp Mole Frac (n-Butane)													
Comp Mole Frac (i-Pentane)													
Comp Mole Frac (n-Pentane)													
Comp Mole Frac (n-Hexane)													
Comp Mole Frac (n-Heptane)													
Comp Mole Frac (n-Octane)													
Comp Mole Frac (n-Nonane)													
Comp Mole Frac (n-Decane)													
Comp Mole Frac (Nitrogen)													
Comp Mole Frac (CO ₂)													
Comp Mole Frac (H ₂ S)													
Comp Mole Frac (M-Mercaptan)													
Comp Mole Frac (E-Mercaptan)													
Comp Mole Frac (Propane)		1.0000	1.0000	1.0000	1.0000	1.0000	1.0000	1.0000	1.0000	1.0000	1.0000	1.0000	1.0000

Table C21: C₃RU process stream data table 3

		736	740	742	743	744	745	745-1	750	751	760	761	762
Vapour Fraction		1.0000	1.0000	0.0000	0.0373	1.0000	1.0000	1.0000	1.0000	1.0000	1.0000	1.0000	1.0000
Temperature	C	-6.191	-16.90	-16.90	-23.32	-23.32	-23.32	-25.91	21.75	-8.081	33.13	21.90	58.29
Pressure	kPa	368.0	272.5	272.5	216.4	216.4	216.4	104.0	313.0	272.5	675.0	559.5	1184
Molar Flow	kgmole/h	1431	1563	451.6	451.6	451.6	451.6	451.6	451.6	2014	2014	3202	3202
Mass Flow	tonne/h	63.12	68.92	19.91	19.91	19.91	19.91	19.91	19.91	88.83	88.83	141.2	141.2
Liquid Volume Flow	m ³ /h	124.6	136.0	39.30	39.30	39.30	39.30	39.30	39.30	175.3	175.3	278.7	278.7
Heat Flow	kW	-4.240e+004	-4.656e+004	-1.566e+004	-1.566e+004	-1.350e+004	-1.350e+004	-1.350e+004	-1.311e+004	-5.967e+004	-5.823e+004	-9.322e+004	-9.124e+004
Comp Mole Frac (Methane)													
Comp Mole Frac (Ethane)													
Comp Mole Frac (i-Butane)													
Comp Mole Frac (n-Butane)													
Comp Mole Frac (i-Pentane)													
Comp Mole Frac (n-Pentane)													
Comp Mole Frac (n-Hexane)													
Comp Mole Frac (n-Heptane)													
Comp Mole Frac (n-Octane)													
Comp Mole Frac (n-Nonane)													
Comp Mole Frac (n-Decane)													
Comp Mole Frac (Nitrogen)													
Comp Mole Frac (CO ₂)													
Comp Mole Frac (H ₂ S)													
Comp Mole Frac (M-Mercaptan)													
Comp Mole Frac (E-Mercaptan)													
Comp Mole Frac (Propane)		1.0000	1.0000	1.0000	1.0000	1.0000	1.0000	1.0000	1.0000	1.0000	1.0000	1.0000	1.0000

Table C22: C₃RU process stream data table 4

		763	764	765	BYPASS	LIQ	M2-701 LIQ	OUT T2-603	Q:T2-301	Q:T2-352	Q:T2-354	Q:T2-402	Q:T2-602
Vapour Fraction		1.0000	0.0000	0.0000	0.0000	0.0000	0.0000	0.0000					
Temperature	C	58.15	32.45	31.76	32.45	32.45	-23.32	31.76					
Pressure	kPa	1174	1174	1174	1174	1174	216.4	1174					
Molar Flow	kgmole/h	3202	3202	3202	0.0000	3202	0.0000	3202					
Mass Flow	tonne/h	141.2	141.2	141.2	0.0000	141.2	0.0000	141.2					
Liquid Volume Flow	m ³ /h	278.7	278.7	278.7	0.0000	278.7	0.0000	278.7					
Heat Flow	kW	-9.124e+004	-1.059e+005	-1.060e+005	0.0000	-1.059e+005	0.0000	-1.060e+005	1280	194.0	337.0	2159	6247
Comp Mole Frac (Methane)													
Comp Mole Frac (Ethane)													
Comp Mole Frac (i-Butane)													
Comp Mole Frac (n-Butane)													
Comp Mole Frac (i-Pentane)													
Comp Mole Frac (n-Pentane)													
Comp Mole Frac (n-Hexane)													
Comp Mole Frac (n-Heptane)													
Comp Mole Frac (n-Octane)													
Comp Mole Frac (n-Nonane)													
Comp Mole Frac (n-Decane)													
Comp Mole Frac (Nitrogen)													
Comp Mole Frac (CO ₂)													
Comp Mole Frac (H ₂ S)													
Comp Mole Frac (M-Mercaptan)													
Comp Mole Frac (E-Mercaptan)													
Comp Mole Frac (Propane)		1.0000	1.0000	1.0000	1.0000	1.0000	1.0000	1.0000					

Table C23: C₃RU process steam data table 5

		Q:T2-603	Q:T2-623	Q:T2-645	Q:T2-701	Q:T2-603(1)	TO MIXER	TO T2-603	VAP	W:R2-701(1)	W:R2-701(2)	W:R2-701(3)	
Vapour Fraction							0.0000	0.0000	1.0000				
Temperature	C						32.45	32.45	32.45				
Pressure	kPa						1174	1174	1174				
Molar Flow	kgmole/h						0.0000	3202	0.0000				
Mass Flow	tonne/h						0.0000	141.2	0.0000				
Liquid Volume Flow	m ³ /h						0.0000	278.7	0.0000				
Heat Flow	kW	80.53	458.1	281.6	1.469e+004	80.52	0.0000	-1.059e+005	0.0000	389.5	1441	1983	
Comp Mole Frac (Methane)													
Comp Mole Frac (Ethane)													
Comp Mole Frac (i-Butane)													
Comp Mole Frac (n-Butane)													
Comp Mole Frac (i-Pentane)													
Comp Mole Frac (n-Pentane)													
Comp Mole Frac (n-Hexane)													
Comp Mole Frac (n-Heptane)													
Comp Mole Frac (n-Octane)													
Comp Mole Frac (n-Nonane)													
Comp Mole Frac (n-Decane)													
Comp Mole Frac (Nitrogen)													
Comp Mole Frac (CO ₂)													
Comp Mole Frac (H ₂ S)													
Comp Mole Frac (M-Mercaptan)													
Comp Mole Frac (E-Mercaptan)													
Comp Mole Frac (Propane)							1.0000	1.0000	1.0000				

APPENDIX D

NORMAL DISTRIBUTION FOR UNCERTAIN MATERIAL FLOWS

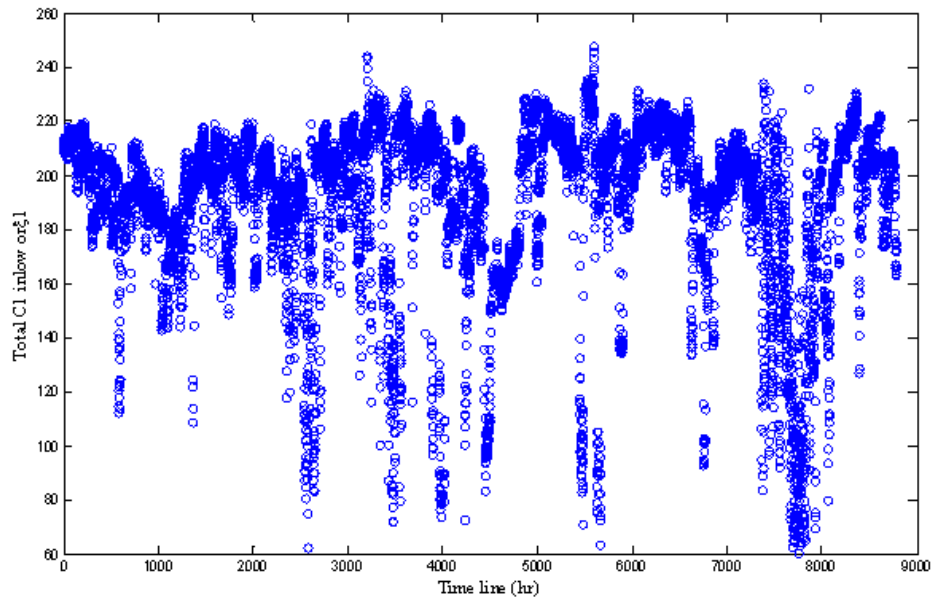


Fig. D.1 Total C₁ or methane inflow from the plant inlet

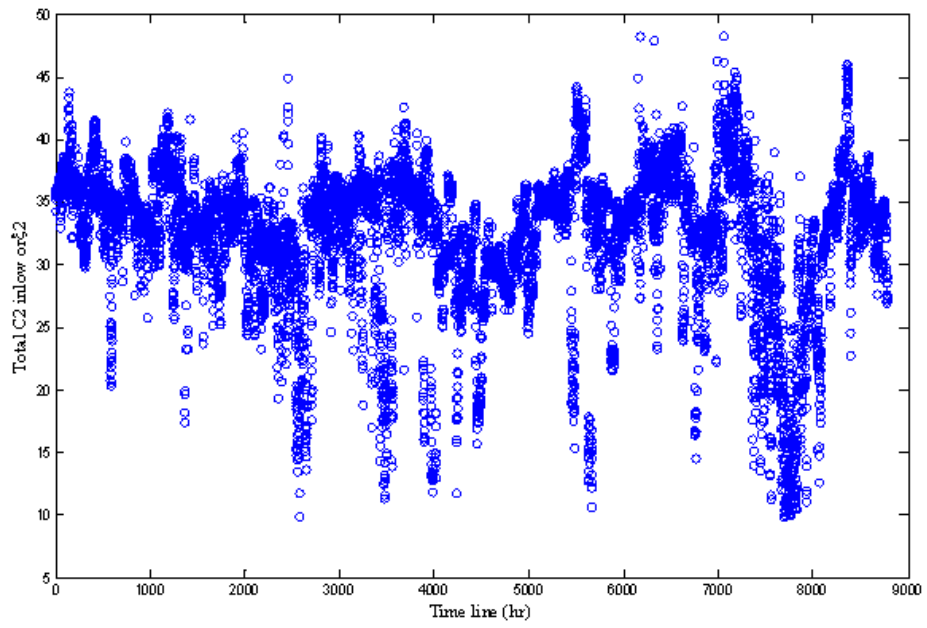


Fig. D.2 Total C₂ or ethane inflow from the plant inlet

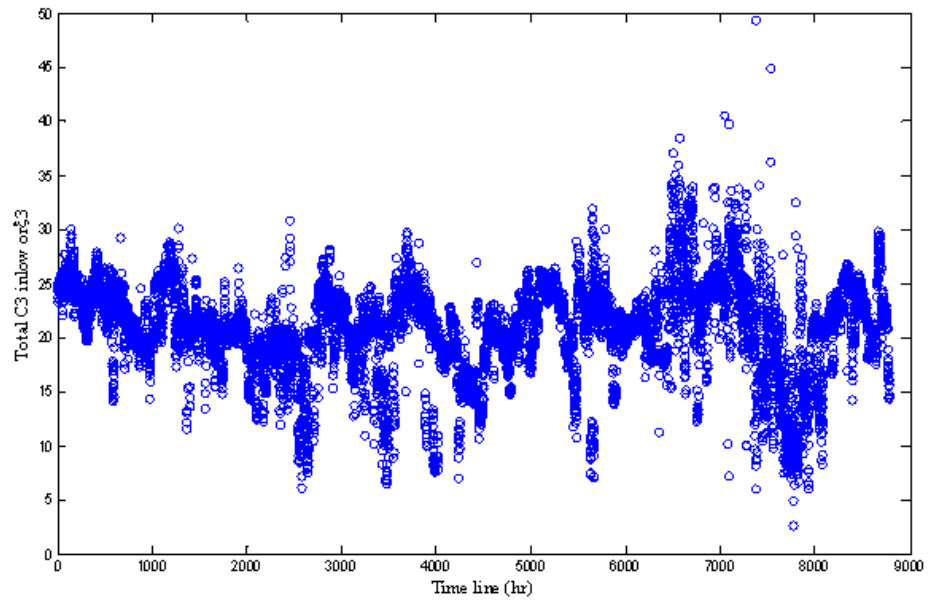


Fig. D.3 Total C₃ or propane inflow from the plant inlet

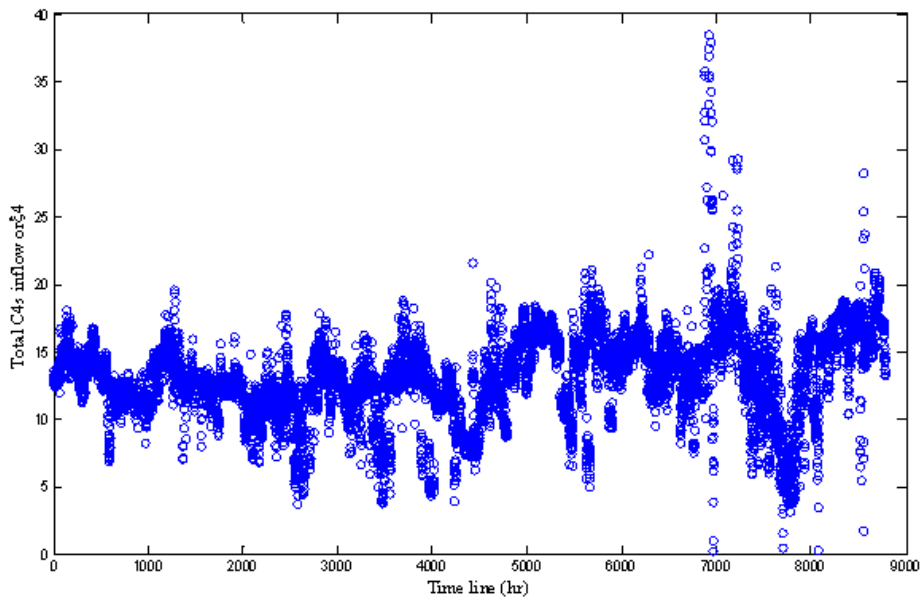


Fig. D. 4 Total C_{4s} or butanes inflow from the plant inlet

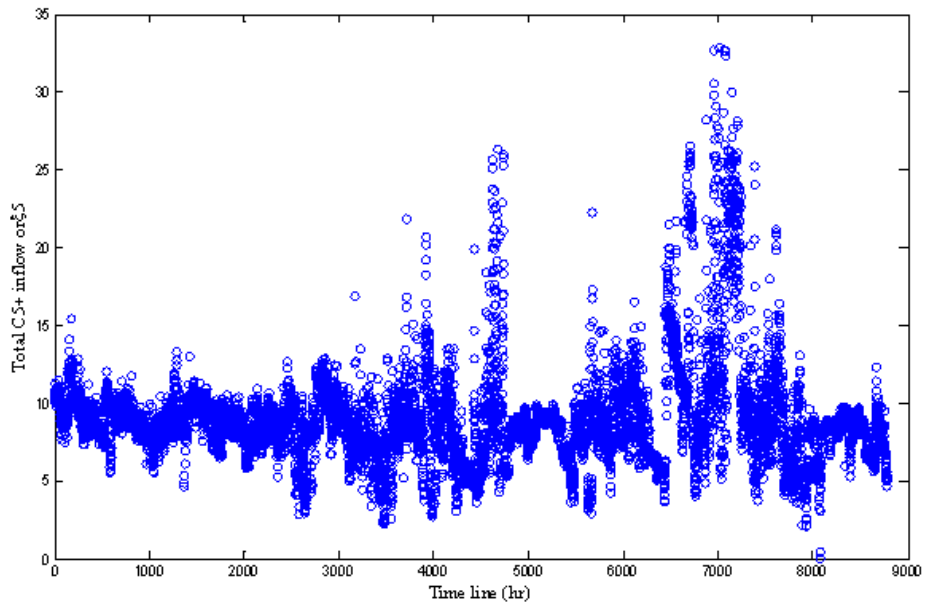


Fig. D. 5 Total C_{5+} or condensates inflow from the plant inlet

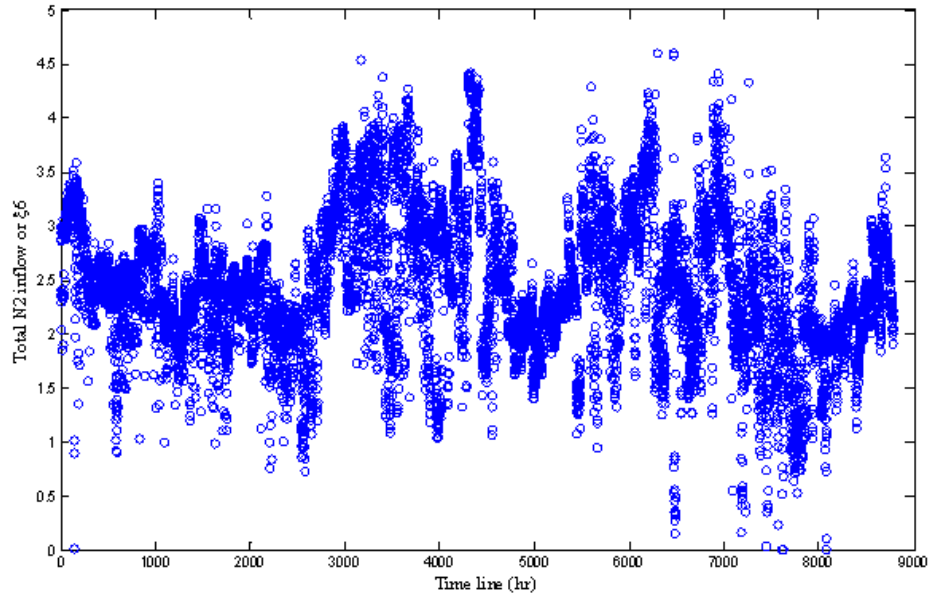


Fig. D.6 Total N₂ or Nitrogen inflow from the plant inlet

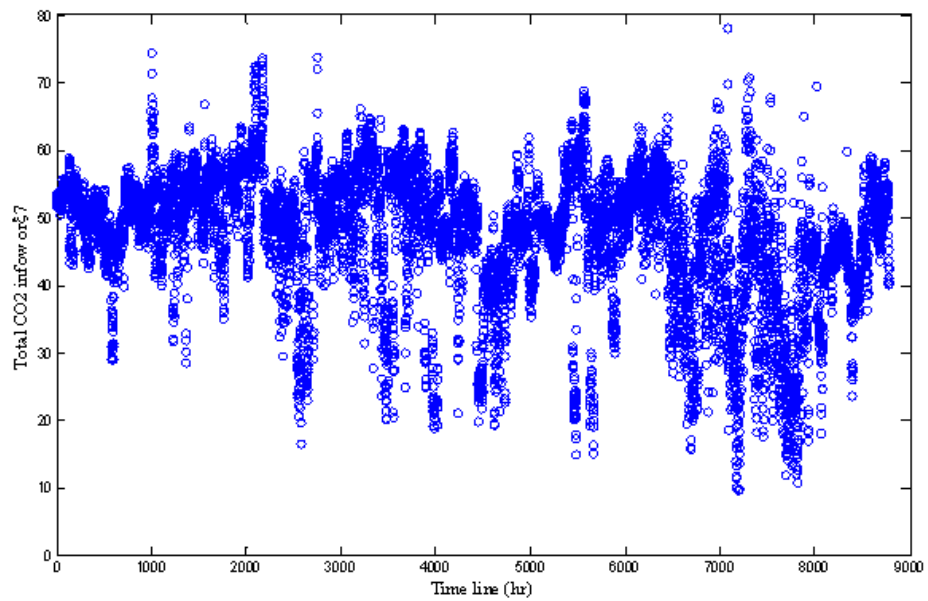


Fig. D.7 Total CO₂ or Carbon dioxide inflow from the plant inlet

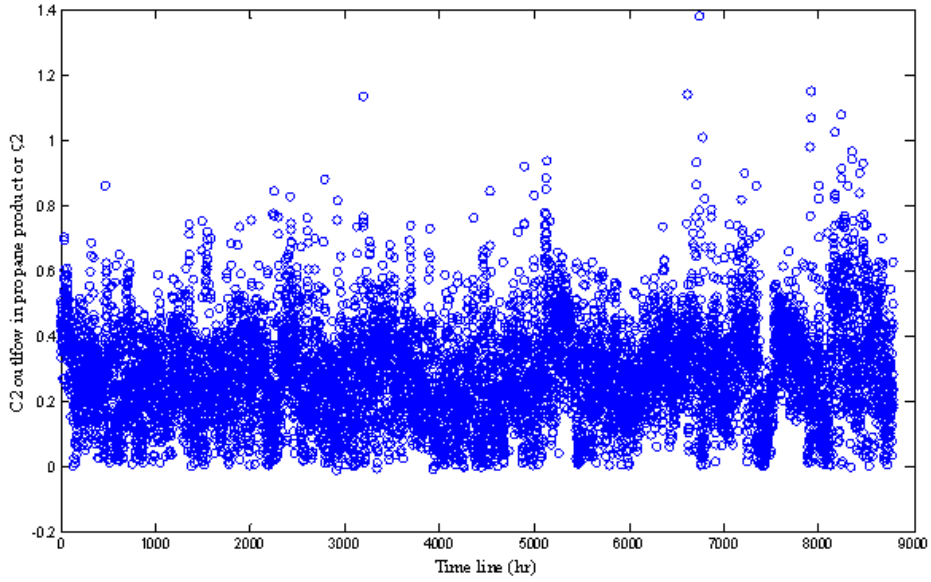


Fig. D. 8 C₂ outflow for propane product from the plant outlet

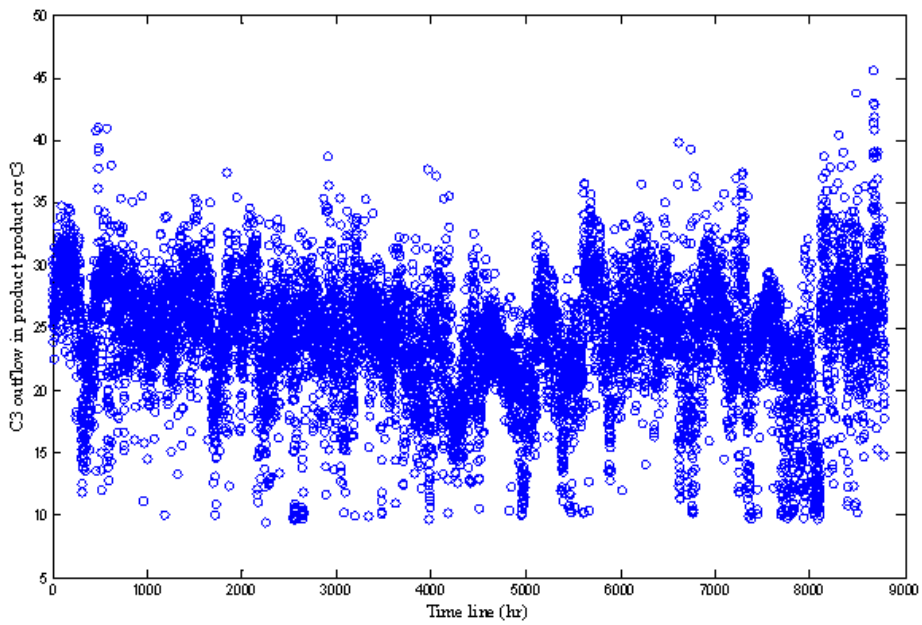


Fig. D.9 C₃ outflow for propane product from the plant outlet

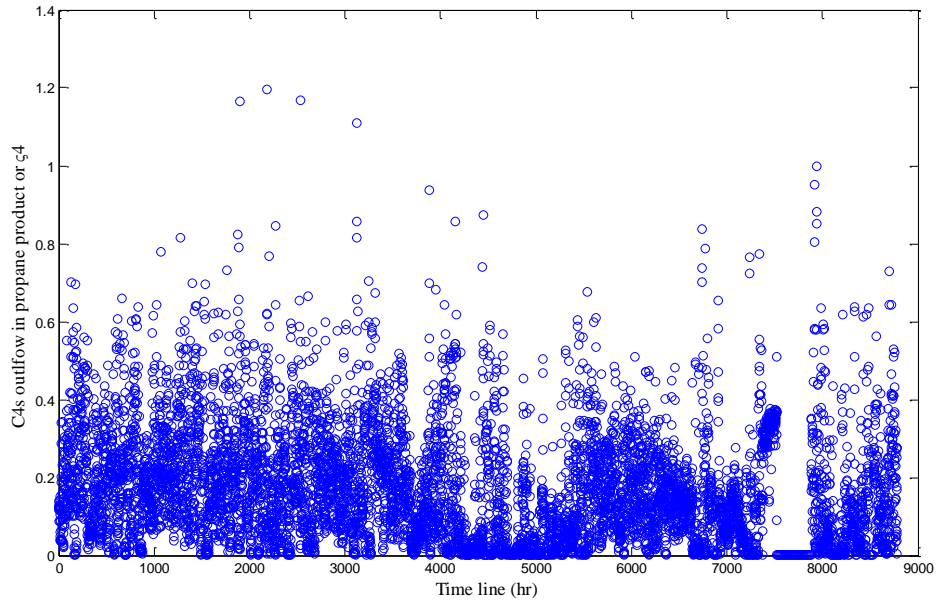


Fig. D.10 C4s outflow for propane product from the plant outlet

APPENDIX E

GAMS OPTIMIZATION CODE

NB: All the GAMS optimization code used for the three case studies (case study 1, 2 and 3) are represented below. 'Notes' written in asterisk (*) are only used for explanation purpose and are not part of the program.

\$Title Gas plant optimization

*Notes

* The following sets, tables and scalars defined are common in all
*the three case studies.

Sets

a Index for feed component flows /ru1*ru7/
b Index for product component flows /pu1*pu7/
c Index for utility flows /u1*u6/
d Index for energy product flows /q1*q4/
e Index for set of confidence level in percentage /50*100/
f Index for inlet energy flow
/QA2101,QT2151,QAGRU,QL2301,QL2302,QT2101,QL2104,QT2451,QL2451,
QL2452,QT2404,WP2404,WP2403,WP2402,WP2401,WR2401,WR2151,WR2501,
QT2604SalesGas,QL2501,QT2603,QT2604PRU,QT2601,QT2621,QT2641,QL2
661,QL2662,WP2621,WP2641,QT2645,QT2623,QT2354,QT2352,QT2301,QT2
602,QT2402,WR27011,WR27012,WR27013,QR1,QR2,QR3,QR4/
g Index for Outlet energy flow
/QT2301,QT2402,WRT2401,QT2501,WRT2151,QT2602,QT2622,QT2642,QT26
23,QT2645,QT2643,QT2644,QT2701,QT2603,QP1,QP2,QP3,QP4,QP5,Q

i Index for raw material flow /R1*R4/
 j Index for product flow /P1*P6/
 k Index for raw material and product components
 /C1,C2,C3,iC4,C4,iC5,C5,C6,C7,C8,C9,C10,C6+,N2,CO2/
 l Index for Deethanizer Depropanizer & Debutanizer columns feed
 and bottoms/Ds-Feed,De-Feed,Dp-Feed,Db-Feed,De-
 Bottom,DpBottom,Db-Bottom/;

Table x(k,i) mass fraction in the raw material streams

*	Phase1gas	Phase2gas	Phase3gas	Phase2liquid
	R1	R2	R3	R4
C1	0.6706315661	0.7115876835	0.3462174656	0.0995669976
C2	0.1186013726	0.0856698874	0.2634824801	0.0333836461
C3	0.0806649561	0.0571473408	0.2167484976	0.0875645643
iC4	0.0256342823	0.0280976366	0.0458911557	0.0734480379
C4	0.0218473996	0.0125542632	0.0323937569	0.0545613996
iC5	0.0104863259	0.0085340786	0.0058641488	0.0651236937
C5	0.0057855591	0.0040815158	0.0027924518	0.0390742162
C6	0.0037143033	0.0032795487	0.0003668867	0.0855628551
C7	0.0021594385	0.0019066789	0.0002326934	0.1266234378
C8	0.0012022370	0.0011161635	0.0001326332	0.1959016323
C9	0.0000000000	0.0000000000	0.0000000000	0.1349842425
C10	0.0000000000	0.0000000000	0.0000000000	0.0010274147
N2	0.0058964675	0.0027371568	0.0017346943	0.0000000000
CO2	0.0533760920	0.0832880462	0.0841431359	0.0031778622
C6+	0.0070759788	0.0063023911	0.0007322133	0.5440995824 ;

Table y(k,j) mass fraction in the product streams

*	Salesgas	Ethane	Propane	Butane	Condensate	CO2
	P1	P2	P3	P4	P5	P6
C1	0.9278570484	1.838005E-03	1.117286E-13	2.41179E-31	1.57575E-31	0
C2	0.0613998937	9.827804E-01	1.088324E-02	3.38162E-12	1.23998E-31	0
C3	0.0029865137	3.443157E-05	9.836914E-01	9.91422E-03	5.11162E-15	0
iC4	0.0001119604	4.515036E-09	5.329154E-03	5.53721E-01	1.19789E-05	0
C4	0.0000302948	3.250589E-10	9.622190E-05	4.33798E-01	3.10034E-03	0
iC5	0.0000012549	1.299845E-12	6.380700E-09	2.55221E-03	1.84500E-01	0
C5	0.0000002353	2.137020E-13	4.342608E-10	1.41547E-05	1.05403E-01	0
C6	0.0000000055	1.411487E-14	8.451347E-13	3.40890E-14	1.38607E-01	0
C7	0.0000000001	1.001356E-15	1.440899E-14	3.12771E-20	1.69835E-01	0
C8	0.0000000000	1.629144E-16	1.595709E-15	4.33937E-24	2.40233E-01	0
C9	0.0000000000	1.827375E-17	2.166259E-16	1.51697E-26	1.56713E-01	0
C10	0.0000000000	2.931575E-20	5.526174E-19	6.18688E-30	1.19290E-03	0
N2	0.0073789116	4.111901E-10	1.490759E-24	4.12215E-48	2.69323E-48	0
CO2	0.0002338818	1.534717E-02	5.247252E-09	7.44194E-25	2.98168E-32	1
C6+	5.435342E-09	6.525873E-15	5.019555E-13	9.52754E-14	7.06985E-01	0

*The temperature (Degree C), pressure (KPa) and flow rates *(ton/h) of R1, R2, R3, R4 at the existing condition is given below

*	R1	R2	R3	R4
*Temperature	24.54	17	28.64	27.44
*Pressure	7261.325	7261.325	6511.325	6661.325
*Flow rates	254.34	40	1.25	31.7

* The composition of each feed is shown in the above table 1, where

* C1 = methane, C2 = Ethane, C3 = Propane, iC4 = iso-butane, C4 = n-butane, iC5 = iso-pentane, C5 = n-pentane, C6+= n-hexane (C6) + n-heptane (C7) + n-octane (C8) + n-nonane (C9) + n-decane (C10), N2 =

*Nitrogen, CO₂ = Carbon dioxide. The main products from the plant are
*SalesGas, Ethane, Propane and Butane. While, Carbon dioxide and
*Condensate are the byproducts from the plant. The product flow rates
*are represented as: P1=Salesgas product, P2 =Ethane, Product, P3
*=Propane product, P4=Butane product, P5=Condensate product and
*P6=Carbon dioxide product.

*The composition of each product are obtained from rigorous HYSYS
*simulation and are given in the above table2 The total product flow
*rate is represented as P. And $P = P1 + P2 + P3 + P4 + P5 + P6$

* All the temperature is degree C, Pressure in KPa and the flow rates
*in ton/h. The composition of each and products are in mass fraction.

Scalars

CR1 cost of raw material R1 / 35.63 /
CR2 cost of raw material R2 / 28.87 /
CR3 cost of raw material R3 / 15.13 /
CR4 cost of raw material R4 / 21.44 /
CR12 average cost of raw material R1 and R2 / 33.179 /
CP1 cost of sales gas in dollar per ton /101.94/
CP2 cost of Ethane in dollar per ton/61.03/
CP3 cost of propane in dollar per ton /166.7/
CP4 cost of butane in dollar per ton /212.0/
CP5 cost of condensate in dollar per ton /0.0/
CP6 cost of carbon dioxide in dollar per ton/0.0 /
Cstm steam cost in dollar per Kw-h /0.008352072/
Crefg Refrigeration cost in dollar per kw-h /0.015740443/
Ccompress compression cost in dollar per Kw-h /0.007870222/
Celetric Electricity cost in dollar per Kw-h / 0.057822037/
Cfuel Heater fuel cost in dollar per Kw-h / 0.001393724/
Ccooling cooling cost for raw material in dollar per Kw-h
/0.000154057/;

*NOTES

* unit conversion : 1MMSCFD = 1062.8 MMBTU/day = 44.3 MMBTU/h.

* specific heat capacity of water at 4 degree C in Kwh per ton.K
*/1.16278/

* specific heat capacity of C3 refrigerant in Kwh per ton.K
*/0.720087695/

* All the costs for the utility consumption are in \$/kWhr.

*** CASE STUDY 1**

*** (I)Single chance constrained optimization**

Table m1(e,a) values for total feed component inflows (ru1-ru4)

*	C1 inflow ru1	C2 inflow ru2	C3 inflow ru3	C4s inflow ru4
50	190.05523730	32.26080945	20.78197572	13.08167633
51	189.26906564	32.11571083	20.67445828	13.00212372
52	188.48239952	31.97052096	20.56687322	12.92252107
53	187.69474231	31.82514816	20.45915262	12.84281813
54	186.90559297	31.67949997	20.35122795	12.76296421
55	186.11444385	31.53348270	20.24302979	12.68290793
56	185.32077829	31.38700098	20.13448749	12.60259701
57	184.52406824	31.23995736	20.02552881	12.52197802
58	183.72377165	31.09225179	19.91607964	12.44099611
59	182.91932974	30.94378116	19.80606355	12.35959473
60	182.11016405	30.79443868	19.69540143	12.27771535
61	181.29567320	30.64411337	19.58401104	12.19529713
62	180.47522944	30.49268937	19.47180652	12.11227652
63	179.64817476	30.34004524	19.35869789	12.02858696
64	178.81381660	30.18605315	19.24459043	11.94415836
65	177.97142306	30.03057803	19.12938405	11.85891667
66	177.12021757	29.87347654	19.01297253	11.77278329
67	176.25937272	29.71459597	18.89524273	11.68567451
68	175.38800340	29.55377297	18.77607360	11.59750020

	ru1	ru2	ru3	ru4
69	174.50515884	29.39083206	18.65533510	11.50816582
70	173.60981347	29.22558396	18.53288698	11.41756593
71	172.70085638	29.05782363	18.40857732	11.32558868
72	171.77707895	28.88732801	18.28224081	11.23211175
73	170.83716043	28.71385333	18.15369683	11.13700152
74	169.87965088	28.53713198	18.02274710	11.04011124
75	168.90295094	28.35686880	17.88917287	10.94127910
76	167.90528756	28.17273652	17.75273166	10.84032567
77	166.88468486	27.98437048	17.61315325	10.73705100
78	165.83892862	27.79136202	17.47013483	10.63123106
79	164.76552291	27.59325047	17.32333504	10.52261327
80	163.66163631	27.38951326	17.17236667	10.41091112
81	162.52403491	27.17955353	17.01678743	10.29579738
82	161.34899758	26.96268449	16.85608843	10.17689550
83	160.13220784	26.73810948	16.68967933	10.05376869
84	158.86861377	26.50489610	16.51686924	9.92590577
85	157.55224398	26.26194224	16.33684150	9.79270247
86	156.17596182	26.00793075	16.14862010	9.65343665
87	154.73113088	25.74126765	15.95102392	9.50723439
88	153.20715016	25.45999638	15.74260315	9.35302297
89	151.59079212	25.16167564	15.52154879	9.18946390
90	149.86523339	24.84320043	15.28556006	9.01485482
91	148.00858737	24.50053128	15.03164373	8.82698104
92	145.99159365	24.12826780	14.75579813	8.62288170
93	143.77380097	23.71894415	14.45249110	8.39846353
94	141.29687398	23.26179376	14.11374467	8.14782360
95	138.47192573	22.74041134	13.72740259	7.86196744
96	135.15297512	22.12785409	13.27350037	7.52612324

	ru1	ru2	ru3	ru4
97	131.07274725	21.37479283	12.71548528	7.11324548
98	125.64879517	20.37372908	11.97370145	6.56439645
99	117.09997536	18.79592872	10.80455832	5.69934243
100	1.96145017	0.45444403	0.94187442	0.95151064;

Table m2(e,a) values for total feed component inflows (ru5-ru7)

*	C5+ inflow			N2 inflow			CO2 inflow		
	ru5	ru6	ru7	ru5	ru6	ru7	ru5	ru6	ru7
50	9.06038102	2.43898383	47.22380042						
51	8.97642799	2.42254694	46.97958470						
52	8.89242215	2.40609971	46.73521539						
53	8.80831047	2.38963176	46.49053820						
54	8.72403946	2.37313261	46.24539750						
55	8.63955489	2.35659166	45.99963559						
56	8.55480160	2.33999809	45.75309197						
57	8.46972320	2.32334087	45.50560262						
58	8.38426181	2.30660866	45.25699914						
59	8.29835774	2.28978978	45.00710797						
60	8.21194924	2.27287215	44.75574940						
61	8.12497207	2.25584317	44.50273664						
62	8.03735922	2.23868974	44.24787466						
63	7.94904040	2.22139808	43.99095908						
64	7.85994166	2.20395373	43.73177475						
65	7.76998485	2.18634138	43.47009431						
66	7.67908704	2.16854480	43.20567654						
67	7.58715986	2.15054668	42.93826440						
68	7.49410881	2.13232852	42.66758296						
69	7.39983235	2.11387044	42.39333685						

	ru5	ru6	ru7
70	7.30422096	2.09515100	42.11520750
71	7.20715602	2.07614697	41.83284981
72	7.10850845	2.05683309	41.54588835
73	7.00813723	2.03718173	41.25391284
74	6.90588750	2.01716259	40.95647286
75	6.80158849	1.99674223	40.65307160
76	6.69505086	1.97588358	40.34315827
77	6.58606360	1.95454532	40.02611908
78	6.47439026	1.93268116	39.70126623
79	6.35976432	1.91023892	39.36782436
80	6.24188340	1.88715940	39.02491393
81	6.12040218	1.86337499	38.67153037
82	5.99492329	1.83880789	38.30651774
83	5.86498577	1.81336785	37.92853518
84	5.73005015	1.78694924	37.53601336
85	5.58947876	1.75942723	37.12709733
86	5.44250951	1.73065260	36.69957017
87	5.28822012	1.70044479	36.25074908
88	5.12547855	1.66858215	35.77734096
89	4.95287227	1.63478813	35.27523683
90	4.76860476	1.59871100	34.73921069
91	4.57033881	1.55989315	34.16246370
92	4.35494978	1.51772284	33.53590643
93	4.11811800	1.47135432	32.84697313
94	3.85361401	1.41956795	32.07754257
95	3.55194582	1.36050532	31.20000297
96	3.19752452	1.29111434	30.16900689
97	2.76180858	1.20580694	28.90152826

	ru5	ru6	ru7
98	2.18260016	1.09240562	27.21663625
99	1.26969599	0.91367110	24.56103790
100	0.02561980	0.49358855	0.20549879;

Variables Z;

Positive Variables

ru1, ru2, ru3, ru4, ru5, ru6, ru7, ru, R1, R2, R3, R4, R, P1, P2, P3, P4, P5, P6, P;

Equations

OBJ, EQN1, EQN2, EQN3, EQN4, EQN5, EQN6, EQN7, EQN8, EQN9, EQN10, EQN11, CON1, CON2, CON3, CON4, CON5, CON6, CON7;

OBJ.. Z =E= CP1*P1 + CP2*P2 + CP3*P3 + CP4*P4 + CP5*P5 + CP6*P6 - (CR12)*(ru1+ ru2 + ru3 + ru4 + ru5 + ru6 + ru7)- CR3*R3 - CR4*R4;

EQN1..y('C1','P1')*P1 + y('C1','P2')*P2 + y('C1','P3')*P3 + y('C1','P4')*P4 + y('C1','P5')*P5 + y('C1','P6')*P6 - x('C1','R3')*R3 - x('C1','R4')*R4 =E= ru1;

EQN2.. y('C2','P1')*P1 + y('C2','P2')*P2 + y('C2','P3')*P3 + y('C2','P4')*P4 + y('C2','P5')*P5 + y('C2','P6')*P6 - x('C2','R3')*R3 - x('C2','R4')*R4 =E= ru2;

EQN3..y('C3','P1')*P1 + y('C3','P2')*P2 + y('C3','P3')*P3 + y('C3','P4')*P4 + y('C3','P5')*P5 + y('C3','P6')*P6 - x('C3','R3')*R3 - x('C3','R4')*R4 =E= ru3;

EQN4..(y('iC4','P1') + y('C4','P1'))*P1 + (y('iC4','P2')+ y('C4','P2'))*P2 +(y('iC4','P3')+ y('C4','P3'))*P3 + (y('iC4','P4')+ y('C4','P4'))*P4 +(y('iC4','P5')+ y('C4','P5'))*P5 + (y('iC4','P6')+ y('C4','P6'))*P6 - (x('iC4','R3')+ x('C4','R3'))*R3 - (x('iC4','R4')+ x('C4','R4'))*R4 =E= ru4;

EQN5..(y('iC5','P1') + y('C5','P1')+ y('C6+', 'P1'))*P1 + (y('iC5','P2')+ y('C5','P2')+ y('C6+', 'P2'))*P2 +(y('iC5','P3')+ y('C5','P3')+ y('C6+', 'P3'))*P3 + (y('iC5','P4')+ y('C5','P4')+ y('C6+', 'P4'))*P4 +(y('iC5','P5')+ y('C5','P5')+ y('C6+', 'P5'))*P5 + (y('iC5','P6')+y('C5','P6')+ y('C6+', 'P6'))*P6 -(x('iC5','R3')+ x('C5','R3')+ x('C6+', 'R3'))*R3 - (x('iC5','R4')+ x('C5','R4')+ x('C6+', 'R4'))*R4 =E= ru5;

EQN6..y('N2','P1')*P1 + y('N2','P2')*P2 + y('N2','P3')*P3 + y('N2','P4')*P4 + y('N2','P5')*P5 + y('N2','P6')*P6 - x('N2','R3')*R3 - x('N2','R4')*R4 =E= ru6;

EQN7..y('CO2','P1')*P1 + y('CO2','P2')*P2 + y('CO2','P3')*P3 +
 y('CO2','P4')*P4 + y('CO2','P5')*P5 + y('CO2','P6')*P6 -
 x('CO2','R3')*R3 - x('CO2','R4')*R4 =E= ru7;

CON1..y('C1','P1')*P1 + y('C1','P2')*P2 + y('C1','P3')*P3 +
 y('C1','P4')*P4 + y('C1','P5')*P5 + y('C1','P6')*P6 -
 x('C1','R3')*R3 - x('C1','R4')*R4 =L= m1('50','ru1');

CON2..y('C2','P1')*P1 + y('C2','P2')*P2 + y('C2','P3')*P3 +
 y('C2','P4')*P4 + y('C2','P5')*P5 + y('C2','P6')*P6 -
 x('C2','R3')*R3 - x('C2','R4')*R4 =L= m1('50','ru2');

CON3..y('C3','P1')*P1 + y('C3','P2')*P2 + y('C3','P3')*P3 +
 y('C3','P4')*P4 + y('C3','P5')*P5 + y('C3','P6')*P6 -
 x('C3','R3')*R3 - x('C3','R4')*R4 =L= m1('50','ru3');

CON4..(y('iC4','P1') + y('C4','P1'))*P1 + (y('iC4','P2')+
 y('C4','P2'))*P2 + (y('iC4','P3')+ y('C4','P3'))*P3 +
 (y('iC4','P4')+ y('C4','P4'))*P4 + (y('iC4','P5')+
 y('C4','P5'))*P5 + (y('iC4','P6')+ y('C4','P6'))*P6 -
 (x('iC4','R3')+ x('C4','R3'))*R3 - (x('iC4','R4')+
 x('C4','R4'))*R4 =L= m1('50','ru4');

CON5.. (y('iC5','P1') + y('C5','P1')+ y('C6+', 'P1'))*P1 +
 (y('iC5','P2')+y('C5','P2')+ y('C6+', 'P2'))*P2 + (y('iC5','P3')+
 y('C5','P3')+y('C6+', 'P3'))*P3 + (y('iC5','P4')+ y('C5','P4')+
 y('C6+', 'P4'))*P4 + (y('iC5','P5')+ y('C5','P5')+
 y('C6+', 'P5'))*P5 + (y('iC5','P6')+y('C5','P6')+
 y('C6+', 'P6'))*P6 - (x('iC5','R3')+ x('C5','R3')+
 x('C6+', 'R3'))*R3 - (x('iC5','R4')+ x('C5','R4')+
 x('C6+', 'R4'))*R4 =L= m2('50','ru5');

CON6..y('N2','P1')*P1 + y('N2','P2')*P2 + y('N2','P3')*P3 +
 y('N2','P4')*P4 + y('N2','P5')*P5 + y('N2','P6')*P6 -
 x('N2','R3')*R3 - x('N2','R4')*R4 =L= m2('50','ru6');

CON7..y('CO2','P1')*P1 + y('CO2','P2')*P2 + y('CO2','P3')*P3 +
 y('CO2','P4')*P4 + y('CO2','P5')*P5 + y('CO2','P6')*P6 -
 x('CO2','R3')*R3 - x('CO2','R4')*R4 =L= m2('50','ru7');

EQN8.. ru =E= ru1 + ru2 + ru3 + ru4 + ru5 + ru6 + ru7;

EQN9.. R =E= R3 + R4;

EQN10.. P =E= P1 + P2 + P3 + P4 + P5 + P6;

EQN11.. P - R - ru =E= 0;

R3.up = 10.706112016;

R3.lo = 0;

R4.up = 35.5858020881;

R4.lo = 0;

P1.up = 298.518112183;

P1.lo = 0;

```

P2.up = 37.310810089;
P2.lo = 0;
P3.up = 47.706112016;
P3.lo = 0;
P4.up = 29.585802088;
P4.lo = 0;
P5.up = 43.111991264;
P5.lo = 0;
P6.up = 57.659376734;
P6.lo = 0;

Model Gas / all /;

Option LP = CPLEX;

Solve Gas using LP maximizing Z;

Display
    ru1.l, ru2.l, ru3.l, ru4.l, ru5.l, ru6.l, ru7.l, R3.l, R4.l, P1.l, P2.l, P
    3.l, P4.l, P5.l, P6.l, ru.l, R.l, P.l;

```

*** (II) Joint chance constrained optimization**

Scalars

```

SM1 supply mean value for ru1 /190.0552373/
SV1 supply STDEV for ru1 /31.36042668/
SM2 supply mean value for ru2 /32.26080945/
SV2 supply STDEV for ru2 /5.787991076/
SM3 supply mean value for ru3 /20.78197572/
SV3 supply STDEV for ru3 /4.28887593/
SM4 supply mean value for ru4 /13.08167633/
SV4 supply STDEV for ru4 /3.173357683/
SM5 supply mean value for ru5 /9.060381024/
SV5 supply STDEV for ru5 /3.348890816/
SM6 supply mean value for ru6 /2.438983829/
SV6 supply STDEV for ru6 /0.655668375/

```

SM7 supply mean value for ru7 /47.22380042/

SV7 supply STDEV for ru7 /9.74177713/;

Variables

Z, zu1, zu2, zu3, zu4, zu5, zu6, zu7;

Positive Variables

ru1, ru2, ru3, ru4, ru5, ru6, ru7, ru, R1, R2, R3, R4, R, P1, P2, P3, P4, P5, P6, P;

Equations

OBJ, EQN1, EQN2, EQN3, EQN4, EQN5, EQN6, EQN7, EQN8, EQN9, EQN10, EQN11, EQN12,

EQN13, EQN14, EQN15, EQN16, EQN17, EQN18, CON1;

OBJ..Z =E= CP1*P1 + CP2*P2 + CP3*P3 + CP4*P4 + CP5*P5 + CP6*P6 -
(CR12)*(ru1+ ru2 + ru3 + ru4 + ru5 + ru6 + ru7)- CR3*R3 -
CR4*R4;

EQN1..y('C1','P1')*P1 + y('C1','P2')*P2 + y('C1','P3')*P3 +
y('C1','P4')*P4 + y('C1','P5')*P5 + y('C1','P6')*P6 -
x('C1','R3')*R3 - x('C1','R4')*R4 =E= ru1;

EQN2..y('C2','P1')*P1 + y('C2','P2')*P2 + y('C2','P3')*P3 +
y('C2','P4')*P4 + y('C2','P5')*P5 + y('C2','P6')*P6 -
x('C2','R3')*R3 - x('C2','R4')*R4 =E= ru2;

EQN3..y('C3','P1')*P1 + y('C3','P2')*P2 + y('C3','P3')*P3 +
y('C3','P4')*P4 + y('C3','P5')*P5 + y('C3','P6')*P6 -
x('C3','R3')*R3 - x('C3','R4')*R4 =E= ru3;

EQN4..(y('iC4','P1') + y('C4','P1'))*P1 + (y('iC4','P2')+
y('C4','P2'))*P2 +(y('iC4','P3')+ y('C4','P3'))*P3 +
(y('iC4','P4')+ y('C4','P4'))*P4 +(y('iC4','P5')+
y('C4','P5'))*P5 + (y('iC4','P6')+ y('C4','P6'))*P6 -
(x('iC4','R3')+ x('C4','R3'))*R3 - (x('iC4','R4')+
x('C4','R4'))*R4 =E= ru4;

EQN5..(y('iC5','P1') + y('C5','P1')+ y('C6+', 'P1'))*P1 +
(y('iC5','P2')+ y('C5','P2')+ y('C6+', 'P2'))*P2
+(y('iC5','P3')+ y('C5','P3')+ y('C6+', 'P3'))*P3 +
(y('iC5','P4')+ y('C5','P4')+ y('C6+', 'P4'))*P4
+(y('iC5','P5')+ y('C5','P5')+ y('C6+', 'P5'))*P5 +
(y('iC5','P6')+y('C5','P6')+ y('C6+', 'P6'))*P6 -(x('iC5','R3')+
x('C5','R3')+ x('C6+', 'R3'))*R3 - (x('iC5','R4')+ x('C5','R4')+
x('C6+', 'R4'))*R4 =E= ru5;

EQN6..y('N2','P1')*P1 + y('N2','P2')*P2 + y('N2','P3')*P3 +
y('N2','P4')*P4 + y('N2','P5')*P5 + y('N2','P6')*P6 -
x('N2','R3')*R3 - x('N2','R4')*R4 =E= ru6;

EQN7..y('CO2','P1')*P1 + y('CO2','P2')*P2 + y('CO2','P3')*P3 +
y('CO2','P4')*P4 + y('CO2','P5')*P5 + y('CO2','P6')*P6 -
x('CO2','R3')*R3 - x('CO2','R4')*R4 =E= ru7;

EQN8.. zu1 =E= (ru1 - SM1)/SV1;

```

EQN9.. zu2 =E= (ru2 - SM2)/SV2;
EQN10.. zu3 =E= (ru3 - SM3)/SV3;
EQN11.. zu4 =E= (ru4 - SM4)/SV4;
EQN12.. zu5 =E= (ru5 - SM5)/SV5;
EQN13.. zu6 =E= (ru6 - SM6)/SV6;
EQN14.. zu7 =E= (ru7 - SM7)/SV7;
CON1.. (1 - errorf(zu1))*(1 - errorf(zu2))*(1 - errorf(zu3))*
        (1 - errorf(zu4))*(1 - errorf(zu5))*(1 - errorf(zu6))*
        (1 - errorf(zu7)) =G= 0.50;
EQN15.. ru =E= ru1 + ru2 + ru3 + ru4 + ru5 + ru6 + ru7;
EQN16.. R =E= R3 + R4;
EQN17.. P =E= P1 + P2 + P3 + P4 + P5 + P6;
EQN18.. P - R - ru =E= 0;

R3.up = 10.706112016;
R3.lo = 0;
R4.up = 35.5858020881;
R4.lo = 0;
P1.up = 298.518112183;
P1.lo = 0;
P2.up = 37.310810089;
P2.lo = 0;
P3.up = 47.706112016;
P3.lo = 0;
P4.up = 29.585802088;
P4.lo = 0;
P5.up = 43.111991264;
P5.lo = 0;
P6.up = 57.659376734;
P6.lo = 0;

```

Model Gas / all /;

Option NLP = CONOPT3;

Solve Gas using NLP maximizing Z;

Display

zu1.l, zu2.l, zu3.l, zu4.l, zu5.l, zu6.l, zu7.l, ru1.l, ru2.l, ru3.l, ru4.l, ru5.l, ru6.l, ru7.l, R3.l, R4.l, P1.l, P2.l, P3.l, P4.l, P5.l, P6.l, ru.l, R.l, P.l;

*** CASE STUDY 2**

***(I) Single chance constrained optimization**

Table m1(e,b) values for total feed component outflows (pu1-pu4)

*	C1 outflow	C2 outflow	C3 outflow	C4s outflow
	pu1	pu2	pu3	pu4
50	0.00000000	0.29099634	24.48603967	15.66600984
51	0.00000125	0.29484201	24.61206710	15.73571295
52	0.00000249	0.29869011	24.73817379	15.80545989
53	0.00000374	0.30254305	24.86443936	15.87529471
54	0.00000499	0.30640329	24.99094413	15.94526182
55	0.00000624	0.31027332	25.11776947	16.01540623
56	0.00000750	0.31415565	25.24499821	16.08577376
57	0.00000876	0.31805287	25.37271500	16.15641121
58	0.00001003	0.32196764	25.50100673	16.22736665
59	0.00001130	0.32590269	25.62996298	16.29868963
60	0.00001258	0.32986085	25.75967647	16.37043142
61	0.00001387	0.33384505	25.89024361	16.44264534
62	0.00001517	0.33785837	26.02176504	16.51538706
63	0.00001648	0.34190403	26.15434623	16.58871491
64	0.00001780	0.34598542	26.28809821	16.66269030
65	0.00001914	0.35010611	26.42313830	16.73737812
66	0.00002049	0.35426991	26.55959099	16.8128472

	pu1	pu2	pu3	pu4
67	0.00002185	0.35848086	26.69758892	16.88917096
68	0.00002323	0.36274330	26.83727398	16.96642781
69	0.00002463	0.36706186	26.97879858	17.04470207
70	0.00002605	0.37144158	27.12232713	17.12408467
71	0.00002749	0.37588787	27.26803770	17.20467411
72	0.00002895	0.38040667	27.41612406	17.28657754
73	0.00003044	0.38500442	27.56679791	17.36991206
74	0.00003195	0.38968822	27.72029170	17.45480623
75	0.00003350	0.39446589	27.87686181	17.54140185
76	0.00003508	0.39934611	28.03679247	17.62985611
77	0.00003670	0.40433854	28.20040042	17.72034421
78	0.00003835	0.40945402	28.36804062	17.81306246
79	0.00004005	0.41470474	28.54011317	17.90823214

Table m1(e,b) values for total feed component outflows (pu1-pu4)

*	C1 outflow	C2 outflow	C3 outflow	C4s outflow
	pu1	pu2	pu3	pu4
80	0.00004180	0.42010456	28.71707196	18.00610431
81	0.00004360	0.42566931	28.89943542	18.10696568
82	0.00004547	0.43141718	29.08780005	18.21114617
83	0.00004739	0.43736929	29.28285781	18.31902849
84	0.00004939	0.44355035	29.48541855	18.43106056
85	0.00005148	0.44998957	29.69643951	18.54777179
86	0.00005366	0.45672186	29.91706474	18.66979493
87	0.00005595	0.46378946	30.14867869	18.79789571
88	0.00005836	0.47124424	30.39298077	18.93301403
89	0.00006092	0.47915090	30.65209142	19.07632265
90	0.00006365	0.48759172	30.92870751	19.22931316

	pu1	pu2	pu3	pu4
91	0.00006659	0.49667378	31.22633758	19.39392605
92	0.00006979	0.50654021	31.54967222	19.57275560
93	0.00007330	0.51738887	31.90519599	19.76938828
94	0.00007722	0.52950513	32.30226034	19.98899617
95	0.00008170	0.54332378	32.75511432	20.23946013
96	0.00008696	0.55955892	33.28715947	20.53372305
97	0.00009342	0.57951797	33.94124134	20.89548190
98	0.00010201	0.60605003	34.81072922	21.37637726
99	0.00011555	0.64786786	36.18114975	22.13432787
100	0.00029791	1.21108509	54.63845756	32.34267443;

Table m2(e,b) values for total feed component outflows (pu5-pu7)

*	C5+ outflow	N2 outflow	CO2 outflow
	pu5	pu6	pu7
50	0.15582874	0.00000000	0.70140516
51	0.15924002	0.00000000	0.70787117
52	0.16265345	0.00000000	0.71434125
53	0.16607118	0.00000000	0.72081947
54	0.16949538	0.00000000	0.72730997
55	0.17292826	0.00000000	0.73381692
56	0.17637206	0.00000000	0.74034456
57	0.17982907	0.00000000	0.74689725
58	0.18330165	0.00000000	0.75347943
59	0.18679221	0.00000000	0.76009571
60	0.19030326	0.00000000	0.76675083
61	0.19383743	0.00000000	0.77344976
62	0.19739742	0.00000000	0.78019765
63	0.20098610	0.00000000	0.78699990

	pu5	pu6	pu7
64	0.20460647	0.00000000	0.79386223
65	0.20826170	0.00000000	0.80079065
66	0.21195518	0.00000000	0.80779154
67	0.21569048	0.00000000	0.81487171
68	0.21947144	0.00000000	0.82203844
69	0.22330220	0.00000000	0.82929956
70	0.22718720	0.00000000	0.83666348
71	0.23113126	0.00000000	0.84413936
72	0.23513963	0.00000000	0.85173714
73	0.23921804	0.00000000	0.85946766
74	0.24337277	0.00000000	0.86734287
75	0.24761078	0.00000000	0.87537592
76	0.25193975	0.00000000	0.88358138
77	0.25636825	0.00000000	0.89197551
78	0.26090590	0.00000000	0.90057651
79	0.26556352	0.00000000	0.90940493

Table m2(e,b) values for total feed component outflows (pu5-pu7)

*	C5+ outflow	N2 outflow	CO2 outflow
	pu5	pu6	pu7
80	0.27035341	0.00000000	0.91848404
81	0.27528958	0.00000000	0.92784045
82	0.28038819	0.00000000	0.93750475
83	0.28566798	0.00000000	0.94751246
84	0.29115085	0.00000000	0.95790511
85	0.29686272	0.00000000	0.96873183
86	0.30283455	0.00000000	0.98005131
87	0.30910383	0.00000000	0.99193458

	pu5	pu6	pu7
88	0.31571655	0.00000000	1.00446883
89	0.32273010	0.00000000	1.01776286
90	0.33021748	0.00000000	1.03195502
91	0.33827367	0.00000000	1.04722534
92	0.34702562	0.00000000	1.06381447
93	0.35664886	0.00000000	1.08205510
94	0.36739651	0.00000000	1.10242703
95	0.37965427	0.00000000	1.12566132
96	0.39405555	0.00000000	1.15295862
97	0.41176010	0.00000000	1.18651718
98	0.43529521	0.00000000	1.23112744
99	0.47238946	0.00000000	1.30143874
100	0.97198788	0.00000000	2.24841610 ;

Variables Z;

Positive Variables

pu1, pu2, pu3, pu4, pu5, pu6, pu7, pu, R1, R2, R3, R4, R, P1, P2, P3, P4, P5, P6, P;

Equations

OBJ, EQN1, EQN2, EQN3, EQN4, EQN5, EQN6, EQN7, EQN8, CON1, CON2, CON3, CON4;

OBJ.. Z =E= CP1*P1 + CP2*P2 + (CP34)*(pu2 + pu3 + pu4 + pu5) +
CP5*P5 + CP6*P6 - CR1*R1 - CR2*R2 - CR3*R3 - CR4*R4 ;

EQN1..x('C2', 'R1')*R1 + x('C2', 'R2')*R2 + x('C2', 'R3')*R3 +
x('C2', 'R4')*R4 - y('C2', 'P1')*P1 - y('C2', 'P2')*P2 -
y('C2', 'P5')*P5 - y('C2', 'P6')*P6 =E= pu2;

EQN2.. x('C3', 'R1')*R1 + x('C3', 'R2')*R2 + x('C3', 'R3')*R3 +
x('C3', 'R4')*R4 -y('C3', 'P1')*P1 - y('C3', 'P2')*P2 -
y('C3', 'P5')*P5 - y('C3', 'P6')*P6 =E= pu3;

EQN3..(x('iC4', 'R1') + x('C4', 'R1'))*R1 + (x('iC4', 'R2')+
x('C4', 'R2'))*R2 +(x('iC4', 'R3')+ x('C4', 'R3'))*R3 +
(x('iC4', 'R4')+ x('C4', 'R4'))*R4 - (y('iC4', 'P1') +
y('C4', 'P1'))*P1 - (y('iC4', 'P2')+ y('C4', 'P2'))*P2 -
(y('iC4', 'P5')+ y('C4', 'P5'))*P5 - (y('iC4', 'P6')+
y('C4', 'P6'))*P6 =E= pu4;

$$\begin{aligned} \text{EQN4..} & (x('iC5','R1') + x('C5','R1') + x('C6+','R1'))*R1 + \\ & (x('iC5','R2') + x('C5','R2') + x('C6+','R2'))*R2 + \\ & (x('iC5','R3') + x('C5','R3') + x('C6+','R3'))*R3 \\ & + (x('iC5','R4') + x('C5','R4') + x('C6+','R4'))*R4 - \\ & (y('iC5','P1') + y('C5','P1') + y('C6+','P1'))*P1 - \\ & (y('iC5','P2') + y('C5','P2') + y('C6+','P2'))*P2 - \\ & (y('iC5','P5') + y('C5','P5') + y('C6+','P5'))*P5 - (y('iC5','P6') \\ & + y('C5','P6') + y('C6+','P6'))*P6 =E= pu5; \end{aligned}$$

$$\begin{aligned} \text{CON1..} & x('C2','R1')*R1 + x('C2','R2')*R2 + x('C2','R3')*R3 + \\ & x('C2','R4')*R4 - y('C2','P1')*P1 - y('C2','P2')*P2 - \\ & y('C2','P5')*P5 - y('C2','P6')*P6 =E= m1('50','pu2'); \end{aligned}$$

$$\begin{aligned} \text{CON2..} & x('C3','R1')*R1 + x('C3','R2')*R2 + x('C3','R3')*R3 + \\ & x('C3','R4')*R4 - y('C3','P1')*P1 - y('C3','P2')*P2 - \\ & y('C3','P5')*P5 - y('C3','P6')*P6 =G= m1('50','pu3'); \end{aligned}$$

$$\begin{aligned} \text{CON3..} & (x('iC4','R1') + x('C4','R1'))*R1 + (x('iC4','R2') + \\ & x('C4','R2'))*R2 + (x('iC4','R3') + x('C4','R3'))*R3 + \\ & (x('iC4','R4') + x('C4','R4'))*R4 - (y('iC4','P1') + \\ & y('C4','P1'))*P1 - (y('iC4','P2') + y('C4','P2'))*P2 - \\ & (y('iC4','P5') + y('C4','P5'))*P5 - (y('iC4','P6') + \\ & y('C4','P6'))*P6 =G= m1('50','pu4'); \end{aligned}$$

$$\begin{aligned} \text{CON4..} & (x('iC5','R1') + x('C5','R1') + x('C6+','R1'))*R1 + \\ & (x('iC5','R2') + x('C5','R2') + x('C6+','R2'))*R2 + \\ & (x('iC5','R3') + x('C5','R3') + x('C6+','R3'))*R3 \\ & + (x('iC5','R4') + x('C5','R4') + x('C6+','R4'))*R4 - \\ & (y('iC5','P1') + y('C5','P1') + y('C6+','P1'))*P1 - \\ & (y('iC5','P2') + y('C5','P2') + y('C6+','P2'))*P2 - \\ & (y('iC5','P5') + y('C5','P5') + y('C6+','P5'))*P5 - (y('iC5','P6') \\ & + y('C5','P6') + y('C6+','P6'))*P6 =E= m2('50','pu5'); \end{aligned}$$

$$\text{EQN5.. } pu =E= pu1 + pu2 + pu3 + pu4 + pu5 + pu6 + pu7 ;$$

$$\text{EQN6.. } R =E= R1 + R2 + R3 + R4;$$

$$\text{EQN7.. } P =E= P1 + P2 + P5 + P6;$$

$$\text{EQN8.. } R - P - pu =E= 0;$$

$$R1.up = 334.582214355;$$

$$R1.lo = 0;$$

$$R2.up = 220.314773560;$$

$$R2.lo = 0;$$

$$R3.up = 10.706112016;$$

$$R3.lo = 0;$$

$$R4.up = 35.5858020881;$$

$$R4.lo = 0;$$

```

P1.up = 298.518112183;

P1.lo = 0;

P2.up = 37.310810089;

P2.lo = 0;

P5.up = 43.111991264;

P5.lo = 0;

P6.up = 57.659376734;

P6.lo = 0;

Model Gas / all /;

Option LP = CPLEX;

Solve Gas using LP maximizing Z;

Display
    pu1.1,pu2.1,pu3.1,pu4.1,pu5.1,pu6.1,pu7.1,R1.1,R2.1,R3.1,R4.1,P
    1.1,P2.1,P5.1,P6.1,pu.1,P.1,R.1;

```

*** (II) Joint chance constrained optimization**

Scalars

```

SM1 supply mean value for ru1 /4.90851E-10/
SV1 supply STDEV for ru1 /4.9669E-05/
SM2 supply mean value for ru2 /0.290996338/
SV2 supply STDEV for ru2 /0.153404194/
SM3 supply mean value for ru3 /24.48603967/
SV3 supply STDEV for ru3 /5.027240429/
SM4 supply mean value for ru4 /15.66600984/
SV4 supply STDEV for ru4 /2.780460351/
SM5 supply mean value for ru5 /0.155828737/
SV5 supply STDEV for ru5 /0.13607626/
SM6 supply mean value for ru6 /8.78535E-16/
SV6 supply STDEV for ru6 /7.92836E-15/
SM7 supply mean value for ru7 /0.70140516/
SV7 supply STDEV for ru7 /0.257929429/;

```

Variables

Z, zu1, zu2, zu3, zu4, zu5, zu6, zu7;

Positive Variables

pu1, pu2, pu3, pu4, pu5, pu6, pu7, pu, R1, R2, R3, R4, R, P1, P2, P3, P4, P5, P6, P;

Equations

OBJ, EQN1, EQN2, EQN3, EQN4, EQN5, EQN6, EQN7, EQN8, EQN9, EQN10, EQN11, EQN12, EQN13, EQN14, CON1;

OBJ.. Z =E= CP1*P1 + CP2*P2 + (CP34)*(pu2 + pu3 + pu4 + pu5) +
CP5*P5 + CP6*P6 - CR1*R1 - CR2*R2 - CR3*R3 - CR4*R4 ;

EQN1..x('C2', 'R1')*R1 + x('C2', 'R2')*R2 + x('C2', 'R3')*R3 +
x('C2', 'R4')*R4 - y('C2', 'P1')*P1 - y('C2', 'P2')*P2 -
y('C2', 'P5')*P5 - y('C2', 'P6')*P6 =E= pu2;

EQN2.. x('C3', 'R1')*R1 + x('C3', 'R2')*R2 + x('C3', 'R3')*R3 +
x('C3', 'R4')*R4 -y('C3', 'P1')*P1 - y('C3', 'P2')*P2 -
y('C3', 'P5')*P5 - y('C3', 'P6')*P6 =E= pu3;

EQN3..(x('iC4', 'R1') + x('C4', 'R1'))*R1 + (x('iC4', 'R2')+
x('C4', 'R2'))*R2 +(x('iC4', 'R3')+ x('C4', 'R3'))*R3 +
(x('iC4', 'R4')+ x('C4', 'R4'))*R4 - (y('iC4', 'P1') +
y('C4', 'P1'))*P1 - (y('iC4', 'P2')+ y('C4', 'P2'))*P2 -
(y('iC4', 'P5')+ y('C4', 'P5'))*P5 - (y('iC4', 'P6')+
y('C4', 'P6'))*P6 =E= pu4;

EQN4.(x('iC5', 'R1') + x('C5', 'R1')+ x('C6+', 'R1'))*R1 +
(x('iC5', 'R2') +x('C5', 'R2')+ x('C6+', 'R2'))*R2 +
(x('iC5', 'R3')+ x('C5', 'R3') +x('C6+', 'R3'))*R3
+(x('iC5', 'R4')+ x('C5', 'R4')+ x('C6+', 'R4'))*R4 -
(y('iC5', 'P1') + y('C5', 'P1')+ y('C6+', 'P1'))*P1 -
(y('iC5', 'P2') +y('C5', 'P2') + y('C6+', 'P2'))*P2 -
(y('iC5', 'P5')+ y('C5', 'P5')+y('C6+', 'P5'))*P5 - (y('iC5', 'P6')
+ y('C5', 'P6')+ y('C6+', 'P6'))*P6 =E= pu5;

EQN5..x('C2', 'R1')*R1 + x('C2', 'R2')*R2 + x('C2', 'R3')*R3 +
x('C2', 'R4')*R4 - y('C2', 'P1')*P1 - y('C2', 'P2')*P2 -
y('C2', 'P5')*P5 - y('C2', 'P6')*P6 =E= m1('50', 'pu2');

EQN6..(x('iC5', 'R1') + x('C5', 'R1')+ x('C6+', 'R1'))*R1 +
(x('iC5', 'R2') +x('C5', 'R2')+ x('C6+', 'R2'))*R2 +
(x('iC5', 'R3')+ x('C5', 'R3') +x('C6+', 'R3'))*R3
+(x('iC5', 'R4')+ x('C5', 'R4')+ x('C6+', 'R4'))*R4 -
(y('iC5', 'P1') + y('C5', 'P1')+ y('C6+', 'P1'))*P1 -
(y('iC5', 'P2') +y('C5', 'P2') + y('C6+', 'P2'))*P2 -
(y('iC5', 'P5')+ y('C5', 'P5')+y('C6+', 'P5'))*P5 - (y('iC5', 'P6')
+ y('C5', 'P6')+ y('C6+', 'P6'))*P6 =E= m2('50', 'pu5');

EQN7.. zu2 =E= (pu2 - SM2)/SV2;

EQN8.. zu3 =E= (pu3 - SM3)/SV3;

```

EQN9.. zu4 =E= (pu4 - SM4)/SV4;
EQN10..zu5 =E= (pu5 - SM5)/SV5;
CON1.. (errorf(zu3))*(errorf(zu4))=G= 0.5;
EQN11.. pu =E= pu1 + pu2 + pu3 + pu4 + pu5 + pu6 + pu7 ;
EQN12.. R =E= R1 + R2 + R3 + R4;
EQN13.. P =E= P1 + P2 + P5 + P6;
EQN14.. R - P - pu =E= 0;

      R1.up = 334.582214355;
      R1.lo = 0;
      R2.up = 220.314773560;
      R2.lo = 0;
      R3.up = 10.706112016;
      R3.lo = 0;
      R4.up = 35.5858020881;
      R4.lo = 0;
      P1.up = 298.518112183;
      P1.lo = 0;
      P2.up = 37.310810089;
      P2.lo = 0;
      P5.up = 43.111991264;
      P5.lo = 0;
      P6.up = 57.659376734;
      P6.lo = 0;

Model Gas / all /;
Option NLP = CONOPT3;
Solve Gas using NLP maximizing Z;
Display
      pu1.l,pu2.l,pu3.l,pu4.l,pu5.l,pu6.l,pu7.l,R1.l,R2.l,R3.l,R4.l,P
      1.l,P2.l,P5.l,P6.l,pu.l,P.l,R.l;

```

*** CASE STUDY 3**

***(I) Single chance constrained optimization**

Table s1(k,l) values for column feed composition

	De-Feed	Dp-Feed	Db-Feed
C1	0.0006249083	4.03248E-14	1.90633E-31
C2	0.3445260150	0.003927954	1.33712E-12
C3	0.3259828270	0.357536934	0.003920158
iC4	0.1180269411	0.141852222	0.218952764
C4	0.0873733029	0.110852646	0.17340164
iC5	0.0467667449	0.071932743	0.112556303
C5	0.0242576152	0.040729516	0.063731254
C6	0.0204153112	0.053623676	0.083907309
C7	0.0138600701	0.065666637	0.102751456
C8	0.0097597637	0.092854413	0.145293358
C9	0.0030868275	0.060562293	0.094764466
C10	0.0000114333	0.000460966	0.000721293
N2	0.0000000001	5.38041E-25	3.25824E-48
CO2	0.0053082396	1.89383E-09	2.9426E-25;

Table s2(k,l) values for column bottom composition

	De-Bottom	Dp-Bottom	Db-Bottom
C1	1.8592737E-15	1.906329E-31	9.169089E-31
C2	5.0145683E-03	1.337117E-12	3.849503E-31
C3	4.9929712E-01	3.920158E-03	1.082107E-14
iC4	1.8081634E-01	2.189528E-01	1.923905E-05
C4	1.3385521E-01	1.734016E-01	4.979377E-03
iC5	7.1646285E-02	1.125563E-01	2.387119E-01
C5	3.7162476E-02	6.373125E-02	1.363735E-01
C6	3.1276096E-02	8.390731E-02	1.503356E-01

	De-Bottom	Dp-Bottom	Db-Bottom
C7	2.1233518E-02	1.027515E-01	1.583276E-01
C8	1.4951881E-02	1.452934E-01	1.963885E-01
C9	4.7289954E-03	9.476447E-02	1.140816E-01
C10	1.7515754E-05	7.212931E-04	7.827276E-04
N2	2.5169264E-29	3.258237E-48	8.974995E-48
CO2	3.3440230E-10	2.942601E-25	6.324608E-32

;

Table m1(e,c) values for total utility inflows (u1-u4)

*	u1 inflow	u2 inflow	u3 inflow	u4 inflow
	u1	u2	u3	u4
50	-339463.115547	50123.236514	5365.947000	5116.235781
51	-340030.073240	50053.381371	5361.744874	5112.241698
52	-340597.387518	49983.482293	5357.540106	5108.245103
53	-341165.416538	49913.495152	5353.330040	5104.243473
54	-341734.521621	49843.375428	5349.111998	5100.234263
55	-342305.068878	49773.078013	5344.883268	5096.214892
56	-342877.430892	49702.557001	5340.641087	5092.182738
57	-343451.988479	49631.765472	5336.382633	5088.135115
58	-344029.132543	49560.655261	5332.105009	5084.069272
59	-344609.266058	49489.176718	5327.805228	5079.982369
60	-345192.806193	49417.278444	5323.480199	5075.871467
61	-345780.186629	49344.907005	5319.126705	5071.733510
62	-346371.860082	49272.006621	5314.741394	5067.565311
63	-346968.301087	49198.518825	5310.320747	5063.363525
64	-347570.009091	49124.382079	5305.861062	5059.124635
65	-348177.511902	49049.531351	5301.358427	5054.844921
66	-348791.369572	48973.897639	5296.808693	5050.520439
67	-349412.178786	48897.407423	5292.207435	5046.146985

	u1	u2	u3	u4
68	-350040.577856	48819.982057	5287.549924	5041.720063
69	-350677.252444	48741.537060	5282.831077	5037.234841
70	-351322.942146	48661.981307	5278.045413	5032.686110
71	-351978.448117	48581.216086	5273.186993	5028.068225
72	-352644.641963	48499.134007	5268.249358	5023.375047
73	-353322.476159	48415.617715	5263.225448	5018.599866
74	-354012.996347	48330.538375	5258.107513	5013.735315
75	-354717.355934	48243.753875	5252.887005	5008.773268
76	-355436.833571	48155.106673	5247.554446	5003.704718
77	-356172.854195	48064.421202	5242.099275	4998.519627
78	-356927.014607	47971.500717	5236.509657	4993.206746
79	-357701.114793	47876.123444	5230.772251	4987.753393
80	-358497.196655	47778.037797	5224.871924	4982.145185
81	-359317.592381	47676.956426	5218.791389	4976.365691
82	-360164.985498	47572.548694	5212.510758	4970.396007
83	-361042.488898	47464.431058	5206.006958	4964.214204
84	-361953.745836	47352.154632	5199.252986	4957.794614
85	-362903.062654	47235.188829	5192.216926	4951.106902
86	-363895.586040	47112.899522	5184.860631	4944.114809
87	-364937.544250	46984.519327	5177.137940	4936.774461
88	-366036.582339	46849.106290	5168.992189	4929.031997
89	-367202.239499	46705.485085	5160.352677	4920.820219
90	-368446.648127	46552.160871	5151.129482	4912.053654
91	-369785.592024	46387.188919	5141.205619	4902.621111
92	-371240.172702	46207.969302	5130.424690	4892.373935
93	-372839.562111	46010.907727	5118.570480	4881.106615
94	-374625.829514	45790.820821	5105.331186	4868.522784
95	-376663.076881	45539.810547	5090.231700	4854.170859

96	-379056.580334	45244.905782	5072.491749	4837.309193
97	-381999.088569	44882.357861	5050.682733	4816.579919
98	-385910.640612	44400.413564	5021.691446	4789.023961
99	-392075.730765	43640.809702	4975.997590	4745.592360
100	-475109.342903	33410.196542	4360.576595	4160.640216 ;

Table m2(e,c) values for total utility inflows (u5-u6)

*		u5 inflow	u6 inflow
		u5	u6
	50	112.801265	4950.238150
	51	112.608446	4943.927975
	52	112.415506	4937.613831
	53	112.222322	4931.291732
	54	112.028773	4924.957657
	55	111.834733	4918.607530
	56	111.640076	4912.237206
	57	111.444673	4905.842445
	58	111.248389	4899.418896
	59	111.051089	4892.962076
	60	110.852631	4886.467340
	61	110.652866	4879.929862
	62	110.451641	4873.344603

Table m2(e,c) values for total utility inflows (u5-u6)

*		u5 inflow	u6 inflow
		u5	u6
	63	110.248795	4866.706282
	64	110.044158	4860.009340
	65	109.837550	4853.247902

	u5	u6
66	109.628780	4846.415736
67	109.417646	4839.506199
68	109.203932	4832.512189
69	108.987402	4825.426072
70	108.767807	4818.239619
71	108.544873	4810.943911
72	108.318305	4803.529249
73	108.087777	4795.985031
74	107.852935	4788.299619
75	107.613387	4780.460177
76	107.368696	4772.452472
77	107.118380	4764.260645
78	106.861895	4755.866925
79	106.598628	4747.251277
80	106.327885	4738.390976
81	106.048873	4729.260064
82	105.760680	4719.828675
83	105.462246	4710.062161
84	105.152333	4699.919974
85	104.829475	4689.354185
86	104.491924	4678.307512
87	104.137560	4666.710634
88	103.763784	4654.478465
89	103.367350	4641.504832
90	102.944134	4627.654704
91	102.488767	4612.752410
92	101.994073	4596.563091
93	101.450130	4578.762068

	u5	u6
94	100.842631	4558.881113
95	100.149775	4536.206780
96	99.335758	4509.567357
97	98.335028	4476.817572
98	97.004732	4433.282440
99	94.908021	4364.665682
100	66.668772	3440.510953;

Table m3(e,d) values for total energy product outflows (q1 to q4)

*	q1 outflow	q2 outflow	q3 outflow	q4 outflow
	q1	q2	q3	q4
50	15513.612430	13176.853210	3542.491844	-513512.061375
51	15524.692918	13180.981686	3545.742115	-513317.710512
52	15535.780376	13185.112759	3548.994429	-513123.237413
53	15546.881802	13189.249036	3552.250841	-512928.519304
54	15558.004258	13193.393150	3555.513423	-512733.432324
55	15569.154900	13197.547764	3558.784271	-512537.850973
56	15580.341010	13201.715594	3562.065524	-512341.647530
57	15591.570028	13205.899411	3565.359363	-512144.691453
58	15602.849597	13210.102062	3568.668031	-511946.848742
59	15614.187590	13214.326482	3571.993836	-511747.981260
60	15625.592162	13218.575709	3575.339171	-511547.946001
61	15637.071788	13222.852900	3578.706521	-511346.594303
62	15648.635315	13227.161351	3582.098483	-511143.770975

Table m3(e,d) values for total energy product outflows (q1 to q4)

*	q1 outflow	q2 outflow	q3 outflow	q4 outflow
	q1	q2	q3	q4
63	15660.292019	13231.504519	3585.517776	-510939.313349
64	15672.051659	13235.886040	3588.967264	-510733.050216
65	15683.924552	13240.309758	3592.449973	-510524.800646
66	15695.921642	13244.779751	3595.969113	-510314.372656
67	15708.054592	13249.300364	3599.528105	-510101.561704
68	15720.335876	13253.876244	3603.130608	-509886.148979
69	15732.778895	13258.512385	3606.780553	-509667.899439
70	15745.398104	13263.214173	3610.482181	-509446.559554
71	15758.209159	13267.987441	3614.240083	-509221.854691
72	15771.229095	13272.838535	3618.059258	-508993.486066
73	15784.476528	13277.774393	3621.945164	-508761.127174
74	15797.971893	13282.802627	3625.903797	-508524.419575
75	15811.737732	13287.931637	3629.941769	-508282.967884
76	15825.799034	13293.170734	3634.066410	-508036.333786
77	15840.183649	13298.530294	3638.285889	-507784.028816
78	15854.922784	13304.021944	3642.609360	-507525.505599
79	15870.051616	13309.658792	3647.047143	-507260.147106
80	15885.610054	13315.455706	3651.610942	-506987.253381
81	15901.643676	13321.429669	3656.314129	-506706.024959
82	15918.204928	13327.600222	3661.172088	-506415.541938
83	15935.354649	13333.990032	3666.202663	-506114.737231
84	15953.164042	13340.625629	3671.426742	-505802.361943
85	15971.717267	13347.538370	3676.869011	-505476.939879
86	15991.114912	13354.765734	3682.558976	-505136.706774
87	16011.478699	13362.353072	3688.532343	-504779.527606
88	16032.958042	13370.356054	3694.832938	-504402.781680

	q1	q2	q3	q4
89	16055.739373	13378.844144	3701.515449	-504003.198999
90	16080.059803	13387.905687	3708.649429	-503576.620625
91	16106.227809	13397.655618	3716.325363	-503117.635934
92	16134.655794	13408.247593	3724.664223	-502619.011410
93	16165.913886	13419.894037	3733.833246	-502070.747023
94	16200.824277	13432.901291	3744.073608	-501458.421597
95	16240.639763	13447.736132	3755.752795	-500760.061228
96	16287.417834	13465.165161	3769.474337	-499939.577677
97	16344.925526	13486.591937	3786.343228	-498930.897450
98	16421.371983	13515.075102	3808.767480	-497590.032824
99	16541.861061	13559.968096	3844.110877	-495476.664215
100	18164.650530	14164.602795	4320.128229	-467013.069229

;

SM1 Mean for steam flow in deethanizer reboiler QT2601
/190.0552373/

SV1 STDEV for steam flow in deethanizer reboiler QT2601
/31.36042668/

SM2 Mean for steam flow in depropanizer reboiler QT2621
/32.26080945/

SV2 STDEV for steam flow in depropanizer reboiler QT2621
/5.787991076/

SM3 Mean for steam flow in debutanizer reboiler QT2641
/20.78197572/

SV3 STDEV for steam flow in debutanizer reboiler QT2641
/4.28887593/

HR1 mass enthalpy of R1 in Kwh per ton /-1218.251/

HR2 mass enthalpy of R2 in Kwh per ton /-1302.131/

HR3 mass enthalpy of R3 in Kwh per ton /-1092.53/

HR4 mass enthalpy of R4 in Kwh per ton /-731.475/

HR mass enthalpy of R in Kwh per ton /-1181.336/

HP1 mass enthalpy of SalesGas in Kwh per ton /-1344.775/

HP2 mass enthalpy of Ethane in Kwh per ton /-827.0496/
 HP3 mass enthalpy of Propane in Kwh per ton /-761.2430/
 HP4 mass enthalpy of Butane in Kwh per ton /-727.3788/
 HP5 mass enthalpy of Condensate in Kwh per ton /-630.7075/
 HP6 mass enthalpy of Carbon dioxide in Kwh per ton /-2499.214/
 HFA2601 mass enthalpy for A2601 feed flow rate/-784.9980396/
 HDA2601 mass enthalpy for A2601 distillate product flow rate
 /-918.395239/
 HBA2601 mass enthalpy for A2601 bottom rate /-670.80931994/
 HFA2621 mass enthalpy for A2621 feed flow rate/-544.2826258/
 HDA2621 mass enthalpy for A2621 distillate product flow rate
 /-743.863449/
 HBA2621 mass enthalpy for A2621 bottom rate /-594.3653994/
 HFA2641 mass enthalpy for A2641 feed flow rate/-594.7222222/
 HDA2641 mass enthalpy for A2641 distillate product flow rate
 /-711.4224147/
 HBA2641 mass enthalpy for A2641 bottom rate /-561.6348855/

 LamdaDe Mass heat of vaporization Demethanizer column
 distillate /76.3056/

 LamdaDp Mass heat of vaporization Depropanizer column
 distillate /84.3333/

 LamdaDb Mass heat of vaporization Debutanizer column
 distillate /91.2222/

 RVDeC1 Relative volatility of C1 for deethanizer column
 / 5.518842089 /

 RVDeC2 Relative volatility of C2 for deethanizer column
 /2.074708064 /

 RVDeC3 Relative volatility of C3 for deethanizer column
 / 1 /

 RVDeiC4 Relative volatility of iC4 for deethanizer column
 /0.816807757/

RVDeC4 Relative volatility of C4 for deethanizer column
 /0.727794167 /

RVDeiC5 Relative volatility of iC5 for deethanizer column
 /0.287007335 /

RVDeC5 Relative volatility of C5 for deethanizer column
 /0.246130849 /

RVDeC6 Relative volatility of C6 for deethanizer column
 /0.127520172 /

RVDeC7 Relative volatility of C7 for deethanizer column
 /0.06774568 /

RVDeC8 Relative volatility of C8 for deethanizer column
 /0.036294169 /

RVDeC9 Relative volatility of C9 for deethanizer column
 /0.019947132 /

RVDeC10 Relative volatility of C10 for deethanizer column
 /0.011131624/

RVDeN2 Relative volatility of N2 for deethanizer column
 /10.40828629/

RVDeCO2 Relative volatility of CO2 for deethanizer column
 /3.602957374/

RVDpC1 Relative volatility of C1 for depropanizer column
 /4.222088549/

RVDpC2 Relative volatility of C2 for depropanizer column
 /3.864191194 /

RVDpC3 Relative volatility of C3 for depropanizer column
 /1.767247051/

RVDpiC4 Relative volatility of iC4 for depropanizer column
 /1 /

RVDpC4 Relative volatility of C4 for depropanizer column
 /0.817925107 /

RVDpiC5 Relative volatility of iC5 for depropanizer column
 /0.460269772 /

RVDpC5 Relative volatility of C5 for depropanizer column
 /0.394012044 /

RVDpC6 Relative volatility of C6 for depropanizer column
 /0.194536244 /

RVDpC7 Relative volatility of C7 for depropanizer column
 /0.098842222 /

RVDpC8 Relative volatility of C8 for depropanizer column
 /0.050736664 /

RVDpC9 Relative volatility of C9 for depropanizer column
 /0.026701511 /

RVDpC10 Relative volatility of C10 for depropanizer column
 /0.014262384 /

RVDpN2 Relative volatility of N2 for depropanizer column
 /16.62917462/

RVDpCO2 Relative volatility of CO2 for depropanizer column
 /7.053240171/

RVDbC1 Relative volatility of C1 for debutanizer column
 /1.159844002 /

RVDbC2 Relative volatility of C2 for debutanizer column
 /4.077211184 /

RVDbC3 Relative volatility of C3 for debutanizer column
 /4.803255103 /

RVDbiC4 Relative volatility of iC4 for debutanizer column
 /2.465992330 /

RVDbC4 Relative volatility of C4 for debutanizer column
 /1.954124933 /

RVDbiC5 Relative volatility of iC5 for debutanizer column
 / 1 /

RVDbC5 Relative volatility of C5 for debutanizer column
 / 0.834436165 /

RVDbC6 Relative volatility of C6 for debutanizer column
 /0.365948855 /

RVDbC7 Relative volatility of C7 for debutanizer column
 /0.165792493 /

RVDbC8 Relative volatility of C8 for debutanizer column
 /0.07591983 /

RVDbC9 Relative volatility of C9 for debutanizer column
 /0.035778296 /

RVDbC10 Relative volatility of C10 for debutanizer column
 /0.027712408 /

RVDbN2 Relative volatility of N2 for debutanizer column
 /1.159844002 /

RVDbCO2 Relative volatility of CO2 for debutanizer column
/6.414496783 /

Theta1 Parameter to be adjusted using trial and error
/ 1.4067 /

Theta2 Parameter to be adjusted using trial and error
/ 1.1867/

Theta3 Parameter to be adjusted using trial and error
/ 1.17677/

FBtDe Deethanizer column bottom flow in ton per hour
/46.80516005/

FBtDp Depropanizer column bottom flow in ton per hour
/45.153268631/

FBtDb Debutanizer column bottom flow in ton per hour
/27.299321513/

BDe Deethanizer column bottom flow in ton per hour /46.8052 /

BDp Depropanizer column bottom flow in ton per hour /45.1533/

BDb Debutanizer column bottom flow in ton per hour /27.29932 /

qDe Feed quality for demethanizer column / 1 /

qDp Feed quality for demethanizer column / 1 /

qDb Feed quality for demethanizer column / 1 /

T2451 Steam temperature for condensate stabilizer column
/168.000601927959/

T2404 Steam temperature for Demethanizer column
/29.9999917296047/

T2601 Steam temperature for Deethanizer column
/96.3821373746501/

T2621 Steam temperature for Depropanizer column
/129.366255222833/

T2641 Steam temperature for Debutanizer column
/130.957037396502/

T2622in Cooling water temperature in for depropanizer
column/30/

T2622out Cooling water temperature out for depropanizer
column/50/

T2642in Cooling water temperature in for debutanizer
column/30/

T2642out Cooling water temperature out for debutanizer
column/50/

SM11 mean for u1 /-339463.115546777 /

SV11 stdv for u1 /22615.97064 /

SM22 mean for u2 /50123.236514 /

SV22 stdv for u2 /2786.52513 /

SM33 mean for u3 /5365.947 /

SV33 stdv for u3 /167.623 /

SM44 mean for u4 /5116.235781 /

SV44 stdv for u4 /159.32416 /

SM55 mean for u5 /112.801265 /

SV55 stdv for u5 /7.69156 /

SM66 mean for u6 /4950.23815 /

SV66 stdv for u6 /251.7132 /

SM111 mean for q1 /15513.61243 /

SV111 stdv for q1 /442.001234 /

SM222 mean for q2 /13176.85321 /

SV222 stdv for q2 /164.685123 /

SM333 mean for q3 /3542.491844 /

SV333 stdv for q3 /129.6534523 /

SM444 mean for q4 /-513512.061375084 /

SV444 stdv for q4 /7752.66561 /;

*UNIT CONVERSION AND NOTES

*Mass of heat of vaporization for each column is calculated as
*follows: Mass heat of vaporization of demethanizer column distillate
*(ethane product)is 274.7 kJ/kg. After converting using 1Kwh =
*3600KJ, the value becomes 274.7 kJ/kg 1000kg/1ton 1kWh/3600kJ =

*76.3056 kWh/ton. Similarly approach is adapted for salesgas, *propane, butane, condensate *and CO2 For saturated feed the feed *quality is one. All the inlet and outlet energy flows are in KW.

*The utilities (energy sources) used in the plant includes LLP steam, *LP steam,HP steam,C3-refrigerant, cooling-water and electricity.

*P & ID representation for each energy inflow and outflow have been *adopted such as Q:T2-401 (from P&ID) = QT2401 (GAMS), W:P2-401 *(P&ID) = WP2401 (GAMS),W:R2-151 (P&ID) = WR2151 (GAMS), W:RT2-151 *(P&ID) = WRT2151, W:R2-*701(1) (P&ID) = WR27011 etc..

*The compression energy (W:R2-151) for R2-151 is obtained from *expander RT2-151(W:RT2-151), While the compression energy (W:R2-401 *is obtained from expander RT2-401 i.e. W:RT2-151.

*All the mass enthalpy values are in kWh/ton ton/h =kW.

*The energy flow for the raw material is a product of the *corresponding mass

*enthalpy value and its flow rate. Example for PhaselGas: QR1= *HR1*R1,for salesgas, QP1 = HP1*P1 and so on...

Variables

maxf, TR1, TR2, TR3, TR4, TC1, T121, T152, TCO2, T301, T302, TH2O2, T310A, THg, T3061, T161, T108, TH2O1, T441B, T452, T453, T454, T311, TpA2, TpA41, TpA4, TpA6, TpA61, T6011, T603, T503, T504, TS, T505, T764, T765, T4411, T442, T622, T623, TH2O11, T642, TH2O22, T643, T651, T652, QA2101, QT2151, WRT2151, QAGRU, QT2301, QL2301, QL2302, QT2101, QL2104, QT2451, QL2451, QL2452, QT2402, QT2404, WR2401, WRT2401, WP2401, WP2402, WP2403, WP2404, WR2151, WR2501, QT2501, QL2501, QT2604SGas, WR27011, WR27012, WR27013, QT2701, QT2603, QT2645, QT2623, QT2354, QT2352, QT2602, QT2604PRU, QT2601, QT2621, QT2622, QT2641, QT2642, QT2623, QT2643, QT2644, QL2661, QL2662, WP2621, WP2641, QR1, QR2, QR3, QR4, QP1, QP2, QP3, QP4, QP5, QP6, RVDdesum, RVDpsum, RVDbsum, u1, u2, u3, u4, u5, u6, q1, q2, q3, q4, Zu1, Zu2, Zu3, Zu4, Zu5, Zu6, Zq1, Zq2, Zq3, Zq4, Qin, Qout;

Positive Variables

PR1, PR2, PR3, PR4, PC1, P121, P152, PCO2, P301, P302, PH2O2, P310A, PHg, P156, P104, P306, P3061, P161, P108, PH2O1, P109, P441B, M441B, P452, P453, P454, P311, P401, P411, P421, P403, P413, P427, PpA2, MpA2, PpA4, MpA4, PpA6, MpA6, P6011, M6011, M6012, P428, P430, P430C, P432, P501, P504, PS, Psalesgas, P732, P734, P735, P736, P743, P7451, P750, P760, P762, P763, P764, P765, P71X, P71S, P71N, P71I, P71D, P71B, P71Y, P71T, P71O, P71J, P71E, P441, P6101, P461C, P6211, P622, P623, PH2O11, P6301, P6411, P642, PH2O22, P643, P651, P652, DeRmin, DpRmin, DbRmin, NDemin, NDpmin, NDbmin, NDstage, NDer, NDes, NDpstage, NDpr, NDps, NDbstage, NDbr, NDbs, YDe, XDe, YDp, XDp, YDb, XDb, DeRflxratio, DpRflxratio, DbRflxratio, FsteamA2451, FsteamA2404, FsteamA2601, FsteamA2621, FsteamA2641, FrefrigerantA2601, FcoolingA2622, FcoolingA2642, R1, R2, R3, R4, R, P1, P2, P3, P4, P5, P6, P;

Negative variables

T312,T401,T411,T602,T431;

Equations

OBJ,EQN1,EQN2,EQN3,EQN4,EQN5,EQN6,EQN7,EQN8,EQN9,EQN10,EQN11,EQN12,EN
13,EQN14,EQN15,EQN16,EQN17,EQN18,EQN19,EQN20,EQN21,EQN22,EQN23,EQN24,
EQN25,EQN26,EQN27,EQN28,EQN29,EQN30,EQN31,EQN32,EQN33,EQN34,EQN35,EQN
36,EQN37,EQN38,EQN39,EQN40,EQN41,EQN42,EQN43,EQN44,EQN45,EQN46,EQN47,
EQN48,EQN49,EQN50,EQN51,EQN52,EQN53,EQN54,EQN55,EQN56,EQN57,EQN58,EQN
59,EQN60,EQN61,EQN62,EQN63,EQN64,EQN65,EQN66,EQN67,EQN68,EQN69,EQN70,
EQN71,EQN72,EQN73,EQN74,EQN75,EQN76,EQN77,EQN78,EQN79,EQN80,EQN81,EQN
82,EQN83,EQN84,EQN85,EQN86,EQN87,EQN88,EQN89,EQN90,EQN91,EQN92,EQN93,
EQN94,EQN95,EQN96,EQN97,EQN98,EQN99,EQN100,EQN101,EQN102,EQN103,EQN10
4,EQN105,EQN106,EQN107,EQN108,EQN109,EQN110,EQN111,EQN112,EQN113,EQN1
14,EQN115,EQN116,EQN117,EQN118,EQN119,EQN120,EQN121,EQN122,EQN123,EQN
124,EQN125,EQN126,EQN127,EQN128,EQN129,EQN130,EQN131,EQN132,EQN133,EQ
N134,EQN135,EQN136,EQN137,EQN138,EQN139,EQN140,EQN141,EQN142,EQN143,EQ
N144,EQN145, EQN146,EQN147,EQN148,EQN149,EQN150,EQN151,EQN152,EQN153,
EQN154,EQN155,EQN156,EQN157,EQN158,EQN159,EQN160,EQN161,EQN162,EQN163
,EQN164,EQN165,EQN166,EQN167,EQN168,EQN169,EQN170,EQN171,EQN172,EQN13
,EQN174,EQN175,CON1,CON2,CON3,CON4,CON5,CON6,CON7,CON8,CON9,CON10,CON
11;

OBJ.. maxf =E= CP1*P1 + CP2*P2 + CP3*P3 + CP4*P4 + CP5*P5 + CP6*P6 -
CR1*R1 - CR2*R2 - CR3*R3 - CR4*R4 - Cstm*u2 - Crefg*u3 -
Ccompress*u4 - Celetric*u5 - Cfuel*u6 - Ccooling*(q1 + q2 +
q3);

*@PLANT INLET

EQN1.. QR1 =E= HR1*R1;

EQN2.. QR2 =E= HR2*R2;

EQN3.. QR3 =E= HR3*R3;

EQN4.. QR4 =E= HR4*R4;

*INITIAL VALUES @PLANT INLET

R1.1 = 254.34;

TR1.fx = 24.54;

PR1.fx = 7261.325;

R2.1 = 40.00;

TR2.fx = 17.00;

PR2.fx = 7261.325;

R3.1 = 1.25;

TR3.fx = 28.64;
PR3.fx = 6511.325;
R4.1 = 31.7;
TR4.fx = 27.44;
PR4.fx = 6661.325;

* PRE-TREATMENT UNIT (PTU)

EQN5.. QA2101 =E= 3.665870*R + 1.846793E-06 ;
EQN6.. QT2151 =E= 1.11674*R - 9.23396E-07;
EQN7.. QT2151 =E= -224.018062*T121 + 6365.456304;
EQN8.. QT2151 =E= 1.1203339*P121 - 7364.5645971;
EQN9.. WRT2151 =E= WR2151;
EQN10.. QAGRU =E= 4.12105*R - 1.84679E-06;
EQN11.. QAGRU =E= -221.615082*T152 + 7448.893563;
EQN12.. QAGRU =E= 1.113799*P152 - 6130.764800;
EQN13.. QT2301 =E= -1.057621*R + 7467.708257;
EQN14.. QT2301 =E= 205.372037*T301 - 4605.747313;
EQN15.. QT2301 =E= -1.052*P301 + 7364;
EQN16.. QL2301 =E= 12.742000*R - 7.39E-06;
EQN17.. QL2301 =E= -205.874867*T302 + 8968.159282;
EQN18.. QL2301 =E= 1.113451*P302 - 2151.723048;
EQN19.. QL2302 =E= -1.3577E+01*R + 1.4774E-05;
EQN20.. QL2302 =E= -175.715119*T310A - 53.525078;
EQN21.. QL2302 =E= 1.044458*P310A - 6664.211133 ;
EQN22.. QT2101 =E= 0.015329577*R ;

*INITIAL VALUES@PTU

TC1.fx = 26.82 ;
PC1.fx = 69.00;
T121.1 = 27.82;

P121.1 = 6901.00;
 T152.1 = 28.54;
 P152.1 = 6721.00;
 TCO2.fx = 43.00;
 PCO2.fx = 5781.00;
 T301.1 = 30.04;
 P301.1 = 5781.00;
 T302.1 = 23.31;
 P302.1 = 5681.00;
 TH2O2.fx = 25.00 ;
 PH2O2.fx = 2126.00 ;
 T310A.1 = 26.00;
 P310A.1 = 2127.00;
 THg.fx = 25.00 ;
 PHg.fx = 5630.00;
 WRT2151.fx = 0;

*NOTES

*H2O-2 temperature and pressure do not affect QL2301.

*TC1 (Chlorine removed temperature does not affect QA2101).

*Hg Temperature and pressure do not affect QL2302.

*PC1 (Chlorine removed temperature does not affect QA2101).

*H2O-1 temperature and pressure do not affect QL2104.

*TCO2 and PCO2 have no effect on QAGRU

*The heat flows are related using linear equation from HYSYS

*simulation with their respective operating parameters(T,P,F), Re^2

* (R-square obtained from regression for each equation is shown below

*(in EQN9 WRT2151 is set to zero)

*EQUATION	5	6	7	8	9	10	11	12	13	14	15	16	17	18	19	20	21	22
*Re^2	1	1	1	1	-	1	1	1	1	1	1	1	1	1	1	1	1	1

* CONDENSATE TREATMENT UNIT (CTU)

EQN23.. QT2101 =E= 0.015329577*R ;
EQN24.. QT2101 =E= -0.00165*P156 + 13.59192;
EQN25.. QT2101 =E= -0.00165*P104 + 13.59192;
EQN26.. QT2101 =E= -0.00164*P306 + 13.54701;
EQN27.. QT2101 =E= -0.0016*P3061 + 13.603;
EQN28.. QT2101 =E= 0.529*T161 - 10.22;
EQN29.. QT2101 =E= -0.00298*P161 + 21.08051;
EQN30.. QL2104 =E= 5.70323E-01*R - 2.30849E-07;
EQN31.. QL2104 =E= 19.68*T108 - 371.4;
EQN32.. QL2104 =E= -0.028*P108 + 317.3;
EQN33.. QT2451 =E= 8.44861772719*R;
EQN34.. QL2451 =E= -0.1276403130*R + 7.187905;
EQN35.. QL2451 =E= -3.08834*T452 + 101.26369;
EQN36.. QL2451 =E= 0.019830*P452 - 90.379799;
EQN37.. QL2452 =E= 1.03551E-02*R - 3.60702E-09;
EQN38.. QL2452 =E= -3.056977*T453 + 102.441931;
EQN39.. QL2452 =E= 0.021789*P453 - 48.783314;
EQN40.. QL2452 =E= 2.910*T454 - 91.04;
EQN41.. QL2452 =E= -0.021604*P454 + 51.807468;

* INTIAL VALUES @CTU

P156.1 = 5322.00;
P104.1 = 5322.00;
P306.1 = 5322.00;
T3061.1 = 22.85;
P3061.1 = 5322.00;
T161.1 = 27.37;
P161.1 = 5450.0;
T108.1 = 27.1;

P108.1 = 5451.0;
 TH201.fx = 27.10 ;
 PH201.fx = 5450.00 ;
 P109.fx = 2501.00;
 T441B.fx = 30.96 ;
 P441B.fx = 3009.00 ;
 M441B.fx = 0.00 ;
 T452.1 = 46.36;
 P452.1 = 2450.00;
 T453.1 = 32.400;
 P453.1 = 2400.00;
 T454.1 = 32.40;
 P454.1 = 2243.56;

*NOTES

*The condensate stripper section. The heat flows are related linearly.

*H2O temperature and pressure do not affect QL2451.

*P109 does not affect QL2104 and QT2451

*Regression result for each equations given below

*EQUATION 23 24 25 26 27 28 29 30 31 32 33 34 35 36 37 38 39

*Re^2 1 1 1 1 1 1 1 1 1 1 1 1 1 1 1 1 1

*Equation 40 and 41 Re^2 is 1.

*LOW TEMPERATURE SEPARATION UNIT (LTSU)

EQN42.. QT2402 =E= 6.595168*R + 3.693585E-06;

EQN43.. QT2402 =E= -1.853*P311 + 12694;

EQN44.. QT2402 =E= 338.998100*T312 + 12330.011411;

EQN45.. QT2402 =E= -358.70109*T401 - 11078.61000;

EQN46.. QT2402 =E= 2.026609*P401 - 9571.946035;
 EQN47.. QT2404 =E= 14.759517*R - 623.223252;
 EQN48.. QT2404 =E= -99.59*T411 - 1370;
 EQN49.. QT2404 =E= 0.811*P411 - 288.7;
 EQN50.. QT2404 =E= 48.54*MpA2 - 3236;
 EQN51.. QT2404 =E= 47.20*MpA4 + 1293;
 EQN52.. QT2404 =E= 33.64*MpA6 + 1723;
 EQN53.. WRT2401 =E= 6.363551*R + 0.196292;
 EQN54.. WP2404 =E= 0;
 EQN55.. WP2403 =E= 0;
 EQN56.. WP2402 =E= 0;
 EQN57.. WP2401 =E= 0.127383*R - 2.661610;
 EQN58.. WR2401 =E= 6.363551*R + 0.196292;

* INITIAL VALUES @LTSU

T311.fx = 22.00;
 P311.1 = 5682.00;
 T312.1 = -30.00;
 T401.1 = -36.00;
 P401.1 = 5621.00;
 T411.1 = -56.00;
 P411.1 = 5541.00;
 P421.fx = 2331.00;
 P403.fx = 2313.00;
 P413.fx = 2305.00;
 TpA2.fx = -17.69;
 PpA2.fx = 2321.00;
 MpA2.1 = 153.30;
 TpA41.fx = -36.17;
 TpA4.fx = -36.17;

PpA4.fx = 2314.00;
 MpA4.1 = 61.69;
 TpA61.fx = -41.13;
 TpA6.fx = -41.13;
 PpA6.fx = 2310.00;
 MpA6.1 = 73.78;
 P427.fx = 2150.00;
 T6011.fx = 4.61;
 P6011.fx = 2771.00;
 M6011.fx = 825.30;
 M6012.fx = 21.59;
 T602.fx = -3.00;
 T603.fx = 20.00;
 WP2404.fx = 0;
 WP2403.fx = 0;
 WP2402.fx = 0;

*NOTES

*T311 does not affect both QT2402 and QT2404

*P421,P403, p413, PpA2, PpA4 do not affect QT2404

*P427 does not affect WR2401

*Stream 603 is C2product (ethane) and its temperature T603 is fixed
 *at 20C Regression result for each equations given below

*EQUATION 42 43 44 45 46 47 48 49 50 51 52 53 54 55

*Re^2 1 0.99 0.97 0.98 0.98 1 0.98 0.94 0.99 0.92 0.94 - - -

* EQN 56, 57 and 58 - 1 1, respectively.

*@ SALES GAS COMPRESSION UNIT (SGCU)

EQN59.. WR2501 =E= 11.726989*R + 120.185384;

EQN60.. WR2501 =E= -5.839*P432 + 18149;

EQN61.. QT2604SGas =E= -2.228165*R + 78.587516;
 EQN62.. QT2604SGas =E= -4.3702425*P501 + 14045.9674751;
 EQN63.. QL2501 =E= 0.339515*R + 5.426681;
 EQN64.. QL2501 =E= -149.75228*T503 + 9384.82757;
 EQN65.. QT2501 =E= 10.410506*R + 136.117541;
 EQN66.. QT2501 =E= 149.075710*T504 - 5704.669091;
 EQN67.. QT2501 =E= 0.086879*P504 + 3262.531728;
 EQN68.. QT2501 =E= -147.34462*T505 + 9156.71594;

* INTIAL VALUES @SGCU

P428.fx = 2578.00;
 P430.fx = 2440.00;
 P430C.fx = 2440.00;
 T431.fx = -85.00;
 P432.1 = 2240.00;
 P501.1 = 3363.00;
 T503.1 = 61.89;
 T504.1 = 62.03;
 P504.1 = 3193.00;
 TS.fx = 62.03 ;
 PS.fx = 3193.00;
 T505.1 = 38.12;
 Psalesgas.fx = 3600.00;
 WR2151.1 = 0;

* NOTES

*P428, P430, P430C, P431 do not affect WR2501

*Salesgas product pressure Psalesgas is fixed at 3600 KPa

*Regression result for each equations given below

*EQUATION 59 60 61 62 63 64 65 66 67 67 68
 *Re^2 1 1 1 1 1 1 1 1 1 1 1

*C3-REFIGERATION UNIT (CRU)

EQN69.. WR27011 =E= 1.190127*R - 4.616981E-07;
EQN70.. WR27011 =E= 0.248*P732 + 321.7;
EQN71.. WR27011 =E= 0.017*P743 + 385.9;
EQN72.. WR27011 =E= -3.678*P7451 + 772.3;
EQN73.. WR27012 =E= 1.926007*R + 667.207929;
EQN74.. WR27012 =E= 0.197*P750 + 1372;
EQN75.. WR27013 =E= 1.573372*R + 1277.555526;
EQN76.. WR27013 =E= 0.327*P760 + 1760;
EQN77.. QT2701 =E= 11.830983*R + 9409.491316;
EQN78.. QT2701 =E= 2.241*P762 + 12028;
EQN79.. QT2603 =E= 0.248854*R - 1.186106;
EQN80.. QT2603 =E= -0.035839*P764 + 122.030292;

*INITIAL VALUES

P732.1 = 272.50;
P734.fx = 408.00;
P735.fx = 398.00;
P736.fx = 368.00;
P743.1 = 216.40;
P7451.1 = 104.00;
P750.1 = 313.00;
P760.1 = 675.00;
P762.1 = 1184.00;
P763.fx = 1174.00;
T764.fx = 32.45;
P764.1 = 1174.00;
T765.fx = 31.76;
P765.fx = 1174.00;

P71X.fx = 750.00;
 P71S.fx = 750.00;
 P71N.fx = 750.00;
 P71I.fx = 750.00;
 P71D.fx = 750.00;
 P71B.fx = 559.50;
 P71Y.fx = 740.00;
 P71T.fx = 740.00;
 P71O.fx = 740.00;
 P71J.fx = 740.00;
 P71E.fx = 740.00;
 QT2352.fx = 194.00;
 QT2354.fx = 337.00;

*NOTES

- *The relation between P732 and QT2402 is constant
- *The relation between P734 and QT2602, WR27011 is constant
- *The relation between P735 and QT602,WR27011,QT2402 is constant
- *The relation between P736 and QT2402,WR27011 is constant
- *The relation between P763 and QT2701 is constant
- *The relation between T764 and QT2603 is constant
- *The relation between T765 and QT2645,QT623,QT2354,QT2352,QT2301 is constant
- *The relation between P765 and QT2645,QT623,QT2354,QT2352,QT2301 is constant
- *The pressures P71X,P71S,P71N,P71I,P71D,P71B,P71Y,P71T,P71O,P71J,P71E have all a constant relationship with their respective heat flows
- *(QT2645,QT623,QT2354,QT2352,QT2301)QT2352 and QT2354 are adjustable
- *heat flows Regression result for each equations given below

*EQUATION 69 70 71 72 73 74 75 76 77 78 79 80

*Re^2 1 1 1 1 1 1 1 1 1 1 1 1

*PRODUCT RECOVERY UNIT (PRU)

EQN81.. QT2603 =E= -0.087*P441 + 342.5;
 EQN82.. QT2604PRU =E= 0.00491618*R - 0.10583307;
 EQN83.. QT2604PRU =E= -61.89*T4411 + 1998;
 EQN84.. QT2604PRU =E= 61.98*T442 - 2060;
 EQN85.. QT2622 =E= 0.141*P6101 + 10848;
 EQN86.. QT2622 =E= 1.047*P461C + 8418;
 EQN87.. QT2623 =E= 0.020*P6211 + 419.9;
 EQN88.. QL2661 =E= -5.781861E-04*R + 1.877433E-01;
 EQN89.. QL2661 =E= -19.385704*T622 + 390.862903;
 EQN90.. QL2661 =E= 0.002010*P622 - 3.537493;
 EQN91.. QT2641 =E= 0.060*P6301 + 2995;
 EQN92.. QT2645 =E= 4.945232*R - 1338.357190;
 EQN93.. QT2645 =E= 0.012314*P6411 + 268.952399;
 EQN94.. QL2662 =E= -0.000324*R + 0.055658;
 EQN95.. QL2662 =E= -11.773439*T642 + 242.603991;
 EQN96.. QL2662 =E= -0.0025030*P642 + 2.0825160;
 EQN97.. QT2643 =E= -16.72*T651 + 2386;
 EQN98.. QT2644 =E= -0.006841*R + 84.398923;
 EQN99.. QT2644 =E= 16.680985*T651 - 500.679426;
 EQN100.. QT2644 =E= -0.007448*P651 + 86.250342;
 EQN101.. WP2621 =E= 0.013153*R + 3.229547;
 EQN102.. WP2641 =E= 0.070646*R - 18.840286;

*Regression result for each equations given below

*EQUATION	81	82	83	84	85	86	87	88	89	90	91	92	93	94	95	96	97
*Re^2	1	1	1	1	1	1	1	1	1	1	1	1	1	1	1	1	1
*EQUATION	98	99	100	101	102												
*Re^2	1	1	1	1	1												

*The column duties in PRU are calculated using Underwood equation,
 *other equations such as Fenske, Gilliland and Kirkbride have also been
 *evaluated.

* DEETHANIZER COLUMN

EQN103.. RVDesum =E=

$$\begin{aligned}
 &RVDeC1*s1('C1', 'De-Feed') / (RVDeC1 - Theta1) + \\
 &RVDeC2*s1('C2', 'De-Feed') / (RVDeC2 - Theta1) + \\
 &RVDeC3*s1('C3', 'De-Feed') / (RVDeC3 - Theta1) + \\
 &RVDeiC4*s1('iC4', 'De-Feed') / (RVDeiC4 - Theta1) + \\
 &RVDeC4*s1('C4', 'De-Feed') / (RVDeC4 - Theta1) + \\
 &RVDeiC5*s1('iC5', 'De-Feed') / (RVDeiC5 - Theta1) + \\
 &RVDeC5*s1('C5', 'De-Feed') / (RVDeC5 - Theta1) + \\
 &RVDeC6*s1('C6', 'De-Feed') / (RVDeC6 - Theta1) + \\
 &RVDeC7*s1('C7', 'De-Feed') / (RVDeC7 - Theta1) + \\
 &RVDeC8*s1('C8', 'De-Feed') / (RVDeC8 - Theta1) + \\
 &RVDeC9*s1('C9', 'De-Feed') / (RVDeC9 - Theta1) + \\
 &RVDeC10*s1('C10', 'De-Feed') / (RVDeC10 - Theta1) + \\
 &RVDeN2*s1('N2', 'De-Feed') / (RVDeN2 - Theta1) + \\
 &RVDeCO2*s1('CO2', 'De-Feed') / (RVDeCO2 - Theta1);
 \end{aligned}$$

EQN104.. DeRmin + 1 =E=

$$\begin{aligned}
 &RVDeC1*y('C1', 'P2') / (RVDeC1 - Theta1) + \\
 &RVDeC2*y('C2', 'P2') / (RVDeC2 - Theta1) + \\
 &RVDeC3*y('C3', 'P2') / (RVDeC3 - Theta1) + \\
 &RVDeiC4*y('iC4', 'P2') / (RVDeiC4 - Theta1) + \\
 &RVDeC4*y('C4', 'P2') / (RVDeC4 - Theta1) + \\
 &RVDeiC5*y('iC5', 'P2') / (RVDeiC5 - Theta1) + \\
 &RVDeC5*y('C5', 'P2') / (RVDeC5 - Theta1) + \\
 &RVDeC6*y('C6', 'P2') / (RVDeC6 - Theta1) + \\
 &RVDeC7*y('C7', 'P2') / (RVDeC7 - Theta1) +
 \end{aligned}$$

$$\begin{aligned}
&RVDeC8*y('C8', 'P2') / (RVDeC8 - Theta) + \\
&RVDeC9*y('C9', 'P2') / (RVDeC9 - Theta) + \\
&RVDeC10*y('C10', 'P2') / (RVDeC10 - Theta) + \\
&RVDeN2*y('N2', 'P2') / (RVDeN2 - Theta) + \\
&RVDeCO2*y('CO2', 'P2') / (RVDeCO2 - Theta);
\end{aligned}$$

EQN105.. DeRflxratio =E= 1.5*DeRmin;

EQN106.. QT2602 =E= LamdaDe*(3.120 + 1)*P2;

EQN107.. QT2601 =E= QT2602 +

$$\begin{aligned}
&((s1('C1', 'De-Feed') - s2('C1', 'De-Bottom'))*(HDA2601 - HFA2601) + \\
&(s1('C2', 'De-Feed') - s2('C2', 'De-Bottom'))*(HDA2601 - HFA2601) + \\
&(s1('C3', 'De-Feed') - s2('C3', 'De-Bottom'))*(HDA2601 - HFA2601) + \\
&(s1('iC4', 'De-Feed') - s2('iC4', 'De-Bottom'))*(HDA2601 - HFA2601) + \\
&(s1('C4', 'De-Feed') - s2('C4', 'De-Bottom'))*(HDA2601 - HFA2601) + \\
&(s1('iC5', 'De-Feed') - s2('iC5', 'De-Bottom'))*(HDA2601 - HFA2601) + \\
&(s1('C6', 'De-Feed') - s2('C6', 'De-Bottom'))*(HDA2601 - HFA2601) + \\
&(s1('C7', 'De-Feed') - s2('C7', 'De-Bottom'))*(HDA2601 - HFA2601) + \\
&(s1('C8', 'De-Feed') - s2('C8', 'De-Bottom'))*(HDA2601 - HFA2601) + \\
&(s1('C9', 'De-Feed') - s2('C9', 'De-Bottom'))*(HDA2601 - HFA2601) + \\
&(s1('C10', 'De-Feed') - s2('C10', 'De-Bottom'))*(HDA2601 - HFA2601) + \\
&(s1('N2', 'De-Feed') - s2('N2', 'De-Bottom'))*(HDA2601 - HFA2601) + \\
&(s1('CO2', 'De-Feed') - s2('CO2', 'De-Bottom'))*(HDA2601 - HFA2601) +
\end{aligned}$$

```

(y('C1', 'P2') - s1('C1', 'De-Feed'))*(HBA2601 - HFA2601) +
(y('C2', 'P2') - s1('C2', 'De-Feed'))*(HBA2601 - HFA2601) +
(y('C3', 'P2') - s1('C3', 'De-Feed'))*(HBA2601 - HFA2601) +
(y('iC4', 'P2') - s1('iC4', 'De-Feed'))*(HBA2601 - HFA2601) +
(y('C4', 'P2') - s1('C4', 'De-Feed'))*(HBA2601 - HFA2601) +
(y('iC5', 'P2') - s1('iC5', 'De-Feed'))*(HBA2601 - HFA2601) +
(y('C6', 'P2') - s1('C6', 'De-Feed'))*(HBA2601 - HFA2601) +
(y('C7', 'P2') - s1('C7', 'De-Feed'))*(HBA2601 - HFA2601) +
(y('C8', 'P2') - s1('C8', 'De-Feed'))*(HBA2601 - HFA2601) +
(y('C9', 'P2') - s1('C9', 'De-Feed'))*(HBA2601 - HFA2601) +
(y('C10', 'P2') - s1('C10', 'De-Feed'))*(HBA2601 - HFA2601) +
(y('N2', 'P2') - s1('N2', 'De-Feed'))*(HBA2601 - HFA2601) +
(y('CO2', 'P2') - s1('CO2', 'De-Feed'))*(HBA2601 - HFA2601))*(P2 +
FBtDe)/(
y('C1', 'P2') - s2('C1', 'De-Bottom') +
y('C2', 'P2') - s2('C2', 'De-Bottom') +
y('C3', 'P2') - s2('C3', 'De-Bottom') +
y('iC4', 'P2') - s2('iC4', 'De-Bottom') +
y('C4', 'P2') - s2('C4', 'De-Bottom') +
y('iC5', 'P2') - s2('iC5', 'De-Bottom') +
y('C6', 'P2') - s2('C6', 'De-Bottom') +
y('C7', 'P2') - s2('C7', 'De-Bottom') +
y('C8', 'P2') - s2('C8', 'De-Bottom') +
y('C9', 'P2') - s2('C9', 'De-Bottom') +
y('C10', 'P2') - s2('C10', 'De-Bottom') +
y('N2', 'P2') - s2('N2', 'De-Bottom') +
y('CO2', 'P2') - s2('CO2', 'De-Bottom')));

```

EQN108.. NDemin =E= 20.361;

EQN109.. XDe =E= (3.120 - DeRmin)/(3.120 + 1);

EQN110.. NDer + NDes =E= 33.564;

EQN111.. NDer =E= 8.765644*NDes;

*DEPROPANIZER COLUMN

EQN112.. RVDpsum =E=

$$\begin{aligned} & \text{RVDpC1} * \text{s1} (' \text{C1} ', ' \text{Dp-Feed} ') / (\text{RVDpC1} - \text{Theta2}) + \\ & \text{RVDpC2} * \text{s1} (' \text{C2} ', ' \text{Dp-Feed} ') / (\text{RVDpC2} - \text{Theta2}) + \\ & \text{RVDpC3} * \text{s1} (' \text{C3} ', ' \text{Dp-Feed} ') / (\text{RVDpC3} - \text{Theta2}) + \\ & \text{RVDpiC4} * \text{s1} (' \text{iC4} ', ' \text{Dp-Feed} ') / (\text{RVDpiC4} - \text{Theta2}) + \\ & \text{RVDpC4} * \text{s1} (' \text{C4} ', ' \text{Dp-Feed} ') / (\text{RVDpC4} - \text{Theta2}) + \\ & \text{RVDpiC5} * \text{s1} (' \text{iC5} ', ' \text{Dp-Feed} ') / (\text{RVDpiC5} - \text{Theta2}) + \\ & \text{RVDpC5} * \text{s1} (' \text{C5} ', ' \text{Dp-Feed} ') / (\text{RVDpC5} - \text{Theta2}) + \\ & \text{RVDpC6} * \text{s1} (' \text{C6} ', ' \text{Dp-Feed} ') / (\text{RVDpC6} - \text{Theta2}) + \\ & \text{RVDpC7} * \text{s1} (' \text{C7} ', ' \text{Dp-Feed} ') / (\text{RVDpC7} - \text{Theta2}) + \\ & \text{RVDpC8} * \text{s1} (' \text{C8} ', ' \text{Dp-Feed} ') / (\text{RVDpC8} - \text{Theta2}) + \\ & \text{RVDpC9} * \text{s1} (' \text{C9} ', ' \text{Dp-Feed} ') / (\text{RVDpC9} - \text{Theta2}) + \\ & \text{RVDpC10} * \text{s1} (' \text{C10} ', ' \text{Dp-Feed} ') / (\text{RVDpC10} - \text{Theta2}) + \\ & \text{RVDpN2} * \text{s1} (' \text{N2} ', ' \text{Dp-Feed} ') / (\text{RVDpN2} - \text{Theta2}) + \\ & \text{RVDpCO2} * \text{s1} (' \text{CO2} ', ' \text{Dp-Feed} ') / (\text{RVDpCO2} - \text{Theta2}); \end{aligned}$$

EQN113.. DpRmin + 1 =E=

$$\begin{aligned} & \text{RVDpC1} * \text{y} (' \text{C1} ', ' \text{P3} ') / (\text{RVDpC1} - \text{Theta2}) + \\ & \text{RVDpC2} * \text{y} (' \text{C2} ', ' \text{P3} ') / (\text{RVDpC2} - \text{Theta2}) + \\ & \text{RVDpC3} * \text{y} (' \text{C3} ', ' \text{P3} ') / (\text{RVDpC3} - \text{Theta2}) + \\ & \text{RVDpiC4} * \text{y} (' \text{iC4} ', ' \text{P3} ') / (\text{RVDpiC4} - \text{Theta2}) + \\ & \text{RVDpC4} * \text{y} (' \text{C4} ', ' \text{P3} ') / (\text{RVDpC4} - \text{Theta2}) + \\ & \text{RVDpiC5} * \text{y} (' \text{iC5} ', ' \text{P3} ') / (\text{RVDpiC5} - \text{Theta2}) + \\ & \text{RVDpC5} * \text{y} (' \text{C5} ', ' \text{P3} ') / (\text{RVDpC5} - \text{Theta2}) + \\ & \text{RVDpC6} * \text{y} (' \text{C6} ', ' \text{P3} ') / (\text{RVDpC6} - \text{Theta2}) + \\ & \text{RVDpC7} * \text{y} (' \text{C7} ', ' \text{P3} ') / (\text{RVDpC7} - \text{Theta2}) + \end{aligned}$$

$$\begin{aligned} & \text{RVDpC8} * y('C8', 'P3') / (\text{RVDpC8} - \text{Theta2}) + \\ & \text{RVDpC9} * y('C9', 'P3') / (\text{RVDpC9} - \text{Theta2}) + \\ & \text{RVDpC10} * y('C10', 'P3') / (\text{RVDpC10} - \text{Theta2}) + \\ & \text{RVDpN2} * y('N2', 'P3') / (\text{RVDpN2} - \text{Theta2}) + \\ & \text{RVDpCO2} * y('CO2', 'P3') / (\text{RVDpCO2} - \text{Theta2}); \end{aligned}$$

EQN114.. DpRflxratio =E= 1.5*DpRmin;

EQN115.. QT2622 =E= LamdaDp*(2.972 + 1)*P3;

EQN116.. QT2621 =E= QT2622 +

$$\begin{aligned} & ((s1('C1', 'Dp-Feed') - s2('C1', 'Dp-Bottom')) * (\text{HDA2621} - \text{HFA2621}) + \\ & (s1('C2', 'Dp-Feed') - s2('C2', 'Dp-Bottom')) * (\text{HDA2621} - \text{HFA2621}) + \\ & (s1('C3', 'Dp-Feed') - s2('C3', 'Dp-Bottom')) * (\text{HDA2621} - \text{HFA2621}) + \\ & (s1('iC4', 'Dp-Feed') - s2('iC4', 'Dp-Bottom')) * (\text{HDA2621} - \text{HFA2621}) + \\ & (s1('C4', 'Dp-Feed') - s2('C4', 'Dp-Bottom')) * (\text{HDA2621} - \text{HFA2621}) + \\ & (s1('iC5', 'Dp-Feed') - s2('iC5', 'Dp-Bottom')) * (\text{HDA2621} - \text{HFA2621}) + \\ & (s1('C6', 'Dp-Feed') - s2('C6', 'Dp-Bottom')) * (\text{HDA2621} - \text{HFA2621}) + \\ & (s1('C7', 'Dp-Feed') - s2('C7', 'Dp-Bottom')) * (\text{HDA2621} - \text{HFA2621}) + \\ & (s1('C8', 'Dp-Feed') - s2('C8', 'Dp-Bottom')) * (\text{HDA2621} - \text{HFA2621}) + \\ & (s1('C9', 'Dp-Feed') - s2('C9', 'Dp-Bottom')) * (\text{HDA2621} - \text{HFA2621}) + \\ & (s1('C10', 'Dp-Feed') - s2('C10', 'Dp-Bottom')) * (\text{HDA2621} - \text{HFA2621}) + \\ & (s1('N2', 'Dp-Feed') - s2('N2', 'Dp-Bottom')) * (\text{HDA2621} - \text{HFA2621}) + \\ & (s1('CO2', 'Dp-Feed') - s2('CO2', 'Dp-Bottom')) * (\text{HDA2621} - \text{HFA2621}) + \\ & (y('C1', 'P3') - s1('C1', 'Dp-Feed')) * (\text{HBA2621} - \text{HFA2621}) + \end{aligned}$$

```

(y('C2', 'P3') - s1('C2', 'Dp-Feed'))*(HBA2621 - HFA2621) +
(y('C3', 'P3') - s1('C3', 'Dp-Feed'))*(HBA2621 - HFA2621) +
(y('iC4', 'P3') - s1('iC4', 'Dp-Feed'))*(HBA2621 - HFA2621) +
(y('C4', 'P3') - s1('C4', 'Dp-Feed'))*(HBA2621 - HFA2621) +
(y('iC5', 'P3') - s1('iC5', 'Dp-Feed'))*(HBA2621 - HFA2621) +
(y('C6', 'P3') - s1('C6', 'Dp-Feed'))*(HBA2621 - HFA2621) +
(y('C7', 'P3') - s1('C7', 'Dp-Feed'))*(HBA2621 - HFA2621) +
(y('C8', 'P3') - s1('C8', 'Dp-Feed'))*(HBA2621 - HFA2621) +
(y('C9', 'P3') - s1('C9', 'Dp-Feed'))*(HBA2621 - HFA2621) +
(y('C10', 'P3') - s1('C10', 'Dp-Feed'))*(HBA2621 - HFA2621) +
(y('N2', 'P3') - s1('N2', 'Dp-Feed'))*(HBA2621 - HFA2621) +
(y('CO2', 'P3') - s1('CO2', 'Dp-Feed'))*(HBA2621 - HFA2621))*(P3 +
FBtDp)/(
y('C1', 'P3') + s2('C1', 'Dp-Bottom') +
y('C2', 'P3') + s2('C2', 'Dp-Bottom') +
y('C3', 'P3') + s2('C3', 'Dp-Bottom') +
y('iC4', 'P3') + s2('iC4', 'Dp-Bottom') +
y('C4', 'P3') + s2('C4', 'Dp-Bottom') +
y('iC5', 'P3') + s2('iC5', 'Dp-Bottom') +
y('C6', 'P3') + s2('C6', 'Dp-Bottom') +
y('C7', 'P3') + s2('C7', 'Dp-Bottom') +
y('C8', 'P3') + s2('C8', 'Dp-Bottom') +
y('C9', 'P3') + s2('C9', 'Dp-Bottom') +
y('C10', 'P3') + s2('C10', 'Dp-Bottom') +
y('N2', 'P3') + s2('N2', 'Dp-Bottom') +
y('CO2', 'P3') + s2('CO2', 'Dp-Bottom')));

```

EQN117.. NDpmin =E= 16.228;

EQN118.. XDp =E= (2.972 - DpRmin)/(2.972 + 1);

EQN119.. NDpr + NDps =E= 26.94;

EQN120.. NDpr =E= 0.819352*NDps;

*DEBUTANIZER COLUMN

EQN121.. RVDbsum =E=

$$\begin{aligned} & \text{RVDbC1*s1('C1', 'Db-Feed')} / (\text{RVDbC1} - \text{Theta3}) + \\ & \text{RVDbC2*s1('C2', 'Db-Feed')} / (\text{RVDbC2} - \text{Theta3}) + \\ & \text{RVDbC3*s1('C3', 'Db-Feed')} / (\text{RVDbC3} - \text{Theta3}) + \\ & \text{RVDbiC4*s1('iC4', 'Db-Feed')} / (\text{RVDbiC4} - \text{Theta3}) + \\ & \text{RVDbC4*s1('C4', 'Db-Feed')} / (\text{RVDbC4} - \text{Theta3}) + \\ & \text{RVDbiC5*s1('iC5', 'Db-Feed')} / (\text{RVDbiC5} - \text{Theta3}) + \\ & \text{RVDbC5*s1('C5', 'Db-Feed')} / (\text{RVDbC5} - \text{Theta3}) + \\ & \text{RVDbC6*s1('C6', 'Db-Feed')} / (\text{RVDbC6} - \text{Theta3}) + \\ & \text{RVDbC7*s1('C7', 'Db-Feed')} / (\text{RVDbC7} - \text{Theta3}) + \\ & \text{RVDbC8*s1('C8', 'Db-Feed')} / (\text{RVDbC8} - \text{Theta3}) + \\ & \text{RVDbC9*s1('C9', 'Db-Feed')} / (\text{RVDbC9} - \text{Theta3}) + \\ & \text{RVDbC10*s1('C10', 'Db-Feed')} / (\text{RVDbC10} - \text{Theta3}) + \\ & \text{RVDbN2*s1('N2', 'Db-Feed')} / (\text{RVDbN2} - \text{Theta3}) + \\ & \text{RVDbCO2*s1('CO2', 'Db-Feed')} / (\text{RVDbCO2} - \text{Theta3}); \end{aligned}$$

EQN122.. DbRmin + 1 =E=

$$\begin{aligned} & \text{RVDbC1*y('C1', 'P4')} / (\text{RVDbC1} - \text{Theta3}) + \\ & \text{RVDbC2*y('C2', 'P4')} / (\text{RVDbC2} - \text{Theta3}) + \\ & \text{RVDbC3*y('C3', 'P4')} / (\text{RVDbC3} - \text{Theta3}) + \\ & \text{RVDbiC4*y('iC4', 'P4')} / (\text{RVDbiC4} - \text{Theta3}) + \\ & \text{RVDbC4*y('C4', 'P4')} / (\text{RVDbC4} - \text{Theta3}) + \\ & \text{RVDbiC5*y('iC5', 'P4')} / (\text{RVDbiC5} - \text{Theta3}) + \\ & \text{RVDbC5*y('C5', 'P4')} / (\text{RVDbC5} - \text{Theta3}) + \\ & \text{RVDbC6*y('C6', 'P4')} / (\text{RVDbC6} - \text{Theta3}) + \\ & \text{RVDbC7*y('C7', 'P4')} / (\text{RVDbC7} - \text{Theta3}) + \\ & \text{RVDbC8*y('C8', 'P4')} / (\text{RVDbC8} - \text{Theta3}) + \end{aligned}$$

```

RVDbC9*y('C9', 'P4') / (RVDbC9 - Theta3) +
RVDbC10*y('C10', 'P4') / (RVDbC10 - Theta3) +
RVDbN2*y('N2', 'P4') / (RVDbN2 - Theta3) +
RVDbCO2*y('CO2', 'P4') / (RVDbCO2 - Theta3);

EQN123.. DbRflxratio =E= 1.5*DbRmin;

EQN124.. QT2642 =E= LamdaDb*(1.722 + 1)*P4;

EQN125.. QT2641 =E= QT2642 +
((s1('C1', 'Db-Feed') - s2('C1', 'Db-Bottom'))*(HDA2641 -
HFA2641) +
(s1('C2', 'Db-Feed') - s2('C2', 'Db-Bottom'))*(HDA2641 -
HFA2641) +
(s1('C3', 'Db-Feed') - s2('C3', 'Db-Bottom'))*(HDA2641 -
HFA2641) +
(s1('iC4', 'Db-Feed') - s2('iC4', 'Db-Bottom'))*(HDA2641 -
HFA2641) +
(s1('C4', 'Db-Feed') - s2('C4', 'Db-Bottom'))*(HDA2641 -
HFA2641) +
(s1('iC5', 'Db-Feed') - s2('iC5', 'Db-Bottom'))*(HDA2641 -
HFA2641) +
(s1('C6', 'Db-Feed') - s2('C6', 'Db-Bottom'))*(HDA2641 -
HFA2641) +
(s1('C7', 'Db-Feed') - s2('C7', 'Db-Bottom'))*(HDA2641 -
HFA2641) +
(s1('C8', 'Db-Feed') - s2('C8', 'Db-Bottom'))*(HDA2641 -
HFA2641) +
(s1('C9', 'Db-Feed') - s2('C9', 'Db-Bottom'))*(HDA2641 -
HFA2641) +
(s1('C10', 'Db-Feed') - s2('C10', 'Db-Bottom'))*(HDA2641 -
HFA2641) +
(s1('N2', 'Db-Feed') - s2('N2', 'Db-Bottom'))*(HDA2641 -
HFA2641) +
(s1('CO2', 'Db-Feed') - s2('CO2', 'Db-Bottom'))*(HDA2641 -
HFA2641) +
(y('C1', 'P4') - s1('C1', 'Db-Feed'))*(HBA2641 - HFA2641) +
(y('C2', 'P4') - s1('C2', 'Db-Feed'))*(HBA2641 - HFA2641) +

```

```

y('C3', 'P4') - s1('C3', 'Db-Feed'))*(HBA2641 - HFA2641) +
(y('iC4', 'P4') - s1('iC4', 'Db-Feed'))*(HBA2641 - HFA2641) +
(y('C4', 'P4') - s1('C4', 'Db-Feed'))*(HBA2641 - HFA2641) +
(y('iC5', 'P4') - s1('iC5', 'Db-Feed'))*(HBA2641 - HFA2641) +
(y('C6', 'P4') - s1('C6', 'Db-Feed'))*(HBA2641 - HFA2641) +
(y('C7', 'P4') - s1('C7', 'Db-Feed'))*(HBA2641 - HFA2641) +
(y('C8', 'P4') - s1('C8', 'Db-Feed'))*(HBA2641 - HFA2641) +
(y('C9', 'P4') - s1('C9', 'Db-Feed'))*(HBA2641 - HFA2641) +
(y('C10', 'P4') - s1('C10', 'Db-Feed'))*(HBA2641 - HFA2641) +
(y('N2', 'P4') - s1('N2', 'Db-Feed'))*(HBA2641 - HFA2641) +
(y('CO2', 'P4') - s1('CO2', 'Db-Feed'))*(HBA2641 - HFA2641))*(P4
+ FBtDb)/(

```

```

y('C1', 'P4') - s2('C1', 'Db-Bottom') +
y('C2', 'P4') - s2('C2', 'Db-Bottom') +
y('C3', 'P4') - s2('C3', 'Db-Bottom') +
y('iC4', 'P4') - s2('iC4', 'Db-Bottom') +
y('C4', 'P4') - s2('C4', 'Db-Bottom') +
y('iC5', 'P4') - s2('iC5', 'Db-Bottom') +
y('C6', 'P4') - s2('C6', 'Db-Bottom') +
y('C7', 'P4') - s2('C7', 'Db-Bottom') +
y('C8', 'P4') - s2('C8', 'Db-Bottom') +
y('C9', 'P4') - s2('C9', 'Db-Bottom') +
y('C10', 'P4') - s2('C10', 'Db-Bottom') +
y('N2', 'P4') - s2('N2', 'Db-Bottom') +
y('CO2', 'P4') - s2('CO2', 'Db-Bottom')));

```

EQN126.. NDbmin =E= 16.228;

EQN127.. XDb =E= (1.722 - DbRmin)/(1.722 + 1);

EQN128.. NDbbr + NDbs =E= 10.601;

EQN129.. NDb_r =E= 1.314964*NDb_s;

*@PLANT OUTLET

EQN130.. QP1 =E= HP1*P1;

EQN131.. QP2 =E= HP2*P2;

EQN132.. QP3 =E= HP3*P3;

EQN133.. QP4 =E= HP4*P4;

EQN134.. QP5 =E= HP5*P5;

*INITIAL VALUES @PRU

P441.1 = 3009.00;

T4411.1 = 32.27;

T442.1 = 32.27;

P6101.1 = 1600.00;

P461C.1 = 2471.00;

P6211.1 = 1860.00;

T622.1 = 20.16;

P622.1 = 1780.00;

T623.fx = 20.16;

P623.fx = 1760.00;

TH2011.fx = 20.16;

PH2011.fx = 1760.00;

P6301.1 = 561.3;

P6411.1 = 860.00;

T642.1 = 20.16;

P642.1 = 770.00;

TH2022.fx = 20.61;

PH2022.fx = 750.00;

T643.1 = 20.16;

P643.1 = 750.00;
T651.1 = 34.94;
P651.1 = 570.00;
T652.1 = 30.00;
P652.1 = 550.00;

*NOTES

*P6101 does not affect QT2621, Stream 623 is C3product (propane) and its temperature is fixed at T623 =20.16 C and pressure P623=1760 kpa

*H2011 and H2022 are influents and their temp and pressure kept constant.P6301 does not affect QT2642. Stream 643 is C4product (butane) and its temperature is fixed at T643 =20.16 C and pressure P643=750 kpa P651 and R have constant relationship with QT2643

*Stream 652 is C5+product (condensate) and its temperature is fixed at T652 =30.16 C and pressure P652 =500 kpa

*P652 is called Ried pressure for the condensate normally this pressure has also a significant effect on the quality of the condensate produced. The feed FDe,FDp,FDb can be represented from material balance around the column,i.e.,FD = Distillate + bottom (flow rate,hence FDe can be manipulated by either Distillate or bottom flow rates,these have been left as a spec in HYSYS.

*The above equation is based on energy balance around a column for multi-component separation. The minimum number of theoretical stage for deethanizer is equal to

$$*ND_{emin} = E = \log_{10}(2842007.179) / \log_{10}(RV_{DeC2})$$

$$*X_{De} = E = (DeRflxratio - DeRmin) / (DeRflxratio + 1);$$

*Actual number of stage for deethanizer column is evaluated using:

$$*(ND_{estage} - ND_{emin}) / (ND_{estage} + 1) = E = 0.381973109;$$

$$*ND_{estage} = E = ND_{er} + ND_{es}$$

*NDer = number of stage for the rectification section for deethanizer

*NDes = number of stage for the stripping section for deethanizer
*column. The same correlation goes for depropanizer and debutanizer

*QP6 for carbon dioxide is obtained from the overall energy balance
*equation

* KEY PROCESS VARIABLES

*@PLANT INLET

*TR1, PR1, TR2, PR2, TR3, PR3, TR4, PR4

*@Pre-treatment unit (PTU)

*T121, P121, T152, P152, T301, P301, T302, P302,

*@Condensate treatment unit (CTU)

*P104, T161, P161, T108, P108, T454, P454

*@Low temperature separation unit (LTSU)

*T311, P311, T312, T401, P401, T411, P411

*@Sales gas compression unit (SGCU)

*P432, P501, T503, T504, T505

*C3-refrigeration unit (CRU)

*P732, P743, P7541, P750, P760, P762, T764

*@Product recovery unit (PRU)

*P441, T4411, T442, P6101, T623, P623, T651, P651

*@PLANT OUTLET

*Psalesgas (C1product), T603 (C2product), T623 (C3product), P623 (C3product),

*T643 (C4product), P643 (C4 product), T652 (C5+product), P652 (C5+product),

*TCO2 (CO2 product), PCO2 (CO2 product)

*MATERIAL BALANCE EQUATION

*component material balance for: C1, C2, C3, C4s, C5+, N2 and CO2

EQN135..y('C1', 'P1')*P1 + y('C1', 'P2')*P2 + y('C1', 'P3')*P3 +
y('C1', 'P4')*P4 + y('C1', 'P5')*P5 + y('C1', 'P6')*P6 =E=
x('C1', 'R1')*R1 + x('C1', 'R2')*R2 +
x('C1', 'R3')*R3+x('C1', 'R4')*R4;

$$\text{EQN136..} y('C2', 'P1') * P1 + y('C2', 'P2') * P2 + y('C2', 'P3') * P3 + y('C2', 'P4') * P4 + y('C2', 'P5') * P5 + y('C2', 'P6') * P6 = E = x('C2', 'R1') * R1 + x('C2', 'R2') * R2 + x('C2', 'R3') * R3 + x('C2', 'R4') * R4;$$

$$\text{EQN137..} y('C3', 'P1') * P1 + y('C3', 'P2') * P2 + y('C3', 'P3') * P3 + y('C3', 'P4') * P4 + y('C3', 'P5') * P5 + y('C3', 'P6') * P6 = E = x('C3', 'R1') * R1 + x('C3', 'R2') * R2 + x('C3', 'R3') * R3 + x('C3', 'R4') * R4;$$

$$\text{EQN138..} (y('iC4', 'P1') + y('C4', 'P1')) * P1 + (y('iC4', 'P2') + y('C4', 'P2')) * P2 + (y('iC4', 'P3') + y('C4', 'P3')) * P3 + (y('iC4', 'P4') + y('C4', 'P4')) * P4 + (y('iC4', 'P5') + y('C4', 'P5')) * P5 + (y('iC4', 'P6') + y('C4', 'P6')) * P6 = E = (x('iC4', 'R1') + x('C4', 'R1')) * R1 + (x('iC4', 'R2') + x('C4', 'R2')) * R2 + (x('iC4', 'R3') + x('C4', 'R3')) * R3 + (x('iC4', 'R4') + x('C4', 'R4')) * R4;$$

$$\text{EQN139..} (y('iC5', 'P1') + y('C5', 'P1') + y('C6+', 'P1')) * P1 + (y('iC5', 'P2') + y('C5', 'P2') + y('C6+', 'P2')) * P2 + (y('iC5', 'P3') + y('C5', 'P3') + y('C6+', 'P3')) * P3 + (y('iC5', 'P4') + y('C5', 'P4') + y('C6+', 'P4')) * P4 + (y('iC5', 'P5') + y('C5', 'P5') + y('C6+', 'P5')) * P5 + (y('iC5', 'P6') + y('C5', 'P6') + y('C6+', 'P6')) * P6 = E = (x('iC5', 'R1') + x('C5', 'R1') + x('C6+', 'R1')) * R1 + (x('iC5', 'R2') + x('C5', 'R2') + x('C6+', 'R2')) * R2 + (x('iC5', 'R3') + x('C5', 'R3') + x('C6+', 'R3')) * R3 + (x('iC5', 'R4') + x('C5', 'R4') + x('C6+', 'R4')) * R4;$$

$$\text{EQN140..} y('N2', 'P1') * P1 + y('N2', 'P2') * P2 + y('N2', 'P3') * P3 + y('N2', 'P4') * P4 + y('N2', 'P5') * P5 + y('N2', 'P6') * P6 = E = x('N2', 'R1') * R1 + x('N2', 'R2') * R2 + x('N2', 'R3') * R3 + x('N2', 'R4') * R4;$$

$$\text{EQN141..} y('CO2', 'P1') * P1 + y('CO2', 'P2') * P2 + y('CO2', 'P3') * P3 + y('CO2', 'P4') * P4 + y('CO2', 'P5') * P5 + y('CO2', 'P6') * P6 = E = x('CO2', 'R1') * R1 + x('CO2', 'R2') * R2 + x('CO2', 'R3') * R3 + x('CO2', 'R4') * R4;$$

*Total material balance

$$\text{EQN142..} R = E = R1 + R2 + R3 + R4;$$

$$\text{EQN143..} P = E = P1 + P2 + P3 + P4 + P5 + P6;$$

$$\text{EQN144..} P - R = E = 0;$$

*Upper and lower bound for decision variables

$$R1.up = 334.582214355;$$

$$R1.lo = 0;$$

$$R2.up = 220.314773560;$$

$$R2.lo = 0;$$

R3.up = 10.706112016;
R3.lo = 0;
R4.up = 35.5858020881;
R4.lo = 0;
P1.up = 298.518112183;
P1.lo = 0;
P2.up = 37.310810089;
P2.lo = 0;
P3.up = 47.706112016;
P3.lo = 0;
P4.up = 29.585802088;
P4.lo = 0;
P5.up = 43.111991264;
P5.lo = 0;
P6.up = 57.659376734;
P6.lo = 0;

* Steam and cooling water usage by the absorbers and distillation
*columns

EQN145.. FsteamA2451 =E= (QT2451)*(3.6)/2177.565671 ;
EQN146.. FsteamA2404 =E= (QT2404)*(3.6)/2496.919669 ;
EQN147.. FsteamA2601 =E= (QT2601)*(3.6)/2307.147807 ;
EQN148.. FsteamA2621 =E= (QT2621)*(3.6)/2233.649564 ;
EQN149.. FsteamA2641 =E= (QT2641)*(3.6)/2232.423954 ;
EQN150.. FrefrigerantA2601 =E= QT2602/36.00438475;
EQN151.. FcoolingA2622 =E= QT2622/23.2556;
EQN152.. FcoolingA2642 =E= QT2642 /23.2556;

*ENERGY BALANCE

*Energy inflow using raw material

EQN153.. $QR1 + QR2 + QR3 + QR4 =E= u1$;
 *Energy inflow using steam
 EQN154.. $QT2451 + QT2404 + QT2601 + QT2621 + QT2641 =E= u2$;
 *Energy inflow using refrigerant
 EQN155.. $QT2354 + QT2352 + WR27011 + WR27012 + WR27013 =E= u3$;
 *Energy inflow using compression
 EQN156.. $WR2501 + QT2604SGas + QL2501 =E= u4$;
 *Energy inflow using electricity
 EQN157.. $WP2401 + WP2402 + WP2403 + WP2404 + WP2621 + WP2641 =E= u5$
 ;
 *Energy inflow using fuel
 EQN158.. $QA2101 + QT2151 + QAGRU + QL2301 + QL2302 + QT2101 + QL2104$
 $+ QL2451 + QL2452 + QL2661 + QL2662 + QT2604PRU =E= u6$;
 *Energy out flow due to cooling water
 EQN159.. $QT2622 + QT2642 + QT2643 + QT2644 =E= q1$;
 *Energy out flow due to sales gas for cooling
 EQN160.. $QT2701 =E= q2$;
 *Energy out flow due to refrigeration for cooling
 EQN161.. $QT2501 =E= q3$;
 *Energy out flow due to products
 EQN162.. $QP1 + QP2 + QP3 + QP4 + QP5 + QP6 =E= q4$;
 CON1.. $QR1 + QR2 + QR3 + QR4 =L= m1('50', 'u1')$;
 CON2.. $QT2451 + QT2404 + QT2601 + QT2621 + QT2641 =L= m1('50', 'u2')$;
 CON3.. $QT2352 + QT2354 + WR27011 + WR27012 + WR27013 =L=$
 $m1('50', 'u3')$;
 CON4.. $WR2501 + QT2604SGas + QL2501 =L= m1('50', 'u4')$;
 CON5.. $WP2401 + WP2402 + WP2403 + WP2404 + WP2621 + WP2641 =L=$
 $m2('50', 'u5')$;
 CON6.. $QA2101 + QT2151 + QAGRU + QL2301 + QL2302 + QT2101 + QL2104 +$
 $QL2451 + QL2452 + QL2661 + QL2662 + QT2604PRU =L= m2('50', 'u6')$;
 CON7.. $QT2622 + QT2642 + QT2643 + QT2644 =G= m3('50', 'q1')$;

```

CON8.. QT2701 =G= m3('50','q2');
CON9.. QT2501 =G= m3('50','q3');
CON10.. QP1 + QP2 + QP3 + QP4 + QP5 + QP6 =G= m3('50','q4');

```

*TOTAL Energy balance

```
EQN163.. Qin =E= u1 + u2 + u3 + u4 + u5 + u6;
```

```
EQN164.. Qout =E= q1 + q2 + q3 + q4;
```

```
EQN165.. Qout - Qin =E= 0
```

```
Model Gas / all /;
```

```
Option LP = CPLEX;
```

```
Solve Gas using LP maximizing Z;
```

* (II) JOINT CHANCE CONSTRAINED OPTIMIZATION

* All the formulation in the single chance constrained optimization
*up to equation 162 remains the same. The only changes in the joint
*chance constrained formulation is shown below.

```
EQN163.. Zu1 =E= (u1 -SM11)/SV11;
```

```
EQN164.. Zu2 =E= (u2 -SM22)/SV22;
```

```
EQN165.. Zu3 =E= (u3 -SM33)/SV33;
```

```
EQN166.. Zu4 =E= (u4 -SM44)/SV44;
```

```
EQN167.. Zu5 =E= (u5 -SM55)/SV55;
```

```
EQN168.. Zu6 =E= (u6 -SM66)/SV66;
```

```
EQN169.. Zq1 =E= (q1 -SM111)/SV111;
```

```
EQN170.. Zq2 =E= (q2 -SM222)/SV222;
```

```
EQN171.. Zq3 =E= (q3 -SM333)/SV333;
```

```
EQN172.. Zq4 =E= (q4 -SM444)/SV444;
```

```
CON11..(1 - erf(Lossu1))*(1 - erf(Lossu2))*(1 -
erf(Lossu3))*(1 - erf(Lossu4))*(1 - erf(Lossu5))*(1 -
erf(Lossu6))*(erf(Lossq1))*(erf(Lossq2))*(erf(Lossq
3))*(erf(Lossq4)) =G= 0.5 ;
```

*TOTAL Energy balance

EQN173.. Qin =E= u1 + u2 + u3 + u4 + u5 + u6;

EQN174.. Qout =E= q1 + q2 + q3 + q4;

EQN175.. Qout - Qin =E= 0;

Model Gas / all /;

Option NLP = CONOPT3;

Solve Gas using NLP maximizing Z;

Display

TR1.1, PR1.1, TR2.1, PR2.1, TR3.1, PR3.1, TR4.1, PR4.1, QR1.1, QR2.1, QR3.1, QR4.1, TC1.1, PC1.1, T121.1, P121.1, T152.1, P152.1, TCO2.1, PCO2.1, T301.1, P301.1, T302.1, P302.1, TH2O2.1, PH2O2.1, T310A.1, P310A.1, THg.1, PHg.1, QA2101.1, QT2151.1, WRT2151.1, QAGRU.1, QT2301.1, QL2301.1, QL2302.1, P156.1, P104.1, P306.1, T3061.1, P3061.1, T161.1, P161.1, T108.1, P108.1, P109.1, T441B.1, P441B.1, M441B.1, T452.1, P452.1, T453.1, P453.1, QT2101.1, QL2104.1, QT2451.1, QL2451.1, QL2452.1, T311.1, P311.1, T312.1, T401.1, P401.1, T411.1, P411.1, P421.1, P403.1, P413.1, P427.1, T454.1, P454.1, TpA2.1, PpA2.1, MpA2.1, TpA41.1, TpA4.1, PpA4.1, MpA4.1, TpA61.1, TpA6.1, PpA6.1, MpA6.1, T6011.1, P6011.1, M6011.1, M6012.1, T602.1, T603.1, QT2402.1, QT2404.1, WR2401.1, WRT2401.1, WP2401.1, WP2402.1, WP2403.1, WP2404.1, P428.1, P430.1, P430C.1, P432.1, P501.1, T503.1, T504.1, P504.1, TS.1, PS.1, T505.1, Psalesgas.1, WR2151.1, WR2501.1, QT2604SGas.1, QL2501.1, QT2501.1, P732.1, P734.1, P735.1, P736.1, P743.1, P7451.1, P750.1, P760.1, P762.1, P763.1, T764.1, P764.1, T765.1, P765.1, P71X.1, P71S.1, P71N.1, P71I.1, P71D.1, P71B.1, P71Y.1, P71T.1, P71O.1, P71J.1, P71E.1, WR27011.1, WR27012.1, WR27013.1, QT2701.1, QT2603.1, QT2354.1, QT2352.1, P441.1, T4411.1, T442.1, P6101.1, P461C.1, P6211.1, T622.1, P622.1, T623.1, P623.1, TH2O11.1, PH2O11.1, P6301.1, P6411.1, T642.1, P642.1, TH2O22.1, PH2O22.1, T643.1, P643.1, T651.1, P651.1, T652.1, P652.1, QT2604PRU.1, QT2623.1, QL2661.1, QT2645.1, QL2662.1, QT2643.1, QT2644.1, WP2621.1, WP2641.1, RVDsum.1, DeRmin.1, DeRflxratio.1, NDemin.1, XDe.1, NDer.1, NDes.1, RVDpsum.1, DpRmin.1, DpRflxratio.1, NDpmin.1, XDp.1, NDpr.1, NDps.1, RVDbsum.1, DbRmin.1, DbRflxratio.1, NDbmin.1, XDb.1, NDbr.1, NDbs.1, QP1.1, QP2.1, QP3.1, QP4.1, QP5.1, QP6.1, FsteamA2451.1, FsteamA2404.1, R1.1, R2.1, R3.1, R4.1, P1.1, P2.1, P3.1, P4.1, P5.1, P6.1, R.1, P.1, u1.1, u2.1, u3.1, u4.1, u5.1, u6.1, q1.1, q2.1, q3.1, q4.1, QT2601.1, QT2602.1, QT2621.1, QT2622.1, QT2641.1, QT2642.1, FsteamA2601.1, FsteamA2621.1, FsteamA2641.1, FrefrigerantA2601.1, FcoolingA2622.1, FcoolingA2642.1, Qin.1, Qout.1

